Synthesis and Evaluation of Novel Heterocyclic Compounds as Anticancer Agents

AMJED ABDULRAZAQ AHMED MAL ULLAH

School of Science, Engineering, and Environment

University of Salford , Salford, UK

Submitted as partial fulfillment of the requirement of the degree of Doctor of philosophy

Contents

Table of Figures

List of schemes

List of Tables

Acknowledgements

This thesis would not have seen the light without the backing of many people, for those, I am extremely thankful.

At the leading age, I wish to express my sincere gratitude to my sponsor the Iraqi Ministry of Higher Education represented by the Iraqi cultural attaché in London, for granting the opportunity and supporting this study at the university of Salford Manchester in UK.

I would like to express my faithful gratefulness to my supervisor Dr. John Hadfield for his kindness support and guidance during my Ph.D. I would also like to extend my thanks to Dr. Steve Rossington and Dr. Jim Wilkinson for their wise advice and knowledge.

A big thanks go to my lab mates Natalie Barnes, Andrew McGown, and Patrick Killoran who guided me during the lab work in my first year, I will never forget you guys. I would also like to thank my friend Al-Ameen Mohammed for his patience when I lose my patience and kind comfort during the tough time. You are holding the torch now. My warm thanks would go for my office mates Steven Austin, Henry, Graham Burry, Ibraham, Mudasar Zafar, Grace, Jessica, Zucchi. My warmest appreciation also goes to the two placement students Shaymaa and Khiran.

A huge thanks also go for Kiri Ameen the most expert man with a magic touch in NMR without his help, I would have been blind. He was my eyes to read organic chemistry. I would also to extend my thanks to all technician at SEE school especially Mark Parlby and Geoff Parr.

A special huge appreciation goes for Dr. Muna Abubaker for her support in cell culture lab, you were really the kindest sister I have ever met in the university of Salford.

Wholehearted appreciation to my soulmate, my wife, for her generosity, kindness and excessive support during this difficult time without your standing on my side in my life I would be lost. My special token of appreciation also goes to my beloved kids, Zahraa and Mustafa, sprinkling joy and happiness in my life, you have made me stronger and more fulfilled in my endeavours.

Finally, I would like to thank my family- my father and mother, brothers, and sister for your constant support. I would like to extend my thanks to my friends Mujahid, Hassanien, and Muhtady thank you for your encouragement.

Abstract

There is a clear need for anti-cancer therapies that have effective cytotoxic efficiency and marginal toxicity, preferably zero. For this goal, researchers have been persevering to develop new drugs from natural resources. Among them are agents that target tubulin, which is a protein found in all eukaryotic cells. This protein is an essential component for mitosis and has several different binding sites at which a variety of chemically different agents interact. These binding sites include the colchicine, vinca alkaloids, rhizoxin /maytansine and tubulin sulfhydryl binding sites. Combretastatin A-4 is one of the most potent natural products targeting tubulin and prevents microtubule polymerisation that leads to mitosis arrest and apoptosis in endothelial cells. Moreover, it can cause selective vascular shutdown for the tumour cell and results in haemorrhagic necrosis for the solid tumour. However, cis-combretastatin is more active than the trans isomer. Toxicity to normal cells has limited its use as an effective chemotherapy. Another problem with this isomer is the *in vivo* instability, by which the unstable cis isomer converts to the more stable inactive trans-isomer.

To overcome this problem, many combretastatin analogues have been synthesized and evaluated in terms of antimitotic and cytotoxic activity as well as toxicity. 6-(4-Methoxy-3-nitrophenyl)-5-(3,4,5-trimethoxyphenyl)-1,2,4-triazin-3(2H)-one, and series of : 2,3-diaryl-3H-imidazo[4,5-b]pyridine, and N-((2-arylamino)pyridine)benzenesulphonamide derivatives, which related to E7010, have been synthesised as possible active analogues of combretastatin A-4.

These heterocyclic analogues have been characterized and examined for their ability to suppress the growth of A549, U-2 OS, BEAS-2B, Saos-2, Hep-G2, and A204 mammalian cell lines by MTT assay, and flowcytometry. 3-Hydroxy-4-methoxy-N-(2-((3,4,5-trimethoxybenzyl)amino)pyridin-3-yl)benzenesulfonamide, was the most potent compound evaluated with an IC_{50} of 1.15µM in the Carcinoma A549 cell line. It is also caused cells to hold up in the G2/M phase of the cell cycle (37.34 %).

Abbreviations

Ac	Acetyl group CO-CH_3
aq.	Aqueous
Ar.	Argon gas
b/t	Between
Brine	Aqueous sodium chloride saturated
^{13}C NMR	Carbon nuclear resonance
CA-4	Combretastatin A-4
$CDCl_3$	Deuterated Chloroform
$CHCl_3$	Chloroform
chemo	chemotherapy
d	Doublet
DCM	dichloromethane
dd	doublet of doublet
DIPEA	Diisopropyl ethylamine
DMF	dimethylformamide
DMSO	dimethyl sulfoxide
DP	Population doubling
EG	Ethylene glycol
eq.	Equivalent(s)
et.al	From Latin Et alia (and other)
ESI	Electron spray ionization
EtOAc	Ethyl acetate
EtOH	Ethanol
GI	Gastrointestinal
^{1}H NMR	Proton nuclear resonance
Hr.	Hours
HCl	Hydrochloric acid
HPLC	High performance liquid chromatography
HRMS	High resolution mass spectroscopy
Hz	Hertz
IC_{50}	Half maximal inhibition concentration

In vitro	Latin (in glass)
In vivo	Latin (within the living)
FTIR	Fourier transform infrared
J	Coupling constant
Lit.	In the literatures
M	Molar
m	Multiplet
Mp	Melting point
Me	Methyl group CH_3
MeOH	Methanol
mg	Milligram(s)
$MgSO_4$	Magnesium Sulphate
min.	Minute(s)
Misc.	Miscellaneous
mM	Millimolar
µM	Micromolar
MOD	Mode of drug action
mmol.	millimole(s)
MTT	3-(4,5-dimethylthiazol-2-yl)-2,5-diphenyltetrazolium bromide
N/V	Nausea/ vomiting
NADH	Nicotine amide adenine
nM	Nanomolar
n-BuLi	Normal-butyl lithium
NMR	Nuclear magnetic resonance
OMe	Methoxy group OCH_3
PBS	Phosphate buffer solution
PH	Power of hydrogen
Ph	Phenyl
R_f	Retention factor in TLC
RT	Room temperature
RNA	Ribonucleic acid

s	Singlet
Sat	Saturated
SiO_2	Silica (silicon dioxide)
SN_1	Substitution nucleophilic unimolecular
SN_2	Substitution nucleophilic bimolecular
SN_{Ar}	Nucleophilic aromatic substitution
S/E	Side effect
t	Triplet
TBAF	Tetra-n-butylammonium fluoride
THF	Tetrahydro furan
TLC	Thin layer chromatography

Chapter 1

Introduction

1 Introduction

1.1 Cancer

Cancer is a global concern as it is a major cause of death. In 2018, there were 9.6 million deaths and 18.1 million new cases were recorded (Bray *et al.*, 2018). Moreover, it is expected in the next few years to surpass 29.5 million new cancer cases and 16.5 million cancer-related deaths. In Europe, as an example, there are 4.23 million new cases and 1.95 million deaths in 2018 (WHO, 2020) . These frightening statistics challenge researchers from all over the world to figure out ways to combat this problem. In 2014, 38316 documents were published all over the world on cancer research (SJR, 2016) and total spend (excluding industries) surpassed €11billions in the 2004/2005 fiscal year (Eckhouse *et al.*, 2008).

Currently, this malady refers to a group of conditions affecting tissues, which is characterized by uncontrolled cell division and growth. The resulting tumour can spread to other tissues, by either invasion or metastasis. Although each tumour has a unique feature, the process by which cancer produced is similar, where a healthy cell in the human body starts to divide in an uncontrolled way due to mutations that occur to numbers of regulatory genes that control the growth, division, differentiation, and survival of the cell (NIH, 2007).

Healthy cell production occurs at the behest of nearby cells, which ensure the appropriate size and structure of the tissue, whereas, the division of a cancer cell happens rapidly and in an unnatural way that affects the size and structure of tissues. Furthermore, losing control of growth with the possibility of spreading throughout the body, a series of extensive mutations that happen in specific genes within the cell, whether it was acquired or inherited, leads to cancer (Vogelstein & Kinzler, 2004).

Genes, which were found in all eukaryotic cells, are a specific series of DNA regulated as chromosomes that are situated in the nucleus of the cell. Functionally, every gene codes for a specific protein that identifies the order in which amino acids must join. Consequently, alterations or mutations in these genes result in modifications in the quantity or the activity of the produced proteins.

Oncogenes are genes that have the possibility to cause cancer (cancer-causing gene) (ACS, 2020). A proto-oncogene is a normal gene that has the ability to become an

oncogene because of changes in its DNA sequences. These genes organize cell growth and proliferation as they mainly code for many proteins which stimulate the cell for division and prevent cell differentiation or regulate programmed cell death (apoptosis) (Robertson, 2014).

As a result, mutations or defects of proto-oncogenes can lead to unregulated cell division by increasing the production of these proteins and ultimately cancer might ensue.

Anti-oncogenes are genes that suppress cell growth through the suppression of cell cycle regulation or promote apoptosis and sometimes do both (Sherr, 2004). Mutations of anti-oncogenes deactivate its control overgrowth leading to deregulation of cellular proliferation. These genes might be considered more important than proto-oncogenes (Weinberg, 2014, p. 231). Consequently, any mutations that occur for these two genes (proto-oncogenes, anti-oncogenes) can disrupt the precise balance between stimulation and suppression of the cellular process leading to unrestrained growth.

DNA can be subjected to an environmental attack that causes damage to the DNA, which if not repaired, leads to mutations and death-related diseases. A good example of the diseases and DNA damage that can be induced by the environment is skin cancer. Moreover, through cell division, the replication of DNA is susceptible to errors that cause spontaneous damage to the DNA (Uryga *et al.*, 2016). However, cells have numerous mechanisms to identify and correct any damage that occurs to DNA, regardless of the environment or replication errors that causes this damage.

Three possible responses can occur to the cell that has major DNA damage, or one that does not have the ability to repair damage effectively as shown in figure 1:

1. Senescence. The cell may stop dividing, i.e., permanent dormancy. The capability of the cells to replicate and divide is terminated after a specific number of populations doublings (DP) which induce cell signalling to cease cells replication. One of the most investigated mechanisms is the telomere uncapping, where the telomere length steadily shortening as the cells approach the end of their reproduction life.
2. Apoptosis. The apoptotic signalling cascade may be triggered if there is sufficient DNA damage, which drives the cell into programmed cell death.
3. Malignancy. The cell may develop its immortal character to grow and start uncontrolled proliferation.

When the cell become tumorous, the mutation will be passed on to the next cell during cell division (Braig *et al.*, 2005).

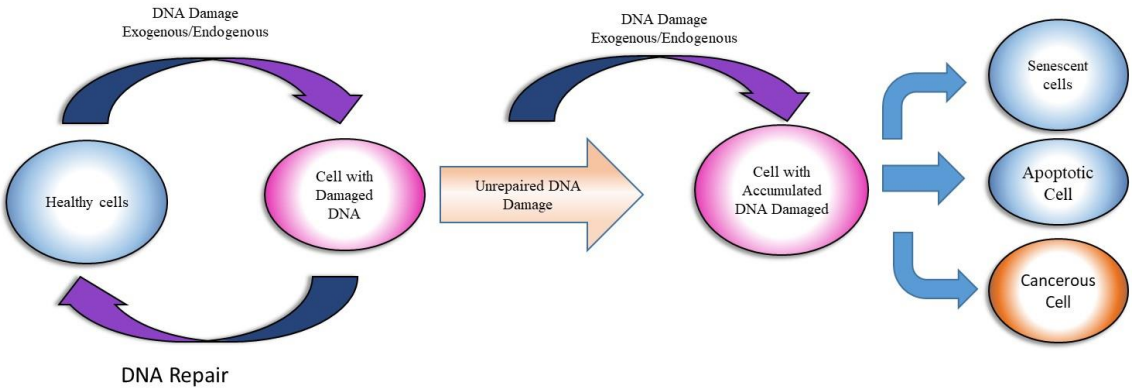

Figure 1: The cell responses toward DNA damage and the repair pathway which leads to senescence, apoptosis, or malignancy (Merck, 2020).

1.2 Types of Cancer

More than 100 distinguished kinds of cancer and subtypes have been found in the human body. These types are classified according to the kind of tissue where the cancer originates from, generally, there are five main groups (CRUK, 2020b) :-

1- Carcinoma is the most common one that is derived from the epithelial cells, which forming tissues that line the inner or outer surfaces of the body. The most common subtypes of carcinoma are adenocarcinoma, squamous cell carcinoma, transitional cell carcinoma, and basal cell carcinoma which are very familiar in older people and can be develop in the colon, breast, lung, pancreas, and prostate.

2- Sarcoma comprises cancers that stem from connective tissues (i.e. bone, cartilage, fat, nerves, lymph vessels, blood vessels, and fibrous tissues). Osteosarcoma is the most common primary malignancy of the bone (Ottaviani & Jaffe, 2010).

3- Leukaemia comprises cancers that usually start in bone marrow which is a blood-forming tissue and results in the production of an uncontrolled amount of abnormal white blood cells. This kind of cancer is quite widespread among children aged less than 15 years old, who represent almost 30% of childhood cancer incidences (Steliarova-Foucher *et al.*, 2017).

4- Lymphoma and myeloma are immune system cancers that originate in the lymphatic system cells such as plasma cells, T cell and B cells. Hodgkin and Non-Hodgkin lymphoma are the main types of lymphoma.
5- Central nervous system cancers are known as brain and spinal cord cancers.

1.3 Causes of cancer

The majority of cancer diseases are related to the environment, lifestyle or behavioural factors, genetic birth defects, and aging as well. The most known environmental factors that have been identified causing cancer include tobacco, radiation, and UV-light (both ionizing and non-ionising), chemicals, environmental pollutants, lack of physical activity, obesity, and infections (Anand *et al.*, 2008). Carcinogens are specific substances capable of causing cancer in living tissues. An example is tobacco smoking (figure 2); these carcinogens are responsible for nearly one-third of all cancer deaths and 90% of lung cancers (Kuper *et al.*, 2002). Most carcinogens and radiation act by damaging DNA and inducing mutations.

Tumour promoters are another type of carcinogen involved in cancer development by inducing cell proliferation. The proliferation, which induced by these chemicals, leads to mutations that inevitably occur during DNA replication.

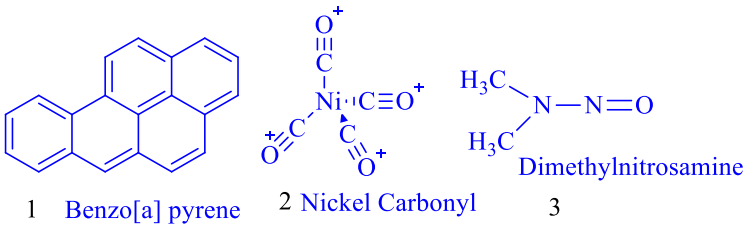

Figure 2: Structure of tobacco smoke carcinogens (Cooper., 2000).

Cancer is often considered as a disease of elderly people as the cancer statistics indicate that more than half (53%) of all new cancer cases are for adults aged 50-74, and over third (36%) is for elderly people aged 75+ as shown in figure 3. For most cancers types, incidence increases with age for both sexes as the development of cancer is a multistep process in which cell DNA damage that results from biological process or exposure to risk factors accumulating over periods of many years. In addition, this fact could be a good indication of the multistep development of cancer.

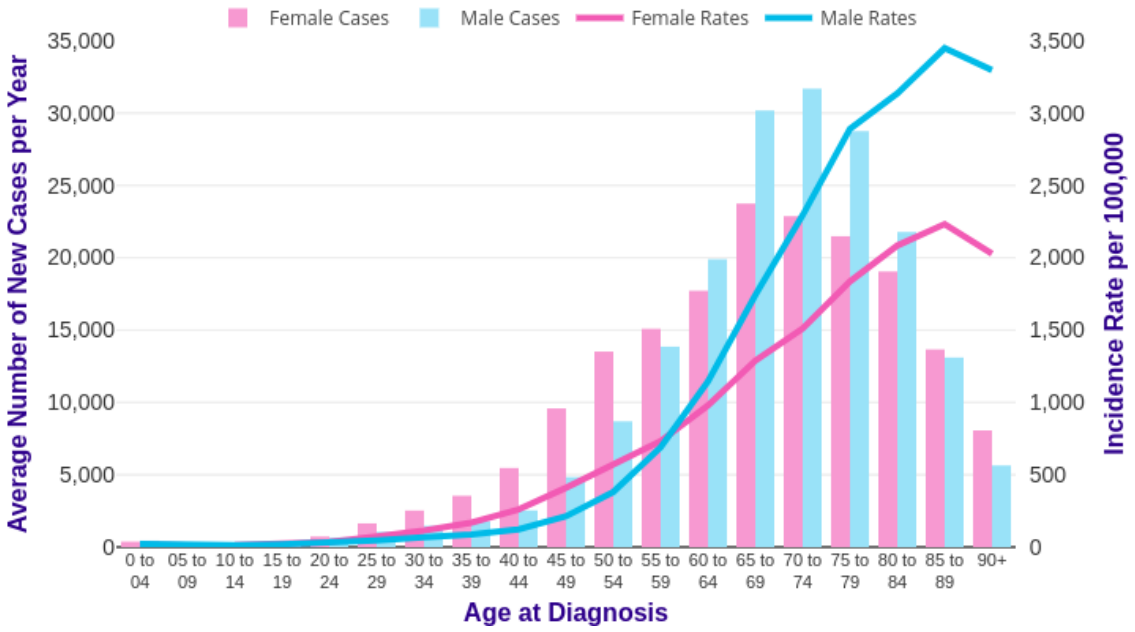

Figure 3: New cancer cases per year and incidence rates for specific ages. UK, 2015-2017 (CRUK, 2020a).

1.4 **Cancer Therapy**

The cancer risk factors, which are a combination of environmental and genetic factors, are the causes of most cancers. However, a great number of these factors can be avoided and controlled (Danaei *et al.*, 2005). Therefore, the essential way to reduce cancer encumbrance is by the primary prevention of cancer risk factors through lifestyle and environmental interventions. It has been shown that avoiding the risk factors such as tobacco, alcohol, sexually transmitted infections, obesity, and air pollutants can prevent more than 30% of cancer mortality (Kushi *et al.*, 2012). A second alternative, which is still effective, is the early reliable detection of premalignant stages of tumour development that could lead to early treatment. Many cancers can be cured if they are diagnosed before they metastasise throughout the body. For instance, minor surgical operations are completely effective to cure the early premalignant stages of colon cancer. There are numerous options for cancer therapy, however, the type of treatment will depend on the type of cancer, location, and how advanced it is. Traditionally, there are three approaches for treating cancer: surgery, radiotherapy, and systemic therapy. Cancer treatment usually involves combinations of treatment such as surgery and systemic therapy and/or radiation therapy.

These drugs, systemic therapies, include hormonal therapy, chemotherapy, immunotherapy, and targeted drugs. Hormone therapy has a vital role in the treatment of breast and prostate cancer, since these types of cancers use hormones to develop or grow which means they are hormone sensitive or hormone-dependent cancers. Furthermore, targeted therapies play a pivotal role in some kinds of cancers because they interfere with particular molecules that have a significant role in the progression, growth, and metastasis process which leads to blocking the growth and spread of cancer (Caley & Jones, 2012).

As cancer cells tend to grow and divide quickly, they are sensitive to chemotherapy, which interrupts the cell cycle and slows down or stops cancer cells' reproduction. Some drugs are specific in affecting the cancer cell at one stage of the cycle, whilst non-specific drugs work on cancer cells in all stages of the cell cycle without considering if they are dividing or resting.

The selectivity of chemotherapy can be improved to target the cancer cell rather than the healthy cell as the fact that any tissue or organ, as well as cancer cells, are surrounded by an intensive area of sugar-containing molecules called polysaccharides. Structurally, these polysaccharides vary depending on the different tissues and organs of the body. The polysaccharides of tumour regions are also different from normal tissue in terms of the chemical compositions. Consequently, using the appropriate carrier for the drug can identify particular kinds of polysaccharides would considerably minimize the side effect of chemotherapy (Longmuir *et al.*, 2009).

For better outcomes, a combination of chemotherapy drugs can be used to treat certain types of cancer. Combined chemotherapy drugs should be potent against tumours and exert their action through different action mechanisms on the cancer cells. One drug may act by disrupting DNA replication and the second may prevents protein synthesis. The biggest advantage of this strategy is lessening the toxicity of the chemotherapy by using small doses and minimising the chances of developing resistance to any one agent. A typical example of combination chemotherapy is shown in the lung cancer medication where cisplatin and etoposide are used in addition to external radiation. Cisplatin acts on disruption of the cell replication by cross-linking DNA strands, whereas etoposide causes irreversible damage to the DNA. These two drugs form a good combination in treating small-sized lung cancer as they have cooperative lethal effects on cancer and distinctive

side effects that make them a potent combination in the treatment of lung cancer (Sundstrøm *et al.*, 2002).

As with any other drugs, chemotherapy has undesirable secondary effects (side effects) as it disrupts the normal function of the healthy and cancer cells alike by interfering with DNA directly (inducing apoptosis), or by targeting the essential proteins which are necessary for cell division (inhibition replication) (Feng & Chien, 2003). Consequently, the main concern of utilising chemotherapy drugs is their inability to discriminate between the healthy and carcinogenic cells, the latter of which have a fast-growing nature. For the same reason some normal cells such as hair, bone marrow, and intestinal epithelial cells that grow rapidly, they interact with anticancer drugs, resulting in high toxicity. Thus, the usual adverse effects of chemotherapy include myelosuppression, nausea and vomiting, hair loss and reduced fertility.

1.5 Types of chemotherapy

Numerous types of chemotherapies are used to treat cancers, which can be classified or grouped into different categories depending on the chemical structures of the chemotherapy drugs and how they act on cancer cells. These categories are changeable with the development of new drugs.

In spite of some drugs working with different groups, some classification is useful in understanding the action mechanisms such as specific and non-specific cell cycle drugs figure 4 (Nussbaumer *et al.*, 2011; Shapiro & Harper, 1999; Thurston, 2006).

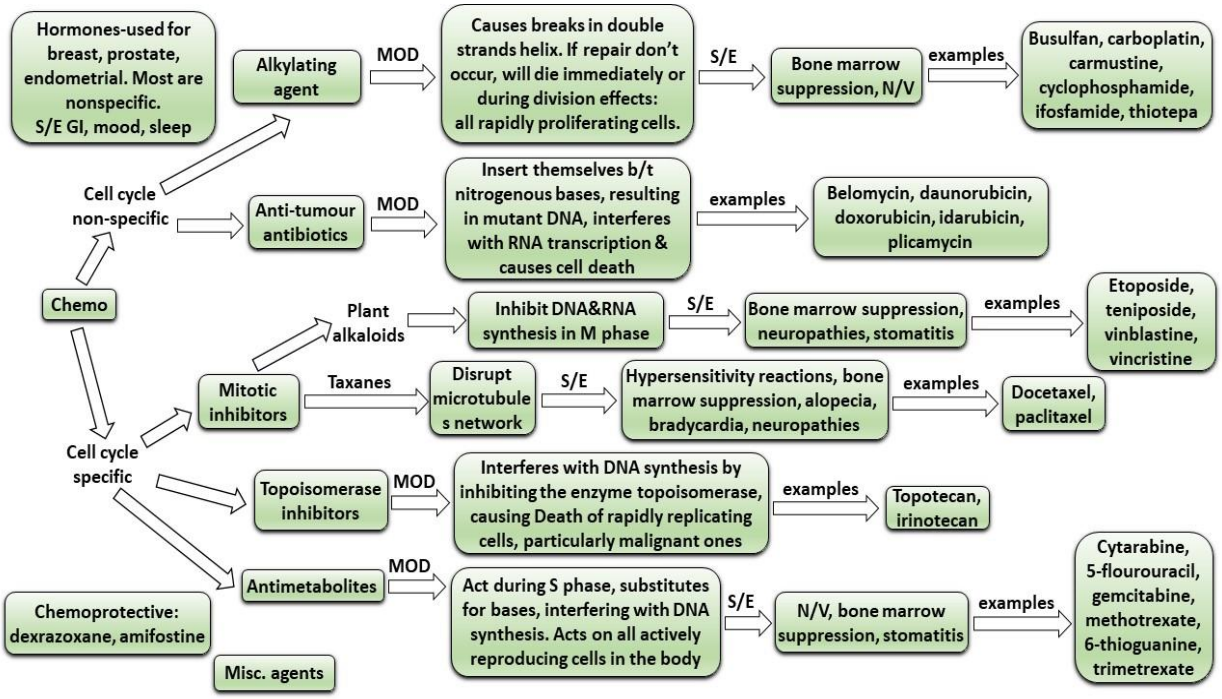

Figure 4: Classification of chemotherapy drugs base on action mechanisms.

Chemotherapies are classified according to the Anatomical Therapeutic Chemical (ATC) Classification System criteria (L01) into six major groups (Missailidis, 2008, p. 53):-

1- Platinum coordination complex.
2- Antimicrotubule agents.
3- Antimetabolites.
4- Antitumour antibiotics.
5- Alkylating agents.
6- Others not included in these five categories.

1.5.1 Platinum drugs

Platinum-based antineoplastic drugs are used in chemotherapy with coordination complexes utilised widely since the discovery of the antineoplastic activity of cisplatin in the 1970s to treat different types of cancer, such as epithelial malignancies (Johnstone *et al.*, 2014). Approximately half of all patients under chemotherapy treatment receive one of the platinum drugs (Markus *et al.*, 2005). One of the well-known platinum drugs is cisplatin, which is used extensively in the treatment of lung cancer, cervix, stomach, head-and-neck, colon, bladder, testes, oesophagus, ovaries, and uterus as a combination system with first-line chemotherapy.

Moreover, it is used with the other advanced cancers as a second -line treatment of cancers like kidney, pancreas, liver, prostate, and breast in addition to curing metastatic melanomas, glioblastomas, and peritoneal or pleural mesotheliomas.

The side effect of high dose treatment with cisplatin is nephrotoxicity and peripheral neurotoxicity, which is still the main limitation for using cisplatin in high doses. However, this side effect on kidney function can be significantly reduced by the pre-hydration of the patients treated with cisplatin and using diuretics (Donzelli *et al.*, 2004).

The antitumour efficiency of cisplatin may be accredited to the reactivity of the chlorine ligand toward displacement reaction, which leads to DNA crosslinking that is either interstrand or intrastrand (figure-5) (Boulikas, 2007). This DNA cross-linking inhibits nuclear functions such as replications and transcriptions, as well as, arresting the proliferation and growth of tumour cells by a four-step process that starts with cellular uptake, aquation/activation, DNA bindings, and cellular processing of DNA lesions that ultimately leads to cell death (Johnstone *et al.*, 2015).

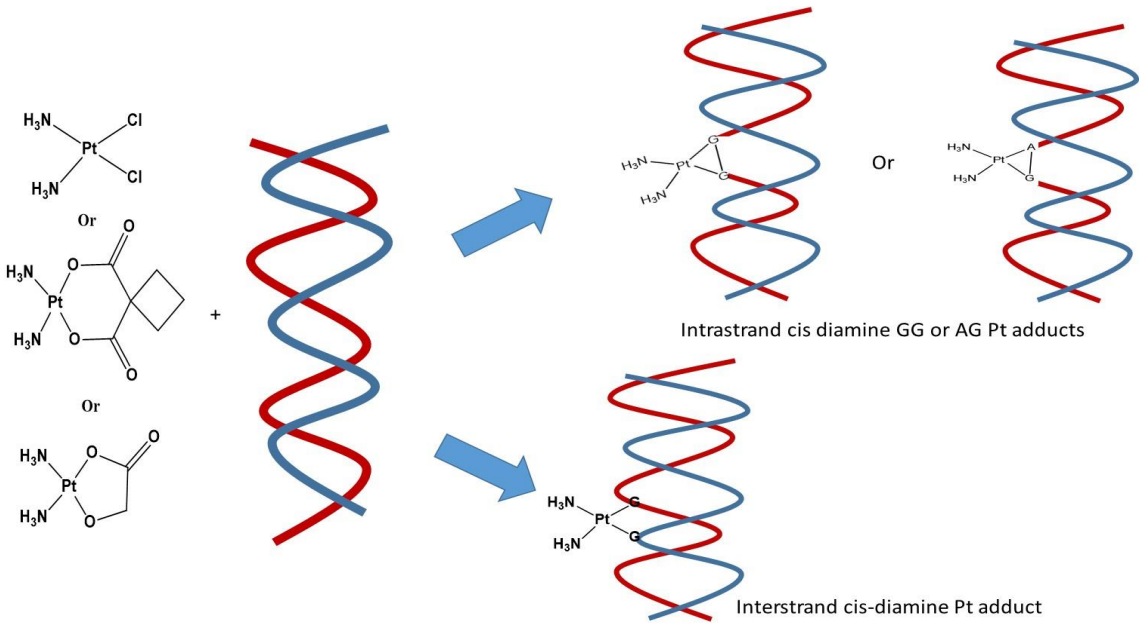

Figure 5: DNA adduct formation with platinum compounds.

1.5.2 Antimetabolites

Metabolites are chemical compounds required for normal biochemical reactions in cells such as oxidation (adding oxygen or removing electrons), reduction (adding hydrogen), transferring (transfer groups like amine, phosphates, carboxyl, etc.). As a result, they have different functions from which stimulating and inhibiting effects on enzymes, signalling, structure, defence, catalytic activity as coenzymes, fuel, and interaction with other organisms (e.g. pigments, odorants, and pheromones).

Antimetabolites, therefore, are chemicals that inhibit the use of metabolites and possess a similar composition to natural molecules used in nucleic acids synthesis (DNA and RNA) such as folic acid, pyrimidines, and purines. However, some structural differences are essential to intervene with normal cell function.

Antimetabolites can be used as drugs in cancer treatment as they can bind to proteins and interfere with one or more enzymes that are necessary for DNA synthesis and therefore cell division and growth of the tumour.

Generally, antimetabolites exert their action during the S phase of the cell cycle when integrated into RNA and DNA, or inhibit enzymes that are necessary for the production of nucleic acid (Avendano & Menendez, 2015, p. 25). Some of them prevent the synthesis of triphosphate derivatives, which are critical precursors of DNA synthesis; therefore, they suppress the process of replication. Other antimetabolites work on changing the

metabolites that are usually integrated with DNA and RNA. As a result, these drugs are more effective during the S phase and have a small impact through the G_0 phase of the cell cycle. As a result, antimetabolites are most potent against tumours that have a high growth fraction. Moreover, apart from 5-fluorouracil, antimetabolites have a non-linear dose response curve which means that no more cell will be killed after a certain concentration despite increasing the dose amount. However, increasing drug's time exposure will increase the potentiality for killing cells (Nargund, 2008).

The main group of antimetabolites, shown in figure-5, which are used in cancer treatment are; folate analogues or dihydrofolate reductase inhibitors, i.e. methotrexate; purine analogues, i.e. fludarabine and 6-mercaptopurine;, adenosine analogues, i.e. cladribine;, pyrimidine analogues or sugar-modified nucleoside analogues, i.e. cytarabine;, fluorouracil, and substituted urea, i.e. hydroxyurea as shown in figure .

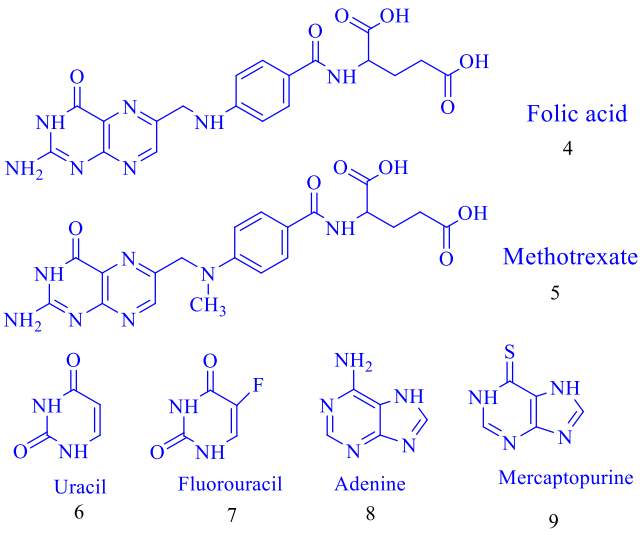

Figure 6: Structural relationships between several antimetabolites and their respective analogues.

1.5.3 Antitumour antibiotic drugs

Antitumour antibiotics are drugs used in cancer treatment, unlike the normal antibiotics that are utilised to cure infections. They exert their function by changing the DNA of the tumour cells to prevent them from growing and proliferating. One of the most common types of drug in this family are anthracycline antibiotics, which are derived from the *Streptomyces* bacterium *Streptomyces peucetius* . The first one brought to the light was

daunorubicin (known as daunomycin), and then doxorubicin (trade name Adriamycin, which is a 14-hydroxy derivative of daunomycin) was developed (Di Marco *et al.*, 1964) and used effectively in the curing of solid tumours such as small cell lung cancer, breast cancer, bladder cancer, stomach cancer, ovarian carcinoma, liver, and thyroid tumours (Arcamone, 1985).

In the more than 50 years since the invention of anthracyclines in the 1960s, the mechanism of action is not yet completely clear, and more than one mechanism has been suggested to understand the action by which these drugs inhibit cancers.

One of the exceptional mechanisms proposed by (Kiyomiya *et al.*, 2001), is based on the selective transfer of the anthracyclines to the nuclei of neoplastic and proliferating cells. Using passive diffusion, anthracyclines enter the cell and bind to the cytoplasmic proteasomes, for which they have a great affinity. This complex of anthracycline-proteasome then moves to the nuclei of neoplastic and normal proliferative cells because proteasomes are located principally in these nuclei, whereas, they are located in the cytosomes in the non-proliferative cells (Stępiński, 2012), (Amsterdam *et al.*, 1993). After proteasome-drug complex dissociation, anthracyclines will bind to the DNA because they have a higher affinity to the DNA. The effects of the anthracyclines is related to this higher affinity. Proteasome-drug complex not only transports anthracyclines to the nucleus, but also inhibits the activity of proteasomes, which results in the inhibition of protein degradation that interacts in cell growth and metabolism, leading to the stimulation of cell apoptosis.

The first mechanism to describe anthracyclines' behaviour was the DNA intercalation mechanism, which suggests that the intercalation of anthracyclines into DNA, results in the inhibition of macromolecular synthesis (Marco & Arcamone, 1975). Furthermore, numerous mechanisms explain the effects of anthracyclines such as DNA binding proteins (Gniazdowski *et al.*, 2005), anthracyclines-p53 interaction (Perego *et al.*, 2001), free radical generation (Gille & Nohl, 1997), and antiangiogenic mechanism (Al-Husein *et al.*, 2012).

Like any other chemotherapies, non-differentiated cytotoxicity to proliferating normal cells leads to undesirable side effects such as nausea, vomiting, and alopecia. The most serious toxicity of anthracyclines, however, is cardiotoxicity and myelosuppression that limits the usage of anthracyclines. The cardiotoxicity of anthracyclines might be arise

from the many factors that occur in the heart such as the inhibition or poisoning of topoisomerase-IIB (or both of them) in cardiomyocytes (Zhang *et al.*, 2012), ryanodine receptors intervention of the sarcoplasmic reticulum, generation of free radical, and the accumulation of anthracycline's metabolic products.

Alternative methodologies to stop the irreversible anthracyclines cardiotoxicity have been utilised which involve changes in drug administration routes, reducing the total dosage, liposomes' capsulation, combined therapy, utilising cardioprotectors, and the preparation of anthracycline analogues (Cortes-Funes & Coronado, 2007).

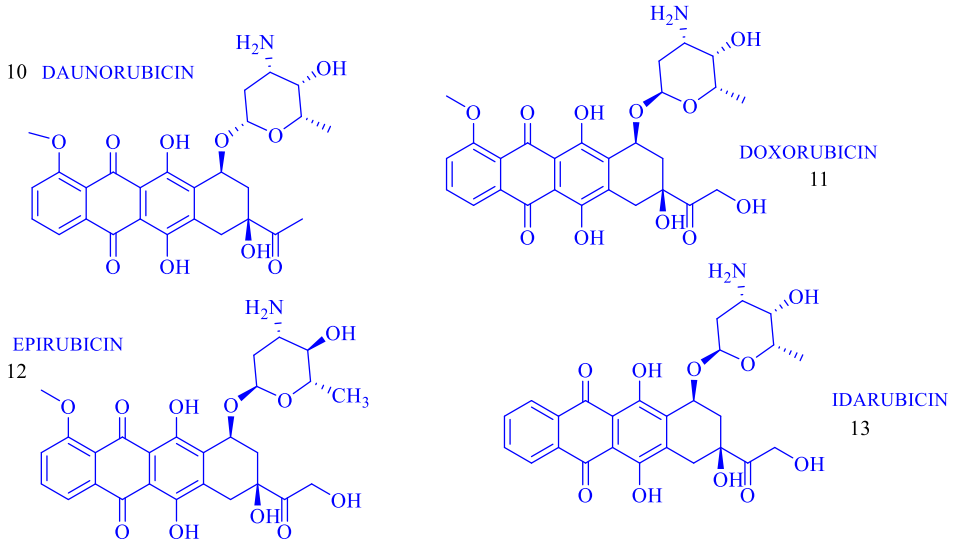

Figure 7 : Structures of some anthracyclines drugs. (Bhattacharya & Mukherjee, 2015)

1.5.4 Alkylating agents

Alkylating agents are one of the earliest kind of antineoplastic chemotherapy drugs that are used to treat all tumour cells, starting in the early 1940s, and still widely used today. They are compounds that have the ability to bind an alkyl group covalently to the biological molecules in a physiological environment of temperature, aqueous media, and Ph (Avendano & Menendez, 2015, p. 198).

Alkylating agents exert their effect on the double helix structures of the DNA molecules through binding an alkyl group to some of these DNAs. This effect is attributed to the ability of the DNA heteroatom to be alkylated, as well as, the sensitivity of all cancer cells to DNA damage. Consequently, the DNA would not be able to bind together as they should, which cause damage to the DNA strands and, ultimately, tumour cell death. This binding is a fundamental mutation for cancer cells to lose their ability to multiply. The

alkylating agents form covalent linkages by nucleophilic or electrophilic groups such as the phosphate, sulfhydryl, hydroxyl, carboxyl, amino, and imidazole groups, which allow them to react with the nucleophilic sites on the DNA and RNA bases or proteins that are essential for cell metabolism and protein synthesis. However, the nature of the alkylating agent is determined by the binding site on the duplex DNA; therapeutically beneficial drugs always act as carbon electrophiles (Gates, 2009) . Their interaction with resting and proliferating cells occurs at any phase of the cell cycle. The cytotoxicity, however, will be higher during the late G_1 and S phases as the cell does not have enough time to correct the damage before DNA synthesis can occur.

Numerous impacts could result on the DNA because of the alkylation of its bases, which prevents DNA replication and RNA transcription from the targeted DNA molecule. In addition, this leads to damaging the DNA by a hydrolytic reaction and by the action of repaired enzymes, inducing mispairing of the nucleotides by modification of the hydrogen bonding that normally occurs between the bases.

Moreover, mono-alkylation (i.e. attachment at one side) prevents enzymes accessing the DNA and thus inhibits cell growth. Dialkylating agents can attach either at two sites on the opposite strand (interstrand crosslinking) or on the same strand (intrastrand crosslinking also known as limpet attachment)). The interstrand DNA crosslinking that occurs at the N7 position of guanine on the opposite strands, which is caused by compounds like bischloroethylnitrosourea (BCNU, carmustine), melphalan and chlorouracil, prevents cell division because it prevents the separation of strands (Noll *et al.*, 2006) as illustrated in figure-8. Intrastrand crosslinking is much less common and can be caused by cisplatin, as well as it being considerably less cytotoxic than their dialkylating counterparts, as there is a direct correlation between the degree of interstrand crosslinking and cytotoxicity (Zwelling *et al.*, 1979).

The ability of alkylating agents to attack cancer cells in all phases of the cell cycle makes them favourable for use in a wide range of cancers, especially those with slow growth cancers like solid tumours and leukaemia. However, they are also utilized to cure cancers of lung, breast, lymphoma, sarcoma, ovarian, myelomas, and Hodgkin's disease.

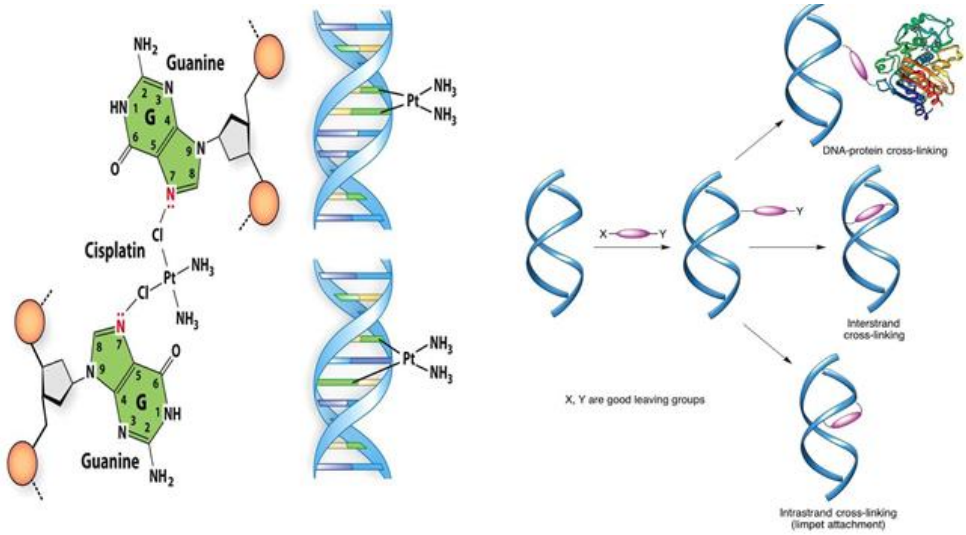

Figure 8: Different types of cross-linking produced on DNA by bis-alkylating agents (Cox *et al.*, 2015, p. 426).

At present, there are several classes of alkylating agents with different classifications; however, they all work by the same chemical mechanism (Colvin, 2003) by which the electrophilic alkyl group becomes attached with cellular nucleophilic sites by a covalent bond. Kinetically, this reaction divides alkylating agents into two categories: alkylating agents which react with the biological molecules directly through the SN_1 mechanism, and those forming an active intermediate that reacts with the biological molecule through the SN_2 mechanism. While busulfan is considered as an SN_2 mechanism agent, nitrogen mustards and nitrosoureas are a good example of the SN_1 mechanism. Major classes of clinically useful alkylating agents are classified into:

a- Alkylsulfonates

This class (alkyl alkane sulfonate busulfan) is considered as the earliest alkylating agents that clearly exert their action through the SN_2 mechanism and exhibit electrophilic selectivity towards thiol groups. Busulfan is prescribed in the treatment of chronic myelogenous leukaemia as it has a greater effect on myeloid cells than the lymphoid cell (Blackburn *et al.*, 1956) . Hepsulfam is a sulfamate analogue of Busulfan which had a broad spectrum of cytotoxic activity in preclinical studies.

b- Nitrogen mustards

This group is the most frequently used among the alkylating agents and only five agents are currently used today from thousands of nitrogen mustards that have been evolved and trialled clinically: -

nitrogen mustard (mechlorethamine), cyclophosphamide, ifosfamide, melphalan, and chlorambucil, which have a common characteristic feature of a bischloroethyl group that is used in alkylation attack.

The first step in the alkylation process is an intramolecular displacement of the chloride ion by the nitrogen atom. The chloride ion acts as a good leaving group, to form a highly reactive cyclic electrophilic aziridinium ion that is attacked by nucleophilic moieties in DNA to form the first product of alkylation. The remaining chloroethyl group to achieve the bifunctional crosslinking will form a second aziridinium ion.

The ability of nitrogen mustards to cross-link the double strands of DNA makes them beneficial drugs in the treatment of lymphoma, leukaemia, multiple myeloma, and ovarian carcinoma. This double cross-linking leads to the inhibition of DNA's replication and transcription, and eventually, if these DNA lesions are not repaired, will lead to cell cycle arrest, apoptosis, and the inhibition of tumour growth (Balcome *et al.*, 2004).

c- Aziridines and Epoxides

This group of alkylating agents are analogues of nitrogen mustards and have the same mechanism of alkylation by the aziridinium intermediates, but the aziridinium ring is uncharged and chemically less potent than those in nitrogen mustards. However, they have equivalent therapeutic properties. Currently, aziridines are represented by thiotepa, mitomycin C, and diaziquone (AZQ).

Epoxides are chemically related to aziridines and alkylated DNAs through the same mechanism and they are represented by dibromodulcitol and dianhydrogalactitol. The former is a prodrug to an epoxide as it is hydrolysed to dianhdrogalactitol.

d- Triazine, hydrazine, and related compounds

Nitrogen containing compounds like triazines and hydrazines are pro-drugs that decompose or metabolize spontaneously to produce alkyl diazonium intermediates, which have the ability to alkylate DNA. Methyldiazonium does not have sufficient time to reach

its target for alkylation as its half-life is very short at approximately 0.4 sec. In aqueous solution, therefore, these drugs undergoes spontaneous activation by which metabolic oxidative demethylation occurs by way of N-methyl oxidation utilizing a microsomal P450 enzyme, as illustrated in Figure 9 (Avendano & Menéndez, 2015; Skibba *et al.*, 1970).

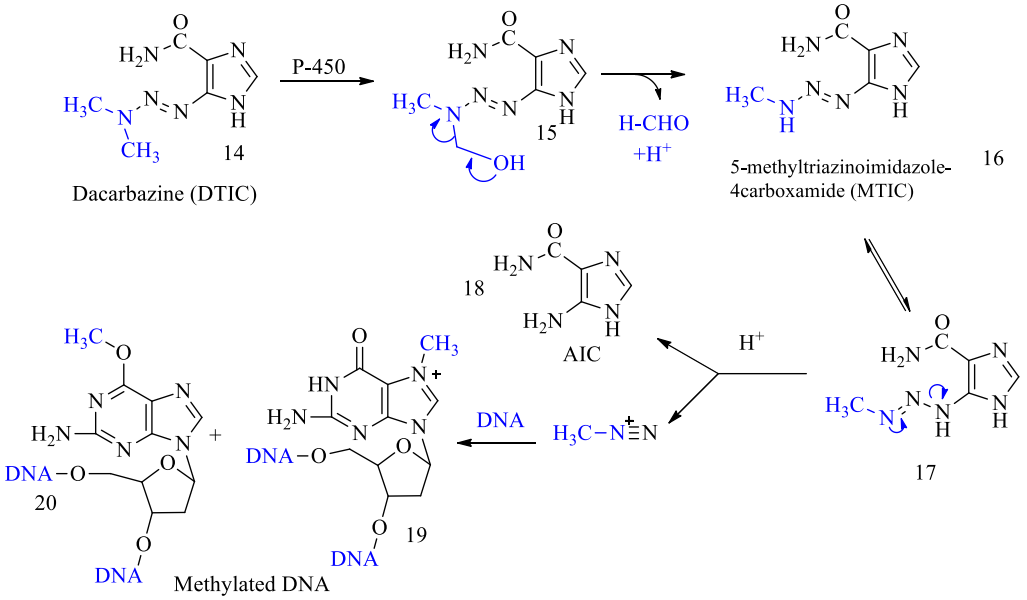

Figure 9: DNA methylation by dacarbazine and formation of methyl diazonium.

The most well-known triazine drugs are dacarbazine which is known commercially as DTIC-Dome and temozolomide that is sold commercially as Temodar (TMZ). DTIC is employed to cure neuroblastoma, metastatic malignant melanoma, rhabdomyosarcoma, soft tissue sarcomas, Hodgkin's disease, fibrosarcoma, islet cell carcinoma, and medullary thyroid carcinoma. As TMZ has a favourable toxicity and pharmacokinetics, it is utilised in the treatment of specific types of brain tumours- anaplastic astrocytoma and glioblastoma multiform (GBM) - as well as being used as a combination chemotherapy with other classes of anticancer drugs to improve the response rate.

1.5.5 Antimicrotubule agents

Microtubules are rigid hollow cylinders approximately 25 nm in diameter, which consist of α-tubulin and β-tubulin heterodimers. These α/β-tubulin dimers polymerise in a linear

fashion to construct a mono microtubule, which expands by the addition of more dimers. Tubulin acts as a building block for microtubules (a highly dynamic structure) that undergoes polymerisation and depolymerisation within the cell, where both are very sensitive to external factors.

Microtubules are polar structures as they have two characteristic ends: - a plus (+) and a minus (-). Both α-and β-tubulin bind to GTP that acts as a polymerisation regulator, before binding to the (+) end of the microtubule. However, GTP linked with the β -tubulin is hydrolysed to GDP shortly after polymerisation because of a reduction of its binding affinity for the adjacent molecules, and therefore, separates rapidly from the ends of the microtubules. In contrast to the GDP-dimer, the GTP-dimer has a tendency to remain in microtubules.

If the GTP is hydrolysed rapidly at the (+) end faster than the addition of the new dimers, the microtubules will alternate between cycles of growth and shrinkage. This behaviour is known as dynamic instability. Consequently, hydrolysis of GTP is crucial for the microtubule dynamic instability, as well as, for the polymerisation-depolymerisation equilibrium.

Microtubules are involved in maintaining cell structures and together with important components they form the cytoskeleton. They have a pivotal role in cell division, signalling, vesicle transport, shape, and polarity (Nogales, 2000).

The mitotic spindle is a bipolar apparatus found in eukaryotic cells, created by microtubules, that functions to accurately and precisely segregate the replicated chromosomes into two daughter cells during cell division, as well as to transfer the chromosomes from the mother cells to the daughter cells (Stanton *et al.*, 2011) .

Because of their pivotal role in the mitotic process, microtubules serve as a target for antitumour drugs known as microtubule-targeting agents that exert their action by disrupting the polymerisation-depolymerisation equilibrium.

They are classified according to their effect on tubulin polymerisation to microtubule stabilising (stimulate microtubules polymerisation) or microtubule destabilising agents (inhibit microtubules polymerisation). The latter is subclassified into those that target Vinca-binding sites and those that interact with colchicine-binding sites. Most of these drugs are natural products from plants and marine organisms. Microtubules and tubulin are considered as the most preferred target identified to date for natural cytotoxic

compounds that have multifarious structures and are able to bind effectively to identical sites on microtubules (Giannakakou *et al.*, 2000) .

The common mechanism by which these drugs work is suppressing microtubule dynamics by binding to the various sites on tubulin and at diverse positions on the microtubules, whereby mitosis is blocked at the metaphase/ anaphase transition and stimulates cell death (Kavallaris *et al.*, 2001).

Microtubule-targeting agents (MTAs) bind to tubulin through several sites such as the lulimalide, taxane/epothilone, vinca alkaloid, and colchicine sites.

1.6 Colchicine Binding Sites

The colchicine site is named from the tropolone alkaloid colchicine that was isolated from the poisonous meadow saffron *Colchicum autumnale L* by the French chemists Pelletier and Caventou for the first time in 1820. This plant is widely used in traditional medicine for curing acute gout and stopping severe attacks of familial Mediterranean fever. Colchicine (**21**), figure 10, was the first compound to be characterized as a tubulin binder in the sixties by Weissenberg (Nunez *et al.*, 1979) . However, minor improvement was made in the research regarding the structural relationship protein and ligand until the position of sites was finally confirmed by means of x-ray crystallography (Ravelli *et al.*, 2004) .

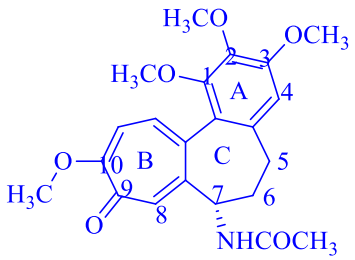

21

Figure 10: Colchicine structure with labelled rings.

Colchicine and its analogues block cell division by disrupting the microtubule by depolymerising microtubules at the higher doses and stabilize microtubules dynamics at low concentration. Firstly, it connects to soluble tubulin to form the colchicine-tubulin complex (CTC) that copolymerises with the normal tubulin to end up with microtubules formation. However, this CTC prevents further polymerisation of the microtubule by

suppressing their dynamics, the conjugated tubulin binding to free tubulin is supressed (Yan Lu *et al.*, 2012).

The structure of colchicine consists of three rings, (figure 10): the methoxy ring (ring A), which is a trimethoxy benzene ring, the tropone ring (ring C), which is a methoxy tropone ring, and the third one a seven-membered ring (ring B) with an acetamido group situated at its C-7 position. The structure-activity-relationships (SAR) studies for the CTC showed that the binding with tubulin requires the methoxy group in C1, C2, C10 and 9- keto group, whereas the 7-acetamido is not necessary for the binding with tubulin and could be replaced with any other group, however, it's thought that it affects the conformation of the colchicine analogues. The trimethoxyphenyl group ring (A) is not only necessary for the stabilizing of the CTC, but also significant for antitubulin activity in association with ring C. Ring B appears to be responsible for the irreversible nature of colchicine binding to tubulin, however, its expansion leads to reduced activity (Chen *et al.*, 2009).

The colchicine-binding site is situated in a far down pocket between the tubulin heterodimer; however, it is mostly buried in the β-subunit. An X-ray structure study showed that the binding affinity of the inhibitors is improved by considerable conformational modifications to allow the inhibitors to access the site, because of the hindered location of the binding sites (Y. Lu *et al.*, 2012).

Owing to the great efficiency of colchicine binding site inhibitors (CBSIs) to inhibit mitosis, cancer cells are more susceptible to colchicine poisoning than normal cells, as they proliferate in significantly increased rates. Moreover, CBSIs have an advantage over other microtubules targeting agents through their action on the tumour vasculature that inhibits angiogenesis, through which fresh blood vessels can be built from pre-existing microvesseles (angiogenesis inhibitors) or damage the current tumour vasculature (vascular disrupting agents, (VDA)). Another advantage of these compounds is that most of them have no multidrug resistance (MDR) issues.

However, the low therapeutic index and toxicity, such as gastrointestinal upset, bone marrow damage, neutropenia, and anaemia, limits the pharmaceutical utility of colchicine against the disease of cancer. The major limitation of using CBSIs clinically is the over-expression of the MDR1 gene that encrypt the P-glycoprotein (Pgp) drug efflux pump. Consequently, over-expression of Pgp deceases intracellular concentration of the drugs, thereby mitigating the drug cytotoxicity.

Similar to colchicine, podophyllotoxin, steganacin, and combretastatins share the same binding site on tubulin (colchicine binding site), (figure 11). However, combretastatins (CAs) surpass the other compounds in activity. The combretastatin family is one of the most studied groups of antimitotic agents, which consists of several closely related stilbenes, phenanthrene and biphenyl derivatives isolated from the African willow tree *Combretum caffrum.* The most effective among them is combretastatin A-4 (**25**) (figure 11) due to its rapid binding to tubulin at the colchicine site.

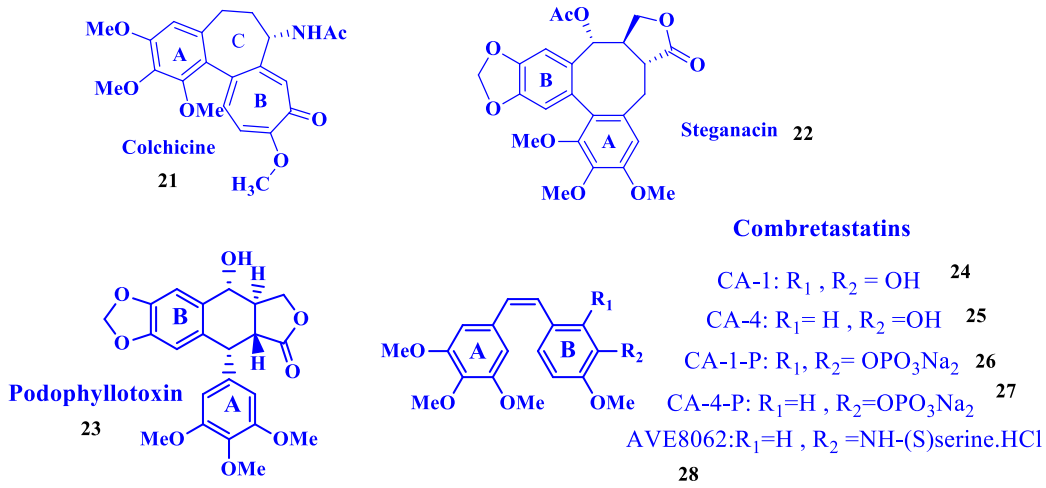

Figure 11: The structure of some known colchicine binding site inhibitors. (Sanghai *et al.*, 2014).

1.7 **Combretastatin A-4 (CA-4)**

Combretastatin A-4 (**25**) is a natural stilbenoid phenol that is extracted from the African willow tree *Combretum Caffrum*. It is a well-known drug that the people of Xhosa in South Africa have used it for decades as a remedy for different health issues such as heart disease, worm treatment, wound dressings and scorpion sting. It is considered one of the most powerful inhibitors of tubulin polymerisation with exceptional tubulin inhibition in a low concentration ($IC_{50}\approx$ 2-3 µM) (Ahmed *et al.*, 2003).

Combretastatin A- 4 has similarities with colchicine as both bear a trimethoxy benzene ring, however, the tropone ring in colchicine can be considered as related to the isovanillin ring in CA-4.

The structure-activity relationship (SAR) researches demonstrated that the trimethoxy phenyl group on ring (A) and para-methoxy group on ring (B) are crucial for its cytotoxic activity (Fürstner & Nikolakis, 1996) .

However, the cis-double bond in CA-4 is associated with stability problem because of its susceptibility to undergo cis-trans isomerisation by the effect of heat, light, and protic media (Tron *et al.*, 2006). As a result, the double bond may be considered as a source of weakness in terms of metabolic stability (Greene *et al.*, 2010; Nathwani *et al.*, 2013) . Another fact that can be concluded from SAR publication on substituted stilbenes is the difficulty of making modifications in the substitution pattern of the two aromatic rings as both of them directly interact with tubulin (Gaukroger *et al.*, 2003). For this reason, many researchers have attempt to change this double bond with a more stable moiety that capable of maintain the correct structure of two adjacent rings of stilbene.

Indeed, in the search for more active and lower toxicity drugs that have additional functionalities such as dual-action drugs it is better to think that the double-bond group is replaced with a ring. Several combretastatin analogues have been synthesised in which the double bond was replaced with five-member heterocyclic such as thiophene, thiazole, dioxolane, oxadiazole, pyrazole, and tetrazole or small alkyl group, where some of these agents proved effective to inhibit the assembly of tubulin (Ohsumi *et al.*, 1998b), (Ohsumi *et al.*, 1998a).

In comparison with CA-4, some of the thiophene (**34**, **35)** (Flynn *et al.*, 2001) and triazole (**41)** derivatives (figure-12) showed potent antimitotic activity and reduced cytotoxicity. The thiazole (**37)** (Ohsumi *et al.*, 1998a) and tetrazole (**39)** (Romagnoli *et al.*, 2012) both exhibited potent antimitotic activity and strong antitumour activity *in vivo*. Of the oxygen heterocycles the S**,** S-diastereo isomer of the dioxolane (dioxostatin) showed very effective ability to inhibit the assembly of tubulin (Pettit *et al.*, 2000).

Furthermore, several analogues have been tested, each of them with a similar two-ring structure bonded by a two-carbon alkene unit, the A ring in most analogues display the 3,4,5-trimethoxy unit. Whereas, changing the substituents on ring-B has been shown to improve the anti-tumour activity (Ohsumi *et al.*, 1998a). The double bond substituted nitrile combretastatin (**31)** (with substitution on the side of the olefinic bond distal to the trimethoxy ring) shows potent antitubulin activity (Ohsumi *et al.*, 1998b). Moreover, a smaller group attached to the side of the olefinic bond proximal to the trimethoxylated ring has also provided compounds with strong cytotoxic properties. These include cyano and formyl groups in (**32**, **33)** (Nam, 2003)(figure-12).

However, other small groups such as COOH, $CONH_2$, do not show antimitotic properties (Borrel *et al.*, 2005). The most interesting substituents of the combretastatin double bond are the methyl (**29)** and ethyl (**30)** substituted agents which are more effective at inhibiting the assembly of tubulin than CA-4. However, they are considerably less cytotoxic to human leukaemia K562 cells at (40- and 120-fold respectively) (Hadfield *et al.*, 2005). 1,5-Diaryl and 4,5-diaryl- 1,2,3-triazole derivatives of combretastatin A-4 analogues have been synthesised. 1,5- (N-C geometry) (**40)** and 4,5-(C-C geometry) (**41)** were evaluated as being antimitotic microtubule destabilising agents (Demchuk *et al.*, 2014), where the latter analogues were found to be significantly more active than the 1,5-(N-C geometry) analogues.

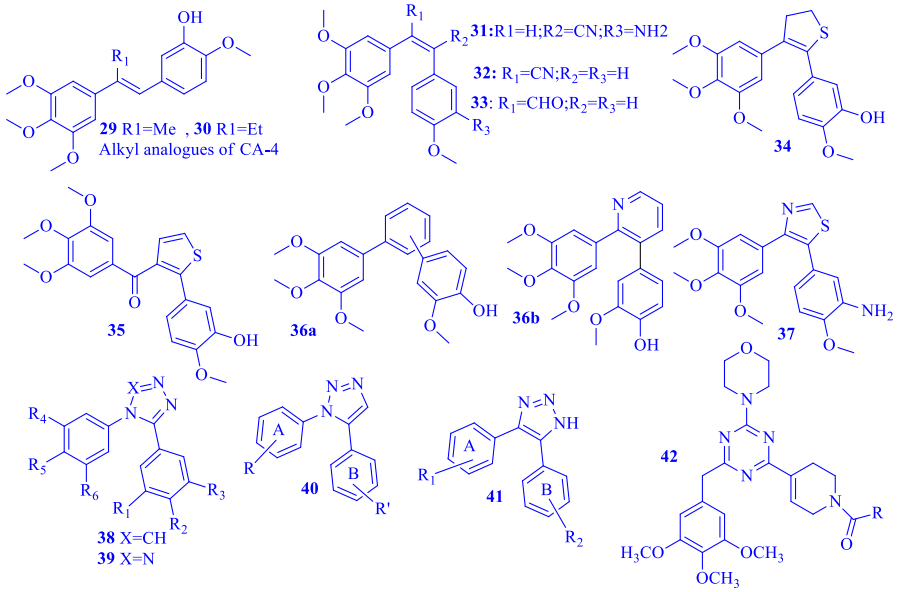

Figure 12: Structure of some synthesized combretastatin analogues.

The ethenyl group of CA-4 was not only replaced by various 5-membered heterocyclic rings, but further modified with a 4 member-ring of β-lactam(Nathwani *et al.*, 2013), and 6-member ring of cyclohexyl and cyclohexene (Nowikow *et al.*, 2019) , phenyl and pyridine analogues, where the synthesised compound was evaluated for their anti-tubulin, apoptotic, and cytotoxicity activities. These compounds (**36a, 36b)** (figure 12) show potent cytotoxicity in promyelocytic leukaemia HL-60 Cells with (IC_{50}<1µM) and apoptosis activity in K-562, P-glycol-protein expressing cell line; however they have low anti-tubulin activity (Simoni *et al.*, 2005). In a recent study, substituted 1,3,5-triazine (**42)** (figure 12) have been tested against several human cancer cell lines and showed encouraging antiproliferative and cytotoxic activity (Narva *et al.*, 2017).

Moreover, fused hetero-bicyclic compounds have been explored such as benzodiazole (Vasilevsky *et al.*, 2008), pyrazolo[1,5-a]pyrimidines (Almansa *et al.*, 2001), benzimidazole (Yang *et al.*, 2005), and 2,3-diaryl-3H-imidazo[4,5-b]pyridine (Marie Kirwen *et al.*, 2017). However, the latter, synthesised only 8 compounds, among which only one compound bears a trimethoxy moiety.

Combretastatin A-4 has several drawbacks that limit its use as an efficient anticancer drug, such as, poor aqueous solubility and bioavailability, short biological half-life, isomerisation of the olefinic bond, and a few other detrimental adverse side effects.

However, to address the aqueous solubility problem, the combretastatin A-4 sodium phosphate prodrug (CA-4P) was developed in the 1990s (Pettit *et al.*, 1995), which is a water-soluble prodrug of combretastatin A-4 and has an improved bioavailability profile. However, this soluble prodrug is converted to its natural form CA-4 by *in vivo* dephosphorylation reaction.

The most intriguing character of combretastatin A-4P is its ability to selectively compromise the vascular network in tumours. As some research has shown, microtubule targeting agents, especially colchicine binding site inhibitors, have the ability to induce irreversible vascular shutdown within solid tumours while leaving normal vasculature intact. CA-4P can cause rapid, selective, and extensive vascular damage that leads to haemorrhagic necrosis within 1hr of treatment and considerable tumour growth delay (Dark *et al.*, 1997) .

The findings from the literatures above, it has become a prompting motive to explore a new heterocyclic linker replacing the unstable olefin of combretastatin A-4 **25** with imidazo[4,5,b] pyridine derivatives **43a, 43b** and substituted 5,6-diaryl-1,2,4-triazine-3(h)-one **59a, 59b** (figure-13).

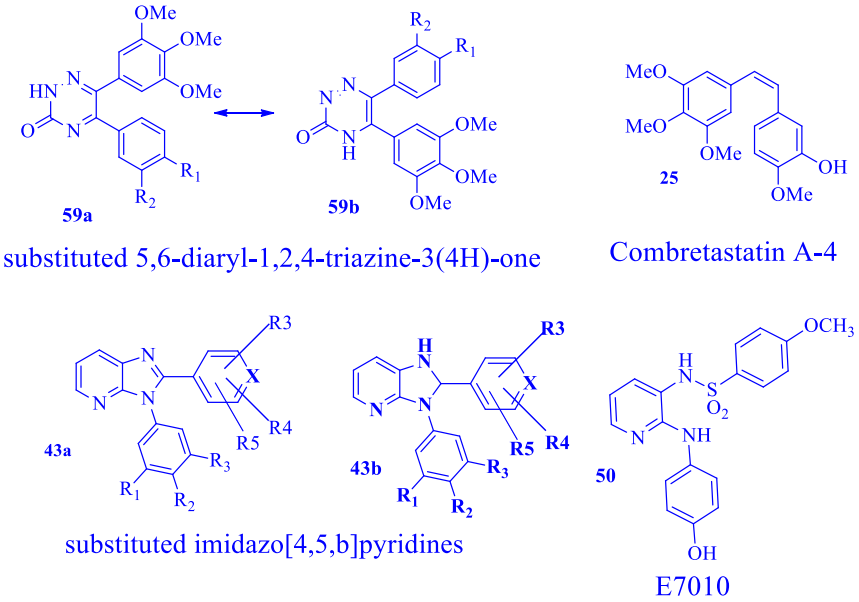

Figure 13: General structures for combretastatin A-4 and designed analogues.

Imidazopyridines are important organic scaffolds that cover a wide range of biologically active compounds such as antiviral, anticancer, antihypertensive, antiparasitic, and antihypertensive agents (Dyminska, 2015). They have also been used as agonists for $GABA_A$ receptors (Langer & Arbilla, 1988), RAF inhibitors (Newhouse *et al.*, 2013), aromatase inhibitors (Dowsett *et al.*, 1994), and many other biological activities. They are found in different isomeric cores such imidazo[1,5-a]pyridines, imidazo[1,2-a]pyridines, imidazo[4,5-c]pyridines, and imidazo[4,5-b]pyridines. The most popular examples for the first two isomers are zolimidine (Parisio & Clementi, 1976) and miroprofen drugs (Mikashima & Goto, 1982).

Imidazo[4,5-b]pyridines have been closely examined as anticancer agents due to their effect on aurora kinases A and B, a phosphotransferase enzymes essential for chromosomes separation during the cellular division (Bavetsias *et al.*, 2007; Lan *et al.*, 2011). Similar to combretastatin A-4, imidazo[4,5-b]pyridines also possess anti-angiogenic influence on tumour vascular because of their inhibition effect on Januse Kinase 1(JAK-1), a group of protein kinases that are involved in angiogenesis process (Vasbinder *et al.*, 2016).

1.8 **E7010**

N-(2-((4-hydroxyphenyl)amino)pyridin-3-yl)-4-methoxybenzenesulfonamide **50** (figure 13) is a synthetic antimicrotubule that has gained an increasing interest since its discovery by (Koyanagi *et al.*, 1994). This anticancer sulphonamide administrated orally for more than one week as capsules provided in a daily dose of 25-100 µg/Kg and revealed high potency against 26 human cancer diseases (Yoshimatsu *et al.*, 1997) such as M5076 fibrosarcoma, P388 Leukaemia, Lewis lung carcinoma, colon 38 carcinoma, and human heterographt carcinoma, and many other cancer disease. Literatures have explored a wide range of analogues with different organic scaffold with the aim to enhance its pharmacological activity. These include (figure-14), arylsulfonyl indole-benzamide **44** (Lai *et al.*, 2019), quinazolines **47**, **48** (Li *et al.*, 2019), pyrimidino[2,1-b]quinazolin-6-on **45,** and imidazo[2,1-b]quinazolin-5-one **46** (Segaoula *et al.*, 2016), and styrylbenzenesulfonamides **49** (Mahesh *et al.*, 2017).

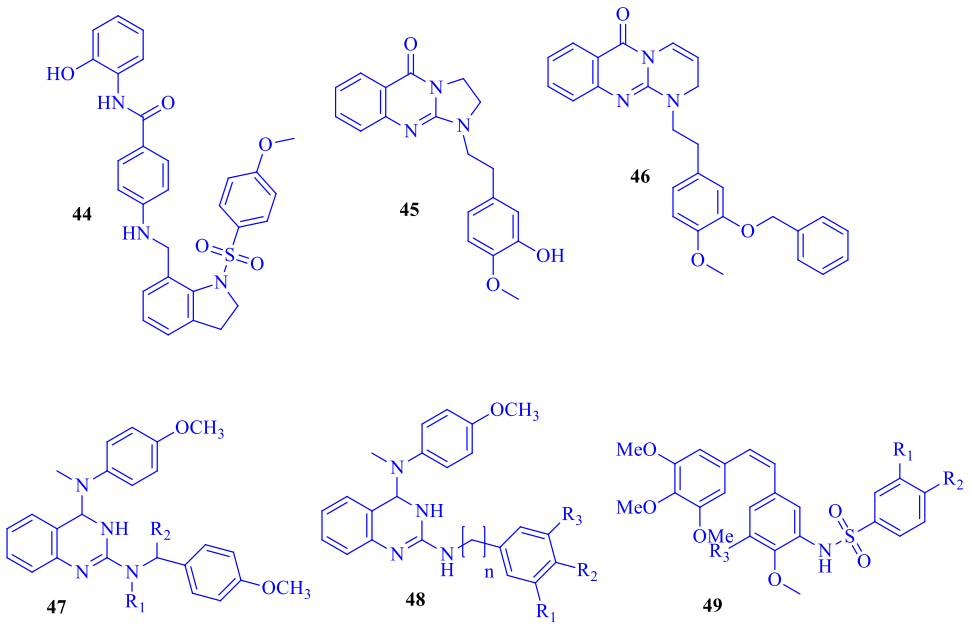

Figure 14: Structure of some E7010 analogues.

This study exploring the synthesis of E7010 analogues (figure-15) that have combretastatin A-4 pharmacophores of trimethoxy moiety aiming to enhance its biological activity.

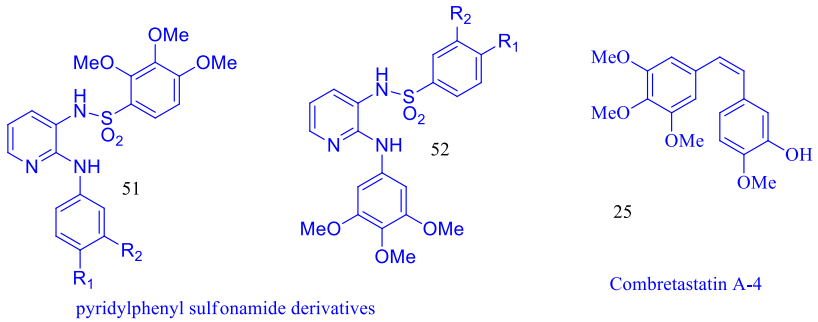

Figure 15: General structure of substituted pyridyl-phenyl sulphonamide as E7010 analogues and CA-4.

1.9 Aims of the project

The aim of this project is to develop Microtubule Targeting Agents (MTAs), which selectively damage rapidly proliferating endothelial cells by interaction with tubulin. These agents are heterocyclic compounds bearing a trimethoxy moiety which is an important motif for antimitotic behaviour and expected to increase the stability of a tubulin-drug linkage, and also work in a similar mechanism to combretastatin A-4 (**25)**.

1.10 Objectives

1- To modify the known antimitotic agent E7010 (50) (figure 13) with a trimethoxy moiety (structures 51, 52, figure15) by the reaction of substituted 2,3-diamino pyridines with substituted benzene sulphonyl chlorides.

2- To synthesise substituted imidazo[4,5, b]pyridines (structure 43, figure 13) as combretastatin A-4 (25) analogues.

3- To synthesise 5,6-diaryl-1,2,4-triazine-3(4H)-one derivatives (structure 59a, 59b figure 13).

4- To evaluate the cytotoxic activity of the synthesised compounds by the MTT assay.

5- To determine the mechanism of action for the most potent analogues through flow cytometric analysis (FACs).

Chapter 2

Synthesis of substituted 5,6-diaryl-1,2,4-triazine-3(4H)-one analogues

2 Synthesis of substituted 5,6-diaryl-1,2,4-triazine-3(4H)-one analogues.

2.1 Material and methods.

General:

The chemical lab work has been carried out at Salford university laboratories, and the products were characterized and identified by melting point, FT-IR, NMR, and mass spectrometry. Other chemicals and anhydrous solvents were obtained from Across Organic, Fisher, and Fluorochem. Anhydrous THF were obtained freshly through distilling commercial THF with benzophenone and sodium metal under an inert atmosphere.

Chromatography:

TLC (thin layer chromatography) was used to follow chemical reactions and determination of SiO_2 mixtures for column chromatography. A precoated, with fluorescent indicator F254, silica gel was used to carry out the TLCs, supported on aluminum plates (200µm, 60Å). The desired products were spotted and visualized by using UV254. The eluent mixtures were given as volumetric ratio of two solvents (v/v), and R_f values were recorded to the closest 0.01 decimal fractions. However, silica gel powder of 60Åpore size distribution and 40-63 µm was utilized for flash chromatography.

NMR SPECTRA

^{1}H- and ^{13}C- NMR

A Bruker AC-400 instrument was used to obtain ^{1}H-NMR spectra at 400MHz in deuterated solvents, $CDCl_3$ was used as a solvent (unless stated otherwise). ^{13}C- NMR spectra were measured using 100 MHz.

Chemical shifts (δH) values are presented in parts per million (ppm) with reference to tetramethyl silane (TMS), which is considered as the standard reference to be at (0) ppm. J- coupling values (coupling constant) are measured in frequency unit (Hertz, Hz), and recorded to 2 decimal points. Topspin software was used to analyse NMR spectra in according to the literature database (Pretsch, 2000; Silverstein *et al.*, 2014)

FT-IR

Bruker vector 22 instrument was used to measure FT-infrared spectra and transmittance peaks were recorded as wavenumbers in cm^{-1} unit.

Synthesis of substituted 5,6-diaryl-1,2,4-triazine analogues

Melting point

Gallenkamp apparatus was used to measure melting points for all synthesised compounds.

Mass spectrometry:

HRMS (high resolution mass spectrometry) was measured at:

1- EPSRC UK National Mass Spectrometry Facility (NMSF) at Swansea University.
2- Department of chemistry at MMU and Cambridge University.

HPLC:

An Agilent 1100 series instrument was used to separates triazine isomers.

Plate reader for MTT assay:

A Multiskan Ascent 354 microplate photometer was used to obtain the optical density of formazan at 570 nm.

Synthesis of substituted 5,6-diaryl-1,2,4-triazine analogues

2.2 Introduction:

Cancer research is a scientific field that has strategic priority for researchers, and especially chemists, to develop and design new compounds that have anti-tumour activity to overcome the disease of cancer.

Consequently, this project outlines the possibility of synthesizing new heterocyclic compounds of substituted 5,6-diaryl-1,2,4-triazine-3(4H)-one, pyridyl-phenyl sulfonamide and imidazopyridine derivatives as analogues of combretastatin A-4 and E7010. Synthesis was carried out through catalytic multistep reactions which involve preparation of intermediates to reach the final product.

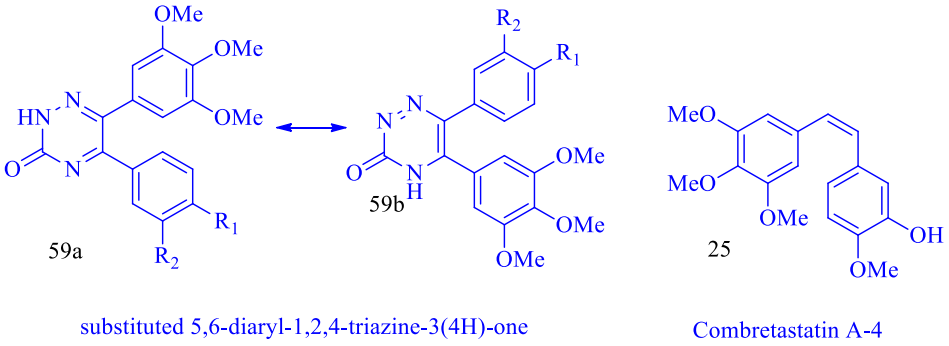

Figure 16: General structures of combretastatin A-4 and substituted 5,6-diaryl-1,2,4-triazine-3(4H)-one.

The aim is to replace the cis-double bond bridge of combretastatin-A4, which is considered metabolically unstable (Nathwani *et al.*, 2013; Tarade *et al.*, 2017), with a rigid six-member heterocyclic ring such as 1,2,4-triazine. The target analogue, 5,6-diaryl-1,2,4-triazine-3(2H)-one, has been synthesised using three chemical reactions, starting from the synthesis of substituted diarylalkynes by palladium-catalyzed cross-coupling reaction. The diarylalkynes were oxidized by DMSO as a source of oxygen and Pd as catalyst to produce substituted aromatic diketone derivatives. These ethane-dione (benzil) derivatives, which are considered as combretastatin A-4 analogues (Mousset *et al.*, 2008), were reacted with semicarbazide hydrochloride, to produce the required compounds as shown in scheme-1.

Synthesis of substituted 5,6-diaryl-1,2,4-triazine analogues

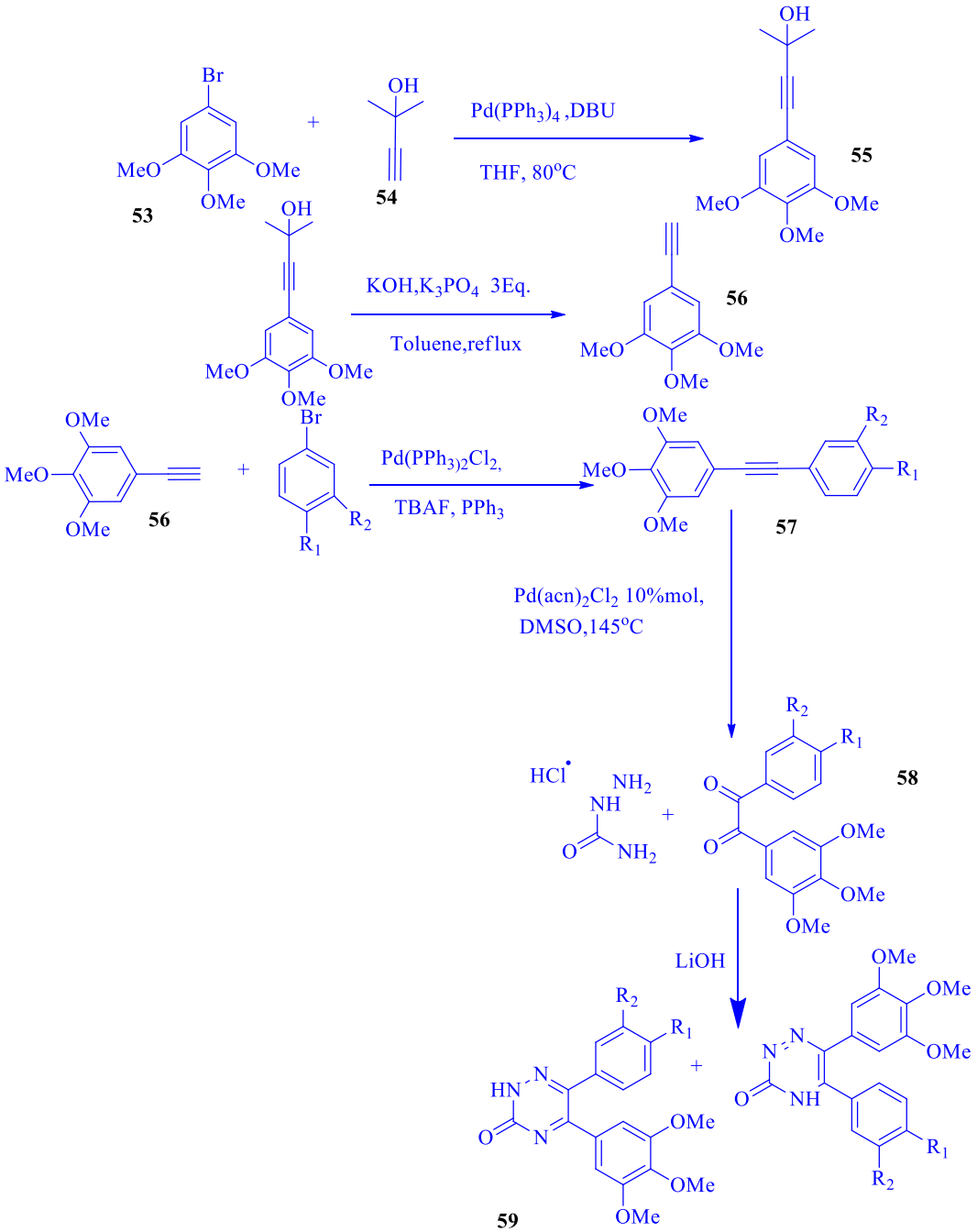

Scheme 1: Synthesis of Substituted 5,6-diaryl-1,2,4-triazine derivatives as combretastatin A-4 analogues.

Synthesis of substituted 5,6-diaryl-1,2,4-triazine analogues

2.3 General procedures and chemical experiments.

2-Methyl-4-(3,4,5-trimethoxyphenyl)but-3-yn-2-ol (**55**)

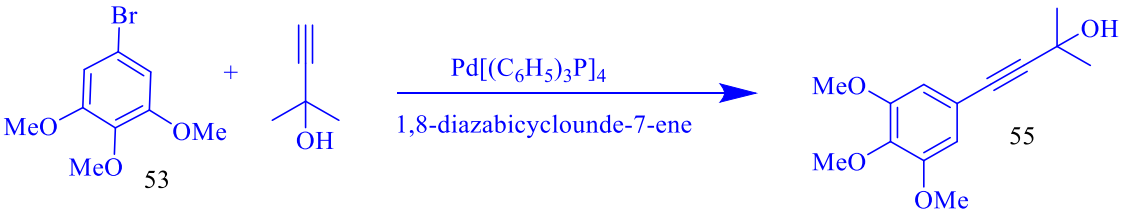

To a stirred solution of 5-bromo-1,2,3-trimethoxybenzene (0.5 g, 2 mmol., 1 eq.)in anhydrous THF (10 cm^3) was added tetrakis(triphenylphosphine) palladium (0) (34 mg, 6 mol %, 0.06 eq.), 1,8-diazabicyclounde-7-ene (0.89 cm^3, 6 mmol., 3eq.), and 2-methylbut-3-yn-2-ol (0.24 cm^3, 2.4 mmol., 1.4 eq.). The mixture was stirred at 80°C and monitored by TLC (hexane: ethyl acetate 6:4, R_f = 0.4). After the consumption of all starting material, the mixture was cooled to the room temperature, diluted with water (20 cm^3) and extracted with ethyl acetate (3×20 cm^3). The organic layer was washed with water and brine, dried over $MgSO_4$, and concentrated in vacuum. The crude product was purified by silica gel chromatography (SiO_2: hexane: ethyl acetate 7:3, R_f = 0.29). The above titled compound **55** was obtained as pale yellow solid (0.477 g, 1.90 mmol., 94%). MP =74-75°C. HRMS (ESI): calculated for $C_{14}H_{19}O_4$ (M+H) = 251.1283, found (M+H) = 251.1278, ΔMs=0.5ppm.

^{1}H NMR: δ (ppm)=1.60 [6 H, s, 2 x (CH_3)], 2.0 [1 H, s, OH], 3.85 [3 H, s, (OCH_3)], 3.90 [6 H, s, 2 x (OCH_3)], 6.60 [2 H, s, Ar-H].

^{13}C NMR: δ (ppm)=31.50 [2 x (CH_3)], 56.11[2 x (OCH_3)], 60.93[(OCH_3)], 65.58 [CHOH], 82.07 [C≡C], 92.87 [C≡C-OH], 108.85 [C-H, Ar-C-H *ortho* to methoxy], 117.75 [Ar-C- C≡C], 138,72 [C-O, Ar-C-OCH_3], 152.98 [C-O, 2 x Ar-C-OCH_3].

FT-IR : ν_{max} (cm^{-1}): 3514 (OH str.), 2981 (C-H str., aromatic), 2840 (C-H, Str., Aliphatic), 2220 (C≡C), 1507,1454 (C=C Str., aromatic), 1125 (C-O-CH_3, Asy. Str.).

5-Ethynyl-1,2,3-trimethoxybenzene (**56**)

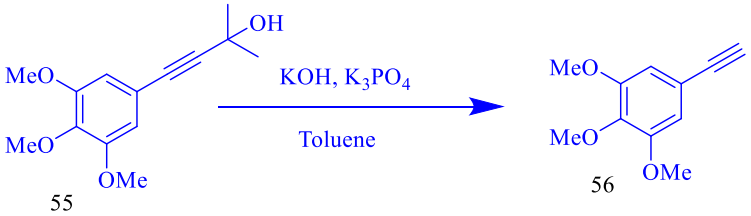

To a vigorously stirred solution of 2-methyl-4-(3,4,5-trimethoxyphenyl)but-3-yn-2-ol (1 g, 4 mmol.) in boiling anhydrous toluene (40 cm^3) under an argon atmosphere, was added

potassium hydroxide (0.224 g, 12 mmol., 3 eq.), and potassium phosphate (0.838 g, 12 mmol, 3 eq.) The reaction mixture was monitored by TLC until the complete conversion of the starting material (4-6 hour). The mixture was cooled to room temperature, filtered through a plug of Celite, and washed several times with toluene. The required product was obtained after evaporation of the solvent as a yellow thick oily liquid that solidified later to a brown solid. Further purification by column chromatography was necessary to obtain pure yellow crystalline solid, (SiO_2: hexane: ethyl acetate 8:2, R_f = 0.18), (0.636 g, 3.308 mmol., 83%, Mp = 73-74 °C, lit. Mp = 68-69 °C).

^{1}H NMR: δ (ppm)= 3.05 (1H, s, C≡CH), 3.85 [9 H, s, 3 x (OCH_3)], 6.75 [2H, s, ArH].

^{13}C NMR: δ(ppm) = 56.15 [2 x (OCH_3)], 60.96 [(OCH_3)], 76.23 [C≡CH terminal alkyne], 83.70 [(Ar-C≡C)], 109.33 [C-H, Ar-CH *ortho* to methoxy], 117.03[Ar-C- C≡C, 139.29 [C-O, Ar-C-OCH_3], 153.06 [C-O, 2 x Ar-C-OCH_3].

FT-IR: ν_{max} (cm^{-1}): 3243 (C-H str., alkyne), 2989 (C-H, Str., aromatic), 2939 (C-H, str., aliphatic), 2027 (C≡C str.), 1562 (C=C, Str., aromatic), 1125 (C-O-CH_3, asy. str.). Spectral data in accordance with the literature (Lawrence *et al.*, 1999).

2.3.1 Synthesis of substituted diarylalkyne through the Sonogashira reaction. **(Liang *et al.*, 2006)**:

To a stirred solution of aryl halide (2 mmol., 1 eq.), in dry THF (10 cm^3) was added 3,4,5-trimethoxyphenylethyne (56) (0.46 g, 2.4 mmol., 1.2 eq.), PPh_3 (47 mg, 0.180 mmol., 0.09 eq.), $Pd(PPh_3)_2Cl_2$ (84 mg, 0.120 mmol., 0.06 eq.), and tetrabutylammoniumfloride trihydrate (1.893 g, 6 mmol., 3 eq.). The mixture was heated at 80°C until the complete conversion of the starting material, cooled to room temperature, diluted with water (20 cm^3) and extracted with ethyl acetate (3×20 cm^3). The organic layer was washed with water, brine, dried over $MgSO_4$, and concentrated in vacuum. The residue was purified by flash column chromatography on silica gel.

Following the above procedure diarlalkynes (60-74) were synthesised.

2-Methoxy-5-(3,4,5-trimethoxyphenyl)ethynyl)benzaldehyde (60)

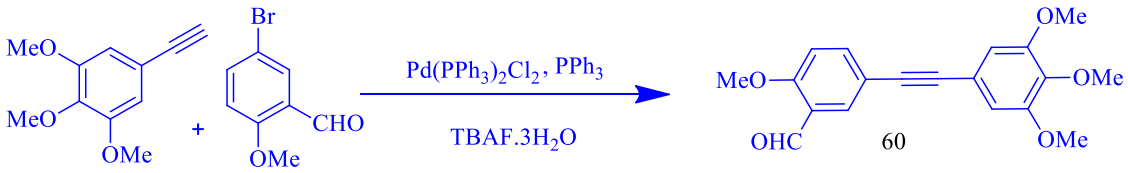

60

Synthesis of substituted 5,6-diaryl-1,2,4-triazine analogues

The above titled diarylalkyne was synthesised from 5-bromo-2-methoxybenzaldehyde (0.43 g, 2 mmol., 1eq.). and obtained as pale-yellow solid (0.501 g, 1.54 mmol., 77%, MP = 144-145 °C), after purification by flash column chromatography (SiO_2: Hexane: ethyl acetate, 7:3, R_f = 0.42). HRMS (ESI) calculated for $C_{19}H_{19}O_5(M+H)^+$ = 327.1227, found for (M+H) = 327.1228, ΔMs=0.1ppm.

^{1}H NMR: δ (ppm)= 3.89[3H, s, (OCH_3)], 3.90 [6 H, s, 2 x (OCH_3)], 3.98[3 H, s, (OCH_3)], 6.77 [2 H, s, Ar-H trimethoxy ring], 7.00 [1H, d, J = 8.68 Hz, Ar-H *meta* to carbonyl group], 7.70 [1 H, dd, J = 2.16 Hz, 8.64 Hz, Ar-H *para* to carbonyl group], 8.00 [1 H, d, J = 2.16 Hz, Ar-H *ortho* to carbonyl group], 10.46 [1 H, s, CHO].

^{13}C NMR : δ (ppm)= 55.89 [(OCH_3)], 56.16 [2 x (OCH_3)], 60.99 [(OCH_3)], 87.09 [Ar-C≡C)], 89.12 [Ar-C≡C)], 108.72 [C-H, Ar-CH *ortho* to methoxy (trimethoxy ring)], 111.93 [C-H, Ar-CH *meta* to carbonyl group], 115.89 [C-C, Ar-C-C≡C], 118.08 [C-C, Ar-C-C≡C], 124.78 [C-C, Ar-C-CHO], 131.97 [C-H, Ar-CH *ortho* to carbonyl group], 138.54 [C-H, Ar-CH *para* to carbonyl group], 138.88 [C-O, Ar-C-OCH_3], 153.12 [C-O, 2 x Ar-C-OCH_3], 161.40 [C-O, Ar-C-OCH_3], 188.94 [CHO].

FT-IR: ν_{max} (cm^{-1}): 3010, 2975 (C-H str., aromatic), 2924 (C-H str., aliphatic), 2227 (C≡C), 1684 (C=O str., aldehyde), 1574,1606(C=C str., aromatic), 1122 (C-O-CH_3, asym. str.) .

1,2,3-Trimethoxy-5-(phenylethynyl)benzene (61)

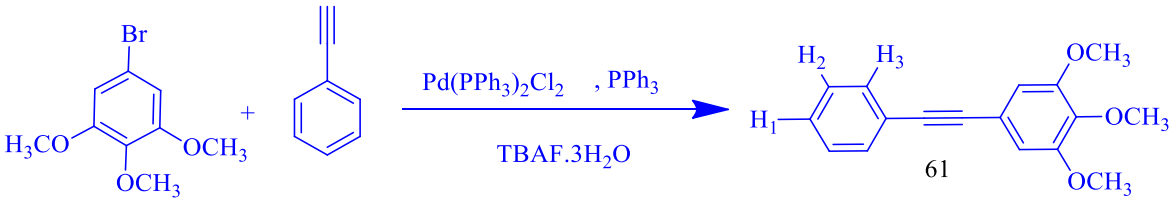

The above diarylalkyne was synthesised from 5-bromo-1,2,3-trimethoxybenzene (0.5 g, 2 mmol.) and phenylacetylene (0.26 cm^3, 2.4 mmol, 1.2 eq.), and obtained as brown crystalline solid (0.441 g, 1.64 mmol., 82%), after purification by column chromatography (SiO_2: Hexane: ethyl acetate 9:1, R_f = 0.36), MP = 74-75°C (lit. Mp = 75.5-77°C, (Hadfield & McGown, 1998).

^{1}H NMR: δ(ppm) = 3.80[3 H, s, (OCH_3)], 3.85 [6 H, s, 2 x (OCH_3)], 6.80 [2 H, s, Ar-H *ortho* to MeO], 7.35 (3 H, m, Ar-H), 7.55 [2 H, dd, J = 3.90 Hz, 1.90 Hz, Ar-H].

^{13}C NMR : δ(ppm) = 56.17 [2 x (OCH_3)], 61.00 [(OCH_3)], 88.49 [(C≡C)], 89.42 [(C≡C)], 108.82 [C-H, Ar-C-H, *ortho* to methoxy (trimethoxy ring)], 118.28 [C-C, Ar-C-C≡C],

123.16 [C-C, Ar-C-C≡C], 128.28 [C-H, Ar-CH1], 128.38 [2 x C-H, Ar-C-H2], 131.56 [2 x C-H, Ar-C-H3], 138.86 [C-O, Ar-C-OCH_3], 153.11 [C-O, 2 x Ar-C-OCH_3].

FT-IR : ν_{max} (cm^{-1}): 2973 (C-H, str., aromatic), 2837 (C-H, str., aliphatic), 1502, 1453 (C=C, str., aromatic), 1125 (C-O-CH_3, asy. Str.).

Spectral and physical data in accordance with literature (Hadfield & McGown, 1998).

2-Methoxy-5-((3,4,5-trimethoxyphenyl)ethynyl)benzonitrile (62)

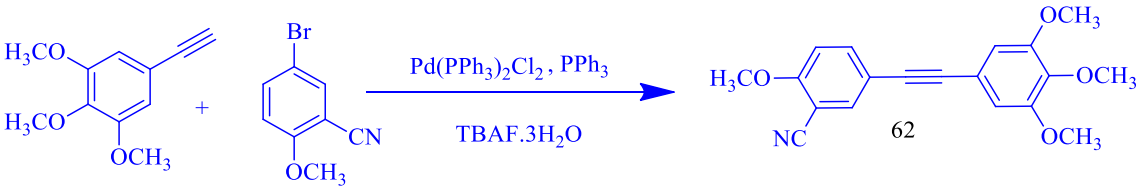

Using 5-bromo-2-methoxybenzonitrile (0.5 g, 2 mmol.) the above diarylalkyne (**62**) was obtained as yellow solid (0.629 g, 1.94 mmol., 97%), after purification by column chromatography (Hexane: ethyl acetate 7:3, R_f = 0.36) MP 133-135 °C. HRMS (ESI): calculated for $C_{19}H_{18}NO_4$ (M+H) = 324.1235, found (M+H)=324.1231, ΔMs= 0.4ppm.

^{1}H NMR :δ (ppm)= 3.8[3 H, s, (OCH_3)], 3.85 [6 H, s, 2 x (OCH_3)], 3.98 (3 H, s, CH_3O), 6.77 [2 H, s, Ar-H, trimethoxy ring], 6.97 (1H, d, J = 8.95 Hz, Ar-H *meta* to CN group), 7.69 [1H, dd, J = 1.77 Hz, 8.95 Hz, Ar-H *para* to CN group], 7.74 (1H, d, J = 1.77Hz, Ar-H *ortho* to CN group).

^{13}C NMR: δ (ppm) = 56.18 [2 x (OCH_3)], 56.29 [(OCH_3)], 61.00 [(OCH_3)], 88.49 [(C≡C)], 89.42 [(C≡C)], 102.37 [C≡N], 108.76 [C-H, Ar-CH ortho to methoxy (trimethoxy ring)], 111.56 [C-H, Ar-CH *meta* to CN group], 115.60 [C-C, Ar-C-C≡N], 116.26 [C-C, Ar-C- C≡C], 117.63 [C-C, Ar-C-C≡C], 136.65 [C-H, Ar-CH *ortho* to CN group], 139.09 [C-H, Ar-CH *para* to CN group], 139.09 [C-O, Ar-C-OCH_3], 153.36 [C-O, 2 x Ar-C-OCH_3], 160.74 [C-O, Ar-C-OCH_3].

FT-IR: ν_{max} (cm^{-1}): 3052, 2997 (C-H str., aromatic), 2940 (C-H str., aliphatic), 2226 (C≡N), 1570 (C=C str., aromatic), 1122 (C-OCH_3 asy.str.) .

2-Methoxy-5-((3,4,5-trimethoxyphenyl)ethynyl)aniline (**63**)

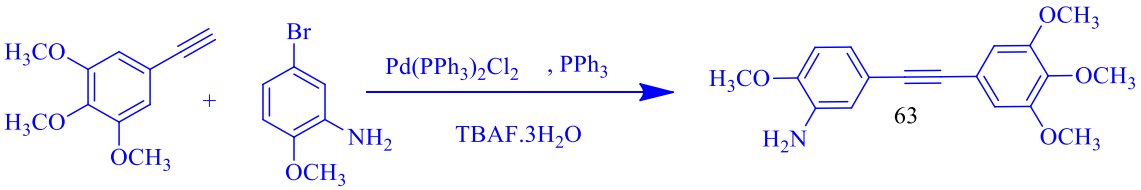

Synthesis of substituted 5,6-diaryl-1,2,4-triazine analogues

Using 5-bromo-2-methoxyaniline (0.404 g, 2 mmol.) the above diarlyalkyne (**63**) was obtained as brownish yellow crystalline solid (0.358 g, 1.14 mmol., 57%), TLC (hexane: ethyl acetate 6:4, R_f = 0.46), chromatography (SiO_2: hexane: ethyl acetate 8:2) MP = 78-89 °C (lit. Mp= 96.29 °C (Lara-Ochoa & Espinosa-Pérez, 2007)).

^{1}H NMR: δ (ppm) = 3.88[3 H, s, (OCH_3)], 3.87[9 H, s, 3 x (OCH_3)], 3.7 [2 H, s, NH_2], 6.76[3H, (1H, d, J = 8.2 Hz Ar-H *meta* to amine group), (2 H, s, Ar-H trimethoxy ring], 6.90[1H, d, J = 2.0 Hz, Ar-H *ortho* to NH_2 group], 6.95[1H, dd, J = 2.04 Hz, 8.24 Hz, Ar-H *para* to NH_2 group].

^{13}C NMR : δ(ppm) =55.50[(OCH_3)], 56.12 [2 x (OCH_3)], 6O.98 [(OCH_3)], 87.44 [(C≡C)], 88.96 [(C≡C)], 108.62 [C-H, Ar-CH ortho to methoxy (trimethoxy ring)], 110.16[C-H, Ar-C-H *meta* to NH_2 group], 115.35 [C-C, Ar-C-C≡C], 117.63 [C-H, Ar-CH *ortho* to NH_2 group], 117.76 [C-C, Ar-C-C≡C], 122.62 [C-H, Ar-CH *para* to NH_2 group], 135.90 [C-N, Ar-C-N], 138.47 [C-O, Ar-C-OCH_3], 147.72 [C-O, Ar-C-OCH_3, *ortho* to NH_2], 153.04 [C-O, 2 x Ar-C-OCH_3].

FT-IR: ν_{max} (cm^{-1}): 3483, 3383 (N-H_2 Str.), 2933 (C-H str., aromatic), 2837 (C-H str., aliphatic), 2199 (C≡C str., aromatic), 1606 (N-H bend.), 1505 (C=C str., aromatic), 1126 (C-OCH_3 asy. str.).

2-Methyl-5-((3,4,5-trimethoxyphenyl)ethynyl)phenol (64)

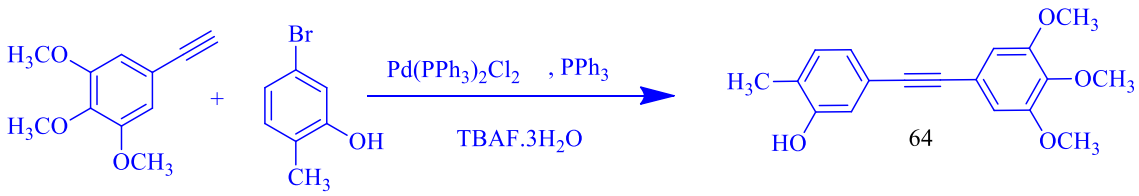

64

Using 5-bromo-2-methylphenol (0.374 g, 2 mmol.) the above diarylalkyne (**64**) was obtained as brownish yellow crystalline solid (0.255 g, 0.854 mmol., 43%), purified by column chromatography (SiO_2: hexane: ethyl acetate 8:2, TLC hexane: ethyl acetate 6:4, R_f = 0.36), MP 124-125 °C. HRMS (ESI) calculated for $C_{18}H_{19}O_4$ (M+H) = 299.1283, found for (M+H) = 299.1279, ΔMs=0.4 ppm.

^{1}H NMR:δ (ppm) = 2.24 [3H, s, CH_3], 3.85 [3H, s, OCH_3], 3.86 [6H, s, 2x(OCH_3)], 4.69 [1H, s, OH], 6.73 [2H, s, Ar-H trimethoxy ring], 6.91[1H, d, J =1.28 Hz, Ar-H *ortho* to OH], 7.0 [1H, dd, J =1.31 Hz, 7.74 Hz, Ar-H *para* to OH], 7.08 [1H, d, J =7.76 Hz, Ar-H *meta* to OH].

^{13}C NMR: δ (ppm) = 15.85 [CH_3], 56.16 [2 x (OCH_3)], 61.02 [(OCH_3)], 88.38 [C≡C], 88.66 [C≡C], 108.76 [C-H, Ar-C-H *ortho* to methoxy], 117.64 [C-H, Ar-C-H *meta* to OH], 118.34 [C-C, Ar-C-C≡C], 121.56 [C-C, Ar-C-C≡C], 124.14 [Ar-CH *ortho* to OH], 124.99 [C-C, Ar-C-CH_3], 131.02 [C-H, Ar-C-H *para* to OH], 138.65 [C-O, Ar-C-OCH_3], 153.09 [C-O , 2 x Ar-C-OCH_3], 153.65 [C-O, Ar-C-OH].

FT-IR: ν_{max} (cm^{-1}): 3350 (O-H str.), 3014, 2997 (C-H str., aromatic), 2940 (C-H str. aliphatic), 1582 (C=C str., aromatic), 1230 (C-O-CH_3, asy. str.).

2-Methoxy-5-((3,4,5-trimethoxyphenyl)ethynyl)phenol (65):

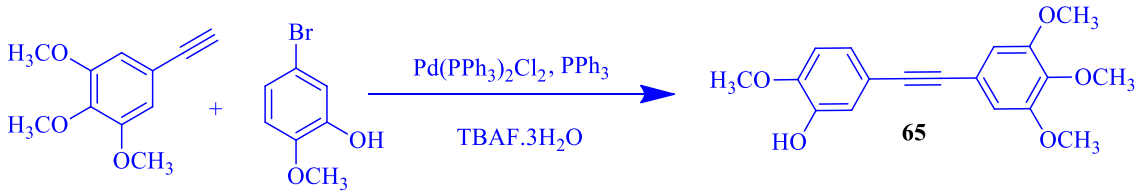

Using 5-bromo-2-methoxypenol (0.406 g, 2 mmol.) the above diarylalkyne (**65**) was obtained as light brown solid (0.134 g, 0.426 mmol., 42%), Mp 96-97°C (lit. Mp = 96-98°C (Lawrence *et al.*, 1999)). After purification by column chromatography (SiO_2: hexane: ethyl acetate 8:2, TLC hexane: ethyl acetate 6:4, R_f=0.42).

^{1}H NMR:δ(ppm)= 3.84 [3 H, s, (OCH_3)], 3.85 [6 H, s, 2x(OCH_3)], 3.89 [3 H, s, (OCH_3)], 5.62 (I H, s, OH), 6.73 [2 H, s, Ar-H trimethoxy ring), 6.78 (1 H, d, J =8.37 Hz, Ar-H *meta* to OH), 7.02(1 H, dd, J =1.96 Hz, 8.37 Hz, Ar-H *para* to OH), 7.06 (1H, d, J =1.96Hz, Ar-H *ortho* to OH).

^{13}C NMR:δ (ppm)= 55.94 [CH3O], 56.14 [2 x (CH3O)], 60.98 [CH3O], 87.89 [C≡C], 88.41 [C≡C], 108.67 [C-H, Ar-C-H *ortho* to methoxy (trimethoxy ring)], 110.49 [C-H, Ar-CH *meta* to OH], 115.97 [C-C, Ar-C-C≡C], 117.50 [C-H, Ar-C-H *ortho* to OH], 118.53 [C-C, Ar-C-C≡C], 124.22 [C-H, Ar-C-H *para* to OH], 138.60 [C-O, Ar-C-OCH_3], 145.36 [C-O, Ar-C-OCH_3], 147.02 [C-O, Ar-C-OH], 153.06 [C-O, 2 x Ar-C-OCH_3].

FT-IR: ν_{max} (cm^{-1}): 3533 (O-H str.), 3014, 2997 (C-H str., aromatic), 2936 (C-H str., aliphatic), 1582 (C=C str., aromatic), 1232 (C-OCH_3, asy. str.)

Spectral data identical with literature (Lawrence *et al.*, 1999).

Synthesis of substituted 5,6-diaryl-1,2,4-triazine analogues

2-Methoxy-5-((3,4,5-trimethoxyphenyl)ethynyl)nitrobenzene (**66**)

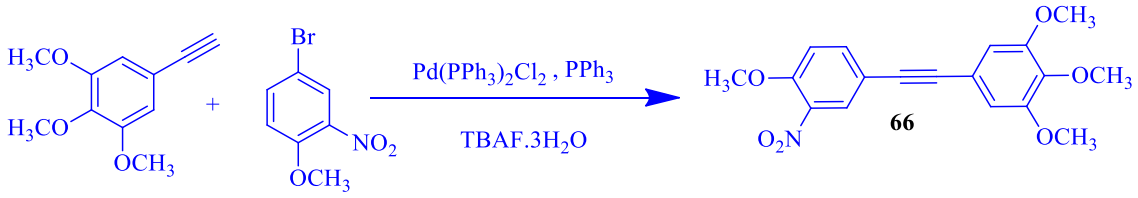

Using 4-bromo-2-nitroanisole (0.406 g, 2 mmol.) the above diarylalkyne (**66)** was obtained as a light green solid (0.56 g, 1.62 mmol., 82%), Mp 132-133°C. After purification by column chromatography (SiO_2: hexane: ethyl acetate 8:2, TLC hexane: ethyl acetate 6:4, R_f=0.38).

HRMS (ESI) calculated for $C_{18}H_{18}O_6N_1$ $(M+H)^+$ =344.1129, found for (M+H)= 344.1130 $C_{18}H_{18}O_6N_1$, ΔMs=0.1ppm.

^{1}H NMR:δ (ppm) = 3.88 [3 H, s, (OCH_3)], 3.89 [6 H, s, 2 x (OCH_3)], 3.99 [3 H, s, (OCH_3)], 6.76 [2 H, s, Ar-H trimethoxy ring], 7.06 [1H, d, J = 8.76 Hz, Ar-H *meta* to NO_2 group], 7.67 [1H, dd, J = 8.76 Hz, 2.12 Hz, Ar-H *para* to NO_2 group], 8.01 [1H, d, J= 2.09 Hz, Ar-H *ortho* to NO_2 group].

^{13}C NMR:δ (ppm) = 56.18 [2 x (OCH_3)], 56.69 [(OCH_3)], 60.01 [(OCH_3)], 85.83 (C≡C), 90.14 (C≡C), 108.79 [C-H, Ar-C-H *ortho* to methoxy (trimethoxy ring)], 113.61 [C-H, Ar-C-H *meta* to NO_2 group], 115.78 [C-C, Ar-C-C≡C], 117.53 [C-C, Ar-C-C≡C], 128.71 [C-H, Ar-C-H *ortho* to NO_2], 136.94 [C-H, Ar-C-H *para* to NO_2], 139.15 [C-O, Ar-C-OCH_3], 139.44 [C-N, Ar-C-NO_2], 152.64 [C-O, Ar-C-OCH_3], 153.17 [C-O, 2 x Ar-C-OCH_3],

FT-IR: ν_{max} (cm^{-1}): 3028, 2980 (C-H str., aromatic), 1576 (asy. str. N=O), 1338 (sym. str. N=O), 1576 (C=C str., aromatic), 1233 (C-OCH_3, asy. str.).

2-Methyl-5-((3,4,5-trimethoxyphenyl)ethynyl)aniline (**67**);

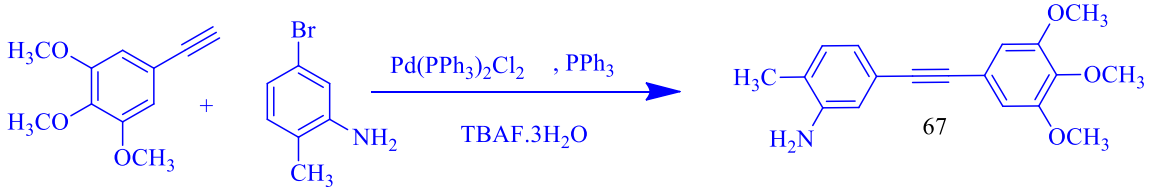

Using 5-bromo-2-methylaniline (0.372 g, 2 mmol.) the above diarylalkyne (**67**) was obtained as light brown solid (0.410 g, 1.37 mmol., 69%), after purification by column chromatography (hexane: ethyl acetate, 7:3, R_f = 0.25). MP 90-91°C. HRMS (ESI): calculated for $C_{18}H_{20}O_3N_1$ (M+H) =298.1443, fond for (M+H) =298.1438, ΔMs=0.5ppm.

^{1}H NMR: δ (ppm) = 2.16 [3 H, s, CH_3], 3.61[2 H, s, NH_2], 3.84 [3 H, s, (OCH_3), 3.85 [6H, s, 2 x (OCH_3)], 6.73 [2 H, s, Ar-H trimethoxy ring], 6.83 [1H, d, J =1.34 Hz, Ar-H *ortho* to NH_2), 6.86 [1H, dd, J =7.74 Hz 1.34 Hz, Ar-H *para* to NH_2), 7.01 [1H, d, J = 7.74 Hz, Ar-H *meta* to NH_2).

^{13}C NMR : δ (ppm) = 17.40 [(CH_3)], 56.13 [(OCH_3)], 60.98 [(OCH_3)], 88.21 (C≡C), 88.91 (C≡C), 108.72 [C-H, Ar-C-H *ortho* to methoxy), 117.51 [C-H, Ar-C-H *meta* to NH_2], 118.58 [C-C, Ar-C-C≡C], 121.35 [C-C, Ar-C-C≡C], 122.09 [C-H, Ar-C-H *ortho* to NH_2], 123.13 [C-C, Ar-C-CH_3], 130.48 [C-H, Ar-C-H *para* to NH_2), 138.61 [C-N, Ar-C-N], 144.45 [C-O, Ar-C-OCH_3], 153.05 [C-O, 2 x Ar-C-OCH_3].

FT-IR: ν_{max} (cm^{-1}): 3473, 3360 (N-H str.), 2936.25 (C-H str., aromatic), 2837 (C-H str., aliphatic), 1622 (N-H bend.) 1574, 1505 (C=C str., aromatic), 1126 (C-OCH_3, asy. str.).

5-((3-Fluoro-4-methylphenyl)ethynyl)-1,2,3-trimethoxybenzene (**68**):

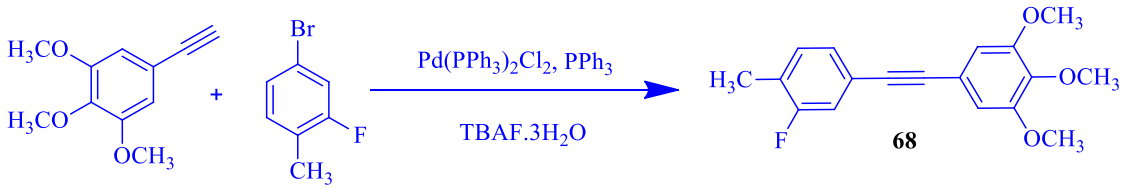

Using 4-bromo-2-flourotoluene (0.252 cm^3, 2 mmol.), the above diarylalkyne (**68**) was obtained as yellow solid (0.525 g, 1.74 mmol., 88%, Mp 126-128°C), after purification by column chromatography (hexane : ethyl acetate 8:2), TLC (hexane : ethyl acetate 6:4, R_f = 0.42). HRMS (ESI): calculated for $C_{18}H_{18}F_1O_3$ (M+H) = 301.1239, found for (M+H) =301.1234, ΔMs=0.5ppm.

^{1}H NMR: δ (ppm) = 2.31 [3 H, d, J =1.44 Hz, (CH_3)], 3.80 [3 H, s, (OCH_3)], 3.81 [6 H, s, 2 x (OCH_3)], 6.69 [2 H, s, Ar-H *ortho* to methoxy], 7.06 -7.12 [3 H, m, Ar-H].

^{13}C NMR: δ (ppm) = 14.61[(CH_3), d, J = 3.46 Hz,], 56.17 [C-O, 2 x (OCH_3)], 61.01 [(OCH_3)], 87.45 [(C≡C), d, J = 3.06 Hz,], 89.48 [(C≡C)], 108.80 [C-H, Ar-C-H trimethoxy ring], 117.78 [C-H, d, J=23.75 Hz, Ar-C-H *ortho* to F], 118.02 [C-C, Ar-C-C trimethoxy ring], 122.07 [1C, d, J= 9.60 Hz, (Ar-C-C)], 125.57[1C, d, J=17.13 Hz, Ar-C-CH_3], 127.17 [C-C, d, J=3.13 Hz, Ar-C-H *para* to F], 131.39 [C-H, d, J = 5.68 Hz, Ar-C-H *metta* to F], 138.94 [C-O, Ar-C-OCH_3], 153.12 [C-O, 2 x Ar-C-OCH_3], 159.60 (C-F, d, J = 245.45 Hz, Ar-C-F).

Synthesis of substituted 5,6-diaryl-1,2,4-triazine analogues

FT-IR: ν_{max} (cm^{-1}): 2994 (C-H str., aromatic), 2824 (C-H str., aliphatic), 1510 (C=C str. aromatic), 1127 (asy. Str. C-OCH_3).

5-((3-Acetyl-4-methoxylphenyl)ethynyl)-1,2,3-trimethoxybenzene (**69**)

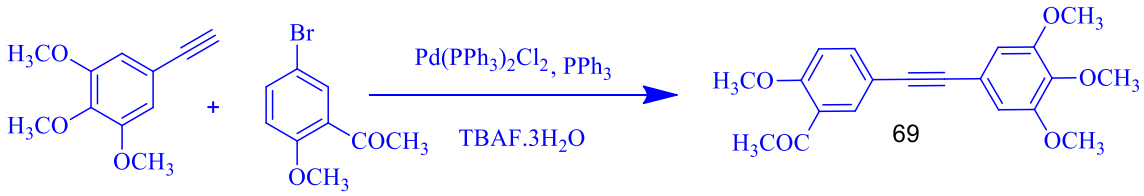

Using 5-bromo-2-methoxyacetophenone (0.458 g, 2 mmol.), the above diarylalkyne (**69)** was obtained as white solid the reaction was monitored by TLC (hexane: ethyl acetate 6:4, Rf = 0.42) column chromatography (hexane: ethyl acetate 8:2) was used to obtain the compound as solid (0.595 g, 1.74 mmol., 88%, Mp 92-94 ^oC). HRMS (ESI): calculated for $C_{20}H_{21}O_5$ $(M+H)^+$ = 341.1389, found (M+H) = 341.1383, ΔMs=0.6ppm.

^{1}H NMR: δ (ppm) = 2.63 [3 H, CH_3], 3.88 [9 H, s, 3 x (OCH_3)], 3.95 [3 H, s, OCH_3], 6.67 [2 H, s, Ar-H trimethoxy ring], 6.95 [1H, d, J = 8.69 Hz, Ar-H *meta* to acetyl group], 7.6 [1H, dd, J = 8.6 Hz, 2.24 Hz, Ar-H *para* to acetyl group], 7.92 [1H, d, J = 2.24 Hz, Ar-H *ortho* to $COCH_3$ group].

^{13}C NMR: δ (ppm) = 31.79 [CH_3], 55.73 [(OCH_3)], 56.15 [2 x (OCH_3)], 60.98 [(OCH_3)], 87.44 [(C≡C)], 88.86 [(C≡C)], 108.66[C-H, Ar-CH ortho to methoxy (trimethoxy ring)], 118.82 [C-H, Ar-CH *meta* to acetyl group], 115.61[C-C, Ar-C-C≡C], 118.25 [C-C, Ar-C-C≡C], 128.27 [C-C, Ar-C-$COCH_3$], 133.84 [C-H, Ar-CH *ortho* to acetyl group], 136.39 [C-H, Ar-CH *para* to acetyl group], 138.75 [C-O, Ar-C-OCH_3], 153.13 [C-O, 2 x Ar-C-OCH_3], 158.64 [C-O, Ar-C-OCH_3], 198.88 [C=O].

FT-IR: ν_{max} (cm^{-1}): 2945 (C-H str. aromatic), 2836 (C-H str., aliphatic), 1660 (str. C=O), 1576 (C=C, aromatic), 1122 (asy. Str. C-O-CH_3).

5-((3-Methyl-4-methoxylphenyl)ethynyl)-1,2,3-trimethoxybenzene (**70**)

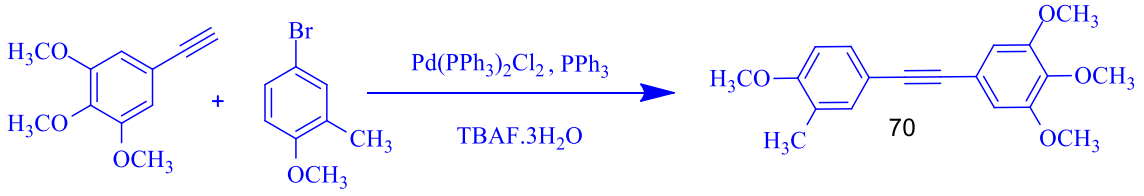

Using 5-bromo-2-methoxyacetophenone (0.458 g, 2 mmol.), the above title compound (**70)** was obtained as white solid (0.489 g, 1.56 mmol., 79%, Mp 122-124 ^oC), after purification by column chromatography (hexane: ethyl acetate 8:2, TLC (hexane: ethyl

acetate 6:4, R_f = 0.56). HRMS (ESI): calculated for $C_{19}H_{21}O_4$ (M+H) = 313.1439, found for (M+H) = 313.1433, ΔMs=0.6ppm.

^{1}H NMR: δ (ppm) = 2.19 [3H, s, (CH_3)], 3.67 [3H, s, (OCH_3)], 3.84 [9H, 2s, 3 x (OCH_3)], 6.73 [2H, s, Ar-H trimethoxy ring], 6.75 [1H, d, J = 8.61 Hz, Ar-H *meta* to CH_3, 7.3 [1H, d, J = 2.15 Hz, Ar-H *ortho* to CH_3], 7.32 [1H, dd, J = 8.61 Hz, 2.15 Hz, Ar-H *para* to CH_3].

^{13}C NMR : δ(ppm) = 16.07 [CH_3], 55.34 [(OCH_3)], 56.12 [2 x (OCH_3)], 60.97 [(OCH_3)], 87.75 (C≡C), 88.78 (C≡C), 108.59 [C-H, Ar-CH ortho to methoxy (trimethoxy ring)], 109.80 [C-H, Ar-CH *meta* to CH_3], 114.64 [C-C, Ar-C-C≡C], 118.78 [C-C, Ar-C-C≡C], 126.86 [C-C, Ar-C-CH_3], 130.51 [C-H, Ar-CH *ortho* to CH_3], 133.77 [C-H, Ar-CH *para* to CH_3], 138.48 [C-O, Ar-C-OCH_3], 153.06 [C-O, 2 x Ar-C-OCH_3], 157.96 [C-O, Ar-C-OCH_3].

FT-IR: ν_{max} (cm^{-1}): 2932 (C-H str. aromatic), 2833 (C-H str., aliphatic), 1573 (C=C aromatic), 1128 (C-O-CH_3 asy. str.).

5-((4-Cyano-3-hydroxyoxylphenyl) ethynyl)-1,2,3-trimethoxybenzene (**71**):

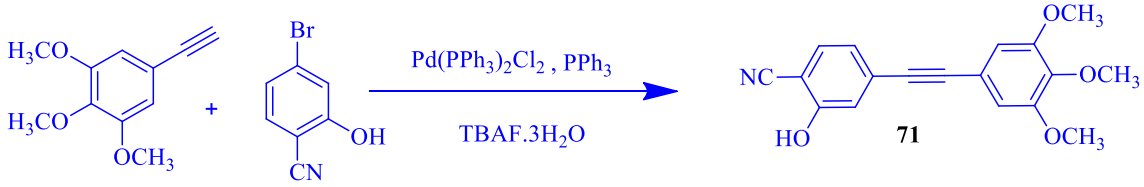

71

Using 5-bromo-2-hydroxybenzonitrile (0.458 g, 2 mmol.), the above diarylalkyne (**71**) was obtained as a yellow solid (0.498 g, 1.61 mmol., 81%, Mp =164-167 ^oC), after purification by column chromatography (hexane: ethyl acetate 8:2, TLC hexane: ethyl acetate 6:4, R_f=0.42). HRMS (ESI): calculated for $C_{18}H_{16}NO_4$ (M+H) =310.1079, found for (M+H) = 310.1074, ΔMs=0.5ppm.

^{1}H NMR: δ (ppm) = 3.85 [9 H, 2 x s, 3 x (OCH_3)], 6.48 [1H, s, OH], 6.75 [2 H, s, Ar-H trimethoxy ring], 7.09 [2 H, m, Ar-H *ortho* and *para* to OH], 7.44 [1H, d, J= 7.88, Ar-H *meta* to OH].

^{13}C NMR :δ (ppm) = 56.22 [2 x (OCH_3)], 61.08 [(OCH_3)], 86.80 [C≡C], 93.61 [C≡C], 99.30 [C≡N], 109.05 [C-H, Ar-CH *ortho* to methoxy], 115.97 [C-C, Ar-C-C≡C], 117.19 [C-C, Ar-C-C≡C], 119.10 [C-H, Ar-CH *meta* to OH], 124.18 [C-H, Ar-CH *ortho* to OH], 129.77 [Ar-C-C≡N], 132.66 [C-H, Ar-CH para to OH], 139.44 [C-O, Ar-C-OCH_3], 153.18 [C-O, Ar-C-OCH_3], 157.05 [C-O, Ar-C-OH].

Synthesis of substituted 5,6-diaryl-1,2,4-triazine analogues

FT-IR: ν_{max} (cm^{-1}): 3285 (OH Str.), 2942 (C-H Str. aromatic), 2839 (C-H Str., aliphatic), 2235 (C≡N str.), 2204 (C≡C str.), 1611 (C=C str., aromatic), 1122 (C-O-CH_3 asy. Str).

2-Amino-4-((3,4,5-trimethoxyphenyl)ethynyl)benzonitrile (72)

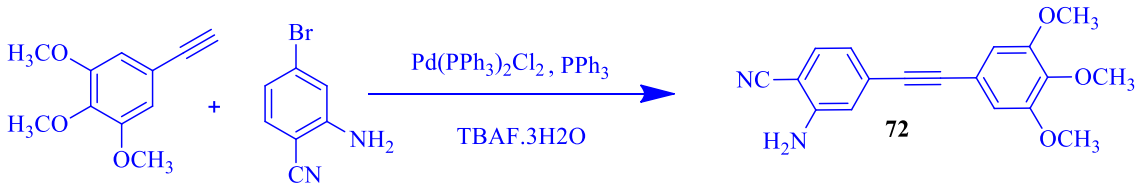

Using 2-amino-4-bromobenzonitrile (0.394 g, 2 mmol.). The above diarylalkyne (**72)** was obtained as a pale-yellow crystalline solid (0.5 g, 1.62 mmol., 81%, Mp 154-155°C), after purification by column chromatography (hexane: ethyl acetate 8:2, TLC hexane: ethyl acetate 6:4, R_f = 0.64). HRMS (ESI): calculated for $C_{18}H_{16}N_2O_3$ $(M)^+$ =309.1234, found $(M)^+$= 309.1236, ΔMs=0.2ppm.

^{1}H NMR: δ (ppm) =3.90 [11H, s, (9 H, s, 3 x (OCH_3), (2 H, NH_2)], 6.78 [2 H, s, Ar-H trimethoxy ring], 6.89 [2 H, m, Ar-H], 7.37 [1H, d, J= 7.87 Hz, Ar-H *meta* to NH_2].

^{13}C NMR: δ (ppm) = 56.20 [2 x (OCH_3)], 61.02 [(OCH_3)], 87.32 (C≡C), 92.62 (C≡C), 95.61 [C≡N], 109.26[C-H, Ar-CH *ortho* to methoxy], 117,36 [C-C, Ar-C-C≡C), 117.64 [C-H, Ar-C-H *ortho* to NH_2], 121.14 [C-H, Ar-CH *para* to NH_2], 128.94 [C-C, Ar-C-C≡C], 132.39 [C-H, Ar-CH *meta* to NH_2], 139.39 [C-O, Ar-C-OCH_3], 149.29 [C-C, Ar-C- C≡N), 153.16 [C-O, 2 x Ar-C-OCH_3].

FT-IR: ν_{max} cm^{-1}: 3446.63, 3354.41 (N-H_2 str), 2937.12 (C-H str., aromatic), 2841.18 (C-H str., aliphatic), 2116.29 (C≡N str.), 1638.65 (N-H bend.), 1575.10-1552.66 (C=C str., aromatic), 1129.76 (C-OCH_3 asy. str.).

2-Methyl-4-((3,4,5-trimethoxyphenyl)ethynyl)benzonitrile (73):

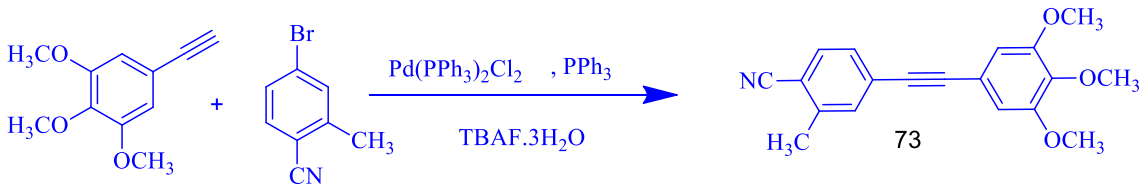

Using 4-bromo-2-methylbenzonitrile (0.394 g, 2 mmol.) the above diarylalkyne (**73**) was procured as a pale-yellow crystalline solid (0.5 g, 1.62 mmol., 82%, Mp = 150-151°C), after purification by column chromatography (hexane: ethyl acetate 8:2, TLC, hexane: ethyl acetate 6:4, R_f =0.46). HRMS (ESI): calculated for $C_{19}H_{18}NO_3$ $(M+H)^+$= 308.1286, found for (M+H) = 308.1281, ΔMs=0.5ppm.

Synthesis of substituted 5,6-diaryl-1,2,4-triazine analogues

^{1}H NMR: δ (ppm) = 2.56 [3 H, (CH_3)], 3.89 [9 H, s, 3 x (CH_3O)], 6.79 [2 H, s, Ar-H trimethoxy ring], 7.40 [1H, dd, J= 8.01 Hz, 1.01 Hz, Ar-H *para* to CH_3], 7.48 [1H, d, J= 1.01 Hz, Ar-H ortho to CH_3), 7.57 [1H, d, J= 8.01 Hz, Ar-H *meta* to CH_3].

^{13}C NMR: δ(ppm) = 20.34 [CH_3], 56.19 [2 x (OCH_3)], 61.01[(OCH_3)], 87.11 [C≡C], 93.34 [C≡C], 108.99 [C-H, Ar-CH ortho to methoxy], 112.00 [C≡N], 117.27 [C-C, Ar-C-C≡C], 117.85 [C-C, Ar-C-C≡C], 127.86 [C-C, Ar-C-CH_3], 129.13 [C-H, Ar-CH meta to CH_3], 132.40 [C-H, Ar-CH *ortho* to CH_3], 132.98 [C-H, Ar-C-H para to CH_3], 141.95 [C-O, Ar-C-OCH_3], 157.96 [C-O, 2 x Ar-C-OCH_3].

FT-IR: ν_{max} (cm^{-1}): 2948 (C-H str., aromatic), 2841 (C-H str., aliphatic), 2203 (C≡N str.), 1603, 1577 (C=C str., aromatic), 1125 (C-O methoxy).

2-Fluoro-4-((3,4,5-trimethoxyphenyl)ethynyl)benzonitrile (74)

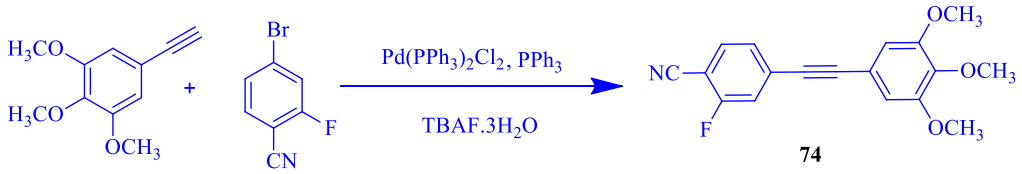

74

Using 4-bromo-2-flourobenzonitrile (0.4 g, 2 mmol.) the above diarylalkyne was procured as a white needle crystalline solid (0.442 g, 1.41 mmol., 71%, Mp 156-158°C), after purification by flash chromatography (hexane: ethyl acetate 8:2), TLC, (hexane: ethyl acetate 6:4, R_f = 0.56). HRMS (ESI): calculated for $(M)^+$= 311.0957, found for $(M)^+$= 311.0955, ΔMs=0.2ppm.

^{1}H NMR :δ (ppm) =3.91 [9H, s, 3 x (CH_3O)], 6.8 [2H, s, Ar-H trimethoxy ring], 7.35[1H, dd, J = 9.35 Hz, 1.26 Hz, Ar-H *ortho* to F], 7.41 [1H, dd, J = 8.06 Hz, 1.36 Hz, Ar-H *para* to F], 7.61[1H, dd, J = 8.01 Hz, 6.72 Hz, Ar-H *meta* to F].

^{13}C NMR :δ(ppm) = 56.23 [2 x (OCH_3)], 61.04 [(OCH_3)], 85.93 [C≡C, d, J = 3.32 Hz], 95.20 [C≡C], 100.73 [C-C, d, J =15.81 Hz, Ar-C-C≡N)], 109.14 [C-H, Ar-CH *ortho* to methoxy], 113.72 [C-C, Ar-C-C trimethoxy ring], 116.60 [C≡N], 118.92 [C-H, d, J = 21.06, Ar-CH *ortho* to F], 127.81 [1C, d, J= 3.47, Ar-CH *meta* to F], 130.49 [1C, d, J=9.68, Ar-C-C fluorine ring], 133.31 [C-H, ,Ar-C-H para to F], 1393.87 [C-O, Ar-C-OCH_3], 1532.24 [C-O, 2 x Ar-C-OCH_3], 161.49 [C-F, d, J = 259.42 Hz, Ar-C-F].

FT-IR: ν_{max} (cm^{-1}): 3054 (C-H str., aromatic), 2942 (C-H str., aliphatic), 2219 (C≡N str.), 1615, 1576 (C=C str., aromatic), 1127 (C-OCH_3 asy. str).

Synthesis of substituted 5,6-diaryl-1,2,4-triazine analogues

2.3.2 Synthesis of substituted 1,2-diarlyketone:

To a stirred solution of diarylalkyne (2 mmol., 1eq.) in anhydrous DMSO (15 cm^3), was added cupric bromide (0.044 g, 0.2 mmol., 0.1 eq.), and bis(acetonitrile)palladium(II) dichloride (0.051 g, 0.2 mmol., 0.1 eq.). The mixture was irradiated in a microwave reactor for 2 hrs at 100 W, 120°C, and 60-second pre-mixing. After conversion the starting material, mixture was diluted with water and extracted with ethyl acetate (3 x 30 cm^3). The organic layer was washed with brine, dried over anhydrous $MgSO_4$, filtered, and evaporated under reduced pressure. Column chromatography was used to purify the solid product on silica gel.

Following the above procedure 1,2-diketones (75- 86) were synthesised.

1-Phenyl-2-(3,4,5-trimethoxyphenyl)ethane-1,2-dione (75)

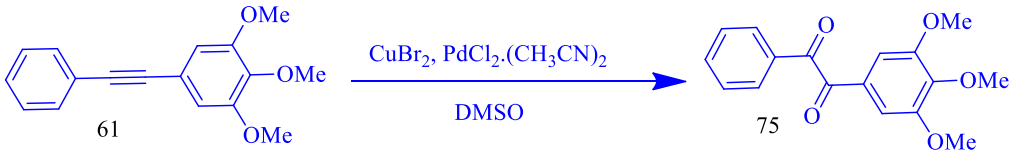

The above titled diketone (75) was synthesized from 1,2,3-trimethoxy-5-(phenylethynyl) benzene (58) (0.536 g, 2 mmol., 1 eq.), and obtained as greenish yellow solid (0.490 g, 1.6 mmol., 81.66%), after purification by column chromatography (eluent: hexane: ethyl acetate, 8:2, R_f = 0.26), MP =108-112 °C (lit. Mp =102, (Giraud *et al.*, 2006)).

^{1}H NMR: δ (ppm) =3.90 [6 H, s, 2 x (OCH_3)], 3.97 [3 H, s, (OCH_3)], 7.25 [2 H, s, Ar-H trimethoxy ring], 7.55 [2 H, s, Ar-H *ortho* to methoxy], 7.55 [2 H, t, J=7.65, Ar-H], 7.69 [1H, t, J=7.41Hz, Ar-H], 7.99 [2 H, d, J=7.68, Ar-H1].

^{13}C NMR: δ (ppm) = 56.36 [2 x (OCH_3)], 61.07 [OCH_3], 107.20 [C-H, 2 x Ar-CH *ortho* to methoxy], 127.92 [C-C, Ar-C-C), 129.03 [C-H, 2 x Ar-C-H], , 129.97 [C-H, 2 x Ar-C-H), 133.09 [C-C, Ar-C-C], 134.90 [C-H, Ar-CH], 144.30 [Ar-C-OCH_3], 153.42 [C-O, 2 x Ar-C-OCH_3], 193.35 [C=O], 194.33 [C=O].

FT-IR: ν_{max} (cm^{-1}): 2943 (C-H str. aromatic), 2833 (C-H str., aliphatic), 1667 (C=O, str.), 1597 (C=C str., aromatic), 1123 (C-O-CH_3, asy. Str.). Spectral data identical with literature (Lv *et al.*, 2015).

Synthesis of substituted 5,6-diaryl-1,2,4-triazine analogues

1-(3-Formyl-4-methoxyphenyl)-2-(3,4,5-trimethoxyphenyl)ethane-1,2-dione (76)

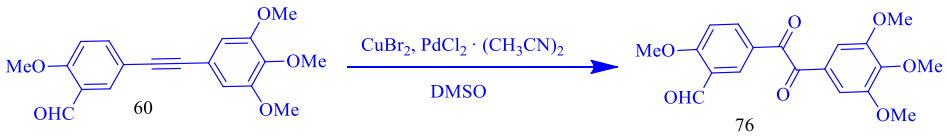

The above titled diketone (**76**) was synthesized from (**60**) (0.472 g, 2 mmol.), and obtained as orange solid (0.615 g, 1.716 mmol., 86%, Mp=144-146 ^{o}C)., after purification with column chromatography (SiO_2: hexane: ethyl acetate, 6:4, R_f = 0.26). HRMS (ESI): calculated for $C_{19}H_{18}O_7Na$ (M+Na) =381.0950,found (M+Na)= 381.0945, ΔMs=0.5ppm.

^{1}H NMR: δ (ppm) =3.89 [6H, s, 2 x (CH_3O)], 3.95 [3H, s, (CH_3O)], 4.05 [3H, s, (CH_3O)], 7.14 [1H, d, J=8.86 Hz, Ar-H *meta* to CHO), 7.22 [2 H, s, Ar-H *ortho* to methoxy], 8.24 [1H, dd, J=8.86 Hz, 2.3 Hz, Ar-H *para* to CHO], 8.37 [1H, d, J=2.3 Hz, Ar-H *ortho* to CHO], 10.44 [1H, s, CHO aldehyde] .

^{13}C NMR: δ (ppm) =56.35 [2 x (OCH_3)], 61.04 [(OCH_3)], 107.29 [C-H, 2 x Ar-CH *ortho* to methoxy], 112.36 [Ar-CH meta to CHO], 124.76 [Ar-C-CO], 126.10 [Ar-C-CO], 127.71 [Ar-C-CO], 131.54 [C-H, Ar-CH *ortho* to CHO], 137.10 [C-H, Ar-CH *para* to CHO], 144.38 [C-O, Ar-C-OCH_3], 153.83 [C-O, 2 x Ar-C-OCH_3], 166.02 [C-O, Ar-C-OCH_3 *ortho* to CHO], 188.35 [CHO], 192.11 [C=O], 192.67 [C=O].

FT-IR: ν_{max} (cm^{-1}): 2944 (C-H str., aromatic), 2838, 2725 (CHO overtone.), 1667, 1660 (C=O str.), 1599 (C=C str., aromatic), 1123 (C-O-CH_3 asy. str.).

1-(3-Cyano-4-methoxyphenyl)-2-(3,4,5-trimethoxyphenyl)ethane-1,2-dione (77)

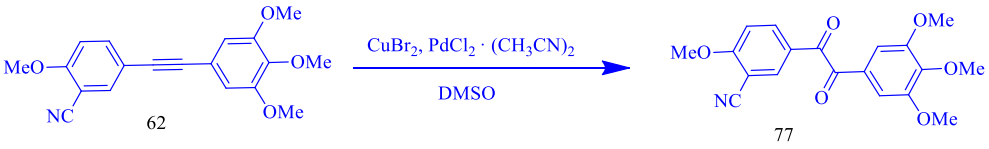

The above titled diketone (**77**) was synthesized from (**62**) (0.646 g, 2 mmol.), and obtained as a yellow solid (0.600 g, 1.68 mmol, 85%, MP 195-197 ^{o}C), after purification with column chromatography (SiO_2: hexane: ethyl acetate, 6:4, R_f = 0.28). HRMS (ESI): calculated for $C_{19}H_{18}NO_6$ (M+H) = 356.1134, found (M+H) = 356.1131, ΔMs=0.3ppm.

^{1}H NMR: δ (ppm) = 3.80 [3H, s, (OCH_3)], 3.83 [6H, s, 2 x (OCH_3)], 4.05 [3H, s, (OCH_3)], 7.21 [2H, s, Ar-H], 7.45 [1H, d, J=9.05 Hz, Ar-H *meta* to CN group], 8.21 [1H, dd, J=9.06 Hz, 2.16 Hz, Ar-H *para* to CN group], 8.31 [1H, d, J=2.16 Hz, Ar-H *ortho* to CN group].

^{13}C NMR: δ (ppm) = 56.39 [2 x (OCH_3)], 56.84 [(OCH_3)], 61.10 [OCH_3)], 103.05 [C≡N], 107.33 [C-H, Ar-CH *ortho* to methoxy], 111.67 [C-H, Ar-CH *meta* to CN], 114.93 [Ar-C-CN], 126.29 [Ar-C-CO], 127.48 [Ar-C-CO], 136.33 [C-H, Ar-CH *ortho* to *nitrile*], 137.10 [C-H, Ar-CH *para* to CN], 144.65 [C-O, Ar-C-OCH_3], 153.45 [C-O, Ar-C-OCH_3], 165.40 [CO, Ar-C-OCH_3], 190.64 [C=O], 192.05 [C=O].

FT-IR: ν_{max} (cm^{-1}): 2949 (C-H str., aromatic), 2839 (C-H str., aliphatic), 2233 (C≡N str.), 1655 (C=O str.), 1601, 1567 (C=C str., aromatic), 1131 (C-O-CH_3 asy. str.).

1-(3-Amino-4-methoxyphenyl)-2-(3,4,5-trimethoxyphenyl)ethane-1,2-dione (78)

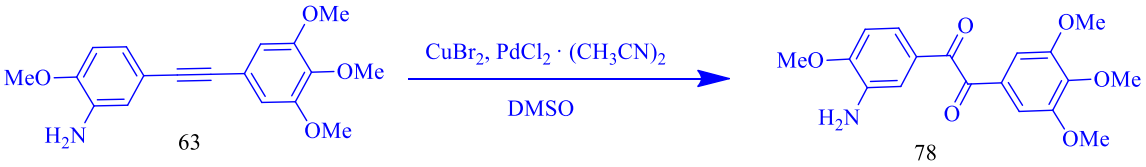

The above titled diketone (**78**) was synthesized from (**60**) (0.626 g, 2 mmol.), and obtained as a green solid (0.220 g, 0.63 mmol., 32%), MP 158-160 ^{o}C [lit. Mp=146-147 (Mousset *et al.*, 2008)], after purification with column chromatography (SiO_2: hexane: ethyl acetate, 7:3, R_f = 0.28).

^{1}H NMR: δ (ppm) = 3.80,3.87 [14H, 2 x s, 4 x (OCH_3) + NH_2], 6.74 [1H, d, J= 8.39 Hz, Ar-H *meta* to NH_2], 7.13 [2H, s, Ar-H trimethoxy ring], 7.25 [1H, dd, J=8.39 Hz 1.96 Hz, Ar-H *para* to NH2], 7.29 [1H, d, J= 1.96 Hz, Ar-H *ortho* to NH_2].

^{13}C NMR: δ (ppm) = 55.83 [(OCH_3)], 56.33 [2 x OCH_3], 61.04 [OCH_3], 107.12 [C-H, 2 x Ar-CH trimethoxy ring), 109.62 [C-H, Ar-CH *meta* to NH_2], 114.23 [C-H, Ar-CH *ortho* to NH_2, 123.18 [C-H, Ar-CH *para* to NH_2], 126.42 [C-C, Ar-C-CO], 128.31 [1C, Ar-C-CO], 136.81 [Ar-C-N], 143.97 [C-O, Ar-C-OCH_3 trimethoxy ring], 152.76 [1C, C-O, Ar-C-OCH_3], 153.34 [C-O, Ar-C-OCH_3 trimethoxy ring] 193.64 [C=O], 193.95 [C=O].

FT-IR: ν_{max} (cm^{-1}): 3497, 3398 (N-H str.), 2936 (C-H str., aromatic), 2833 (C-H, aliphatic), 1667 (N-H bend.), 1655 (C=O Str.), 1604, 1578 (C=C str., aromatic), 1125 (C-O-CH_3, asy. str).

1-(3-Hydroxy-4-methylphenyl)-2-(3,4,5-trimethoxyphenyl)ethane-1,2-dione (79)

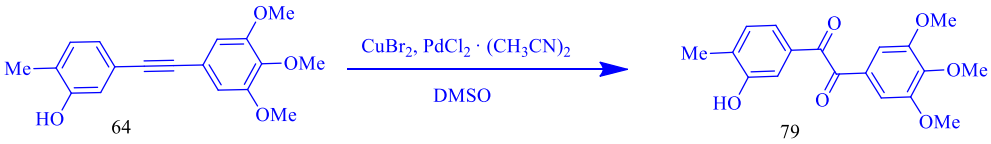

The above titled diketone (**79**) was synthesized form (**61**) (0.596 g, 2 mmol.), and obtained as a yellow solid (0.45, 1.36 mmol., 32%, Mp= 160-162 ^{o}C), after purification by column chromatography (SiO_2: hexane: ethyl acetate, 7:3, R_f = 0.28). HRMS (ESI): calculated for $C_{18}H_{19}O_6$ (M+H) = 331.1181, found for (M+H) =331.1180, ΔMs=0.1ppm. **^{1}H NMR**: δ (ppm) = 2.34 [3 H, s, (CH_3)], 3.88 [6 H, s, 2 x (OCH_3)], 3.96 [3 H, s, (OCH_3)], 5.85 [1H, s, OH], 7.21 [2 H, s, Ar-H *ortho* to methoxy], 7.25 [1H, d, J= 7.8 Hz, Ar-H *meta* to OH], 7.25 [1H, dd, (J=7.8 Hz, 1.56 Hz, Ar-H *para* to OH], 7.44 [1H, d, J= 1.56 Hz, Ar-H *ortho* to OH].

^{13}C NMR: δ (ppm) = 29.70 [(CH_3)], 56.33 [2 x (OCH_3)], 61.08 [(OCH_3)], 107.20 [C-H, Ar-CH *ortho* to methoxy], 114.88 [C-H, Ar-CH *meta* to OH], 123.14 [Ar-CH *ortho* to OH], 127.90 [Ar-C-CO], 131.57 [C-H, Ar-CH *para* to OH], 132.16 [Ar-C-CO], 133.23 [Ar-C-CH_3], 144.25 [Ar-C-OCH_3], 153.37 [C-O, Ar-C-OCH_3], 154.54 [Ar-C-OCH_3], 193.62 [C=O], 194.09 [C=O].

FT-IR: ν_{max} (cm^{-1}) 3358 (OH Str.), 2946 (C-H str. aromatic), 2833 (C-H, str. aliphatic], 1651 (C=O Str.), 1581 (C=C, str. aromatic), 1129 (C-O-CH_3, asy. str.).

1-(3-Hydroxy-4-methoxyphenyl)-2-(3,4,5-trimethoxyphenyl)ethane-1,2-dione (80)

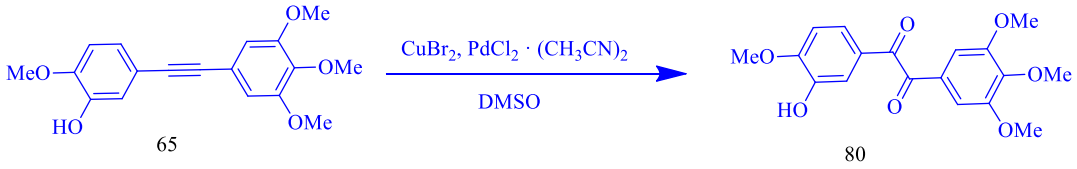

The above titled diketone (**80**) was synthesized from (**65**) (0.628g, 2 mmol), and obtained as a brownish-yellow solid (0.256 g, 0.73 mmol., 37%), MP 154-156 ^{o}C (lit. Mp=153-154 ^{o}C (Mousset *et al.*, 2008)), after purification with column chromatography (SiO_2: hexane: ethyl acetate, 7:3, R_f = 0.28).

^{1}H NMR:δ (ppm) = 3.85 [6 H, s, 2 x (OCH_3)], 3.92 [6 H, s, 2 x (OCH_3)], 6.13 [1H, s, OH], 6.87 [1H, d, J= 8.46 Hz, Ar-H *meta* to OH], 7.19 [2 H, s, Ar-H trimethoxy ring], 7.45 [1H, dd, J= 8.44 Hz, 2.00Hz, Ar-H *para* to OH], 7.52 [1H, d, J= 2.00Hz, Ar-H *ortho* to OH].

^{13}C NMR:δ (ppm) =55.19 [(OCH_3)], 56.30 [2 x (OCH_3)], 60.99 [(OCH_3)], 107.12 [C-H, 2 x Ar-CH trimethoxy ring], 110.25 [Ar-CH *meta* to OH], 114.97 [Ar-CH *ortho* to OH], 124.56 [Ar-CH *para* to OH], 126.65 [Ar-C-CO], 128.09 [Ar-C-CO], 144.07 [Ar-C-OCH_3], 146.06 [Ar-C-OCH_3], 152.46 [Ar-C-OH], 153.32 [2 x Ar-C- OCH_3], 193.31 [C=O], 194.68 (C=O).

FT-IR: ν_{max} (cm^{-1}):3375 (O-H str.), 3096, 2935 (C-H str., aromatic), 2845 (C-H str., aliphatic), 1652 (C=O str.), 1577 (C=C str., aromatic), 1117 (C-O-CH_3 asy. str.).

1-(4-Methoxy-3-nitrophenyl)-2-(3,4,5-trimethoxyphenyl)ethane-1,2-dione (81):

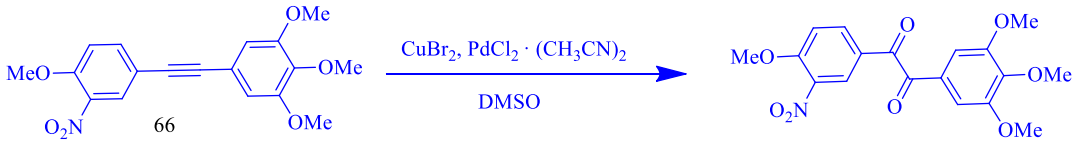

The above titled compound (**81**) was synthesized from (**66**) (0.686 g, 2 mmol.), and obtained as a yellow solid (0.597 g, 1.59 mmol., 80%, Mp =150-153 ^{o}C), after purification by column chromatography (SiO_2: hexane: ethyl acetate, 8:2, R_f = 0.17). HRMS (ESI): calculated for $C_{18}H_{18}NO_8$ (M+H) =376.1032, found for (M+H)= 376.1029, ΔMs=0.3ppm.

^{1}H NMR: δ (ppm) =3.83 [6 H, s, 2 x (OCH_3)], 3.90 [3H, s, (OCH_3)], 4.0 [3H, s, (OCH_3)], 7.13 [1H, d, J= 8.90 Hz, Ar-H *meta* to nitro], 7.17 [2 H, s, Ar-H trimethoxy ring], 8.11 [1H, dd, J= 8.90 Hz, 2.17 Hz, , Ar-H *para* to nitro], 8.40 [1H, d, J= 2.17 Hz, Ar-H *ortho* to nitro].

^{13}C NMR: δ (ppm) =56.40 [2 x (OCH_3)], 57.14 [(OCH_3)], 61.12 [(OCH_3)], 107.39 [Ar-CH trimethoxy ring], 113.62 [Ar-CH *meta* to nitro], 125.63 [Ar-C-CO], 127.43 [Ar-C-CO], 127.67 [Ar-CH *ortho* to nitro], 135.67 [Ar-CH *para* to nitro], 139.83 [Ar-C- OCH_3], 144.68 [Ar-C-NO_2], 153.45 [2 x Ar-C-OCH_3], 157.34 [Ar-C-OCH_3], 190.51 [C=O], 191.74 [C=O].

FT-IR: ν_{max} **(**cm^{-1}**)** 2952 (C-H str., aromatic), 2834 (C-H str., aliphatic), 1651 (C=O, str.), 1581 (C=C str., aromatic), 1129 (C-O-CH_3, asy. str.).

Synthesis of substituted 5,6-diaryl-1,2,4-triazine analogues

1-(3-Amino-4-methylphenyl)-2-(3,4,5-trimethoxyphenyl)ethane-1,2-dione (82):

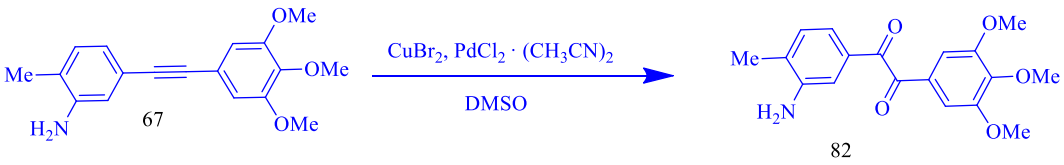

The above titled diketone (**82**) was synthesized from (**67**) (0.594 g, 2 mmol.), and obtained as a green solid (0.263, 0.8 mmol., 40 %, MP = 146-148 ^{o}C), after purification by column chromatography (SiO_2: hexane: ethyl acetate, 6:4, R_f = 0.27). HRMS (ESI) :calculated for C18H20NO5 (M+H) =330.1341, found for (M+H)= 330.1338, ΔMs=0.3ppm.

^{1}H NMR : δ (ppm) =2.12 [3 H, s, (CH_3)], 3.8 [6 H, s, 2 x (OCH_3)], 3.86 [3 H, s, (OCH_3)], 7.07 [1H, d, J = 7.86 Hz, Ar-H *meta* to NH_2], 7.12 [2H, s, Ar-H *ortho* to methoxy], 7.15 [1H, dd, J= 7.84 Hz, 1.78 Hz, Ar-H *para* to NH_2], 7.19 [1H, d, J = 1.78 Hz, Ar-H *ortho* to NH_2].

^{13}C NMR : δ (ppm) = 17.88 [(CH_3)], 56.18 [(OCH_3)], 56.32 [2 x (OCH_3)], 107.11 [2 x Ar-CH, *ortho* to methoxy], 114.67 [Ar-CH *meta* to NH_2], 122.39 [Ar-CH *ortho* to NH_2], 130.93 [Ar-CH *para* to NH_2], 128.12 [Ar-C-CO], 130.32 [Ar-C-CO], 133.67 [Ar-C-CH_3], 138.95 [Ar-C-OCH_3], 145.28 [Ar-C-N], 153.36 [2 x Ar-C-OCH_3], 193.81 [C=O], 194.59 (C=O).

FT-IR: ν_{max} **(**cm^{-1}): 3445, 3360 (N-H str.), 2940 (C-H str., aromatic), 2837 (C-H str., aliphatic), 1655 (N-H bend.), 1635 (C=O str.), 1571 (C=C str., aromatic), 1124 (C-O-CH_3, asy. str.).

1-(3-Fluoro-4-methylphenyl)-2-(3,4,5-trimethoxyphenyl)ethane-1,2-dione (83):

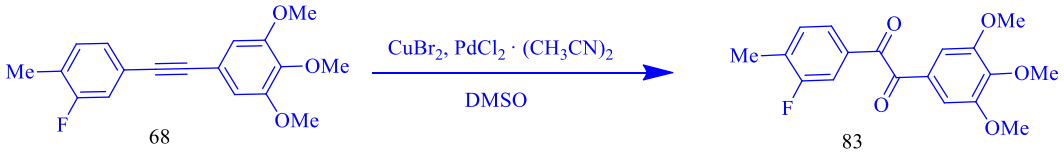

The above titled diketone (**83**) was synthesized from (**68**) (0.60 g, 2 mmol.), and obtained as a green-yellow solid (0.553 g, 1.66 mmol., 87.8%, MP 112-114 ^{o}C), after purification by column chromatography (SiO2: hexane: ethyl acetate, 8:2, R_f = 0.32). HRMS (ESI): calculated for $C_{18}H_{18}FO_5$ (M+H) = 333.1133, found for (M+H) =333.1135, ΔMs=-0.2ppm

^{1}H NMR: δ (ppm) =2.34 [3 H, d, J=1.86 Hz, (CH_3)], 3.82 [6 H, s, 2 x (OCH_3)], 3.88 [3H, s, (OCH_3)], 7.19[2H, s, Ar-H *ortho* to methoxy], 7.28 [1H, t, J=7.69Hz, Ar-H *meta* to flourine], 7.55[2H, m, Ar-H *ortho* and *para* to fluorine].

^{13}C NMR: δ (ppm) = 15.14[CH_3, d, J= 3.52 Hz], 56.36 [(OCH_3)], 61.08 [2 x (OCH_3)], 107.21 [Ar-C-H *ortho* to methoxy], 115.66 [C-H, d, J = 23.67 Hz, Ar-C-H *ortho* to F], 125.89 [C-H, d, J= 3.28 Hz, Ar-C-H *para* to F], 127.73 [Ar-C-CO], 132.07[C-H, d, J = 4.53 Hz, Ar-C-H *meta* to F], 132.72 [C-C, d, J = 6.33 Hz, Ar-C-CO], 133.21 [C-C, d, J=17.47 Hz, (Ar-C-CH_3)], 144.39 [Ar-C-OCH_3], 153.42 [2 xAr-C-OCH_3], 162.57 [C-F, d, J= 248.16 Hz, Ar-C-F), 192.76 [C=O], 192.87 [C=O, d, J = 1.49 Hz C=O] .

FT-IR: ν_{max} (cm^{-1}) 2941 (C-H str. aromatic), 2840 (C-H str., aliphatic), 1668 (C=O str.) 1582 (C=C str., aromatic), 1343 (C-F str.), 1126 (C- OCH_3, asy. str.).

1-(3-Acetyl-4-methoxyphenyl)-2-(3,4,5-trimethoxyphenyl)ethane-1,2-dione (84)

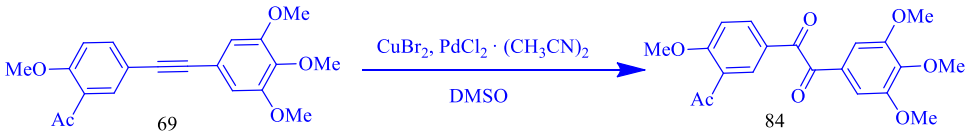

The above titled compound (84) was synthesized from (69) (0.68 g, 2 mmol.), and obtained as a white crystaline solid (0.50 g, 1.34 mmol., 67%, MP =117-119 ^{o}C), after purification by column chromatography (SiO_2: hexane: ethyl acetate, 6:4, R_f = 0.31). HRMS (ESI): calculated for $C_{20}H_{21}O_7$ $(M+H)^+$=373.1282, found for (M+H)= 373.1283, ΔMs=-0.1ppm.

^{1}H NMR: δ (ppm) =2.55 [3 H, s, (CH_3)], 3.82 [6 H, s, 2 x (OCH_3)], 3.86 [3 H, s, (OCH_3)], 3.96 [3 H, s, (OCH_3)], 7.01[1H, d, J= 8.76 Hz, Ar-H *meta* to Ac group], 7.15[2 H, s, Ar-H trimethoxy ring], 8.06 [1H, dd, J= 8.76 Hz, 2.28 Hz, Ar-H *para* to Ac group], 8.22 [1H, d, J= 2.28 Hz, Ar-H *ortho* to Ac group].

^{13}C NMR: δ(ppm) = 29.7 [CH_3], 56.20 [(OCH_3)], 56.37 [2 x (OCH_3)], 61.07 [(OCH_3)], 107.30 [2 x Ar-CH trimethoxy ring], 112.00 [Ar-CH *meta* to Ac group], 126.09 [Ar-C-CO], 127.84 [Ar-C-CO], 128.86 [Ar-C-CO], 133.07 [Ar-CH *ortho* to Ac group], 135.28 [Ar-CH *para* to Ac group], 144.33 [Ar-C-OCH_3], 153.40 [2 x Ar-C-OCH_3 trimethoxy ring], 163.35 [Ar-C-OCH_3], 192.26 [C=O], 192.88 [C=O], 198.49 [C=O].

FT-IR: ν_{max} (cm^{-1}): 2952 (C-H str. aromatic), 2845 (C-H str., aliph.), 1667 (C=O str.) 1580 (C=C str., aromatic), 1123 (C-O-CH_3, asy. str.).

Synthesis of substituted 5,6-diaryl-1,2,4-triazine analogues

1-(4-Methoxy-3-methylphenyl)-2-(3,4,5-trimethoxyphenyl)ethane-1,2-dione (85)

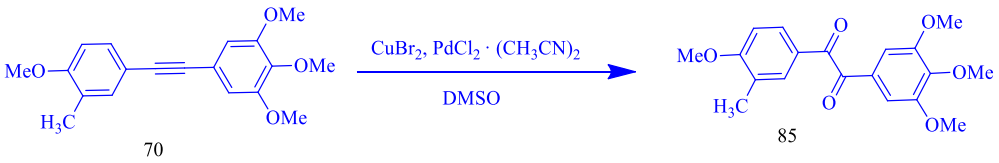

The above titled compound (**85**) was synthesized from (**70**) (0.624 g, 2 mmol.), and obtained as a light green solid (0.569 g, 1.82 mmol., 91%, Mp =128-131 ^{o}C), after purification by column chromatography (SiO_2: hexane: ethyl acetate, 8:2, R_f = 0.32). HRMS (ESI): calculated for $C_{19}H_{21}O_6$ (M+H) =345.1333, found for (M+H) = 345.1335, ΔMs=-0.2ppm.

^{1}H NMR: δ (ppm) =2.02 [3 H, s, (CH_3)], 3.85 [6 H, s, 2 x (OCH_3)], 3.89 [3 H, s, (OCH_3)], 3.92 [3H, s, (OCH_3)], 6.86[1H, d, J = 8.52 Hz, Ar-H *meta* to CH_3 group], 7.20 [2H, s, Ar-H trimethoxy ring], 7.76 [1H, dd, J = 8.5 Hz, 2.02 Hz, Ar-H *para* to CH_3 group], 8.22 [1H, d, J= 2.02 Hz, Ar-H *ortho* to CH_3 group].

^{13}C NMR: δ (ppm) = 16.23 (CH_3), 55.72 [OCH_3], 56.34 [2 x OCH_3], 61.03[OCH_3], 107.18 [2 x Ar-CH *ortho* to methoxy], 109.70 [Ar-CH *meta* to CH_3], 125.62 [Ar-C-CO], 127.74 [Ar-C-CO], 128.25 [Ar-C-CH_3], 130.81 [Ar-CH *ortho* to CH_3 group], 132.10 [Ar-CH *para* to CH_3 group], 144.05 [Ar-C-OCH_3 trimethoxy ring], 153.36 [2 x Ar-C-OCH_3 trimethoxy ring], 163.37 [Ar-C-OCH_3], 193.29 [C=O], 193.83 [C=O].

FT-IR: ν_{max} (cm^{-1}) 2954 (C-H str. aromatic), 2838 (C-H str., aliphatic), 1659 (C=O str.) 1584 (C=C str. aromatic), 1130 (C-O-CH_3, asy. str.).

1-(4-Cyano-3-hydroxyphenyl)-2-(3,4,5-trimethoxyphenyl)ethane-1,2-dione(86)

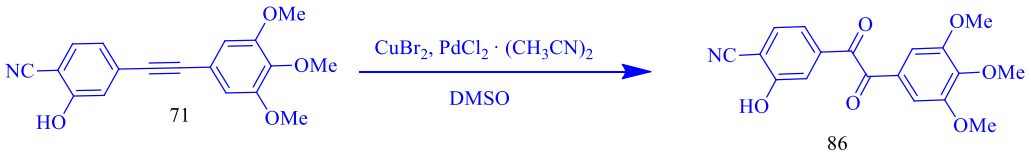

The above titled compound (**86**) was synthesized from (**71**) (0.618 g, 2 mmol.), and obtained as a light green solid (0.4 g, 1.17 mmol., 59 %), Mp >230 ^{o}C, after purification by column chromatography (SiO_2: hexane: ethyl acetate, 7:3, R_f = 0.2). HRMS (ESI): clculated for $C_{18}H_{16}N_1O_6$ (M+H) =342.0972, found for (M+H)= 342.0977,ΔMs=-0.5ppm.

^{1}H NMR: δ (ppm) = 3.79 [3 H, s, (OCH_3)], 3.81[6 H, s, 2 x (OCH_3)], 7.19 [2 H, s, Ar-H *ortho* to meyhoxy], 7.35[1H, dd, J= 8.05 Hz, 1.11Hz, Ar-H *para* to OH], 7.49 [1H, d, J

= 1.11 Hz, Ar-H *ortho* to OH], 7.84 [1H, d, J= 8.05 Hz, Ar-H *meta* to OH], 11.77 [1H, s, OH].

^{13}C NMR: δ (ppm) = 56.21 [2 x (OCH_3)], 60.35 [(OCH_3)], 104.61 [C≡N], 107.13 [Ar-CH *ortho* to meyhoxy], 115.95 [Ar-C-H *meta* to OH], 116.17[Ar-C-CO], 120.09 [Ar-CH *para* to OH], 126.85 [Ar-C-CO], 134.49 [Ar-CH *ortho* to OH], 136.82 [Ar-C-CN], 144.12 [Ar-C-OCH_3],153.21[2x Ar-C-OCH_3], 160.46 [Ar-C-OH], 192.52 [C=O], 193.00 [C=O].

FT-IR: ν_{max} (cm^{-1}) 3324 (OH str.), 2957 (C-H str., aromatic), 2848 (C-H str., aliphatic), 2230 (C≡N str.), 1670 (C=O str.), 1581 (C=C str., aromatic), 1118 (C-O-CH_3, asy. str.).

2.3.3 Synthesis of substituted 1,2,4-traizine-3(2H)-one:

6-(4-methoxy-3-nitrophenyl)-5-(3,4,5-trimethoxyphenyl)-1,2,4-triazin-3(2H)-one(87)

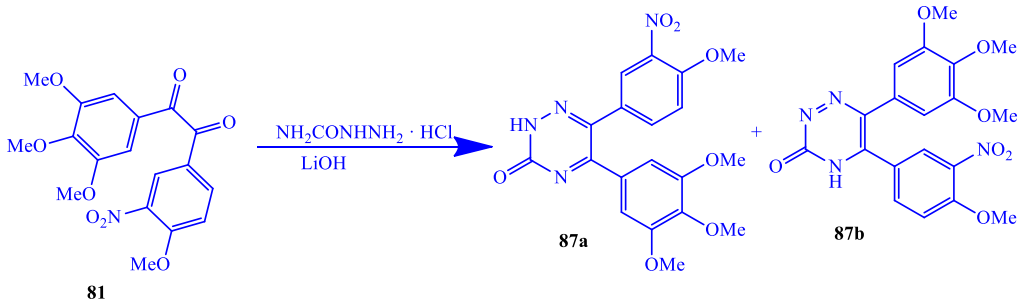

To a stirred solution of semicarbazide hydrochloride (0.133 g, 1.2 mmol., 1.2 eq.), lithium hydroxide (0.028 g, 1.2 mmol., 1.2 eq.) in ethanol was added 1-(4-methoxy-3-nitrophenyl)-2-(3,4,5-trimethoxyphenyl)ethane-1,2-dione (0.375 g, 1 mmol., 1 eq.) and the mixture was heated under reflux for overnight. After cooling, precipitate was filtered , washed with water and purified by column chromatography (SiO_2: ethtylacetate : hexane 8:2, R_f = 0.27) which obtain as a green solid of two isomers (0.217 g, 0.52 mmole, 52.41%). The isomers mixture were further separated by HPLC using silicagel column 4µ Genesis C18 120Å and ethyl acetate - hexane system (8:2) as a mobile phase.

Isomer 1

^{1}H NMR: δ (ppm) = 3.62 [6 H, 2 x (OCH_3)], 3.84 [3 H, (OCH_3)], 3.86 [3 H, (OCH_3)], 6.75[2H, s, Ar-H trimethoxy ring], 7.02 [1H, d, J = 8.86 Hz, Ar-H *meta* to NO_2], 7.4 [1H, dd, J= 8.92 Hz, 2.4 Hz, Ar-H *para* to NO_2], 7.93 [1H, d, J= 2.33 Hz, Ar-H *ortho* to NO_2], 11.46 [1H, s, NH].

^{13}C NMR: δ (ppm) =56.22 [2 x (OCH_3)], 56.84 [OCH_3], 61.13[OCH_3], 107.64 [C-H, Ar-CH trimethoxy ring], 113.36 [C-H, Ar-C-H *meta* to NO_2], 125.98 [C-H, Ar-C-H *ortho* to NO_2], 126.53 [Ar-C-CO], 129.09 [Ar-C-CO], 134.38 [C-H, Ar-C-H *para* to NO_2], 139.58 [1C, Ar-C-OCH_3], 140.90 [Ar-C-NO_2], 141.85 [Ar-C=N], 153.10 [2 x Ar-C-OCH_3], 153.44 [Ar-C-OCH_3], 153.83 [1C, Ar-C=N], 167.10 [Ar-C=O].

Isomer 2

^{1}H NMR:δ (ppm) = 3.68 [6H, 2 x OCH_3], 3.83 [3H, OCH_3], 3.93 [3H, OCH_3], 6.46[2H, s, Ar-H trimethoxy ring], 6.79 [1H, d, J = 8.97 Hz, Ar-H *meta* to NO_2], 7.71 [1H, dd, J = 8.97 Hz, 2.09 Hz, Ar-H *para* to NO_2], 8.07 [1H, d, J = 2.09 Hz, Ar-H *ortho* to NO_2], 10.91 [1H, s, NH].

^{13}C NMR : δ (ppm) =56.36 [2 x (OCH_3)], 56.92 [OCH_3], 61.14[OCH_3], 106.36 [C-H, Ar-CH trimethoxy ring], 113.00 [C-H, Ar-C-H *meta* to NO_2], 126.66 [C-H, Ar-C-H *ortho* to NO_2], 126.78 [Ar-C-CO], 128.48 [Ar-C-CO], 135.73 [C-H, Ar-C-H *para* to NO_2], 139.26 [Ar-C-OCH_3], 139.77 [Ar-C-NO_2], 142.73 [Ar-C=N], 153.48 [2 x Ar-C-OCH_3], 153.70 [Ar-C-OCH_3], 155.42 [Ar-C=N], 164.99 [Ar-C=O].

FT-IR: ν_{max} (cm^{-1}): 3379 (N-H str.), 3010(C-H Str., aromatic), 2948 (C-H Str., aliphatic), 1653 (C=O str.), 1603 (C=N str.), 1507 (C=C str., aromatic), 1123 (C-O-CH_3, asy. str.).

Synthesis of substituted 5,6-diaryl-1,2,4-triazine analogues

2.3.4 Results and Discussion

Synthesis of diarylalkynes:

Diarylalkynes are a very important precursor for a natural product, pharmaceutical, and molecular organic synthesis. Consequently, many protocols for the synthesis of aryl alkynes have been reported, with a various starting materials such as carbonyl compounds (Habrant *et al.*, 2010), haloalkenes or alkyl halides (Okutani & Mori, 2009), and alkenes (Ranu *et al.*, 2003). However, palladium-catalysed cross coupling reactions are widely used in the organic synthesis to couple sp^2 carbon (aryl or alkenyl halide) with sp carbon hybridisation (terminal alkyne), as shown in scheme-2. This reaction is known as the Sonogashira reaction, which is a catalytic process that requires a palladium (0) complex and base, and some reactions use copper iodide as a co-catalyst.

Sonogashira reaction is extensively used among other methodologies in organic synthesis for the synthesis of heterocyclic compounds, natural products, conjugated polymers, pharmaceutical and biomolecules, and many other chemicals (Chinchilla & Najera, 2011).

Scheme 2: General reaction of Sonogashira coupling.

The reaction conditions can be varied depending on the reactivity of the aryl halide and alkyne. For instance, aryl iodide reacts under room temperature conditions, whereas, heating, and a higher percentage of catalyst, are normally used with a deactivated aryl halides (Littke & Fu, 2002). Although, there are different oxidation states of a palladium catalyst, palladium (0) and palladium (II) are the two catalysts most frequently used as they are very stable (Muniz, 2009) · The reaction mechanism consists of two catalytic cycles. However, it is not clearly understood because the difficulty in analysing and isolating of the organometallic compound intermediates, present in the reaction. However, it is suggested that the mechanism consists of four steps. The first one starts when the aryl halide (RX) reacts with the palladium catalyst Pd (0) to form a palladium (II) intermediate. This step is known as oxidative addition, where the oxidation states and coordination number of the metal catalyst increase. The copper cycle produces a π-alkyne complex of copper acetylide, in the presence of a strong base. This copper acetylide reacts with the palladium (II) intermediate, which results from the oxidative addition step, in the

second step of the cycle, which is known as the trans metalation step where copper halide is expelled. The palladium catalyst ligands are converted to the cis conformation in the third step via trans-cis isomerisation reaction to produce cis palladium complex that undergoes a reductive elimination reaction to reproduce the palladium catalyst for the next cycle leaving the required alkyne (Chinchilla & Najera, 2007). The four steps of the mechanism are illustrated in the scheme 2 below.

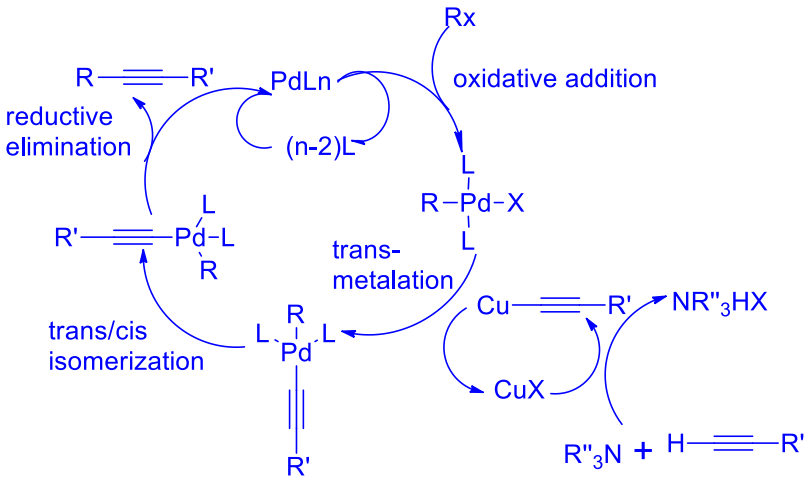

Scheme 3: The catalytic cycle of Sonogashira reaction (Chinchilla & Najera, 2011).

Although the Sonogashira reaction is significantly utilized in numerous arrays of synthetic reactions, it has several complications. The first one arises from using copper iodide as a co-catalyst, where it found that the *in situ* copper acetylide complex often leads to a Glasser reaction that generates a homocoupled product of the terminal alkyne (Siemsen *et al.*, 2000). In addition, copper iodide is environmentally unfriendly and difficult to recover. However, it has been reported that the slow addition of alkyne and using a reductive environment like H_2 could mitigate this problem (Elangovan *et al.*, 2003). For this reasons, many papers have described the Sonogashira reaction without utilizing copper salts and most of these papers increase the reactivity of catalytic system by using an excessive amount of the amine (Chinchilla & Najera, 2011; Leadbeater & Tominack, 2003). Conducting the Sonogashira reaction with zero concentration of copper salt is known as copper-free Sonogashira coupling. The proposed mechanism of this reaction shown in scheme 3.

The substantial amount of base, on the other hand, has created another drawback where it has been shown that some secondary amines react efficiently and reversibly with the

palladium alkyne complex by substituting one (PPh_3) ligand which results in competition between the amine and alkyne to this ligand (Jutand *et al.*, 2005) .

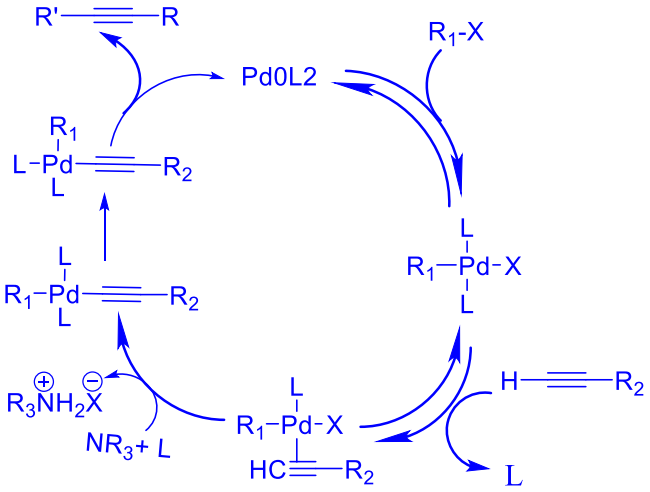

Scheme 4: Proposed copper-free Sonogashira coupling mechanism (Mery *et al.*, 2003).

Optimizing the efficiency of the reaction is widespread in the literature. As a result, many variations have been carried out to effectively improve the performance of the reaction. Among them, using aqueous media (Lipshutz *et al.*, 2008) , free amine (Cheng *et al.*, 2004) , or solvent-free conditions (Kabalka *et al.*, 2000), and surprisingly, palladium free (Thathagar *et al.*, 2004).

Not only is the Sonogashira cross coupling used for asymmetric diarlyalkyne synthesis, but also for the preparation of terminal alkynes by using aryl halides and a protected alkyne such as trimethysilylacetylene (TMSA), and 2-methyl-3-butyne-2-ol (dimethyl ethyl carbinol, DMEC) after removing the protecting group which is trimethylsilane and isopropanol respectively (Csékei *et al.*, 2008; Nagy *et al.*, 2005)

The copper-free Sonogashira reaction has been used to synthesize all the asymmetric diarylalkyne reported in this thesis. Moreover, 5-ethynyl-1,2,3-trimethoxy benzene has been synthesised in same method from 5-bromo-1,2,3-trimethoxybenzene (53) and dimethyl ethynyl carbinol in presence of palladium catalyst, DBU as base, and THF as a solvent to form 2-methyl-4-(3,4,5-trimethoxyphenyl)but-3-yn-2-ol (55) in a good to excellent yield as described in (Caporale *et al.*, 2014). The only difference was using palladium-tetrakis(triphenylphosphine) as a catalyst without the need of using any ligand (scheme-1). This compound was deprotected by using KOH and K_3PO_4 to obtain

Synthesis of substituted 5,6-diaryl-1,2,4-triazine analogues

5-ethynyl-1,2,3-trimethoxybenzene (56) as described in (Smeyanov & Schmidt, 2013). However, the reaction worked best with three equivalent ratios of KOH/K_3PO_4.

Several protocols were investigated to prepare 5-ethynyl-1,2,3-trimethoxybenzene, as it represents essential starting material for the synthesis framework, such as the Corey-Fuchs alkyne synthesis (Burroughs *et al.*, 2015; Coniglio *et al.*, 2012; Li *et al.*, 2013) (scheme-5) , and the Sonogashira Cross-Coupling by trimethylsilylacetylene (Agabekov *et al.*, 2013; Provot *et al.*, 2005) (scheme-6). However, neither one produced a satisfied yield even with the highly expensive aryl halide 5-iodo-1,2,3-trimethoxybenzene.

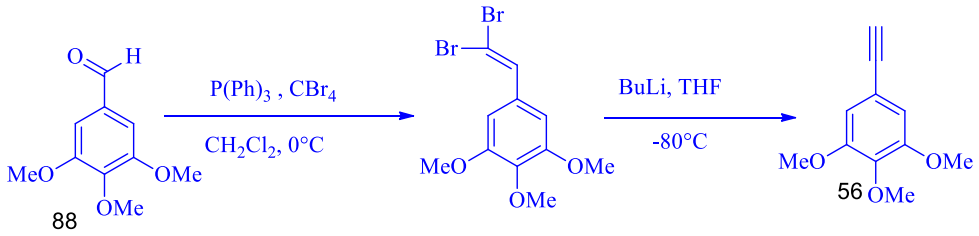

Scheme 5: Corey-Fuchs synthesis for terminal alkyne (Coniglio *et al.*, 2012)

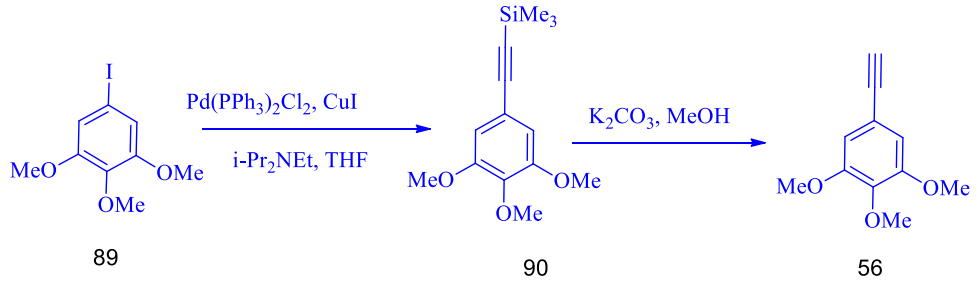

Scheme 6: Sonogashira Cross-Coupling Reaction (Agabekov *et al.*, 2013).

Although the above reaction of alkynylation is feasible and productive, it does not work with some diarylalkyne couplings especially those with hydroxyl and amine groups; even when the reaction is carried out by using a strong nucleophilic base like DBN or DABCO (Liang *et al.*, 2006) . Consequently, the diarylalkyne cross coupling was carried out with a different base, whereby bis(triphenylphosphine) palladium (II) dichloride $PdCl_2(PPh_3)_2$ was used as a catalyst, triphenylphosphine as a ligand and tetrabutylammonium fluoride trihydrate as a base. Anhydrous THF was used as a solvent, as shown in scheme 7.

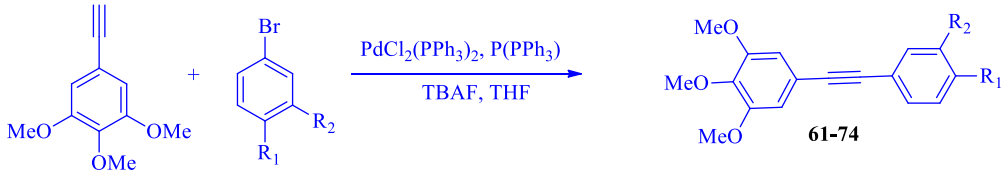

Scheme 7: synthesis of substituted diarylalkyne.

Synthesis of substituted 5,6-diaryl-1,2,4-triazine analogues

Fifteen diarlyalkynes with different substituent groups have been synthesized (scheme 7), illustrated in table 1, and twelve of them are novel. ^{1}H, ^{13}C NMR, IR, and mass spectroscopy have been used to characterize them.

Diarylalkyne	**R_1**	**R_2**	**MP^{o}C**	**%YIELD**
**61	H	H	74-75	82
*60	OCH_3	CHO	144-145	77
*62	OCH_3	CN	133-135	97
63	OCH_3	NH_2	87-89	57
*64	CH_3	OH	124-125	43
65	OCH_3	OH	96-97	41
*66	OCH_3	NO_2	132-133	82
*67	CH_3	NH_2	90-91	69
*68	CH_3	F	126-128	88
*69	OCH_3	$COCH_3$	92-94	93
*70	OCH_3	CH_3	122-124	78
*71	CN	OH	164-167	81
*72	CN	NH_2	154-155	82
*73	CN	CH_3	150-151	81
*74	CN	F	156-158	71

Table 1: Synthesised substituted diarlalkyne with yield.

*This diarylalkynes are novel compounds.

**This diarylalkyne prepared from phenylacetylene and 5-bromo-1,2,3-trimethoxy-benzene, therefore, it is not subject to the equation above.

Synthesis of 1,2-diketone derivatives:

1,2-Diphenyl-1,2-ethanedione, a compound widely known as benzil, has great importance in the cyclocondensation reaction, as it is considered a bis-acceptor species that can be condensed with a bis-donor group. Compounds, such as aromatic diamines, thioureas, and urea derivatives can be used to produce various heterocycles that are utilised in synthesis of numerous biological products. The major path of producing these benzil derivatives is the catalytic oxidation of diarylalkynes as the starting material can be obtained without difficulty by the Sonogashira reaction (Doucet & Hierso, 2007). The

direct oxidation of diarylalkynes has a growing significance because of the variety and availability of the starting material. And also, the feasibility of the oxidation procedures which seems to be a straightforward protocol that varies with the catalyst and oxidant. Many reagents have been used as oxidising agents or catalysts, including, methods that use inorganic reagents such as iodine (I_2) (Yusubov & Filimonov, 1991) or iodine derivatives (PIFA) (Tingoli *et al.*, 2011), potassium permanganate ($KMnO_4$), Sulphur trioxide (SO_3), potassium peroxymonosulfate (Oxone), cerium ammonium nitrate (Yuan *et al.*, 2017), mercuric salts (Jung & Deng, 2014), or copper salt (Xu *et al.*, 2015). Many disadvantages have been reported for these methods such as environmental effects, using harsh conditions, and toxicity (Mori *et al.*, 2010). However, Pd catalysed oxidation reaction is prominent in literature (Takacs & Jiang, 2003), as a result of the functional group tolerance and tremendous selectivity (Ren *et al.*, 2009). Moreover, Cu^{II} salts have been reported to be used with most protocols as a promoter for the catalytic cycle to reactivate Pd^0 into Pd^{II+} by oxidation (Xue *et al.*, 2018). The Wacker oxidation process, in which the alkene is converted to ketone by using Pd catalyst, co-catalyst, and water, have been intensely scrutinized. However, the oxidation of alkynes into benzil derivatives have not been researched so far (Ren *et al.*, 2009; Wang & Jiang, 2008). Despite that, some papers have proposed a feasible mechanism (Gao *et al.*, 2012; Xue *et al.*, 2018), which is not significantly different from the Wacker process version. Here, the first step of the mechanism involves Ꙋ-complex formation between the alkyne and the palladium centre that activate the triple bond to the second step. This intermediate would be efficiently attacked by nucleophilic spices such as dimethyl sulfoxide leading to a vinyl-metal intermediate of zwitterionic or neutral character. At the third step, a second dimethyl sulfoxide molecule attacking the vinyl-palladium intermediate to produce a dimethyl sulphide molecule and different intermediate, upon which β-elimination would occur to afford the desired product and second molecule of dimethyl sulphide.

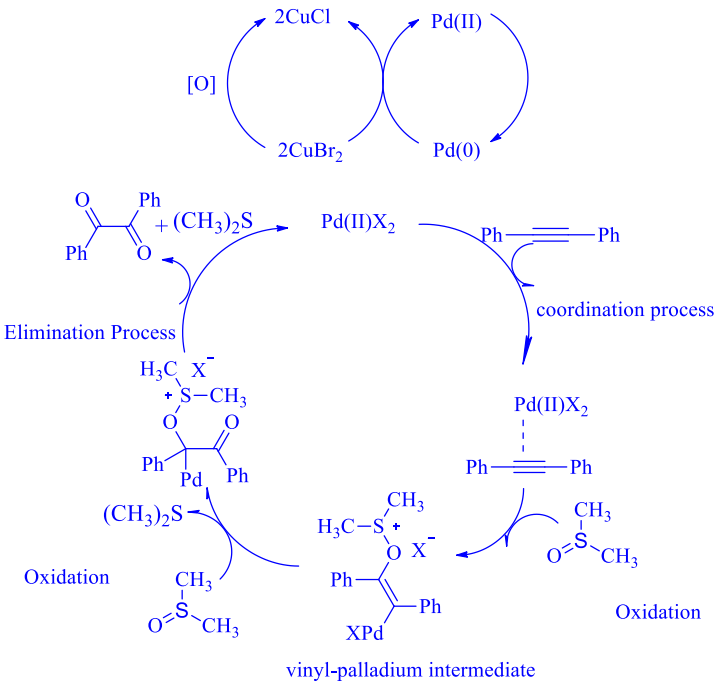

Scheme 8: Suggested mechanism for the oxidation of alkynes (Gao *et al.*, 2012; Xue *et al.*, 2018).

Several methods reported in literatures, was explored to synthesize α-diketones, among them (Mousset *et al.*, 2008), (Xu *et al.*, 2015), and (Gao *et al.*, 2012). However, a modified protocol to (Gao *et al.*, 2012) has been used to synthesis them by using bis(acetonitrile)palladium(II) dichloride complex as catalyst under microwave condition instead of palladium diacetate. Twelve aromatic α-diketones have been synthesized and nine of them are novel compounds. ^{1}H, ^{13}C NMR, IR, and mass spectroscopy have been used to characterize them.

Synthesis of substituted 5,6-diaryl-1,2,4-triazine analogues

α-diketones	R_1	R_2	MP °C	Yield %	Reference
(75)	H	H	120-121	82	(Giraud *et al.*, 2006)
*(76)	OCH_3	CHO	144-146	86	
*(77)	OCH_3	CN	195-197	85	
(78)	OCH_3	NH_2	158-160	32	(Mousset *et al.*, 2008)
*(79)	CH_3	OH	160-162	68	
(80)	OCH_3	OH	154-156	72	(Mousset *et al.*, 2008)
*(81)	OCH_3	NO_2	150-153	80	
*(82)	CH_3	NH_2	146-148	40	
*(83)	CH_3	F	112-114	88	
*(84)	OCH_3	$COCH_3$	117-119	67	
*(85)	OCH_3	CH_3	128-131	91	
*(86)	CN	OH	>230	59	

Table 2: synthesised substituted 1,2-diketones with yield.

* 1,2-diketones are novel compounds.

Synthesis of 1,2,4-triazine-3(2H)-one derivatives

Triazine is a hexaheterocyclic scaffold with three nitrogene atoms found in three isomers figure-17, which aquired exceptional interest due to its broad reach biological activity such as anticancer (Smith *et al.*, 2012), antifungal (Singh *et al.*, 2012), anti-malarial, anti-inflamatory, antiviral, analgesic (Singla *et al.*, 2015), and antihypertensive activity (Heilman *et al.*, 1979).

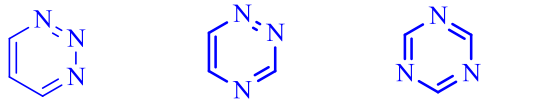

1,2,3-triazine 1,2,4-triazine 1,3,5-triazine

91 92 93

Figure 17: Structures of triazine isomers.

Synthesis of substituted 5,6-diaryl-1,2,4-triazine analogues

1,3,5-Triazine isomers, typically, prepaired from the reaction of Cyanuric acid with substituted amines :

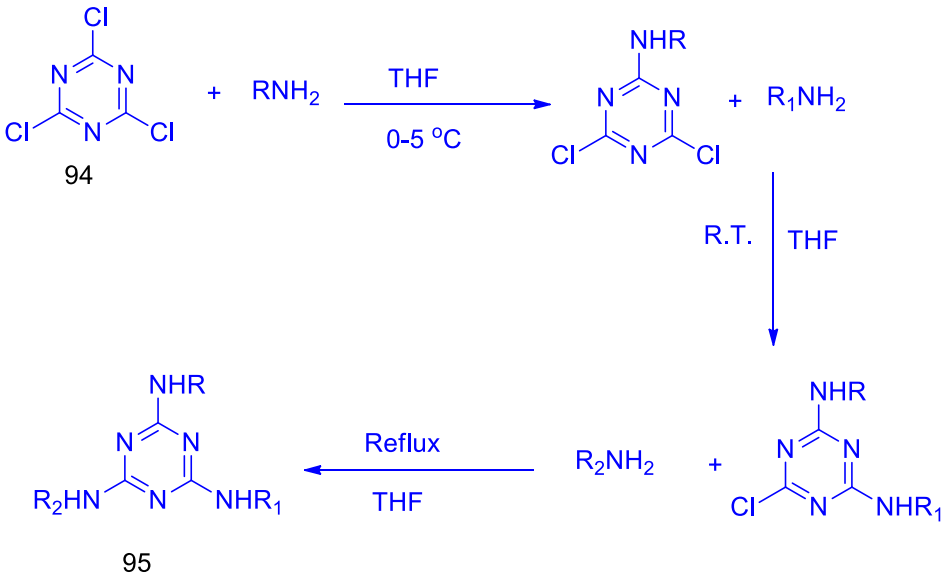

Scheme 9: Synthetic pathway for 1,3,5-triazine synthesis (Singla *et al.*, 2015).

However, 1,2,4-triazines mainlly prepared from benzils derivatives and substituted hydrazines by cyclocondensation reaction. The synthesis of 1,2,4-triazine-3-one from benzil and semicarbazide in acidic medium was invistigated (Mullick *et al.*, 2009) with zero yield product. Consequently, the reaction was carried out in basic medium by using lithium hydroxide as a catalyst and ethanol as a solvent. Semicarbazide hydrochloride was used to prepare triazine analogues, as an alternative for semicarbazide (Arquero *et al.*, 1998). This protocol was operative to prepare compound (**87)**, but it didn't work for compounds 87c, 87d, 87e (scheme 10).

Synthesis of substituted 5,6-diaryl-1,2,4-triazine analogues

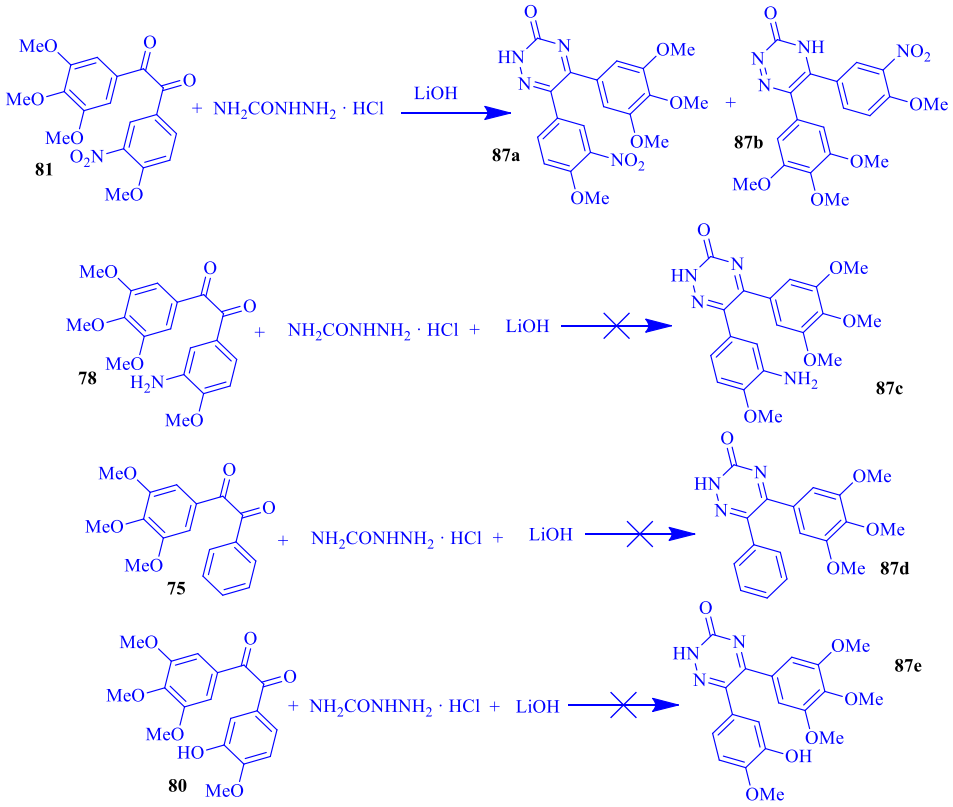

Scheme 10: Explored reactions to prepare 5,6-diaryl-1,2,4-triazine analogues.

Several attempts were carried out to optimize the reaction by using NaOH, KOH, and operating reaction under microwave irriradiation. However, none of these were efficient to produce the required final product. The electronic density around carbonyl group could be a crucial factor for the success of the reaction, as the reaction mechanisim is relying on the attack of nucleophile to the carbonyl group. Therefore, the reaction worked well with the electron withdrawing group NO_2, but no product was produced with the electron donating group like OH, and NH_2 and OCH_3.

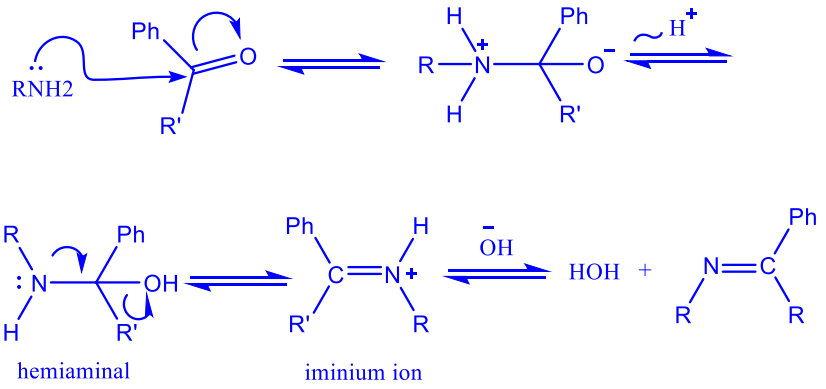

Scheme 11: mechanism of imine formation (Grossman, 1999).

Chapter 3

Synthesis of substituted pyridyl-phenyl sulfonamide derivatives

3 Synthesis of substituted pyridyl-phenyl sulphonamide derivatives:

Sulphonamides are an important organic scaffold having many applications in pharmaceutical industries. They also possess a variety of biological activities including anti-bacterial, anti-hypertensive, anti-epileptic, anti-inflammatory, anti-HIV, and anti-cancer (Lavanya, 2017).

Sulphonamides are synthetically derived from sulfonyl chloride and substituted amines in a basic medium as a catalyst (with, e.g., triethylamine or pyridine). Alternatively, these compounds can be synthesized from aryl iodide and sulphur dioxide with catalytic indium or palladium (Emmett *et al.*, 2014; Kim & Jang, 2007).

Much literature has been published on the synthesis of sulphonamides considering different substrates such as thiol (Veisi *et al.*, 2011), sulfonic acid or sulfonate salts (De Luca & Giacomelli, 2008), and Grignard reagents (Woolven *et al.*, 2011).

This chapter explores the synthesis of pyridinyl-phenyl sulphonamides derivatives synthesized through a multi-step approach. A substituted N-phenyl-3-nitropyridine-2-amine (**97**) was synthesised as the starting material, which was then converted to a substituted pyridine-2,3-diamine (**98**) by reduction of the nitro group to amine. The substituted pyridine diamine efficiently reacted with aryl sulfonyl chlorides (scheme 12).

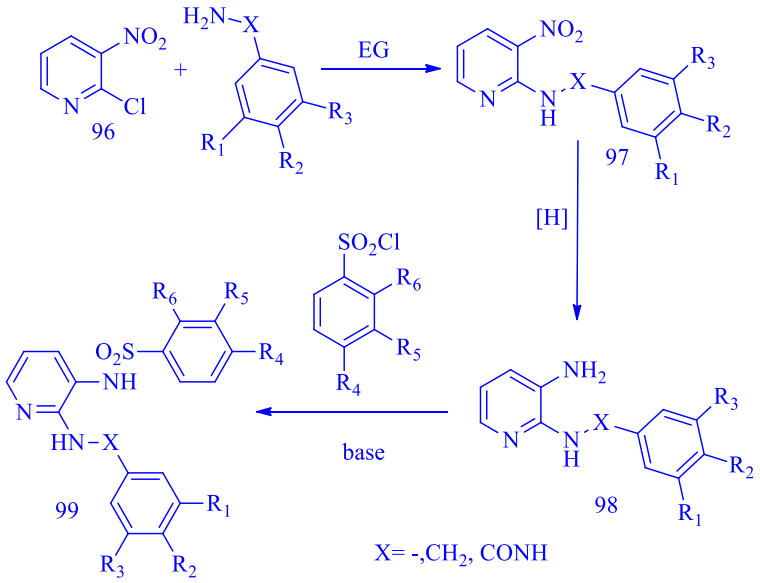

Scheme 12: Synthesis of substituted pyridyl-phenyl sulphonamide derivatives.

3.1 Synthesis of substituted N-phenyl-3-nitropyridine-2-amines.

3-Nitro-N-(3,4,5-trimethoxyphenyl)pyridin-2-amine (100)

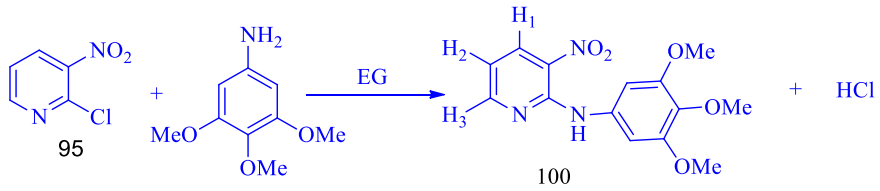

Procedure a: A mixture of 2-chloro-3-nitro pyridine (1.585 g, 10 mmol., 1 eq.) and 3,4,5-trimethoxy aniline (2.015 g, 11 mmol., 1.1 eq.) in ethylene glycol (15 cm^3) was irradiated in a microwave vial for 2 hours at 100 W and 70ºC. After completion of the reaction, water was added, and the mixture was extracted with ethyl acetate (3 x 30 cm^3), and the organic layer dried with anhydrous $MgSO_4$. The solvent was evaporated under reduced pressure and the crude solid was purified by flash chromatography (hexane: ethyl acetate 7:3, R_f=0.21) to obtain a red crystalline solid (2.6 g, 8.51 mmol., 85%). Mp = 144-145 ºC, lit. Mp =140-141(Robison & Finch, 1970)

Procedure b: A mixture of 2-chloro-3-nitro pyridine (1.585 g, 10 mmol., 1 eq.) and 3,4,5-trimethoxy aniline (2.015 g, 11 mmol., 1.1 eq.) in ethylene glycol (15 cm^3) was heated conventionally for 12-14 hrs at 100ºC. After completion of the reaction, water was added, and the mixture extracted with ethyl acetate (3 x 30 cm^3), and the organic layer dried with $MgSO_4$. The solvent was evaporated under reduced pressure and the crude solid was purified by flash chromatography (hexane: ethyl acetate 7:3, R_f =0.21) to obtain a red crystalline solid (2 g, 6.55 mmol., 66%). Mp = 144-145 ºC, lit. Mp =140-141 ºC (Robison & Finch, 1970).

^{1}H NMR :δ (ppm) =3.88 [3 H, s, (CH_3O)], 3.91 [6 H, s, 2 x (CH_3O)], 6.85 [1H, dd, J=8.41 Hz, 4.6 Hz, Py-H2], 6.92 [2 H, s, *ortho* to methoxy], 8.52 [1H, d, J=4.6 Hz, 1.75 Hz, Py-H1], 8.58 [1H, dd, J=8.42 Hz, 1.75 Hz, Py-H3], 10.07 (1H, s, NH)

^{13}C NMR : δ (ppm) = 56.33 [2 x (CH_3O)], 61.08 [(CH_3O)], 100.61 [C-H, *ortho* to methoxy], 113.81[C-H, Py-C-H2], 128.62 [C-O, Ar-C-O-CH_3], 133.60 [C-N, Ar-C-NH], 135.43 [C-N, Py-C-NO_2], 135.71[C-H, Py-C-H1], 150.37 [C-N, Py-C=N], 153.40 [2 x C-O, Ar-C-OCH_3], 155.32 [C-H, Py-C-H3].

FT-IR: ν_{max} **(**cm^{-1}): 3342 (NH str.), 3095 (C-H str., arom.), 2832 (C-H str., aliph.), 1592 (C=C str., arom.), 1504 (N-O asy. str., NO_2), 1420 (N-O sym. str.), 1124 (C-O-CH_3 asy.

str.). Following procedure b N-phenyl-3-nitropyridine-2-amine (102-109) were synthesised.

N-(3-Hydroxy-4-methoxyphenyl)-3-nitropyridin-2-amine (101):

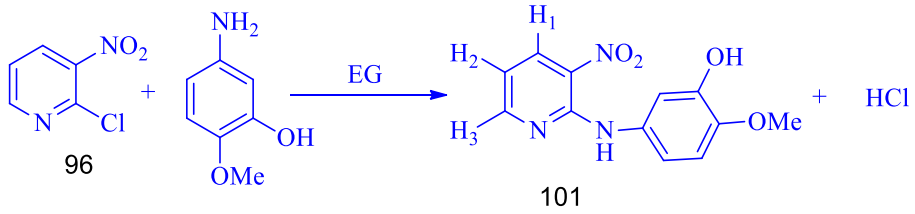

Using 5-amino-2-methoxyphenol (1.530 g, 11 mmol, 1.1 eq), the above 3-nitro-pyridine-2-amine (101) was obtained as a black solid (1.427 g, 6.62 mmol., 55%). Mp =160-162 ºC, after flash column purification (SiO_2, hexane: ethyl acetate 7:3, R_f=0.2).

HRMS (ESI): calculated for $C_{12}H_{14}N_3O_2$ (M+H) = 262.0828, found (M+H) = 262. 0840, ΔMs=1.2ppm.

^{1}H NMR: δ (ppm) =3.93 [3H, s, (CH_3O)], 5.73 [1H, s, OH], 6.80 [1H, dd, J = 8.32, 4.38 Hz, Py-H_2], 6.87 [1H, d, J = 8.6 Hz *meta* to OH, Ar-H], 7.02 [1H, dd, J= 8.6 Hz, 2.2 Hz *para* to OH, Ar-H], 7.32[1H,d, J = 2.2 Hz *ortho* to OH, Ar-H], 8.48 [1H, d, J = 4.33 Hz, Py-H_1], 8.53 [1H, d, J = 8.33 Hz, Py-H_3], 9.98 [1H, s, NH].

^{13}C NMR: δ (ppm) =56.19 [(CH_3O)], 110.41[C-H, Ar-C-H *ortho* to OH], 110.52[C-H, Ar-C-H *para* to OH], 110.81 [C-H, Ar-C-H *meta* to OH], 114.82 [C-H, Py-C-H2], 128.35 [C-O, Ar-C-OH], 131.44 [C-N, Ar-C-NH], 135.53 [C-H, Py-H1], 144.19 [Py-C-NO_2], 145.80 [C-N, Py-C=N], 150.65 [C-O, Ar-C-OCH_3], 155.32 [C-H, Py-C-H3].

FT-IR: ν_{max} (cm^{-1}): 3546.87 (OH Str.), 3340.38 (NH str.), 2998.85 (C-H str., aromatic), 2826.12 (C-H str., aliphatic), 1603.15 (C=C str., aromatic), 1506.10 (N-O asy. str., NO_2), 1446.07 (N-O sym. str., NO_2), 1126.47 (C-O-CH_3 asy. str.).

N-(3-Flouro-4-methoxyphenyl)-3-nitropyridin-2-amine (102):

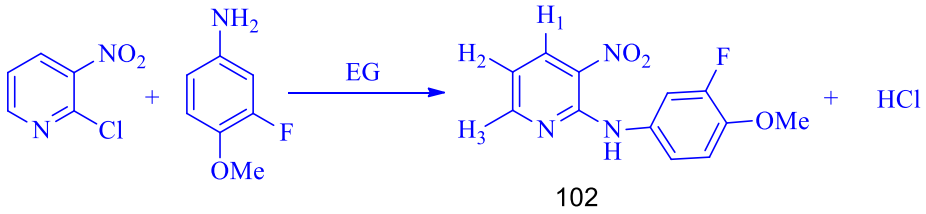

Using 3-fluoro-4-methoxy aniline (1.55 g, 11 mmol., 1.1 eq.), the above 3-nitro-pyridine-2-amine (97) was obtained as a black solid (1.99 g, 7.56 mmol., 76%). Mp =129-130 ºC, after flash column purification (SiO_2: hexane: ethyl acetate 8:2, R_f = 0.15).

HRMS (ESI): calculated for $C_{12}H_{11}N_3O_3F$ (M+H) = 264.0792, found (M+H) = 264.0784, ΔMs=0.8ppm.

^{1}H NMR : δ (ppm) =3.89 [3 H, s, (CH_3O)], 6.82 [1H, dd, J = 8.32 Hz, 4.54 Hz, Py-H_2], 6.98 [1H, t, J= 18.07 Hz *ortho* to F, Ar-H], 7.58 [1H, dt, J = 8.9 Hz, 4.05 Hz *para* to F , Ar-H], 7.61 [1H, dd, J = 12.9 Hz, 2.59 Hz, *meta* to F, Ar-H], 8.45 [1H, dd, J = 4.58 Hz, 1.86 Hz Py-H_1], 8.49 [1H, dd, J = 8.38 Hz, 1.86 Hz, Pyr-H_3], 9.99 (1H, s, NH).

^{13}C NMR : δ (ppm) =56.58 [(CH_3O)], 111.73 [C-H, d, J=22.08 Hz, Ar-C-H *ortho* to F], 113.95 [C-H, d, J=2.8 Hz, Ar-C-H *para* to F], 113.95 [C-H, Py-C-H2], 118.41 [C-H, d, J=3.53 Hz, Ar-C-H *meta* to F], 128.53 [C-N, Py-C-NO_2], 131.07 [C-N, d, J=9.34 Hz, Ar-C-NH], 135.60 [C-H, Py-C-H1], 144.88 [C-O, d, J=10.91 Hz, Ar-C-OCH_3], 150.24 [C-N, Py-C=N], 150.84 [C-F, d, J=245.41 Hz], 155.33 [C-H, Py-C-H3].

FT-IR: ν_{max} (cm^{-1}) 3313 (NH str), 3092 (C-H str., aromatic), 2801 (C-H str., aliphatic), 1608 (C=C str., aromatic), 1501 (N-O asy. str., NO_2), 1438 (N-O sym. str.), 1150 (C-O-CH_3 asy. str.).

N-(4-Hydroxy-3-methylphenyl)-3-nitropyridin-2-amine (103):

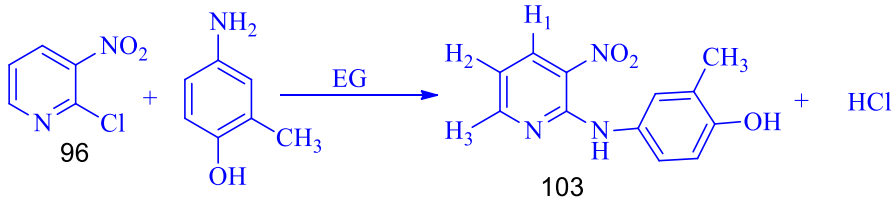

Using 4-amino-2-methyl phenol (1.35g, 11 mmol, 1.1eq), the above 3-nitro-pyridine-2-amine (103) was obtained as a black solid (2.20 g, 8.97 mmol., 90%). Mp =178-180 ºC, after purification column chromatography (hexane: ethyl acetate 8:2, R_f=0.21).

HRMS (ESI): calculated for $C_{12}H_{12}N_3O_3$ (M+H) = 246.0876, found (M+H) = 246.0879, ΔMs=0.3ppm.

^{1}H NMR (d6-acetone): δ(ppm) =2.13 [3H, s, (CH_3)], 6.76 [1H, d, J=8.41 Hz, *meta* to CH_3, Ar-H], 6.88 [1H, dd, J=8.36 Hz, 4.55 Hz, Py-H_2], 7.20 [1H, dd, J=8.41Hz, 2.67Hz, *para* to CH_3, Ar-H], 7.24 [1H, d, J=2.64 *ortho* to CH_3, Ar-H], 8.45 [1H, dd, J=4.6 Hz, 1.75 Hz, Py-H1], 8.49 [1H, dd, J=8.35 Hz, 1.75 Hz, Py-H3], 9.81 (1H, s, NH).

^{13}C NMR (d6-acetone): δ(ppm) =16.31 [(CH_3)], 114.24 [C-H, Ar-C-H *ortho* to CH], 115.40 [C-H, Py-H2], 122.82 [C-H, Ar-C-H *meta* to CH_3], 125.28 [C-C, Ar-C-CH_3], 126.86 [C-H, Ar-C-H *para* to CH_3], 129.36 [C-N, Ar-C-NH], 131.07 [C-N , Py-C-NO_2], 136.18 [C-H, Py-H1], 151.51 [C-O, Ar-COH], 153.52 [C-N, Py-C=N], 156.28 [C-H, Py-H3].

FT-IR ν_{max} (cm^{-1}): 3380 (OH str), 3354 (N-H str.), 3094 (C-H str., aromatic), 2950 (C-H str., aliphatic), 1585 (C=C str., aromatic), 1496 (N-O asy. str., NO_2), 1431 (N-O sym. str.), 1149 (C-O-CH_3 asy. str.).

N-(3-Fluoro-4-hydroxyphenyl)-3-nitropyridin-2-amine (104):

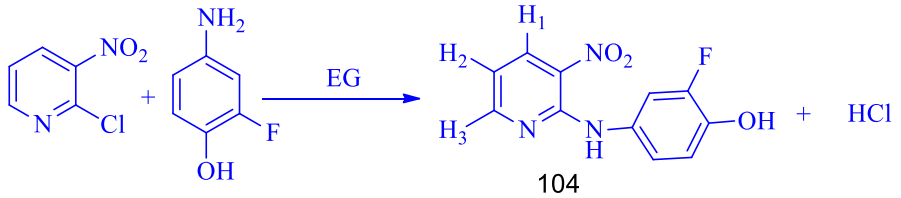

104

Using 4-amino-2-flouro phenol (1.39 g, 11 mmol., 1.1 eq.), the above 3-nitro-pyridine-2-amine (104) was obtained as black solid (2.205 g, 8.8 mmol., 89%). Mp=133-135ºC, after purification by column (hexane: ethyl acetate 8:2, R_f =0.17). HRMS (ESI): calculated for $C_{11}H_9FN_3O_3$ (M+H) =250.0627, found for (M+H) =250.0624, ΔMs=0.3ppm.

^{1}H NMR: δ (ppm) = 5.18 [1H, S, OH], 6.81 [1H, dd, J= 8.35 Hz, 4.55 Hz, Py-H2], 6.98 [1H,dt, J=18.25 Hz, 8.91 Hz *ortho* to F, Ar-H], 7.10 [1H, dd, J=8.84 Hz, 3.82 Hz *para* to F, Ar-H], 7.59 [1H, dd, J=12.23 Hz, 2.51 Hz *meta* to F, Ar-H], 8.45[1H, dd, J= 4.56 Hz, 1.85 Hz,Pyr-H1], 8.52 [1H,dd, J=8.35 Hz, 1.85 Hz , Pyr-H3], 9.98 [1H, s, N-H].

^{13}C NMR : δ (ppm) =111.13 [C-H, d, J=22.3 Hz, Ar-C-H *ortho* to F], 113.94 [1C, C-H, Py-C-H2], 117.25 [C-H, d, J= 2.93 Hz, Ar-C-H *para* to F], 119.47[C-H, d, J=3.30 Hz, Ar-C-H *meta* to F], 130.77 [C-N, d, J=9.37 Hz, Ar-C-NH], 135.66 [C-H, Py-C-H1], 140.73 [C-O, d, J=14.4 Hz, Ar-C-OH], 149.36 [C-F, d, J= 236.30 Hz, Ar-C-F], 150.31 [C-N, Py-C-NO_2], 152.79 [C-N, Py-C=N], 155.28 [C-H, Py-C-H3].

FT-IR: ν_{max} (cm^{-1}): 3330 (NH, OH str.), 3086 (C-H str., aromatic), 2961 (C-H str., aliphatic), 1597 (C=C str., aromatic), 1509 (N-O asy. str., NO_2), 1492 (N-O sym. str.), 1188 (C-O-CH_3 asy. str.).

N-(4-Bromo-3-fluorophenyl)-3-nitropyridin-2-amine (105):

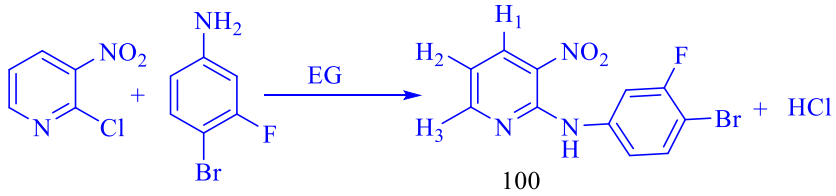

100

Using 4-bromo-3-flouroaniline (2.090 g, 11 mmol., 1.1 eq.), the above 3-nitro-pyridine-2-amine (105) was obtained as orange solid (2.721 g, 8.75 mmol., 88%, Mp =158-159 ºC), after purification by column chromatography (hexane: ethyl acetate 9:1, R_f = 0.26). HRMS (ESI): calculated for $C_{11}H_8BrFN_3O_2$ (M+H) = 311.9783, found (M+H) = 311.9785, ΔMs=0.2ppm.

^{1}H NMR :δ (ppm) = 6.89 [1H, dd, J= 8.37 Hz, 4.61 Hz, Py-H2], 7.17 [1H, dq, J= 2.46 Hz , 1.04 Hz, Ar-H, *para* to F], 7.49 [1H, t, J= 8.17 Hz , Ar-H, *meta* to F], 7.84 [1H, dd, J= 10.86 Hz, 2.46 Hz , Ar-H, *ortho* to F], 8.50 [2H, (1H, dd, J= 4.66 Hz, 1.84 Hz, Py-H1), (1H, dd, J=8.39 Hz, 1.84 Hz, Py-H3)].

^{13}C NMR : δ (ppm) =103.17 [C-Br, d, J=21.41 Hz, *ortho* to F], 110.02 [C-H, d, J= 27.24 Hz , Ar-C-H *ortho* to F], 114.85 [C-H, Py-H2], 118.32 [C-H, d, J= 3.12 Hz , Ar-C-H *meta* to F], 129.09 [C-N, Py-C-NO_2], 113.20 [C-H, d, J=1.36 Hz , Ar-C-H *para* to F], 135.65 [C-H, Py-H1], 138.82 [C-N, d, J=10.07 Hz, Ar-C-NH], 149.42 [C-N, Py-C=N], 154.93 [C-H, Py-H3], 157.84 [C-F, d, J=246.73 Hz].

FT-IR: ν_{max} **(**cm^{-1}): 3317 (NH str.), 3063 (C-H str.), 1591 (NH bend.), 1572 (C=C str., aromatic), 1498 (N-O asy. str., NO_2), 1442 (N-O sym. str.), 1187 (Ar-O-CH_3 asy. str.), 1049 (C-F).

3-Nitro-*N*-(3,4,5-trifluorophenyl)pyridin-2-amine (106)

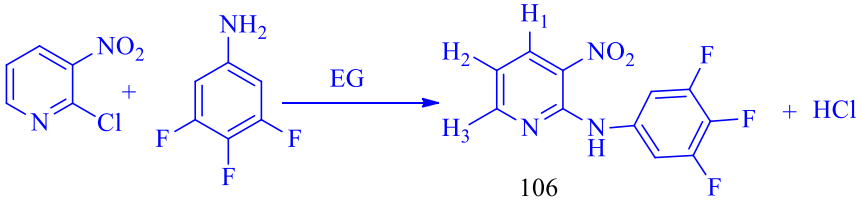

106

Using 3,4,5-trifluoroaniline (1.6181 g, 11 mmol., 1.1 eq), the above 3-nitro-pyridine-2-amine (106) was obtained as a red solid (2.155 g, 7.27 mmol., 80%). Mp =165-167 ºC, after purification by column chromatography (hexane: ethyl acetate 9:1, R_f = 0.26). HRMS (ESI): calculated for $C_{11}H_7F_3N_3O_2$ (M+H) = 270.0490, found (M+H) = 270.0495, ΔMs=0.5ppm.

^{1}H NMR : δ (ppm) = 6.89 [1H, dd, J= 8.33 Hz, 4.59 Hz, Py-H2], 7.37 [2 H, m, Ar-H, *ortho* to F], 8.45 [2 H, (1H, dd, J=4.53 Hz, 1.75 Hz, Py-H1), (1H, dd, J=8.34 Hz,1.75 Hz, Py-H3].

^{13}C NMR: δ (ppm) =106.10 [C-H, dd, J= 18.44 Hz, 7.12 Hz, Ar-C-H], 115.08 [C-H, Pyr-H2], 129.09 [C-N, Py-C-NO_2], 133.71 [C-N, dd, J=11.53 Hz, 4.12, Hz, Ar-C-NH], 135.15 [C-F,dt, J= 248.17 Hz, 15.52 Hz], 149 [C-N, Py-C=N], 149.82 [C-F, ddd, J=247.91, 10.31, 5.37 Hz, Ar-F], 154.86 [C-H, Py-H3].

FT-IR: ν_{max} (cm^{-1}): 3551 (NH str.), 2974 (C-H str., aromatic), 1624 (C=C str., aromatic), 1583 (N-O asy. str., NO_2), 1501 (N-O sym. str.), 1185 (C-O-CH_3 asy. str.).

3-Nitro-N-(2,4,5-trifluorophenyl)pyridin-2-amine (107)

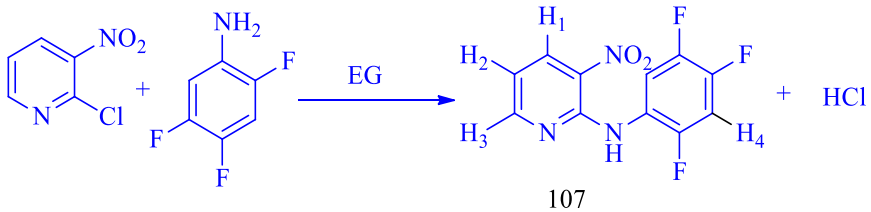

107

Using 2,4,5-trifluoroaniline (1.6181 g, 11 mmol., 1.1eq), The above 3-nitro-pyridine-2-amine (107) was obtained as a yellow crystalline solid (1.524 g, 5.66 mmol., 46%). Mp=127-128 ºC, after column chromatography purification (hexane: ethyl acetate 9:1, R_f = 0.26). HRMS (ESI): calculated for $C_{11}H_7F_3N_3O_2$ (M+H) = 270.0490, found (M+H) = 270.0497, ΔMs=0.7ppm.

^{1}H NMR :δ (ppm) = 6.92 [1H, dd, J= 8.34 Hz, 4.58 Hz, Py-H2], 7.37 [1H, m, Ar-H,], 8.39 [1H, m, Ar-H], 8.50-8.56 [2H, (1H, dd, J= 4.57 Hz, 1.79 Hz, Py-H3), (1H, dd, J=8.34 Hz, 1.80 Hz, Py-H1], 10.21 [1H, NH].

^{13}C NMR : δ (ppm) =104.72 [C-H, dd, J=25.22 Hz, 21.71 Hz, Ar-C-H4], 111.59 [1C, dd, J=24.86 Hz, 1.51 Hz, Ar-C-H], 115.03 [C-H, Py-H2], 122.95-123.20 [C-N, m, Ar-C-NH], 129.38 [C-N, Py-C-NO_2], 135.60 [C-H, Py-H1], 144.26-146.99 [C-F, ddd, J= 248.66 Hz, 15.01 Hz, 11.45 Hz, Ar-C-F], 144.85-147.42 [C-F, ddd, J= 241.44 Hz, 12.64 Hz, 3.95 Hz, Ar-C-F], 147.78-150.21 [C-F, ddd, J=243.85 Hz, 9.01 Hz, 2.98 Hz, Ar-C-F], 149.03 [C-N, Py-C=N], 154.74 [C-H, Py-H3].

FT-IR: ν_{max} (cm^{-1}): 3551 (NH str.), 2974 (C-H str. aromatic), 1624 (C=C str., aromatic), 1583 (N-O asy. str., NO_2), 1501 (N-O sym. str.), 1185 (Ar-O-CH_3).

3-Nitro-N-(4-hydroxy-3-methoxyphenyl)pyridin-2-amine (108):

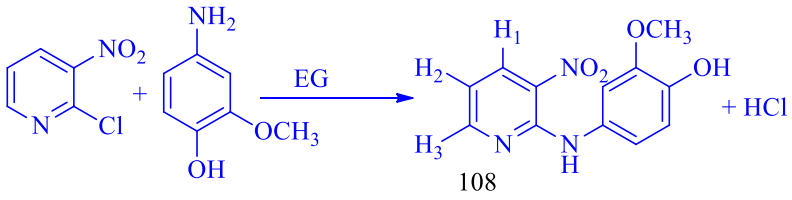

108

Using 4-hydroxy-3-methoxyaniline (1.530 g, 11mmol., 1.1 eq), the above title compound (108) was obtained as a black solid (1.251 g, 4.7 mmol., 48%). Mp=138-140 ºC, after flash column purification (hexane: ethyl acetate 8:2, R_f=0.20). HRMS (ESI): calculated for $C_{12}H_{12}N_3O_4$ (M+H) = 262.0827, found (M+H) = 262.0833, ΔMs=0.6ppm.

^{1}H NMR : δ (ppm) = 3.89 [3H, s, (OCH_3)], 5.42 [1H, s, OH], 6.74 [1H, dd, J= 8.38 Hz, 4.55 Hz, pyr-H2], 6.89 [1H, d, J=8.46 Hz, Ar-H, *ortho* to OH], 6.99 [1H, dd, J= 8.46 Hz, 2.34Hz, Ar-H , *meta* to OH], 7.15 [1H, d, J=2.34 Hz, Ar-H, *ortho* to (OCH_3)], 8.41 [1H, dd, J= 4.55 Hz, 1.75 Hz, Py-H1], 8.47 [1H, dd, J= 8.38 Hz, 1.75 Hz, Py-H3], 9.93 [1H, s, NH].

^{13}C NMR : δ (ppm) =56.05 [(OCH3)], 107.37 [C-H, Ar-C-H *ortho* to methoxy], 113.41 [C-H, Ar-C-H *meta* to methoxy], 114.44 [C-H, Py-C-H2], 116.64 [C-H, Ar-C-H *para* to methoxy], 128.30 [C-O, Ar-C-OCH_3], 130.13 [C-N, Ar-C-NH], 135.59 [C-H, Py-C-H1], 143.36 [C-N, Py-C-NO_2], 146.54 [C-N, Py-C=N], 150.88 [C-O, Ar-C-OH], 155.55 [C-H, Py-C-H3].

FT-IR: ν_{max} (cm^{-1}): 3542 (NH str.), 3308 (OH str.), 2940 (C-H str., aromatic), 2820 (C-H str., aliphatic), 1614 (NH, bend), 1582 (C=C str., aromatic), 1466 (N-O asy. str., NO_2), 1438 (N-O sym. str.), 1107 (C-O-CH_3 asy str.).

3-Nitro-N-(4-hydroxy-3-methylphenyl)pyridin-2-amine (109):

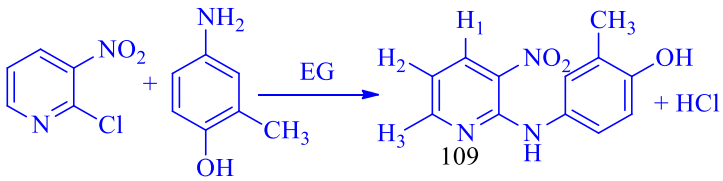

109

Using 4-hydroxy-3-methylaniline (1.354 g, 11 mmol, 1.1 eq), the above 3-nitro-pyridine-2-amine (109) was obtained as a dark brown solid (1.501 g, 6.09 mmol., 61%, Mp=136-139 ºC), after column purification (hexane : ethyl acetate 7:3, R_f =0.22). HRMS (ESI): calculated for $C_{12}H_{12}N_3O_3$ (M+H) = 246.0878, found (M+H) = 246.0886, ΔMs=0.8ppm.

^{1}H NMR: δ (ppm**)** = 2.15 [3H, s, (CH_3)], 4.09 [1H, s, OH], 6.77 [1H, dd, J= 8.32 Hz, 4.51 Hz, Py-H2], 6.90 [1H, dd, J=8.04 Hz, 2.13 Hz, Ar-H, *para* to CH_3], 7.08 [1H, d, J=8.05Hz, Ar-H , *meta* to CH_3], 7.15 [1H, d, J=2.11Hz, Ar-H, *ortho* to (CH_3)], 8.42 [1H, dd, J= 4.51 Hz, 1.77 Hz, Py-H1], 8.49 [1H, dd, J= 8.31 Hz, 1.78 Hz, Py-H3], 9.97 [1H, s, NH].

^{13}C NMR: δ (ppm) =30.96 [(CH3)], 110.24 [C-H, Ar-C-H ortho to CH_3], 113.64 [C-H, Ar-C-H para to CH_3], 115.21 [C-H, Py-C-H2], 121.37 [C-C, Ar-C-CH_3], 128.62 [C-N, Ar-C-NH], 131.21 [C-H, Ar-C-H meta to CH_3], 135.84 [C-H, Py-C-H1], 136.23 [C-N, Py-C-NO_2], 150.56 [C-N, Py-C-NH], 154.50 [C-O, Ar-C-OH], 155.15 [C-H, Py-C-H3].

FT-IR: ν_{max} **(**cm^{-1}): 3437 (OH str.), 3318 (NH St.), 3048 (C-H str.), 2818 (C-H str., aliphatic), 1612 (NH, bend), 1579 (C=C str., aromatic), 1505 (N-O asy. str., NO_2), 1413 (N-O sym. str.).

3-Nitro-N-(3,4,5-trimethoxybenzyl)pyridin-2-amine (110)

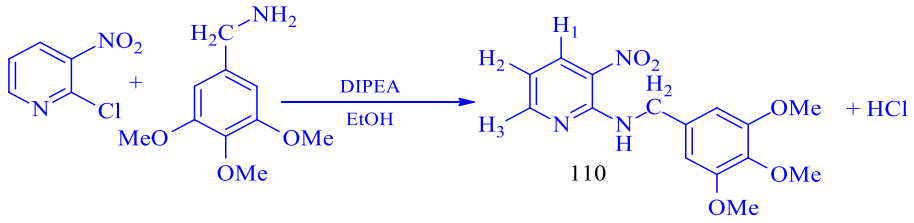

To a stirred solution of 2-chloro-3-nitropyridine (1.585 g, 10 mmol, 1 eq.) in ethanol (10 cm^3), placed in -10 ˚C ice bath, was added diisopropyl-ethylamine (DIPEA) (3.48 cm^3, 20 mmol., 2 eq.) dropwise over 15 min. Thereafter, 3,4,5-trimethoxybenzylamine (1.02 cm^3, 12 mmol, 1.2 eq.) was added and the temperature increased gradually to 80 ˚C and stirred for 6-8 hours. The solvent was evaporated, and water (15 cm^3) was added to the resulting crude product which was extracted with (3 x 30 cm^3) ethyl acetate. The organic layer was separated, dried over anhydrous $MgSO_4$, filtered, and solvent removed by rotary evaporation. Flash column purification (petroleum ether: ethyl acetate 8:2, R_f = 0.17) was carried out to obtain the required product as a yellow solid (2.801 g, 8.77 mmol., 88%, Mp=120-122 ºC). HRMS (ESI): calculated for $C_{15}H_{17}N_3O_5$ (M+H) = 320.1246, found (M+H) = 320.1250, ΔMs=0.4ppm.

^{1}H NMR: δ (ppm) =3.83 [9 H, s, 3 x (OCH_3)], 4.74 [2 H, d, J= 5.62 Hz, (CH_2-NH), 6.59 [2 H, s, Ar-H trimethoxy ring], 6.64 [1H, dd, J= 8.38 Hz, 4.51 Hz , Py-H2], 8.37 [1H,dd, J=4.51 Hz, 1.73 Hz, Py-H1], 8.37 [1H, dd, J=8.33 Hz, 1.73 Hz, Py-H3], 8.46 [1H, t, J= 5.6 Hz, N-H].

^{13}C NMR : δ (ppm) = 45.37 [CH_2], 56.09 [2 x (OCH_3)], 60.78[(OCH_3)], 104.74 [C-H, Ar-H *ortho* to methoxy], 112.17 [C-H, Py-H2], 128.13 [C-O, Ar-C-OCH_3], 133.91 [C-CH_2, Ar-H], 135.31 [C-H, Py-H1], 137.27 [C-N, Py-C-NO_2], 152.23 [C=N, Pyr-N], 153.40 [2 x C-O, Ar-C-OCH_3], 155.67 [C-H, Py-H3].

FT-IR: ν_{max} (cm^{-1}): 3401 (NH str.), 3065 (C-H str., aromatic), 2943 (C-H str., aliphatic), 1592 (C=C str., aromatic), 1571 (N-O asy. str., NO_2), 1493 (N-O sym.str.), 1123 (C-O-CH_3 asy. str.).

3,4,5-Trimethoxy-N'-(3-nitropyridin-2-yl)benzohydrazide (111):

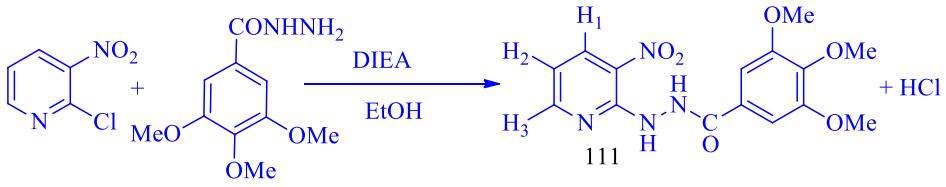

To a stirred solution of 2-chloro-3-nitropyridine (1.585g, 10 mmol, 1eq.) in DMF (10 cm^3), placed in -10 ˚C ice bath, was added DIPEA (3.48 cm^3, 20 mmol., 2.0 eq.) dropwise over 15min. Thereafter, 3,4,5-trimethoxybenzyhydrazide (2.714g, 12 mmol, 1.2 eq) was added and temperature increased gradually to 120 ˚C. The reaction was stirred for 12 hours. After consumption of the starting material, the reaction was cooled, and water (15 cm^3) was added to the mixture, which was extracted with (3 x 30 cm^3) ethyl acetate. The organic layer was separated, dried over anhydrous $MgSO_4$, filtered, and solvent removed by rotary evaporation. Column purification was carried out to obtain the required product as a yellow-orange solid (2.258, 6.48 mmol., 65%) Mp = 184-185ºC, lit. Mp=162-164 ºC (Murty *et al.*, 2016), after column purification (petroleum ether: ethyl acetate 8:2, R_f = 0.4).

^{1}H NMR : δ (ppm) =3.88 [6 H, s, 2 x (OCH_3)], 3.87 [3H, s, (OCH_3)], 6.86 [1H, dd, J= 8.38 Hz 4.69 Hz, Py-H2], 8.41 [1H, dd, J= 4.71 Hz, 1.64 Hz, Py-H1], 8.49 [1H, dd, J= 8.34Hz, 1.764 Hz, Py-H3], 9.38 [1H, d, J= 4.54 Hz, N-H], 10.15 [1H, d, J=4.57Hz, N-H].

^{13}C NMR : δ (ppm) = 56.419 [2 x (OCH_3)], 60.96 [(OCH_3)], 104.71 [C-H, Ar-H *ortho* to methoxy], 114.34 [C-H, Py-H2], 126.82 [C-O, Ar-C-OCH_3], 128.77 [C-C, Ar-C-CO], 135.39 [C-H, Py-H1], 141.67 [C-N, Pyr-NO_2], 149.86 [C-N, Py-C=N], 153.35 [2 x C-O, Ar-C-OCH_3], 154.27 [C-H, Py-H3], 164.69 [1C, C=O].

FT-IR: ν_{max} (cm^{-1}): 3417, 3319 (NH str.), 3081 (C-H str., aromatic), 2842 (C-H, aliphatic), 1612 (C=O Str.), 1587 (C=C str., aromatic), 1510 (N-O asy. str.., NO_2), 1483 (N-O sym. str.), 1127 (C-O-CH_3 asy. str.).

3.2 Synthesis of substituted 2,3-diaminopyridine:

N2-(3,4,5-Trimethoxyphenyl)pyridine-2,3-diamine (112):

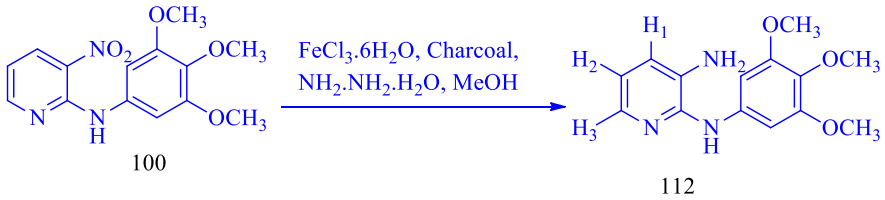

100 112

To a stirred solution of 3-nitro-N-(3,4,5-trimethoxyphenyl)pyridin-2-amine (100) (0.915 g, 3 mmol., 1 eq.) in methanol (25 cm^3) was added iron(III) chloride hexahydrate (0.064 g, 0.23 mmol., 0.08 eq.), and activated charcoal (0.064 g, 5.4 mmol., 1.8 eq.). After heating mixture under reflux for 10 min., (1.31 cm^3, 0.027 mmol., 9 eq.) hydrazine monohydrates 100% was added drop wise over 30 minutes and the mixture heated under reflux until completion of reaction (monitored by TLC). Cooling to room temperature, solvent was evaporated, the resulting sludge was dissolved in ethyl acetate (35 cm^3) and extracted with H_2O (3x 30 cm^3). The organic layer was dried over anhydrous $MgSO_4$ and solvent evaporated to obtain the required product as a dark brown solid (0.685 g, 83%). Mp = 158-160 ºC, lit. Mp =147 ºC (Robison & Finch, 1970) after purification by column chromatography (hexane: ethyl acetate 5:5, R_f = 0.16).

^{1}H NMR : δ (ppm) =3.25 [2 H, s, NH_2], 3.77 [3 H, s, (CH_3O)], 3.79 [6 H, s, 2 x (CH_3O)], 6.38 [1H, s, NH], 6.55 [2 H, s, Ar-H, *ortho* to CH_3O], 6.72 [1H, dd, J=8.41 Hz, 4.6 Hz, pyr-H2], 6.97 [1H, dd, J=4.6 Hz, 1.75 Hz, Pyr-H1], 8.58 [1H, dd, J=8.42 Hz,1.75 Hz,Pyr-H3].

^{13}C NMR: δ (ppm) = 56.04 [2 x (CH_3O)], 60.99 [(CH_3O)], 96.72 [C-H, Ar-C-H *ortho* to meyhoxy], 116.96 [C-H, Py-C-H2], 123.61[C-H, Py-C-H1], 131.04 [C-N, Ar-C-NH], 132.99 [C-O, Ar-C-O-CH_3], 138.30 [C-H, Py-C-H3], 145.70 [C-N, Py-C=N], 153.48 [C-O, 2 x Ar-C-OCH_3].

FT-IR: ν_{max} **(**cm^{-1}): 3405, 3387 (NH_2 str.), 2922 (C-H str., aromatic), 2824 (C-H str., aliphatic), 1602 (NH-ben. Primary amine), 1588 (C=C str., aromatic), 1129 (C-O-CH_3 asy. str.).

Following the above example, substituted 2,3-diaminopyridines (113-115) were synthesised.

N2-(4-hydroxy-3-methylphenyl)pyridine-2,3-diamine (113):

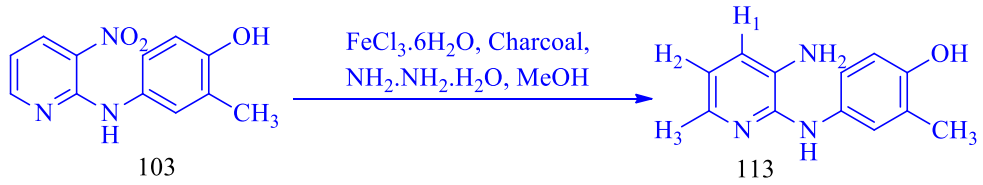

103 113

The above titled compound (113) was synthesised from N-(4-hydroxy-3-methylphenyl)-3-nitropyridin-2-amine (103) (1.45 g, 5.912 mmol., 1 eq.), $FeCl_3.6H_2O$ (0.127 g, 0.47 mmol., 0.08 eq.), activated carbon (0.127 g, 10.641mmol., 1.8 eq.) in 25 cm^3 methanol, and hydrazine monohydrate (2.57 cm^3, 53.2 mmol., 9 eq.), and obtained as brown solid (0.978 g, 0.45 mmol., 77%, Mp=211-213ºC), after purification by column chromatography (SiO_2, hexane: ethyl acetate 7:3, R_f = 0.15). HRMS (ESI): calculated for $C_{12}H_{14}N_3O$ (M+H) = 216.1137, found (M+H) = 216.1139, ΔMs=0.2ppm.

^{1}H NMR (d6-dmso): δ(ppm) = 2.11 [3H, s, (CH_3)], 5.04 [2H,s, NH_2], 6.52 [1H, dd, J= 7.53 Hz, 5.03 Hz, Py-H2], 6.67 [1H, d, J= 8.80 Hz, *meta* to CH_3, Ar-H], 6.83 [1H, dd, J=7.56 Hz, 1.67 Hz, Py-H1], 7.23 [2 H, m, *ortho* and *para* to CH_3, Ar-H], 7.38 [1H, dd, J=5.04 Hz, 1.57 Hz, Py-H3], 7.49 [1H, s, NH], 8.81 [1H, s, OH] .

^{13}C NMR (d6-dmso): δ(ppm) =16.26 [(CH_3)], 114.26 [C-H, Py-H2], 114.40 [C-H, Ar-C-H *meta* to CH_3], 118.40 [C-H, Ar-C-H *ortho* to CH_3], 118.88 [C-H, Py-H1], 122.58 [C-H, Ar-C-H *para* to CH_3], 123.42 [C-C, Ar-CH_3], 131.15 [C-N, Ar-C-NH], 132.96 [C-N , Py-C-NH2], 133.43 [C-H, Py-H3], 144.59 [C=N, Py-C=N], 149.90 [C-O, Ar-O-C].

FT-IR: ν_{max} **(**cm^{-1}): 3380.34 (OH str), 3354.35 (N-H str.), 3094.97 (C-H str., aromatic), 2950.52 (C-H str., aliphatic), 1585.07 (C=C str., aromatic), 1496.31 (N-O asy. str., NO_2), 1431.64 (N-O sym. str.), 1149.04 (C-O-CH_3 asy. str.).

N2-(4-Hydroxy-3-fluorophenyl)pyridine-2,3-diamine (114):

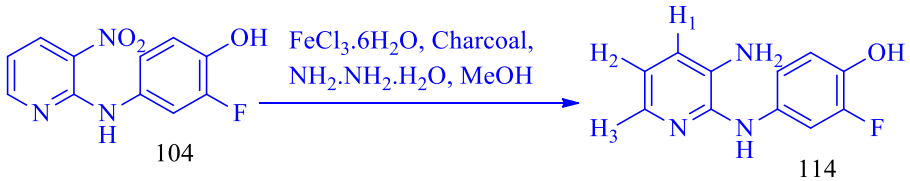

104 114

The above titled compound (114) was synthesised from N-(4-hydroxy-3-fluorophenyl)-3-nitropyridin-2-amine (104) (1.952 g, 7.833 mmol., 1 eq.), $FeCl_3.6H_2O$ (0.169 g , 0.626 mmol., 0.08 eq.), activated carbon (0.169 g, 14.09 mmol., 1.8 eq.) in methanol (25 cm^3), and hydrazine monohydrate (3.42 cm^3, 70.49 mmol., 9 eq.), and obtained as a brown solid (1.089 g, 4.9 mmol., 83%, Mp=195-198ºC), after purification by column chromatography (SiO_2, hexane: ethyl acetate 6:4, R_f = 0.12). HRMS (ESI): calculated for $C_{11}H_{11}FN_3O$ (M+H) = 220.0881, found (M+H) = 220.0886, ΔMs=0.5ppm.

^{1}H NMR (Acetone-d6): δ(ppm) = 4.44 [2 H, S, NH], 6.47 [1H, dd, J= 7.52 Hz, 4.85 Hz, pyr-H_2], 6.72 [1H, dd J=9.94 Hz, 8.84 Hz *meta* to F, Ar-H], 6.87[1H, dd, J= 7.51 Hz, 1.59 Hz,Py-H1], 6.96 [1H, s, N-H], 6.98 [1H, dq, J=8.84 Hz, 1.33 Hz *para* to F, Ar-H], 7.47 [1H,dd, J=4.88 Hz, 1.56 Hz , Pyr-H3], 7.60 [1H, dd, J=14.04 Hz, 2.61 Hz *ortho* to F, Ar-H], 7.96 [1H,s, OH].

^{13}C NMR (d6-acetone): δ(ppm) =108.42 [C-H, d, J=23.43Hz, Ar-C-H *ortho* to F], 114.57 [C-H, Py-C-H2], 116.06 [C-H, d, J= 2.94 Hz, Ar-C-H *para* to F], 118.28[C-H, d, J=8.79Hz, Ar-C-H *meta* to F], 126.06 [C-H, Pyr-C-H1], 133.28[C-N, Py-C-NH_2], 136.24 [C-N, d, J=9.67 Hz, Ar-C-NH], 139.69 [C-O, d, J=13.24 Hz, Ar-C-OH], 142.92 [C-H, Py-C-H3], 149.23 [C-N, Py-C=N], 150.64,153.10 [C-F, d, J= 236.21 Hz, Ar-C-F],.

FT-IR: ν_{max} **(**cm^{-1}): 3330 (NH, OH str.), 3086 (C-H str., aromatic), 2961 (C-H str., aliphatic), 1597(C=C str., aromatic), 1509 (N-O asy. str., NO_2), 1492 (N-O sym. str.), 1188 (C-O-CH_3 asy. Str.).

N2-(3,4,5-trimethoxybenzyl)pyridine-2,3-diamine (115):

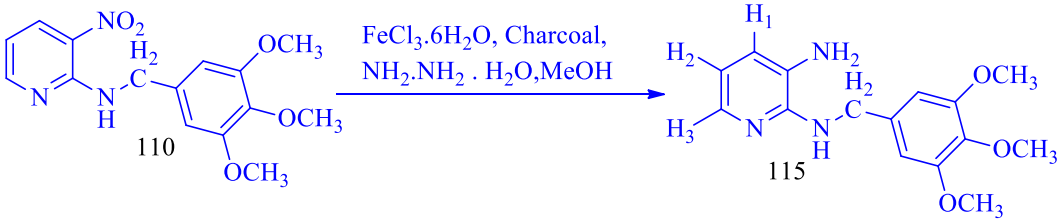

The above titled pyridine-2,3-diamine was synthesised from compound (**110**) (2.075 g, 6.5 mmol., 1 eq.), $FeCl_3.6H_2O$ (0.140 g , 0.519 mmol., 0.08 eq.), activated carbon (0.140 g, 11.69 mmol., 1.8 eq.) in 25 cm^3 methanol, and hydrazine monohydrate (2.9 cm^3, 58.5 mmol., 9 eq.), which was obtained as light brown solid (0.976 g, 3.37 mmol., 52%). Mp =136-138 ºC, after purification by column chromatography (SiO_2, hexane: ethyl acetate 7:3, R_f =0.14). HRMS (ESI): calculated for $C_{15}H_{20}N_3O$ (M+H) = 290.1499, found (M+H) = 290.1508, ΔMs=0.1ppm.

^{1}H NMR from (d6-acetone): δ (ppm) = 3.46 [3 H, s, (OCH_3)], 3.65 [6 H, s, 2 x (OCH_3)], 4.12 [2H, s, NH2], 4.43 [2 H, d, J =5.69 Hz, CH_2], [1H, t, J=5.69 Hz, NH], 6.28 [1H, dd, J=7.42 Hz, 4.97 Hz, Py-H2], 6.60 [2 H, s, Ar-H *ortho* to methoxy], 6.70 [1H, dd, J=7.43 Hz, 1.47 Hz, Py-H1], 7.39 [1H, dd, J=4.97, 1.46 Hz, Py-H3].

^{13}C NMR from : δ (ppm) = 46.43[CH_2], 56.06[2 x (OCH_3)], 60.83 [(OCH_3)], 105[C-H, Ar-C-H *ortho* to methoxy], 113.76 [C-H, Py-H2], 121.92 [C-H, Py-H1], 128.57 [C-C, Ar-C-CH_2], 135.61[C-N, Py-C-NH_2], 136.94 [C-O, Ar-C-OCH_3], 138.68 [C-H, Py-H3], 149.88 [C=N, Py-C=N], 153.22 [C-O, 2 x Ar-C-OCH_3].

FT-IR: ν_{max} **(**cm^{-1}): 3419 (NH, str.), 3383, 3357 (NH_2 str.), 2973 (C-H str., aromatic), 2905 (C-H str., aliphatic), 1610 (NH ben.), 1590 (C=C str., aromatic), 1499 (N-O asy. str., NO_2), 1417 (N-O sym. str.), 1114 (C-O-CH_3 asy. str.).

N2-(3-Hydroxy-4-methoxyphenyl)pyridine-2,3-diamine (116):

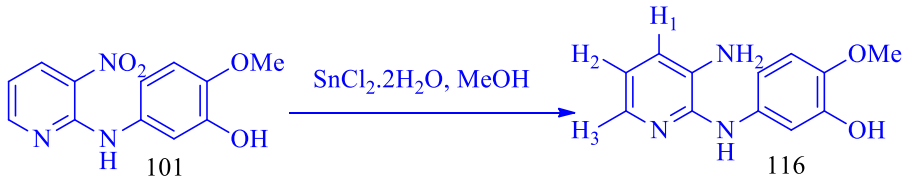

To a stirred solution of N-(3-hydroxy-4-methoxyphenyl)-3-nitropyridin-2-amine (1.2 g, 4.59 mmol., 1 eq.) (101) in methanol (25 cm^3) was added tin (II) chloride dihydrate (3.107g , 13.77 mmol., 3 eq.), and the mixture was heated under reflux for 3-6 hrs. After cooling the reaction to room temperature, solvent was evaporated by rotary evaporation, and the crude solid was neutralised using a saturated solution of sodium bicarbonate $NaHCO_3$. After the addition of ethyl acetate (30 cm^3), the resulting mixture was filtered over Celite and organic layer was separated, dried over anhydrous $MgSO_4$, and solvent evaporated to give crude solid which was purified by flash chromatography (SiO_2, hexane: ethyl acetate 5:5, R_f = 0.18) to afford the product as a black crystalline solid (0.532 g, 2.03 mm0l., 50%). Mp = 170-172 ºC. HRMS (ESI): calculated for $C_{12}H_{12}N_3O_4$ (M+H) = 232.1086, found (M+H) = 232.1086, ΔMs=0.0ppm.

^{1}H NMR (d6-dmso): δ ppm =3.74 [3 H, s, (CH_3O)], 5.04 [2 H, s, NH_2], 6.58 [1H, dd, J = 7.46 Hz, 4.84 Hz, Py-H2], 6.82 [1H, d, J = 8.72 Hz *meta* to OH, Ar-H], 6.88 [1H, d, J = 7.46 Hz, 1.51 Hz , Py-H1], 7.0 [1H, dd, J= 8.72 Hz, 2.62 Hz *para* to OH, Ar-H], 7.27 [1H,d, J = 2.62 Hz *ortho* to OH, Ar-H], 7.46 [1H, s, OH], 7.49 [1H, dd, J = 4.84 Hz, 1.51 Hz, Py-H3], 8.83 [1H, s, NH].

^{13}C NMR (d6-dmso): δ ppm= 56.19 [(CH3O)], 107.75[C-H, Ar-C-H *ortho* to OH], 109.56[C-H, Ar-C-H *meta* to OH], 112.95 [C-H, Ar-C-H *para* to OH], 114.77 [C-H, Py-C-H2], 119.07 [C-H, Py-H1], 131.51 [C-O, Ar-C-OCH_3], 134.40 [C-H, Py-H3], 136.22 [C-N, Ar-C-NH], 142.08 [C-N, Py-C-NH_2], 144.48 [C-N, Py-C=N], 146.56 [C-O, Ar-C-OH].

FT-IR: ν_{max} **(**cm^{-1}): 3372, 3331 (NH str.), 3132 (OH str.), 2964 (C-H str. aromatic), 2838 (C-H str., aliphatic), 1590 (NH-ben.), ,1589 (C=C str., aromatic), 1126 (C-O-CH_3 asy. Str.).

Following the above example, pyridine-2,3-diamine (117) was synthesised.

N2-(3-Fluoro-4-methoxyphenyl)pyridine-2,3-diamine (117):

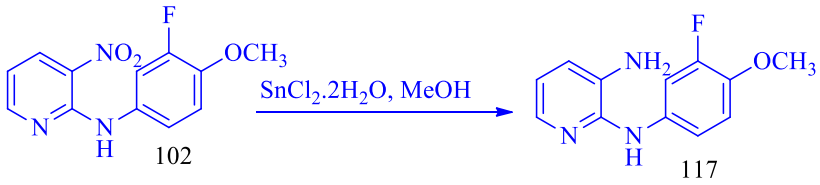

Using N-(3-flouro-4-methoxyphenyl)-3-nitropyridin-2-amine (102) (1.45 g, 5 mmol., 1 eq.), $SnCl_2.6H_2O$ (3.384 g, 15 mmol., 3 eq.) in methanol (25 cm^3), and obtained as a black solid (0.612 g, 2.62 mmol., 53%). Mp =139-140 ºC, after purified with column chromatography (SiO_2, hexane: ethyl acetate 8:2, R_f = 0.16). HRMS (ESI): calculated for $C_{12}H_{13}N_3O$ (M+H) = 234.1043, found (M+H) = 234.1041, ΔMs=0.2ppm.

^{1}H NMR: δ (ppm) =3.45 [2H, s, NH2], 3.83 [3H, s, (CH_3O)], 6.45 [1H, s, NH], 6.72 [1H, dd, J = 7.62,5.10 Hz, Py-H_2], 6.85 [1H, t, J= 17.62 Hz *ortho* to F, Ar-H], 6.92 [1H, dt, J = 9.01 Hz, 2.61 Hz *para* to F, Ar-H], 6.99 [1H, dd, J = 7.69, 1.58 Hz, Py-H_3], 7.22 [1H,dd, J = 13.16 Hz, 2.54 Hz *meta* to F, Ar-H], 7.74 [1H, dd, J = 5.12 Hz, 1.56 Hz Py-H_1].

^{13}C NMR : δ (ppm) =56.97 [(CH_3O)], 108.08 [C-H, d, J=21.95 Hz, , Ar-C-H *ortho* to F], 114.42 [C-H, d, J=3.46 Hz, Ar-C-H *meta* to F], 114.46 [C-H, d, J=3.06 Hz, Ar-C-H *para* to F], 116.90 [C-H, Py-C-H2], 123.87 [C-H, Py-C-H1], 130.25 [C-N, Py-C-NH_2], 135.13 [C-N, d, J=9.52 Hz, Ar-C-NH], 139.13 [C-H, Py-C-H3], 142.454 [C-O, d, J=11.05 Hz, Ar-C-OCH_3], 146.14 [C=N, Py-C=N], 151.38 [C-F, d, J=250.32 Hz, Ar-C-F].

FT-IR: ν_{max} **(**cm^{-1}): 3413.65, 3385.64 (NH str.), 3092.23 (C-H str., aromatic), 2801.48 (C-H str., aliphatic), 1600.56 (NH-ben. Primary amine), 1592.46 (C=C str., aromatic), 1123.15 (C-O-CH_3 asy. str.).

3.3 Synthesis of substituted pyridine-benzenesulfonamide derivatives:

Synthesis of benzene sulfonyl chloride derivatives (Huntress & Carten, 1940):

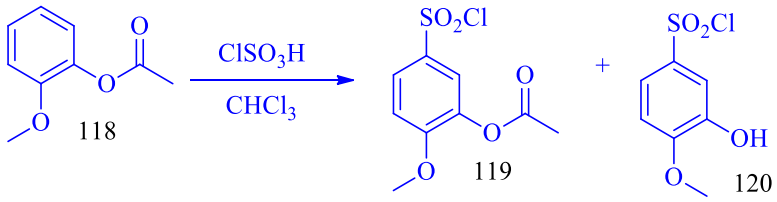

To a stirred solution of 2-methoxyphenyl acetate (118) (4.413 cm^3, 30 mmol., 1 eq.) in chloroform (10 cm^3), placed in -10 ºC ice-bath, was added drop wise chlorosulfonic acid solution (5.97 cm^3, 90 mmol., 3 eq.) in chloroform (5 cm^3) over 30 minutes. After completion of addition, the temperature was increased to 20 ºC and the reaction was monitored by TLC. Following consumption of starting material, the mixture was poured into crushed ice and the organic layer separated, dried over magnesium sulphate and evaporated under vacuum. The sulfonyl chloride mixture product was purified by column chromatography to obtain two products:

3-Hydroxy-4-methoxybenzene-1-sulfonyl chloride (120):

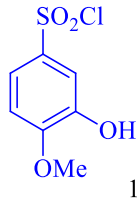

120

The above sulfonyl chloride obtained as a grey solid (1.196 g, 7.53 mmol., 18%, Mp = 65-66 ºC), (SiO_2, hexane: ethyl acetate 9:1, R_f = 0.12). HRMS (ESI): calculated for $C_7H_9O_2$ (M+H) =125.0602, found 125.9868 ΔMs=0.92 ppm, [M^+] calculated for $C_7H_7ClO_2$ =158.0134, found 158.9624, ΔMs=0.94ppm.

^{1}H NMR : δ ppm =3.93 [3 H, s, (OCH_3)], 5.56 [1H, s, OH], 6.89 [1H, d, J=8.62 Hz, Ar-H *meta* to OH], 7.45 [1H, d, J=2.41 Hz, Ar-H *ortho* to OH], 7.49 [1H, dd, J= 8.62 Hz, 2.41Hz, Ar-H *para* to OH].

^{13}C NMR : δ (ppm) =56.55[(OCH_3)], 110.22 [C-H , *ortho* to OH], 113.09 [C-H, *meta* to OH], 120.72 [C-H, *para* to OH], 136.75 [C-S, Ar-C-SO_2], 146.09 [C-O, Ar-C-OCH_3], 152.04 [C-O, Ar-C-OH].

FT-IR: ν_{max} **(**cm^{-1}): 3439 (OH str.), 3025 (C-H str., aromatic), 2850 (C-H str., aliphatic), 1602, 1588 (C=C str., aromatic), 1359 (S=O asy. str.,), 1161 (S=O sym. str.), 1132 (C-O- CH3, asy. str.)

3-Acetoxy-4-methoxy-benzenesulfonyl chloride (**119**):

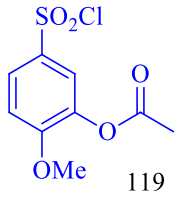

119

The above sulfonyl chloride (**195**) was obtained as a white crystalline solid (0.594 g, 2.24 mmol., 9%). Mp =130 -131 ºC, (lit. MP=128-129 ºC (Kratzl & Nelböck-Hochstetter, 1952)), (SiO_2, hexane: ethyl acetate 9:1, R_f = 0.18).

^{1}H NMR : δ ppm =2.34 [3H, s, (CH_3)], 3.95 [3H, s, (OCH_3)], 7.11 [1H, d, J= 8.86 Hz, Ar-H *meta* to acetate], 7.73 [1H, d, J=2.39 Hz, Ar-H *ortho* to acetate], 7.91[1H, dd, J=8.89Hz, 2.39Hz, Ar-H *para* to acetate].

^{13}C NMR : δ (ppm) =20.47 [(CH_3)], 56.61 [(OCH_3)], 112.29 [C-H, *meta* to acetate], 122.29 [C-H, *ortho* to acetate], 127.10 [C-H, *para* to acetate], 135.74 [C-S, Ar-C-SO_2], 139.82 [C-O, Ar-C-OCH_3], 157.04 [C-O, Ar-C-OAc], 168.10 [C=O].

FT-IR: ν_{max} (cm^{-1}): 3070 (C-H str., aromatic), 2848 (C-H str., aliphatic), 1766 (C=O str.), 1593 (C=C str., aromatic), 1369 (S=O asy. str.), 1161 (S=O sym. str.), 1010 (C-O-CH_3, asy. str.,).

No NMR literature for this compound.

2,3,4-Trimethoxybenzene-1-sulfonyl chloride (Onozuka *et al.*, 2010)(122) :

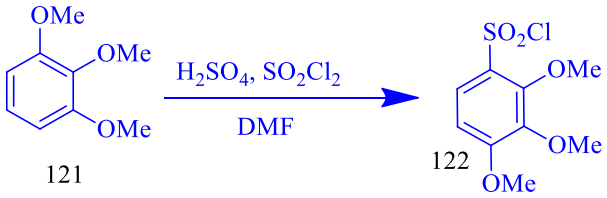

121 122

To a stirred solution of N,N-dimethylformamide (1.3 cm^3, 15 mmol., 1.5 eq.) at room temperature, was added dropwise sulfuryl chloride (1.212 cm^3, 15 mmol., 1.5 eq.), over 30 minutes. Sulfuric acid (0.106 cm^3, 2 mmol., 0.13 eq.) was added to the mixture and stirred for 1 hr. 1,2,3-Trimethoxybenzene (1.681 g, 10 mmol., 1 eq.) was added portion wise over 40 minutes, after increasing the temperature to 90 ºC. The mixture was stirred for a further 2 hours, at the same temperature, and reaction monitored by TLC. After consumption of starting material, the reaction was cooled to the room temperature, ice water (10 cm^3) was added, and the mixture was extracted with ethyl acetate (3x 30 cm^3). The organic layer was washed with brine (10 cm^3), dried over $MgSO_4$, and solvent was

evaporated to give the crude mixture, which was purified by flash chromatography (SiO_2, hexane: ethyl acetate 16:1, R_f = 0.12) to obtain the above sulfonyl chloride (**122**) as a viscous liquid (3.396 g, 12.7 mmol., 85%). lit. Mp (hexane)=38-39 ºC, Bp = 165 ºC (Pifferi & Monguzzi, 1973)).

^{1}H NMR: δ ppm =3.90 [3H, s, (OCH_3)], 3.96 [3H, s, (OCH_3)], 4.14 [3H, s, (OCH_3)], 6.75 [1H, d, J= 9.16 Hz Ar-H], 7.62 [1H, d, J= 9.16Hz, Ar-H].

^{13}C NMR : δ (ppm) =56.54 [(OCH_3)], 61.06 [(OCH_3)], 61.94 [(OCH_3)], 106.09 [C-H , Ar-C-H *ortho* to methoxy], 124.99 [C-H , Ar-C-H *meta* to methoxy], , 129.59 [C-S, Ar-C-SO_2], 142.93 [C-O, Ar-C-OCH_3], 152.26 [C-O, Ar-C-OCH_3], 160.26 [C-O, Ar-C-OCH_3].

FT-IR: ν_{max} **(**cm^{-1}): 3099 (C-H str., aromatic), 2957 (C-H str., aliphatic), 1568, 1474 (C=C str., aromatic), 1382 (S=O asy. str.), 1158 (S=O sym. str.), 1067 (C-O-CH_3, asy. str.).

No NMR data for this copound.

3-Hydroxy-4-methoxy-N-(2-((3,4,5-trimethoxyphenyl)amino)pyridin-3-yl)benzenesulfonamide (**123**):

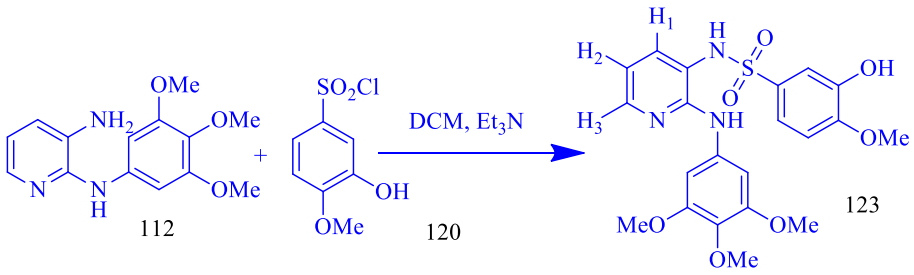

To a stirred solution of (**112**) (0.137 g, 0.5 mmol.,1 eq.) in dichloromethane (15 cm^3) was added 3-hydroxy-4-methoxybenzene-1-sulfonyl chloride (120) (0.111 g, 0.5 mmol., 1 eq.), portion wise, and triethyl amine (0.2 cm^3, 0.015 mmol, 3 eq.). The mixture was stirred for 18 hours at room temperature. After completion of reaction, the solvent was evaporated and water (10 cm^3) was added. The mixture was extracted with ethyl acetate (3 x 30 cm^3), and the organic layer was washed with water, dried over $MgSO_4$, and solvent evaporated. The solid product was purified by column chromatography (SiO_2, hexane: ethyl acetate 6:4, R_f = 0.18) to obtain the above sulphonamide as a white solid (0.196 g, 0.42 mmol., 85%, Mp = 154-156 ºC). HRMS (ESI): calculated for $C_{21}H_{24}N_3O_7S$ (M+H) = 462.1334, found for (M+H) = 462.1338, ΔMs=0.4ppm.

^{1}H NMR from (d6-aceton):δ ppm =3.69 [3H, s, (OCH_3)], 3.79 [6 H, s, 2 x (OCH_3)], 3.87 [3H, s, (OCH_3)], 6.68 [1H, dd, J=7.68 Hz, 4.85 Hz, Py-H2], 7.04 [1H, d, J= 8.48 Hz, Ar-H *meta* to OH], 7.11 [2H, s, Ar-H, *ortho* to trimethoxy], 7.16 [1H, dd, J=7.68 Hz, 1.76 Hz, Py-H1], 7.20 [1H, dd, J=8.48 Hz, 2.24 Hz, Ar-H *para* to OH], 7.28 [1H,d, J=2.25 Hz, Ar-H *ortho* to OH], 7.66 [1H, s, NH], 8.10 [1H, dd, J= 4.87 Hz, 1.76 Hz, Py-H3], 8.37 [2 H, s, NH, and OH labile protons].

^{13}C NMR from (d6-aceton): δ (ppm) =56.32 [2 x (OCH_3)], 56.47 [(OCH_3)], 60.63 [(OCH_3)], 97.84 [C-H, Ar-H *ortho* to methoxy(trimethoxy ring)], 111.83 [C-H, Ar-C-H *meta* to OH], 114.54 [C-H, Ar-C-H *para* to OH], 115.07 [C-H, Py-H2], 119.08 [C-N, Ar-C-NH], 120.99 [C-H, Ar-C-H *ortho* to OH], 132.21 [C-O, Ar-C-OCH_3], 134.00 [C-O, Ar-C-OCH_3], 137.13 [C-H, Py-H1], 137.88 [C-S, Ar-C-SO_2], 147.15 [C-H, Py-H3], 147.73 [C-N, Py-C-NH], 152.41[C=N, Py-C=N], 153.81 [C-O, Ar-C-OH], 154.13[C-O, 2 x Ar-C-OCH_3].

FT-IR: ν_{max} **(**cm^{-1}): 3408 (NH str.), 3230 (OH, str.), 2940 (C-H, aromatic), 2840 (C-H, aliphatic), 1603, (NH ben.), 1587, 1504 (C=C str., aromatic), 1272 (asy. str., S=O), 1151 (sym. str., S=O), 1124 (C-O-CH_3, asy. str.). following the above example pyridinyl-phenyl sulphonamide (**125**) was synthesized.

3-Fluoro-4-methoxy-N-(2-((3,4,5-trimethoxyphenyl)amino)pyridin-3-yl)benzenesulfonamide (**125**):

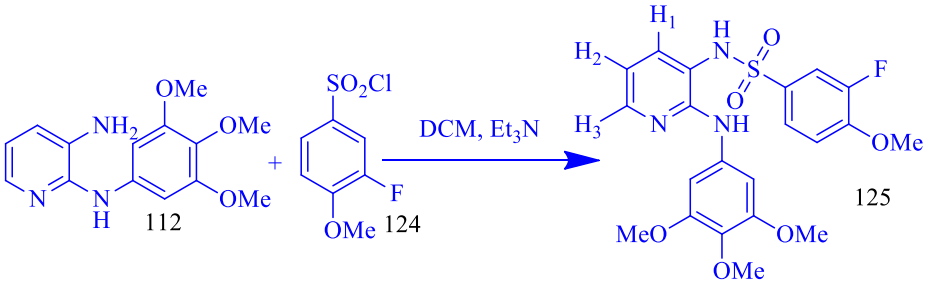

Using N2-(3,4,5-trimethoxyphenyl)pyridine-2,3-diamine (112) (0.137 g, 0.5 mmol.), 3-fluoro-4-methoxybenzenesulfonyl chloride (124) (0.112 g, 0.5 mmol.), and triethylamine (0.2 cm^3, 0.015 mmol.), the above titled sulphonamide (125) was obtained as a pale yellow solid (0.205g, 0.44 mmol., 89%). Mp =140-142 ºC, after purification by column chromatography (SiO_2, hexane: ethyl acetate 6:4, R_f = 0.18). HRMS(ESI): calculated for $C_{21}H_{23}FN_3O_6S$ (M+H) = 464.1280, found (M+H) =464.1290, ΔMs=0.10ppm.

^{1}H NMR from (Acetone-d6):δ ppm =3.55 [3 H, s, (OCH_3)], 3.67 [6 H, s, 2 x (OCH_3)], 3.77 [3H, s, (OCH_3)], 6.54 [1H, dd, J=7.70 Hz, 4.89 Hz, Py-H2], 6.91 [2H, s, Ar-H, ortho

to trimethoxy], 7.03 [1H, dd, J=7.71 Hz, 1.72 Hz, Py-H1], 7.07 [1H, t, J=8.36 Hz, Ar-H *meta* to F], 7.36 [2H, m, 1H *ortho* to F, 1H *para* to F], 7.55 [1H, s, NH], 7.97 [1H, dd, J=4.86 Hz, 1.72 Hz, Py-H3], 8.32 [1H,s, NH].

^{13}C NMR from (Acetone-d6):δ (ppm) =56.29 [2 x (OCH_3)], 56.90 [(OCH_3)], 60.61 [(OCH_3)], 97.79 [C-H, Ar-C-H *ortho* to methoxy (trimethoxy ring)], 114.26 [C-H, d, J=1.95 Hz, para to F], 115.19 [C-H, Py-C-H2], 115.74 [C-H,d, J=21.28 Hz, *ortho* to F], 118.69 [C-NH, trimethoxy ring], 125.95 [C-H, d, J=3.71 Hz, *meta* to F], 131.95 [C-S, d, J= 5.68 Hz, Ar-C-SO_2], 134.07 [C-H, Py-H1], 137.40 [C-O, Ar-C-OCH_3], 137.81 [C-H, Py-H3], 147.46 [C-N, Py-NH], 151.01, 153.50 [C-F, d, J=249.84 Hz,], 152.56 [C-O, d, J=10.22 Hz, , *ortho* to Fe], 153.81 [C-N, Py-N], 154.14 [C-O, 2 x Ar-C-OCH_3].

FT-IR: ν_{max} (cm^{-1}): 3365 (NH str.), 3070 (C-H str., aromatic), 2940 [C-H str., aliphatic], 1599, (NH bend), 1505 (C=C str., aromatic), 1274 (asy. str., S=O, 1202 (sym. str., S=O), 1151 (C-O-CH_3 asy. str).

N-(2-((3-Hydroxy-4-methoxyphenyl)amino)pyridin-3-yl)-2,3,4-trimethoxybenzenesulfonamide (126):

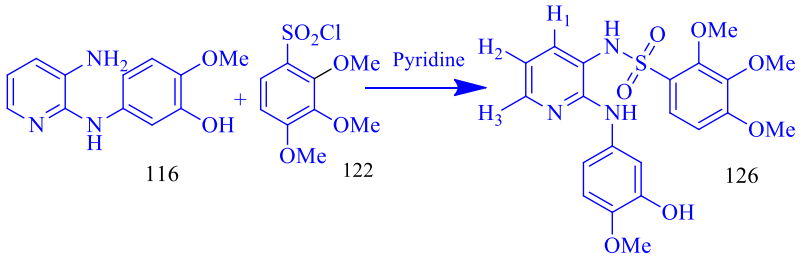

To a stirred solution of 5-((3-aminopyridin-2-yl)amino)-2-methoxyphenol (116) (0.115 g, 0.5 mmol., 1eq.) in pyridine (3 cm^3) was added 2,3,4-trimethoxybenzene-1-sulfonyl chloride (122) (0.160 g, 0.6 mmol., 1.2 eq.) and the mixture was stirred for 1 hour. After completion of the reaction, monitored by TLC, the pyridine was evaporated under reduced pressure by forming azeotropic mixture with toluene multiple times. Water was added and the solid extracted with ethyl acetate (3x30 cm^3). The organic layer was washed with brine (10 cm^3), dried with anhydrous MgSO4, and the solvent was evaporated. The solid product was purified by column chromatography (SiO_2, hexane: ethyl acetate 6:4, R_f = 0.18), and obtained as a pale white solid (0.182 g, 0.39 mmol., 79%) Mp=188-190°C. HRMS (ESI): calculated for $C_{21}H_{24}N_3O_7S$ (M+H) = 462.1349, found (M+H) =462.1348, ΔMs=0.1ppm.

^{1}H NMR (d6-acetone):δ ppm =3.71 [3 H, s, (OCH_3)], 3.78 [3 H, s, (OCH_3)], 3.87 [3 H, s, (OCH_3)], 4.05 [3H, s, (OCH_3)], 6.60 [1H, dd, J= 7.64 Hz, 4.88 Hz, Py-H2], 6.80 [1H, d, J=8.92 Hz, Ar-H ortho to methoxy (trimethoxy ring)], 6.85 [1H, d, J=8.85 Hz, Ar-H *meta* to OH], 7.06 [1H, dd, J=8.69 Hz, 2.62 Hz, Ar-H *para* to OH], 7.36-7.38 [2H, m, 1H *meta* to methoxy trimethoxy ring, 1H, *ortho* to OH] 7.42 [1H, dd, J=7.63 Hz, 1.75, Py-H1], 7.48 [1H, s, OH], 7.82 [1H, s, NH], 7.95 [1H, dd, J=4.89 Hz,1.75 Hz, Py-H3], 8.60 [1H, s, NH].

^{13}C NMR (d6-acetone):δ (ppm) =56.60 [(OCH_3)], 56.78 [(OCH_3)], 61.16 [(OCH_3)], 62.62 [(OCH_3)], 107.93 [C-H, Ar-C-H *ortho* to OH], 108.17 [C-H, Ar-C-H *ortho* to methoxy (trimethoxy ring)], 110.86 [C-H, Ar-C-H *para* to OH], 112.94 [C-H, Ar-C-H *meta* to OH], 114.55 [C-H, Py-H2], 118.53,[C-S, Ar-C-SO_2], 126.17 [C-H, Ar-C-H *meta* to methoxy (trimethoxy ring)], 126.29 [C-O, Ar-C-OCH_3], 136.05 [C-H, Py-H1], 136.32 [C-N, Ar-C-NH], 143.39 [C-O, Ar-C-OCH_3], 143.99 [C-O, Ar-C-OCH_3], 146.64 [C-H, Py-H3], 147.42 [C-N, Py-C-NH], 151.65 [C-N, Py-C=N], 153.31 [C-O, Ar-C-OH], 159.32 [C-O, Ar-C-OCH_3].

FT-IR: ν_{max} **(**cm^{-1}): 3423 (NH str.), 3273 (OH str.), 2926 (C-H str., aromatic), 2850 (C-H str. , aliphatic), 1605, (NH bend.), 1581, 1512 (C=C str., aromatic), 1308 (S=O, asy. str.), 1289 (S=O, sym. str.), 1087 (C-O-CH_3, asy. str.).

Following the above procedure, pyridinyl-phenyl sulphonamide (127- 131) was synthesised.

N-(2-((4-Hydroxy-3-methylphenyl)amino)pyridin-3-yl)-2,3,4-trimethoxybenzenesulfonamide (127):

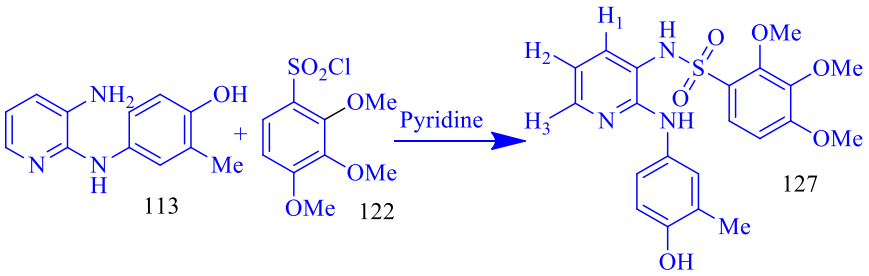

Using 4-((3-aminopyridin-2-yl)amino)-2-methylphenol (113) (0.107 g, 0.5 mmol.) and 2,3,4-trimethoxybenzene-1-sulfonyl chloride (122) (0.160 g, 0.6 mmol., 1.2 eq.), the above titled sulphonamide (127) was obtained as a pale white solid (0.198 g, 0.44 mmol., 89%). Mp =160-162ºC, after purification by column chromatography (SiO_2, hexane:

ethyl acetate 6:4, R_f = 0.18). HRMS (ESI): calculated for $C_{21}H_{24}N_3O_6S$ (M+H) = 446.1390, found (M+H) =446.1385, ΔMs=0.5ppm.

^{1}H NMR from (d6-acetone):δ ppm =2.21 [3H, s, (CH_3)], 3.74 [3H, s, (OCH_3)], 3.91 [3H, s, (OCH_3)], 4.14 [3H, s, (OCH_3)], 6.58 [1H, dd, J= 7.64,4.88 Hz, Py-H2], 6.73 [1H, d, J=8.52 Hz, Ar-C-H *ortho* to methoxy], 6.86 [1H, d, J=8.96 Hz, Ar-H *meta* to CH_3], 7.33 [1H, d, J=2.46 Hz, Ar-H *ortho* to CH_3], 7.39-7.43 [3H, m, 1H *meta* to methoxy, 1H, *para* to CH_3, 1H, Py-H1], 7.74 [1H, s, OH], 7.82 [1H, s, NH], 7.94 [1H, dd, J=4.88,1.72Hz, Py-H3], 8.57[1H, s, NH].

^{13}C NMR from (d6-acetone): δ ppm = 16.45 [CH_3], 56.60 [(OCH_3)], 61.07 [(OCH_3)], 62.57 [(OCH_3)], 107.87 [C-H, Ar-C-H *ortho* to methoxy], 114.15 [C-H, Py-H2], 115.84 [C-H, Ar-C-H *meta* to methoxy], 117.32 [C-C, Ar-C-CH_3], 121.21 [C-H, Ar-C-H *meta* to CH_3], 124.16 [C-S, Ar-C-SO_2], 125.03[C-N, Ar-C-NH], 125.18 [C-H, Ar-H *ortho* to CH_3], 125.75 [C-H, Ar-C-H para to CH_3], 126.37 131.87 [C-O, Ar-C-OCH_3], 135.28 [C-H, Py-H1], 143.92 [C-N, Py-C-NH], 146.74 [C-H, Py-H3], 150.48[C-N, Py-C=N], 150.90 [C-O, Ar-C-OCH_3], 153.70 [C-O, Ar-C-OH], 159.31 [C-O, Ar-C-OCH_3].

FT-IR: ν_{max} (cm^{-1}): 3422 (NH str.), 3272 (OH str.), 2945 (C-H str., aromatic), 2834 (C-H str., aliphatic), 1603 (NH-bend), 1582, 1510 (C=C str., aromatic), 1370 (S=O, asy. str.), 1308 (S=O, sym. str.), 1088 (C-O-CH_3, asy. str.).

N-(2-((3-fluoro-4-methoxyphenyl)amino)pyridin-3-yl)-2,3,4-trimethoxybenzenesulfonamide (128):

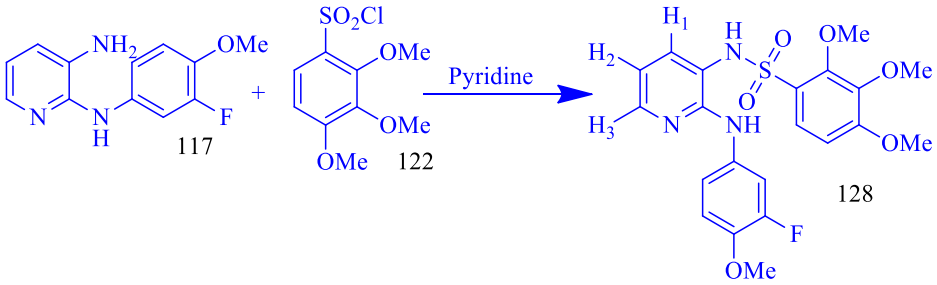

Using N2-(3-fluoro-4-methoxyphenyl)pyridine-2,3-diamine (117) (0.116 g, 0.5 mmol.) and 2,3,4-trimethoxybenzene-1-sulfonyl chloride (122) (0.160 g, 0.6 mmol., 1.2 eq.), the above sulphonamide (128) was obtained as a pink solid (0.185 g, 0.41 mmol., 80%). Mp = 98-99 ºC, after purified using column chromatography (SiO_2, hexane: ethyl acetate 7:3, R_f = 0.15). HRMS (ESI): calculated for $C_{21}H_{23}FN_3O_6S$ (M+H) = 446.1291, found (M+H) =446.1298, ΔMs=0.7ppm.

^{1}H NMR (d6-acetone):δ ppm =3.61 [3H, s, (OCH_3)], 3.70 [3H, s, (OCH_3)], 3.75[3H, s, (OCH_3)], 4.00 [3H, s, (OCH_3)], 6.54 [1H, dd, J= 7.67 Hz, 4.89 Hz, Py-H2], 6.68 [1H, d, J=8.96 Hz, Ar-H *ortho* to methoxy (trimethoxy ring)], 6.92 [1H, t, J=9.3 Hz, Ar-H *meta* to F], 7.15-7.18[1H, ddd, J=1.54 Hz, 2.44 Hz, 8.88 Hz, Ar-H *para* to F], 7.24 [1H, d, J=8.96 Hz, Ar-H *meta* to methoxy (trimethoxy ring)], 7.33[1H, dd, J= 1.74 Hz, 7.69 Hz, Py-H1], 7.68 [1H, dd, J= 2.54 Hz, 14.21 Hz, Ar-H *ortho* to F], 8.01 [2H, (1H, dd, J= 4.89 Hz, 1.74 Hz, Py-H3), (1H, s, NH)], 8.65 [1H, s, NH].

^{13}C NMR (d6-acetone): δ ppm = 56.62 [(OCH_3)], 56.94 [(OCH_3)], 61.18 [(OCH_3)], 62.69 [(OCH_3)], 108.00 [C-H, Ar-C-H *ortho* to methoxy], 108.20 [C-H, d, J = 23.43 Hz, *ortho* to F], 115.03 [C-H, d, J= 2.96 Hz, *para* to F], 115.19 [C-H, Py-C-H2], 115.38 [C-H, d, J=3.49 Hz, *meta* to F], 118.83 [C-S, Ar-C-SO_2], 126.14 [C-O, Ar-C-OCH_3], 126.20 [C-H, meta to methoxy (trimethoxy ring)], 135.76 [C-N, d, J=9.51 Hz, Ar-C-NH, F ring], 136.55 [C-H, Py-H1], 142.99 [C-O, d, J=11.30 Hz, Ar-C-OCH_3, ortho to F], 143.96 [C-N, Py-C-NH], 146.55 [C-H, Py-H3], 151.57 [C-O, Ar-C-OCH_3], 151.57-153.97 [C-F, d, J= 248.14 Hz], 152.92 [C-N, Py-C=N], 159.34 [C-O, Ar-C-OCH_3].

FT-IR: ν_{max} **(**cm^{-1}): 3380, 3234 (NH str.), 2946 (C-H str., aromatic), 2843 (C-H str., aliphatic), 1584 (NH-bend), 1509 (C=C str., aromatic), 1344 (S=O asy. str.), 1315 (S=O sym. str.), 1186 (C-O-CH_3, asy. str.).

N-(2-((3-Fluoro-4-hydroxyphenyl)amino)pyridin-3-yl)-2,3,4-trimethoxybenzenesulfonamide (129):

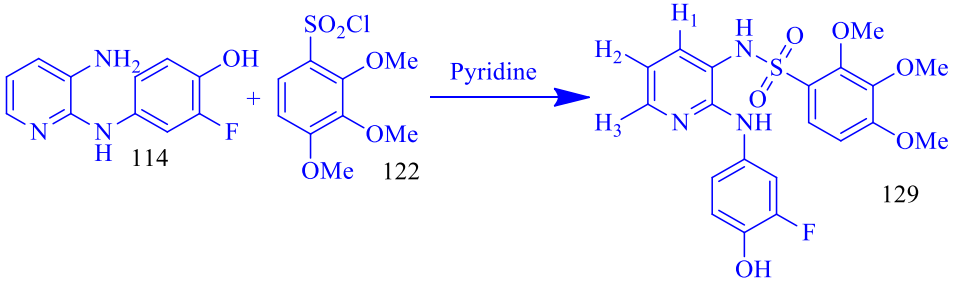

Using 4-((3-aminopyridin-2-yl)amino)-2-fluorophenol (114) (0.109 g, 0.5 mmol., 1eq.) and 2,3,4-trimethoxybenzene-1-sulfonylchloride (122) (0.160 g, 0.6 mmol., 1.2 eq.), the above sulphonamide (129) was obtained as a beige solid (0.178 g, 0.39 mmol., 80%). Mp=189-190 ºC, after purification by column chromatography (SiO_2, hexane: ethyl acetate 7:3, R_f = 0.25). HRMS (ESI): calculated for $C_{20}H_{21}FN_3O_6S$ (M+H) = 450.1135, found (M+H) =450.1136, ΔMs=0.1ppm.

^{1}H NMR (d6-acetone): δ(ppm) = 3.59 [3H, s, (OCH_3)], 3.74 [3H, s, (OCH_3)], 4.00 [3H, s, (OCH_3)], 6.52 [1H, dd, J= 7.68 Hz, 4.87 Hz, Py-H2], 6.69 [1H, d, J=8.93 Hz, Ar-H *ortho* to methoxy], 6.78 [1H, dd, J= 9.85 Hz, 8.65 Hz, Ar-H *meta* to F], 7.04 [1H, ddd, 8.66 Hz, 2.61 Hz, 1.361 Hz, Ar-H *para* to F], 7.24 [1H, d, J=8.93 Hz, Ar-H *meta* to methoxy], 7.31 [1H, dd, J= 7.69,1.71 Hz, Py-H1], 7.67 [1H, dd, J= 13.95 Hz, 2.61 Hz, Ar-H *ortho* to F], 7.83 [1H, s, NH], 7.86 [1H, dd, J= 7.69 Hz, 1.71 Hz, Py-H3], 8.03 [1H, OH], 8.49 [1H, s, NH].

^{13}C NMR from ($CDCl_3$):δ ppm = 56.61 [(OCH_3)], 61.16 [(OCH_3)], 62.67 [(OCH_3)], 107.98 [C-H, *ortho* to methoxy], 108.08 [C-H, d, J= 23.76 Hz, *ortho* to F], 114.93 [C-H, Py-C-H2], 115.96 [C-H, d, J= 2.99 Hz, *para* to F], 118.30 [C-H, d, J= 3.6 Hz, *meta* to F], 118.65 [C-S, *meta* to F], 126.20 [2C, (C-H *meta* to methoxy), (C-O, Ar-C-OCH_3], 134.76 [C-N, d, J= 9.57 Hz, Ar-C-N *meta* to F], 136.46 [C-H, Py-H1], 139.85 [C-OH, d, J= 13.46 Hz, *ortho* to F], 143.97 [C-O, Ar-C-OCH_3], 146.61 [C-H, Py-H3], 150.58-152.94 [C-F, d=234.36 Hz,], 151.58 [C-N, Py-C-N], 153.05 [C-O, Ar-C-OCH_3], 159.33 [C-O, Ar-C-OCH_3].

FT-IR: ν_{max} **(**cm^{-1}): 3373 (NH str.), 3248 (OH str.), 2946 (C-H str., aromatic), 2845 (C-H str., aliphatic), 1608 (NH-bend), 1583, 1512. (C=C str., aromatic), 1346 (S=O asy. str.), 1286 (S=O sym. str.), 1087 (C-O-CH_3, asy. str.).

3-Fluoro-4-methoxy-N-(2-((3,4,5-trimethoxybenzyl)amino)pyridin-3-yl)benzenesulfonamide (130):

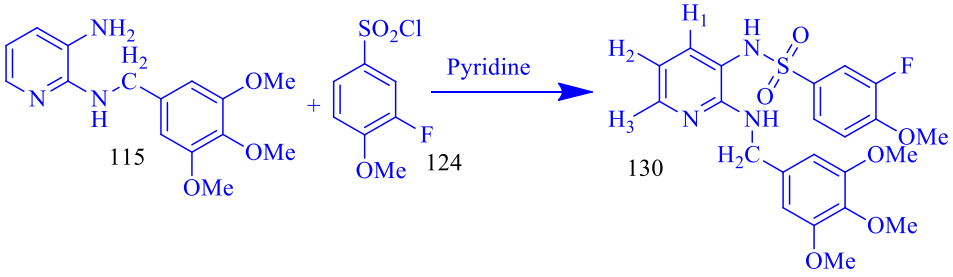

Using N2-(3,4,5-trimethoxybenzyl)pyridine-2,3-diamine (115) (0.144 g, 0.5 mmol., 1eq.) and 3-fluoro-4-methoxybenzene-1-sulfonyl chloride (0.134 g, 0.6 mmol., 1.2 eq), the above sulphonamide (130) was obtain as a white solid (0.190 g, 0.39 mmol., 82%, Mp =155-156ºC), after purified with column chromatography (SiO_2, hexane: ethyl acetate 8:2, R_f =0.15). HRMS (ESI): calculated for $C_{22}H_{25}FN_3O_6S$ $(M+H)^+$ = 478.1448, found (M+H) =478.1441, ΔMs=0.7ppm.

^{1}H NMR (d6-acetone):δ ppm = 3.70 [3H, s, (OCH_3)], 3.80 [6 H, s, 2 x (OCH_3)], 3.98 [3 H, s, (OCH_3)], 4.56 [2 H, d, J=5.81 Hz, CH_2], 6.21 [1H, t, J=5.82 Hz, NH], 6.39 [1H, dd, J=7.56 Hz,4.97 Hz, Py-H2], 6.73 [2 H, s, Ar-H, trimethoxy ring], 6.87 [1H, dd, J=7.56 Hz,1.71 Hz, Py-H1], 7.25 [1H, t, J=8.66 Hz, para to F], 7.48 [2 H, m, ortho and meta to F], 7.93 [1H, dd, J=4.97 Hz, 1.71 Hz, Py-H3], 8.32 [1H, s, NH].

^{13}C NMR (d6-acetone): δ ppm = 45.45 [CH_2], 56.35 [2 x (OCH_3)], 56.93 [(OCH_3)], 60.44 [(OCH_3)], 105.47 [C-H, *ortho* to methoxy (trimethoxy ring)] , 112.53 [CH, Py-C-H2], 114.15 [C-H, d, J= 2.17 Hz, *para* to F], 115.77 [C-H, d, J=20.82 Hz, *ortho* to F], 117.44 [C-C, Ar-C-CH_2], 125.94 [C-H, d, J=3.85 Hz, *meta* to F], 132.23 [C-S, d, J= 5.66 Hz, Ar-C-S], 135.99 [C-H, Py-C-H1], 136.98 [C-N, Py-C-NH], 137.91 [C-O, Ar-C-OCH_3], 147.85 [C-H, Py-C-H1], 150.99-153.47 [C-F, d, J=250.81, Ar-C-F], 152.45 [C-O, d, J=10.55 Hz, Ar-C-OH], 154.32 [C-O, 2 x Ar-C-OCH_3], 156.75 [C-N, Py-C=N].

FT-IR: ν_{max} **(**cm^{-1}): 3440, 3122 (NH str.), 2947 (C-H str., aromatic), 2845 (C-H str., aliphatic), 1596, (NH-bend), 1500 (C=C str., aromatic), 1344 (S=O asy. str.), 1317 (S=O sym. str.), 1128 (C-O-CH_3, asy. str.).

3-Hydroxy-4-methoxy-N-(2-((3,4,5-trimethoxybenzyl)amino)pyridin-3-yl)benzenesulfonamide (131):

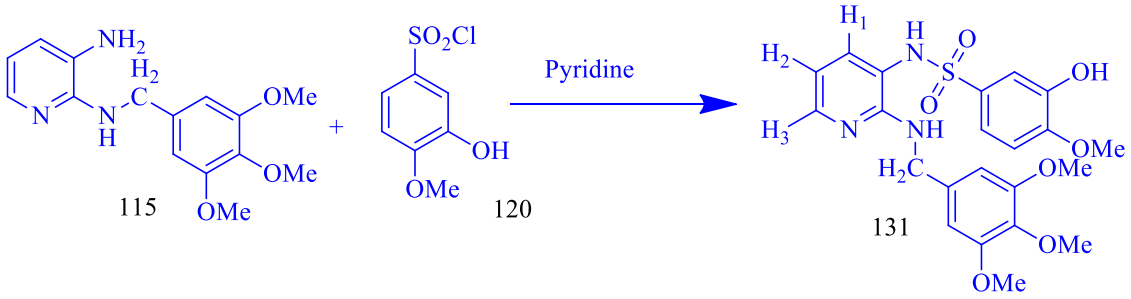

Using N2-(3,4,5-trimethoxybenzyl)pyridine-2,3-diamine (115) (0.144 g, 0.5 mmol., 1 eq.) and 3-hydroxy-4-methoxybenzene-1-sulfonyl chloride (120) (0.134 g, 0.6 mmol., 1.2 eq.) the above sulphonamide (131) was obtained as a white solid (0.205 g, 0.43 mmol., 87%). Mp =162-164 ºC, after purification by column chromatography (SiO_2, hexane: ethyl acetate 8:2, R_f = 0.17). HRMS (ESI): calculated for $C_{22}H_{26}N_3O_7S$ $(M+H)^+$ = 476.1491, found (M+H) = 476.1490, ΔMs=0.1 ppm.

^{1}H NMR from (d6-acetone):δ ppm = 3.56 [3H, s, (OCH_3)], 3.67 [6H, s, (OCH_3)], 3.79 [3H, s, (OCH_3)], 4.43 [2H, d, J=5.99 Hz, CH_2], 6.07 [1H, t, J=6.01 Hz, NH], 6.24 [1H, dd, J=7.56 Hz, 4.92 Hz, Py-H2], 6.61 [2H, s, Ar-H, trimethoxy ring], 6.70 [1H, dd,

J=7.56 Hz,1.74 Hz, Py-H1], 6.90 [1H, d, J=8.38 Hz, meta to OH], 7.06 [2H, (1H, d, J=2.25 Hz ortho to OH), (1H, dd, J=8.38 Hz, 2.28 Hz, para to OH)], 7.77 [1H, dd, J=4.91 Hz,1.71Hz, Py-H3], 8.06 [1H, s, OH], 8.23 [1H, s, NH].

^{13}C NMR (d6-acetone): δ ppm = 45.47 [CH_2], 56.37 [2 x (OCH_3)], 56.47 [(OCH_3)], 60.44 [(OCH_3)], 105.41 [C-H, *ortho* to methoxy (trimethoxy ring)] , 111.70 [C-H, *meta* to OH], 112.48 [CH, Py-C-H2], 114.72 [C-H, *para* to OH], 117.93 [C-CH_2, Ar-C-CH_2], 120.99 [C-H, *ortho* to OH], 128.68 [C-S, Ar-C-S], 132.36 [C-O, Ar-C-OCH_3], 135.78 [C-H, Py-C-H1], 137.05 [C-N, Py-C-NH], 147.57 [C-N, Py-C=N], 147.62 [C-H, Py-C-H3], 152.28 [C-O, Ar-C-OCH_3], 154.32 [C-O, 2 x Ar-C-OCH_3)], 156.78 [C-O, Ar-C-OH].

FT-IR: ν_{max} **(**cm^{-1}): 3378, 3117 (NH str.), 3234 (OH str.), 2970 (C-H str., aromatic), 2840 [C-H str., aliphatic], 1602 (NH-bend), 1508, 1584 (C=C str., aromatic), 1344 (S=O asy. str.), 1316 (S=O sym. str.), 1127 (C-O-CH_3, asy. str.).

3.4 Discussion

Earlier reports have investigated the conditions by which aliphatic and aromatic nucleophilic substitution reactions occur. While aromatic substrates only slightly undergo S_N1, it is practically not feasible for S_N2. This is due to the presence of an electron cloud surrounding the Sp^2 aromatic ring (Clayden *et al.*, 2012). To overcome this problem, the reaction can be achieved by incorporating an electron-withdrawing group adjacent to the leaving group. Other alternatives include transition metal catalysis, strong bases and replacing diazonium group with a suitable nucleophile. Selection of appropriate solvent also plays a significant role on the reaction rate (Smith, 2013) as the reaction proceeds effectively in aprotic solvents than in protic solvents (Acevedo & Jorgensen, 2004).

Nucleophilic aromatic substitution (S_NAr) is a two-step reaction mechanism that differs from both S_N1 and S_N2. It mainly relates to introducing a nucleophile on the aromatic ring through intermediate steps also referred to as Meisenheimer intermediates (scheme 13. The stability of the intermediates according to Meisenheimer depends on three important factors. One contributing factor is the presence of an electron-withdrawing group in ortho and / or para position. The more electron-withdrawing groups present the more stable intermediate and hence the reaction proceeds efficiently. The two other factors are to introduce a good nucleophile along with the presence of a suitable leaving group.(Clayden *et al.*, 2012).

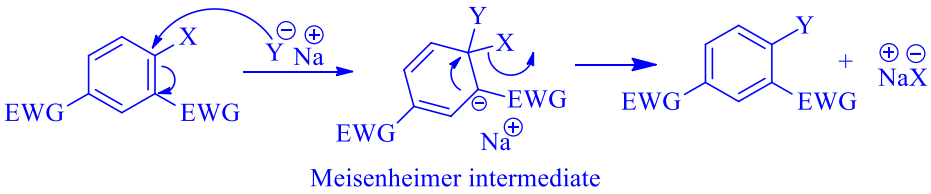

Scheme 13: addition-elimination nucleophilic substitution mechanism S_NAr (Goldstein *et al.*, 2017).

Heterocyclic aromatic substrates such as pyridine, on the other hand, can easily undergo nucleophilic substitution due their electron-deficient nature of the heterocyclic ring. Aromatic heterocycles react faster with leaving groups in position 3 and 4 in comparsion with those in the same position of benzene ring (Isanbor & Emokpae, 2008). Therefore, synthesis of 2-anilino-3-nitropyridine derivatives was carried out using highly

electrophilic 2-chloro-3-nitro-pyridine with activated substituted aniline (scheme 14) to avoid using poisonous and costly catalyst such as palladium.

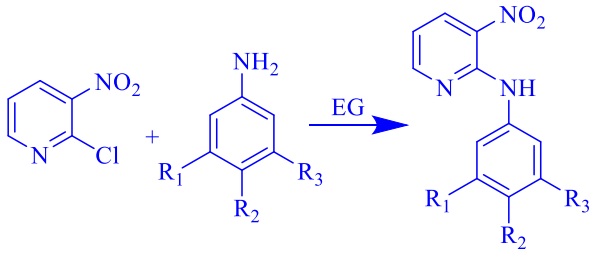

Scheme 14: General reaction for synthesis substituted 2-anilino-3-nitropyridine.

During the optimization process for the synthesis of substituted N-phenyl-3-nitropyridine-2-amine many protocols have been expolred in order to enhance the reaction yield. One useful protocol was available (Wu *et al.*, 2014). A base such as triethylamine was used as a catalyst in alcoholic medium. Different solvents were used to improve the reaction ranging from toluene, ethanol, methanol, isopropanol, and t-butanol. The main difficulty was the requirement of extreme temperature which results in decomposition of the substituted aniline forming a black sludge that makes extraction difficult to carry out. To address this problem, the protocol described in (Kovač *et al.*, 1983) was tested to eliminates the reduction of nitro pyridine and decrease the total reaction steps (scheme 15) .

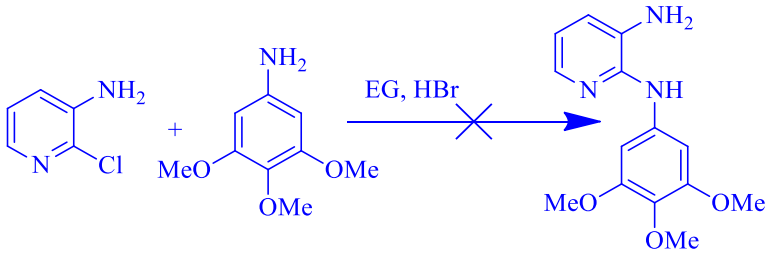

Scheme 15: preparation of substituted diaminopyridine from 2-chloro-3-aminopyridine (Kovač *et al.*, 1983).

This difficulty was resolved and the yield was greatly enhanced under microwave irradiation, however for the heat sensitive aromatic amines conventional heating in an oil bath at a temperature between 80-100 ºC gave good yeilds.

12 substituted N-phenyl-3-nitropyridine-2-amine have been synthesized and 10 of them are novel compounds.

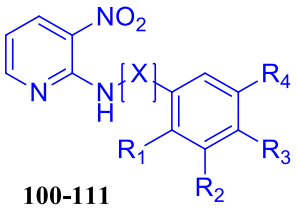

100-111

Scheme 16: General structure of synthesised substituted 3-nitropyridine-2-anilines.

Comp.	R1	R2	R3	R4	X	Mp ºC	Yield %	References
100	H	OCH_3	OCH_3	OCH_3	-	144-145	50	(Robison & Finch, 1970)
*101	H	H	OCH_3	OH	-	160-162	55	
*102	H	H	OCH_3	F	-	129-130	76	
*103	H	H	CH_3	OH	-	178-180	90	
*104	H	H	OH	F	-	133-135	89	
*105	H	H	Br	F	-	158-159	88	
*106	H	F	F	F	-	165-167	80	
*107	F	H	F	F	-	127-128	46	
*108	H	H	OH	OCH_3	-	138-140	48	
*109	H	H	OH	CH_3	-	136-139	61	
*110	H	OCH_3	OCH_3	OCH_3	CH_2	184-185	65	
111	H	OCH_3	OCH_3	OCH_3	CONH	120-122	88	(Murty *et al.*, 2016)

* these compounds are novel.

Table 3: Synthesised substituted 3-nitropyridine-2-anilines with yield.

The reduction of 3-nitropyridine-2-amine derivatives was carried out by $SnCl_2.2H_2O$ and $FeCl_3.6H_2O$, as a catalyst compared to the protocols available from the literature which used ammonium chloride/zinc mixture (Nandini *et al.*, 2014), $Na_2S.9H_2O$ / water (Cao *et al.*, 2011), and zinc/ acetic acid (Hasegawa *et al.*, 2007). The first two reduction mitures produced (0.458g, 1.5 mmol., 15%) and (0.611 g, 2 mmol., 20%) of compound (**100**) respectively, whereas, zinc/ acetic provided no yield.

Several approaches have been reported for the synthesis of aryl sulfonyl chlorides from a variety of substrates, though, most of them are not feasible due to a high amount of starting material present after the reaction.

However, 3,4,5-trimethoxybenzenesulfonyl chloride was reported as the final product for the sulfonation process as reported in (Onozuka *et al.*, 2010). Despite many attempts to obtain the same product with the same procedure at different reaction conditions gave 2,3,4-trimethoxybenzenesulfonyl chloride isomer as a final product.

Several methodologies reported the synthesis of sulfonyl chloride from variuos substrates, however, most of them are unfeasible in terms of starting material availability (Binisti *et al.*, 2001; Ji *et al.*, 2019).

Mass spectroscopy analysis of 3-hydroxy-4-methoxybenzene-1-sulfonyl chloride (120) has shown a big difference from the expected molecular weight, which might be due to transfer of chlorine from the sulfonyl chloride group to the neighbouring carbon under mass spectroscopy condition. This phenomenon is quite familiar with aryl sulfonyl chloride compounds due to the electron attack during process (Davis *et al.*, 1977).

As at the time of this write up, just 6 out of 12 substituted N-phenyl-3-nitropyridine-2-amine, have been reduced to substituted pyridine-2,3-diamine derivatives with 2 variables, (scheme 17). However, five of them are novel (table 4). These pyridine-diamines was converted to substituted pyridinyl-benzen sulphonamide (scheme 18), compound shown in table (table 5).

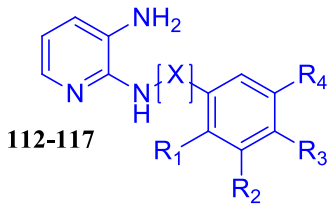

Scheme 17: General structure of substituted 2,3-diaminopyridine.

Comp.	R1	R2	R3	X	Mp ºC	Yield %
112	OCH_3	OCH_3	OCH_3	-	158-160	83
*113	H	OH	CH_3	-	211-213	72
*114	H	OH	F	-	195-198	76
*115	OCH_3	OCH_3	OCH_3	CH_2	136-138	52
*116	H	OCH_3	OH	-	170-172	50
*117	H	OCH_3	F	-	139-140	53

* these compounds are novel.

Table 4: substituted 2,3-diaminopyridines with yield.

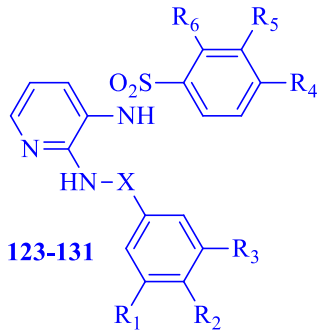

Scheme 18: General structure of substituted pyridinyl-phenyl sulphonamides.

Comp.	R_1	R_2	R_3	R_4	R_5	R_6	X	MP	Yield %
123	OCH_3	OCH_3	OCH_3	OCH_3	OH	H	-	154-156	85
125	OCH_3	OCH_3	OCH_3	OCH_3	F	H	-	140-142	89
126	H	OCH_3	OH	OCH_3	OCH_3	OCH_3	-	188-190	79
127	H	OH	CH_3	OCH_3	OCH_3	OCH_3	-	160-162	89
128	H	OCH_3	F	OCH_3	OCH_3	OCH_3	-	98-99	80
129	H	OH	F	OCH_3	OCH_3	OCH_3	-	189-190	80
130	OCH_3	OCH_3	OCH_3	OCH_3	F	H	CH_2	155-156	82
131	OCH_3	OCH_3	OCH_3	OCH_3	OH	H	CH_2	162-164	87

Table 5: synthesised substituted pyridinyl-phenyl sulphonamide with yield.

Chapter 4

Synthesis of substituted imidazo[4,5,b]pyridines

4 Synthesis of substituted imidazo[4,5,b]pyridines:

4.1 Introduction:

Imidazopyridines have gained great attention in the pharmaceutical and medicinal chemistry due to their structural similarity to purine and benzimidazole (figure 19). Generally, they are prepared by creating the imidazole ring from pyridine derivatives throughout the formation of N-C-N bonds. Some literature describes the formation of N-C-N bond by activating the reaction with Pd or Cu catalysts with *ortho*-halogen derivatives of pyridinyl amide as starting material with substituted amines (Zheng *et al.*, 2007; Zou *et al.*, 2007), (scheme 19), or by the amidation reaction of halogen derivatives of amino pyridines (Rosenberg *et al.*, 2012; Wilson *et al.*, 2014) (scheme 19).

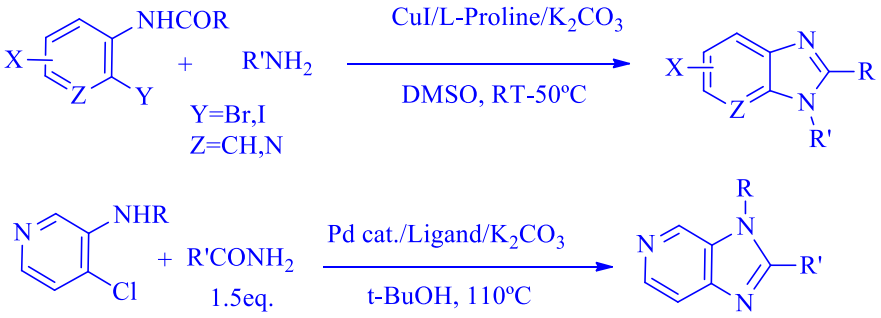

Scheme 19: synthesis of imidazo-pyridines through N-C-N bond formation.

However, the most familiar synthetic route is obtained by condensation dehydration reactions of *ortho*-diamino pyridines with aldehydes or carboxylic acid derivatives in presence of catalyst. The reaction of *ortho*-diamino pyridines with carboxylic acids has been explored, however, the reaction is low yielding and difficult to purify (Sajith & Muralidharan, 2012). Another synthetic route for the synthesis of disubstituted imidazo[4,5,b]pyridine has been reported using Pd-catalysed activation of the carbon centre in imidazole ring (Macdonald *et al.*, 2013; Sajith & Muralidharan, 2012). However, many disadvantages synchronised with these protocols such as limited availability of commercial substrates, poisonous materials, exhausting procedures, and costly catalysts and ligands (Padmaja *et al.*, 2018).

This chapter explores the synthesis of 2,3-disubstituted imidazo[4,5,b]pyridines as a promising analogues of the antimitotic agent combretastatin A-4.

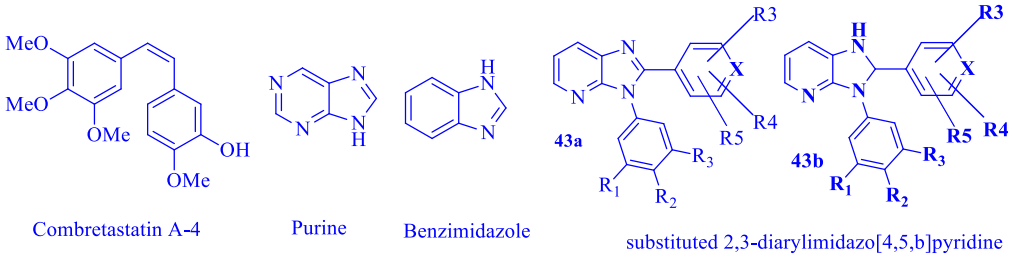

Figure 18: Chemical structure of purine, benzimidazole, combretastatin A-4, and substituted imidazo[4,5,b]pyridine.

4.2 Synthesis of substituted 2,3-diaryl-3H-imidazo[4,5-b]pyridine

2,3-Bis(3,4,5-trimethoxyphenyl)-3H-imidazo[4,5-b]pyridine (132) (Kim Choong Hahn *et al.*, 2015):

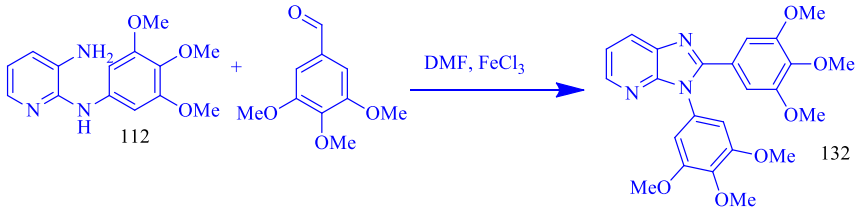

To a stirred solution of compound (112) (0.5 mmol., 0.137 g, 1 eq.) in DMF (15 cm^3) was added 3,4,5-trimethoxybenzaldehyde (0.6 mmol., 0.117 g, 1.2 eq.) and $FeCl_3$ (14 mg, 0.086 mmol., 0.09% eq.). The mixture was irradiated in a microwave vial for 30 minutes at 200 W and 120 °C. After completion of reaction, water (10 cm^3) was added and the product was extracted with ethyl acetate (3 x 30 cm^3), and the organic layer was washed with water (10 cm^3), dried with anhydrous $MgSO_4$, and solvent evaporated under reduced pressure. The crude product was purified by column chromatography (SiO_2: hexane: ethyl acetate 8:2, R_f = 0.5) to obtain the above titled compound as a white solid (0.115 g, 0.25 mmol., 51%, Mp =185-186ºC). HRMS (ESI): calculated for $C_{24}H_{26}N_3O_6$ (M+H) = 452.1822, found (M+H) = 452.1821, ΔMs=0.1ppm.

^{1}H NMR : δ (ppm) =3.67 [6H, s, 2 x (OCH_3)], 3.76 [6H, s, 2 x (OCH_3)], 3.83 [3H, s, (OCH_3)], 3.86 [3H, s, (OCH_3)], 6.61 [2H, s, Ar-H], 6.92 [2H, s, Ar-H], 7.28 [1H, dd, J = 8.05 Hz, 4.86 Hz, Py-H_2], 8.11 [1H, dd, J = 8.05 Hz, 1.4 Hz, Py-H1], 8.36 [1H, dd, J = 4.87 Hz, 1.46 Hz, Py-H3].

^{13}C NMR :δ (ppm) = 55.99 [2 x (OCH_3)], 56.41[2 x (OCH_3)], 60.89 [(OCH_3)], 60.98 [(CH_3O)], 105.61 [C-H, Ar-H *ortho* to methoxy], 106.47 [C-H, Ar-H *ortho* to methoxy], 119.36 [C-H, Py-C-H2], 124.08 [C-C, Ar-C-C=N], 127.16 [C-H, Py-C-H1], 131.29 [C-

O, Ar-C-OCH_3], 134.51 [C-O, 2 x Ar-C-OCH_3], 138.47 [C-N, Ar-C-N], 139.79 [C-N, Py-C-N], 144.83 [C-H, Py-C-H3], 149.64 [C-N, N-C=N,], 152.63 [C=N, Py-C=N], 152.97 [C-O, Ar-C-OCH_3], 154.10 [C-O, Ar-C-OCH_3].

FT-IR: ν_{max} (cm^{-1}): 2996 (C-H, str., aromatic), 2834 (C-H, str., aliphatic), 1589 (C=C, str., aromatic), 1118 (C-O-CH_3, asy. str.).

Following the above procedure the following imidazo[4,5,b]pyridines (133-155) were synthesised

2-(3,4,5-Trimethoxyphenyl)-3-(3-hydroxy-4-methoxyphenyl)- 3H-imidazo[4,5-b]pyridine (133):

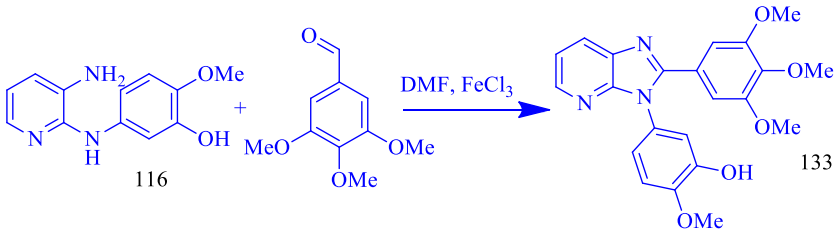

Using N2-(3-hydroxy-4-methoxyphenyl)pyridine-2,3-diamine (116) (0.115, 0.5 mmol.), and 3,4,5-trimethoxybenzaldehyde (0.6 mmol., 0.117 g), and $FeCl_3$ (0.014 g, 0.086 mmol.), the above titled imidazo[4,5,b]pyridine (133) was obtained as a white solid (0.115 g, 0.28 mmol., 56%). Mp = 222-223 ºC, after purification by flash chromatography (SiO_2: hexane: ethyl acetate 7:3, R_f = 0.2). HRMS (ESI): calculated for $C_{22}H_{22}N_3O_5$ = 408.1559, found (M+H) = 408.1554, ΔMs=0.5ppm.

^{1}H NMR from (methanol-d4): δ (ppm) =3.69 [6H, s, 2 x (OCH_3)], 3.78 [3H, s, (OCH_3)], 3.94 [3H, s, (OCH_3)], 6.86 [1H, dd, J = 8.48 Hz, 2.55 Hz, Ar-H *para* to OH], 6.90 [1H, d, J=2.48 Hz, Ar-H *ortho* to OH], 6.95 [2H, s, Ar-H *ortho* to methoxy (trimethoxy ring)], 7.11 [1H, d, J = 8.48 Hz, Ar-H *meta* to OH], 7.41[1H, dd, J = 8.10 Hz, 4.86 Hz, Py-H_2], 8.16 [1H, dd, J = 8.11 Hz, 1.21 Hz, Py-H_1], 8.32 [1H, dd, J = 4.85 Hz, 1.10 Hz, Py-H_3].

^{13}C NMR from (Methanol-d4): δ (ppm) =56.53[2 x (OCH_3)], 56.75[(OCH_3)], 61.18 [(OCH_3)], 108.22 [C-H, ortho to methoxy (trimethoxy ring)], 113.24 [C-H, Ar-C-H *meta* to OH], 116.48 [C-H, Ar-C-H *ortho* to OH], 120.72 [C-H, Ar-C-H *para* to OH], 120.91 [C-H, Py-C-H2], 124.85 [C-C, Ar-C-C], 127.97 [C-H, Py-CH1], 129.27 [C-N, Ar-C-N, trimethoxy ring], 135.02 [C-N, Py-C-N], 141.31 [C-O, Ar-C-OCH_3], 145.68

[C-H, Py-CH3], 149.06 [C-O, Ar-C-OCH_3], 150.25 [2 x C-N, (Py-C=N), (N-C=N)], 154.44 [2 x C-O, Ar- C-OCH_3]. 154.86 [C-O, Ar-C-OH].

FT-IR: ν_{max} (cm^{-1}): 3348 (OH str.), 2939 (C-H, str., aromatic.), 2842 (C-H, str., aliphatic), 1587 (C=C, str., aromatic), 1119 (C-O-CH_3, asy. str.).

2-(3-Fluoro-4-methoxyphenyl)-3-(3,4,5-trimethoxyphenyl)-3H-imidazo[4,5-b]pyridine (134):

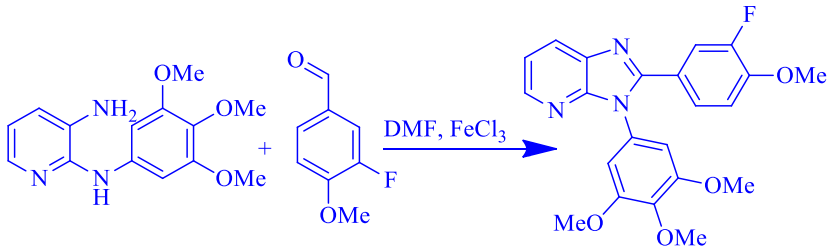

Using N2-(3,4,5-trimethoxyphenyl)pyridine-2,3-diamine (112) (0.5 mmol., 0.137 g), and 3,4,5-trimethoxybenzaldehyde (0.6 mmol., 0.092 g) and $FeCl_3$ (14 mg, 0.086 mmol.) the above titled imidazo[4,5,b]pyridine (134) was obtained as a dark purple solid (0.075 g, 0.18 mmol., 37%). Mp =162-163 ºC), after purification by flash chromatography (SiO_2: hexane: ethyl acetate 8:2, R_f = 0.5). HRMS (ESI): calculated for $C_{22}H_{21}FN_3O_4$ = 410.1516, found (M+H) = 410.1533, ΔMs=1.7ppm.

^{1}H NMR : δ (ppm) =3.72 [6H, s, 2 x (OCH_3)], 3.84 [3H, s, (OCH_3)], 3.86 [3H, s, (OCH_3)], 6.53 [2H, s, Ar-H, *ortho* to methoxy (trimethoxy ring)], 6.84 [1H, t, J = 8.56 Hz, Ar-H *meta* to F], 7.23 [2H, (1H, dd, J = 8.09 Hz, 4.86 Hz, Py-H2), (1H, m, *para* to F], 7.42 [1H, dd, J= 12.21 Hz, 2.01 Hz, Ar-H *ortho* to F], 8.06 [1H, dd, J = 4.84 Hz, 1.2 Hz, Py-H1], 8.33 [1H, dd, J= 8.09 Hz, 1.18 Hz, Py-H3].

^{13}C NMR: δ (ppm) =55.99 [2 x (OCH_3)], 56.32 [(OCH_3)], 60.98 [(OCH_3)], 105.35 [C-H, Ar-C-H *ortho* to methoxy (trimethoxy ring)] 112.86 [C-H, d, J =2.01 Hz, Ar-C-H, *para* to F], 116.87 [C-H, d, J = 20.93 Hz, Ar-C-H, *ortho* to F], 119.40 [C-H, Py-C-H2], 121.81 [C-C, d, J= 6.63 Hz, Ar-C-C], 125.67 [C-H, d, J=3.63 Hz, Ar-C-H *meta* to F], 127.14 [C-H, Py-C-H1], 130.73 [C-N, Ar-C-N, trimethoxy ring], 134.53 [C-O, Ar-C-OCH_3, trimethoxy ring], 138.53 [C-N, Py-C-N], 144.83 [C-H, Py-C-H3], 149.41 [C-O, d, J=10.76 Hz, ortho to F], 150.66 [C-F, d, J= 226.92 Hz, Ar-C-F], 149.55 [C=N, Py-C=N], 153.08 [N-C=N], 154.05 [2 x Ar-C-OCH_3].

FT-IR: ν_{max} (cm^{-1}): 2936 (C-H, str., aromatic), 2837 (C-H, str., aliphatic), 1593 (C=C, Str., aromatic), 1120 (C-O-CH_3, asy. str.).

2-(Benzo[d][1,3]dioxol-5-yl)-3-(3,4,5-trimethoxyphenyl)-3H-imidazo[4,5-b]pyridine (135):

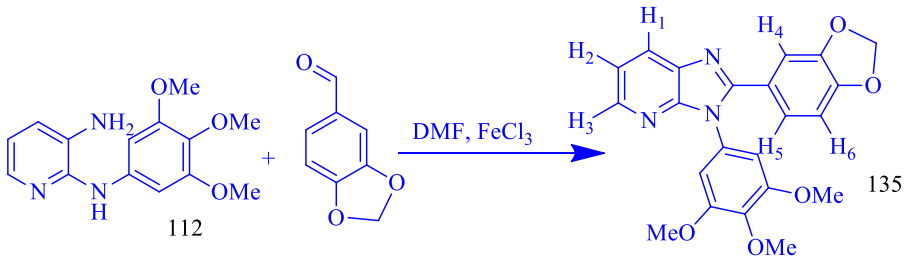

Using N2-(3,4,5-trimethoxyphenyl)pyridine-2,3-diamine (112) (0.5 mmol., 0.137 g), and 3,4-(methylenedioxy)benzaldehyde (0.6 mmol., 0.090 g) and $FeCl_3$ (14 mg, 0.086 mmol.,), the above imidazo[4,5,b]pyridine (135) was obtained as a dark purple solid ((0.105g, 0.25 mmol., 52%). Mp = 225-227 ºC, after purification by flash chromatography (SiO_2: hexane: ethyl acetate 7:3, R_f = 0.25). HRMS (ESI): calculated for $C_{22}H_{20}N_3O_5$ (M+H) = 406.1403, found (M+H) = 406.1390, ΔMs=-1.3ppm.

^{1}H NMR : δ (ppm) =3.76 [6 H, s, 2 x (OCH_3)], 3.88 [3 H, s, (OCH_3)], 5.97 [2H, s, (CH_2)], 6.56 [2H, s, *ortho* to methoxy (trimethoxy ring)], 6.73 [1H, d, J = 8.17 Hz, Ar-H6], 7.10 [1H, dd, J = 8.17Hz, 1.74 Hz, Ar-H5], 7.15 [1H, d, J=1.73 Hz, Ar-H4], 7.25 [1H, dd, J=8.00Hz, 4.842Hz, Py-H2], 8.08 [1H, dd, J= 7.98 Hz, 1.40 Hz, Py-H1], 8.34 [1H, dd, J=4.80Hz, 1.40Hz, Py-H3].

^{13}C NMR: δ (ppm) =56.30 [2 x (OCH_3)], 61.40 [(OCH_3)], 101.58 [(CH_2)], 105.35 [C-H, *ortho* to methoxy (trimethoxy ring)], 108.39 [C-H, Ar-C-H6], 109.35 [C-H, Ar-C-H5], 119.26 [C-H, Py-C-H2], 122.98 [C-C, Ar-C-C], [C-H, Ar-C-H4], 127.03 [C-H, Py-C-H1], 130.91 [C-N , Ar-C-N], 134.61 [C-O, Ar-C-OCH_3], 138.36 [C-N, Py-C-N], 144.60 [C-H, Py-C-H3], 147.79 [C=N , N-C=N], 149.39 [C-O, Ar-C-O], 149.55 [C-O, Ar-C-O], 152.87 [C=N , Py-C=N], 153.94 [2 x Ar-C-OCH_3].

FT-IR: ν_{max} (cm^{-1}): 2936 (C-H, str., aromatic), 2837 (C-H, str., aliphatic), 1593 (C=C, str., aromatic), 1228 (CH2, scissoring), 1120 (C-O-CH_3, asy. str.), 998 (CH_2, waging).

2-(3,4-Dihydroxyphenyl)-3-(3,4,5-trimethoxyphenyl)-3H-imidazo[4,5-b]pyridine (136):

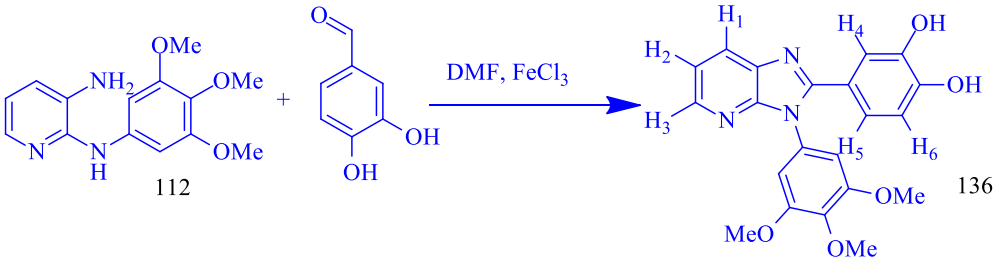

Using N2-(3,4,5-trimethoxyphenyl)pyridine-2,3-diamine (112) (0.5 mmol., 0.137 g), 3,4-dihydroxybenzaldehyd (0.6 mmol., 0.082 g), and $FeCl_3$ (14 mg, 0.086 mmol.), the above imidazo[4,5,b]pyridine (136) was obtained as a dark purple solid ((0.105 g, 0.26 mmol., 53%, Mp >250ºC) after purification by flash chromatography (SiO_2: hexane: ethyl acetate 5:5, R_f = 0.20). HRMS (ESI): calculated for $C_{21}H_{20}N_3O_5$ (M+H) = 394.1403, found (M+H) = 394.1396, ΔMs=0.7ppm.

^{1}H NMR: (d6-dmso):δ (ppm) =3.70 [6 H, s, 2 x (OCH_3)], 3.76 [3 H, s, (OCH_3)], 6.70 [1H, d, J= 8.34 Hz, Ar-H6], 6.77 [2H, s, *ortho* to methoxy (trimethoxy ring)], 6.87 [1H, dd, J = 8.33 Hz, 2.12 Hz, Ar-H5], 7.18 [1H, d, J = 2.12 Hz, Ar-H4], 7.30 [1H, dd, J = 8.05 Hz, 4.87 Hz, Py-H2], 8.09 [1H, dd, J = 8.05 Hz, 1.33 Hz, Py-H1], 8.26 [1H, dd, J = 4.87Hz, 1.32Hz, Py-H3], 9.70 [2H, s, 2 x OH].

^{13}C NMR: (d6-dmso):δ (ppm) =56.17[2 x (OCH_3)], 60.17 [(OCH_3)], 106.19 [C-H, *ortho* to methoxy (trimethoxy ring)], 115.25 [C-H, Ar-C-H6], 115.46 [C-H, C-H, Ar-C-H4], 118.77 [C-H, Py-C-H2], 120.47 [C-C, Ar-C-CN], 120.79 [C-H, Ar-C-H5], 126.19 [C-H, Py-C-H1], 131.40 [C-N, Ar-C-N], 134,52 [C-N, Py-C-N], 137.52 [C-O, Ar-C-OCH_3], 143.32 [C-H, Py-C-H3], 144.95 [C=N, N-C=N], 147.48 [C-O, Ar-C-OH], 149.76 [C=N, Py-C=N], 153.14 [2 x Ar-C-O-CH_3], 153.16 [C-O, Ar-C-OH].

FT-IR: ν_{max} (cm^{-1}) 3529 (OH str.), 2933 (C-H, str., aromatic.), 2837 (C-H, str., aliphatic), 1596 (C=C, str., aromatic), 1123 (C-O-CH_3, asy. str.).

2-(3,4,5-trifluorophenyl)-3-(3,4,5-trimethoxyphenyl)-2,3-dihydro-1H-imidazo[4,5-b]pyridine (137):

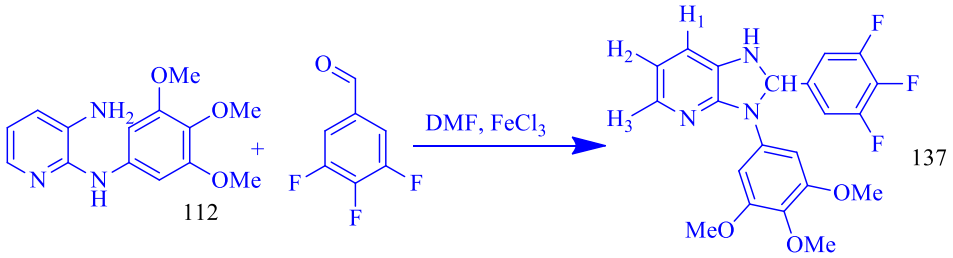

Using N2-(3,4,5-trimethoxyphenyl)pyridine-2,3-diamine (112) (0.5 mmol., 0.137 g), 3,4,5-triflourobenzaldehyd (0.6 mmol., 0.096 g), and $FeCl_3$ (14 mg, 0.086 mmol.), the above imidazo[4,5,b]pyridine (137) was obtained as a dark purple solid (0.105 g, 0.25 mmol., 41%). Mp = 171-173 ºC, after purification by flash chromatography (SiO_2: hexane: ethyl acetate 9:1, R_f = 0.10). HRMS (ESI): calculated for $C_{21}H_{17}F_3N_3O_3$ (M+H) = 418.1378, found for (M+H) = 418.1366, ΔMs=1.3ppm.

^{1}H NMR: δ (ppm) =3.71 [3 H, , (OCH_3)], 3.74 [3 H, (OCH_3)], 3.75 [3 H, (OCH_3)], 4.49 [1H, d, J= 5.90 Hz, N-H,], 5.82 [1H, d, J=5.73 Hz, C-H-NH], 6.12 [1H, s, *ortho* to methoxy (trimethoxy ring)], 6.51 [1H, dd, J = 7.61 Hz, 4.92 Hz, Py-H2], 6.64, [2 H, m, Ar-H, *ortho* to F], 6.73 [1H, dd, J = 7.61 Hz, 1.23 Hz, Py-H1], 7.29 [1H, NH, labile protone], 7.58 [1H, dd, J=4.93 Hz, 1.23 Hz, Py-H3].

^{13}CNMR: δ (ppm) =56.17[(OCH_3)], 60.17 [(OCH_3)], 61.07 [(OCH_3], 61.35 [CH-NH], 98.30 [C-H, ortho to methoxy (trimethoxy ring)], 111.16 [2C-H, dd, J = 16.28 Hz, 5.49 Hz, *ortho* to F], 112.83 [C-quaternary, Ar-C, trimethoxy ring], 115.90 [C-H, Py-C-H2], 126.94 [C-H, Py-C-H1], 130.09 [C-N, Ar-C-N], 135.68 [Ar-C-OCH_3], 137.00 [C-N, Py-C-N], 137.08 [C=C, m, meta to F], 139.25 [C-H, Py-C-H3], 139.37 [C-F, ddd, J= 250.89 Hz, 15.70 Hz, 2.98 Hz], 146.19 [C=N, Py-C=N], 150.98 [Ar-C-OCH_3], 151.05 [2C-F, ddd, J=250.64 Hz, 10.17 Hz, 3.68 Hz, , Ar-C-F], 152.39 [Ar-C-OCH_3].

FT-IR: ν_{max} (cm^{-1}): 3356 (NH str.), 2938 (C-H, str., Aromatic.), 2836 (C-H, str., aliphatic), 1600 (NH, bend.), 1525 (C=C, Str., Aromatic), 1101 (C-O-CH_3, Asy. Str), 1019 (C-F str.).

2-(6-Bromo-3-hydroxy-2-methoxyphenyl)-3-(3,4,5-trimethoxyphenyl)-3H-imidazo[4,5-b]pyridine (138):

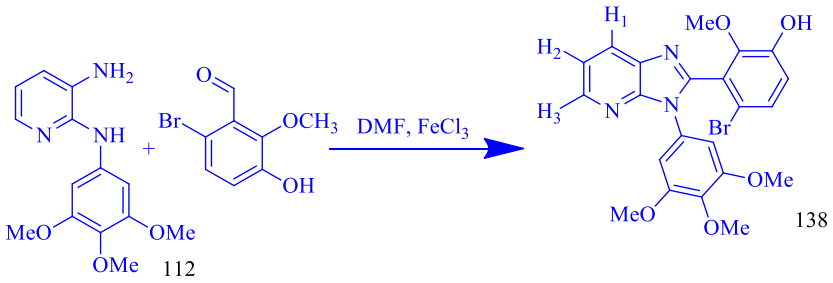

Using N2-(3,4,5-trimethoxyphenyl)pyridine-2,3-diamine (112) (0.5 mmol., 0.137 g, 1eq.), 6-bromo-3-hydroxy-2-methoxybenzaldehyde (0.6 mmol., 0.138 g, 1.2 eq.), and $FeCl_3$ (14 mg, 0.086 mmol.), the above imidazo[4,5,b]pyridine (138) was obtained as a pale yellow solid (0.125 g, 0.25 mmol., 41% , Mp =130-132 ºC) after purification by flash chromatography (SiO_2: hexane: ethyl acetate 1:1, R_f = 0.10). HRMS (ESI): calculated for $C_{22}H_{20}BrN_3O_5$ (M+H) = 486.0659, found for (M+H) = 486.0667, ΔMs=-0.8ppm.

^{1}H NMR : δ (ppm) =3.62 [3 H, s, (OCH_3)], 3.64 [6H, 2 x (OCH_3)], 3.80 [3 H, s, (OCH_3)], 6.55 [1H, d, J = 8.79 Hz, *ortho* to OH], 6.68 [2H, s, Ar-H, trimethoxy ring], 6.82 [1H, d, J = 8.78 Hz, *meta* to OH], 7.18 [1H, dd, J = 8.07 Hz, 4.87 Hz, Py-H2], 7.87(1H, OH), 8.02 [1H, dd, J = 8.06 Hz, 1.29 Hz, Py-H1], 8.33 [1H, dd, J = 4.87 Hz, 1.29 Hz, Py-H3].

^{13}C NMR: δ (ppm) =56.04 [2 x (OCH_3)], 56.32 [(OCH_3)], 60.76 [(OCH_3)], 104.39 [C-H, *ortho* to methoxy (trimethoxy ring)], 113.26 [C-H, Ar-C-H *ortho* to OH], 114.30 [C-Br, Ar-C-Br], 118.92 [C-H, Py-C-H2],119.33 [C-C, Ar-C-C], 122.82 [C-H, Ar-C-H *meta* to OH], 127.80 [C-H, Py-C-H1], 129.76 [C-N, Ar-C-N], 134.47 [C-N, Py-C-N], 137.76 [C-O, Ar-C-OCH_3], 144.86 [C-H, Py-C-H3], 146.87 [2 x C-N, (Py-C-N), (N-C=N)], 146.87 [C-O, Ar-C-OCH_3 *ortho* to OH], 150.56 [C-O, Ar-C-OH], 153.12 [2 x C-O, (Ar-C-OCH_3), trimethoxy ring].

FT-IR: ν_{max} (cm^{-1}): 3345 (OH str.), 2938 (C-H, str., aromatic), 2835 (C-H, str., aliphatic), 1598, 1505 (C=C, Str., aromatic), 1121 (C-O-CH_3, asy. Str).

2-(4-Hydroxy-3-methylphenyl)-3-(3,4,5-trimethoxyphenyl)-3h-imidazo[4,5-b]pyridine (139):

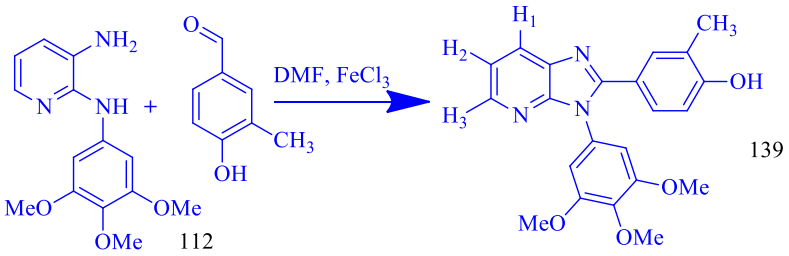

Using N2-(3,4,5-trimethoxyphenyl)pyridine-2,3-diamine (112) (0.5 mmol., 0.137 g), 4-hydroxy-3-methylbenzaldehyde (0.6 mmol., 0.081g), and $FeCl_3$ (14 mg, 0.086 mmol.), the above imidazo[4,5,b]pyridine (139) was obtained as a dark purple solid (0.110 g, 0.28 mmol., 57%). Mp =249-250 ºC, after purification by column chromatography (SiO_2: hexane: ethyl acetate 1:1, R_f = 0.10). HRMS (ESI): calculated for $C_{22}H_{22}N_3O_4$ (M+H) = 392.1605, found for (M+H) = 392.1611, ΔMs=-0.6ppm.

^{1}H NMR (d6-dmso): δ (ppm) =2.09 [3 H, s, (CH_3)], 3.69 [6 H, s, 2 x (OCH_3)], 3.75 [3H, s, (OCH_3)], 6.73 [1H, d, J = 8.38 Hz, Ar-H *meta* to CH_3], 6.79 [2H, s, *ortho* to methoxy (trimethoxy ring)], 7.19 [1H, dd, J=8.40 Hz, 2.0 Hz, Ar-H *para* to CH_3], 7.32 [1H, dd, J=7.97 Hz, 4.81 Hz, Py-H2], 7.50 [1H, d, J = 2.01Hz, Ar-H *ortho* to CH_3], 8.10 [1H, dd, J=7.97 Hz, 1.42 Hz, Py-H1], 8.26 [1H, dd, J = 4.81 Hz, 1.42 Hz, Py-H3], 9.89 [1H, s, OH].

^{13}C NMR (d6-dmso):δ (ppm) =15.97 [(CH_3)], 56.24[2 x (OCH_3)], 60.22 [(OCH_3)], 106.38 [C-H, *ortho* to methoxy (trimethoxy ring)], 114.19 [C-H, Ar-C-H *meta* to CH_3], 118.77 [C-H, Ar-C-H *ortho* to CH_3], 119.94 [C-C, Ar-C-CH_3], 123.90 [C-C, Ar-C-CH], 126.18 [C-H, Py-C-H2], 127.71 [C-H, Ar-C-H *para* to CH_3], 131.43 [C-H, Py-C-H1], 131.71 [C-N, Ar-C-N], 134.52 [C-N, Py-C-N], 137.64 [C-O, Ar-C-OCH_3], 143.33 [C-H, Py-C-H3], 149.76 [C=N, Py-C=N], 153.12 [C=N, N-C=N], 153.19 [2 x C-O, Ar-C-OCH_3 trimethoxy ring], 157.26 [C-O, Ar-C-OH].

FT-IR: ν_{max} (cm^{-1}): 3344 (OH str.), 2926 (C-H, str., aromatic.), 2835 (C-H, str., aliphatic), 1599, 1577 (C=C, str., aromatic), 1125 (C-O-CH_3, asy. str).

2-(2-Methoxypyridin-3-yl)-3-(3,4,5-trimethoxyphenyl)-3H-imidazo[4,5-b]pyridine (140):

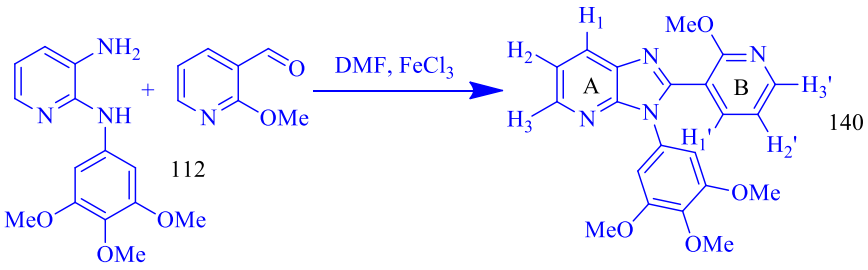

Using N2-(3,4,5-trimethoxyphenyl)pyridine-2,3-diamine (112) (0.5 mmol., 0.137 g), 2-methoxy-3-pyridinecarboxaldehyde (0.6 mmol., 0.068 g), and $FeCl_3$ (14 mg, 0.086 mmol.), the above imidazo[4,5,b]pyridine (140) was obtained as a pale white solid (0.110 g, 0.28 mmol., 56%). Mp =157-159 ºC, after purification by flash chromatography (SiO_2: hexane: ethyl acetate 1:1, R_f = 0.10). HRMS (ESI) calculated for $C_{21}H_{21}N_4O_4$ (M+H) = 393.1557, found for (M+H) = 393.1565, ΔMs=-0.8ppm.

^{1}H NMR: δ (ppm) =3.65 [3 H, s, (OCH_3)], 3.73 [6 H, s, 2 x (OCH_3)], 3.89 [3H, s, (OCH_3)], 6.56 [2H, s, *ortho* to methoxy (trimethoxy ring)], 7.03 [1H, dd, J = 7.32 Hz, 4.96 Hz, Py-H2'], 7.36 [1H, dd, J = 8.03 Hz, 4.85 Hz, Py-H2], 7.98 [1H, dd, J=7.32 Hz, 1.92 Hz, Py-H1'], 8.21 [1H, dd, J = 8.04 Hz, 1.39 Hz, Py-H1], 8.29 [1H, dd, J = 4.97 Hz, 1.91 Hz, Py-H3'], 8.46 [1H, dd, J = 4.85Hz,1.39Hz, Py-H3].

^{13}CNMR: δ (ppm) =53.36[(OCH_3)], 56.19 [2 x (OCH_3)], 60.19 [(OCH_3], 103.97 [C-H, *ortho* to methoxy (trimethoxy ring)], 113.70 [C-C, Py-C-C], 116.78 [C-H, Py-C-H2], 119.36 [C-H, Py-C-H1], 127.58 [C-H, Py-C-H2'], 130.63 [C-N, Ar-C-N], 134.33 [C-O, Ar-C-OCH_3], 137.86 [C-N, Py-C-N, ring A], 140.72 [C-H, Py-C-H1'], 145.23 [C-H, Py-C-H3], 148.24 [C=N, N-C=N], 149.39 [C-H, Py-C-H3'], 150.59 [C-N, Py-C=N, ring A], 153.37 [2 x C-O, Ar-C-OCH_3 trimethoxy ring], 160.91 [O-C=N, Py-C=N, ring B].

FT-IR: ν_{max} (cm^{-1}): 3012 (C-H, str., aromatic), 2825 (C-H, str., aliphatic), 1588, 1579 (C=C, str., aromatic), 1119 (C-O-CH_3, asy. str.).

2-(2-Methylpyridin-3-yl)-3-(3,4,5-trimethoxyphenyl)- 2,3-dihydro-1H-imidazo[4,5-b]pyridine (141):

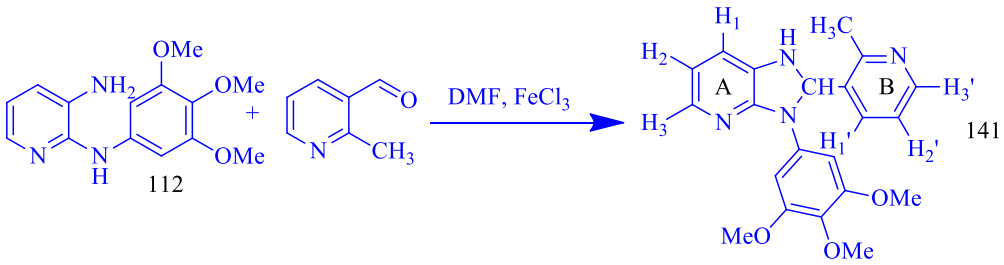

Using N2-(3,4,5-trimethoxyphenyl)pyridine-2,3-diamine (112) (0.5 mmol., 0.137 g), 2-methyl-3-pyridinecarboxaldehyde (0.6 mmol., 0.134 cm^3), and $FeCl_3$ (0.014 g, 0.086 mmol.), the above imidazo[4,5,b]pyridine (141) was obtained as a brown solid (0.118 g, 0.3 mmol., 62% , Mp = 234-235 ºC) after purification by flash chromatography (SiO_2: hexane: ethyl acetate 1:1, R_f = 0.20). HRMS (ESI): calculated for $C_{21}H_{23}N_4O_3$ (M+H) = 379.1770, found for (M+H) = 379.1765, ΔMs=0.5ppm.

^{1}H NMR : δ (ppm) =2.37 [3H, s, (CH_3)], 3.47 [3H, s, (OCH_3)], 3.74 [3H, s, (OCH_3)], 3.80 [3H, s, (OCH_3)], 4.98 [1H, d, J=2.91 Hz, NH], 6.23 [1H, s, CH], 6.28 [1H, s, Ar-H, trimethoxy ring], 6.47 [1H, dd, J= 7.60 Hz, 4.91 Hz, Py-H2'], 6.56 [1H, dd, J= 7.61 Hz, 1.21 Hz, Py-H1'], 6.94 [1H, dd, J=7.42 Hz, 4.81 Hz, Py-H2], 7.17 [1H, s, labile proton], 7.39 [1H, dd, J=7.43 Hz, 1.1.21Hz, Py-H1], 7.67 [1H, dd, J=4.80 Hz, 1.21 Hz, Py-H3], 8.19 [1H, dd, J=4.91 Hz, 1.21 Hz, Py-H3'].

^{13}CNMR : δ (ppm) =18.52 [(CH_3)], 55.80 [(OCH_3)], 56.01 [(OCH_3)], 60.81 [(OCH_3)], 60.97 [CH-NH], 98.75 [C-H, *ortho* to methoxy (trimethoxy ring)], 114.53 [C-quternary, Ar-C- trimethoxy ring], 115.29 [C-H, Py-C-H2], 121.73[C-H, Py-H2'], 125.68 [C-H, Py-C-H1'], 130.34 [C-N, Ar-C-N], 131.99 [C-C, Py-C-CH], 135.79 [C-O, Ar-C-OCH_3], 137.27 [C-H, Py-H1], 137.73 [C-C, Py-C-CH_3 ring B], 137.96 [C-H, Py-C-H3], 146.11 [C-H, Py-C-H3'], 147.71 [C-N, Py-C-NH, ring A], 150.72 [C-O, Ar-C-OCH_3], 152.85 [C-O, Ar-C-OCH_3], 158.56 [C=N, Py-C=N, ring A].

FT-IR: ν_{max} (cm^{-1}): 3240 (NH str.), 2930 (C-H, str., aromatic), 2825 (C-H, str., aliphatic), 1601 (NH bend.), 1547, 1498 (C=C, str., aromatic), 1115 (C-O-CH_3, asy. str).

2-(2-Fluoropyridin-3-yl)-3-(3,4,5-trimethoxyphenyl)-2,3-dihydro-1H-imidazo[4,5-b]pyridine (142):

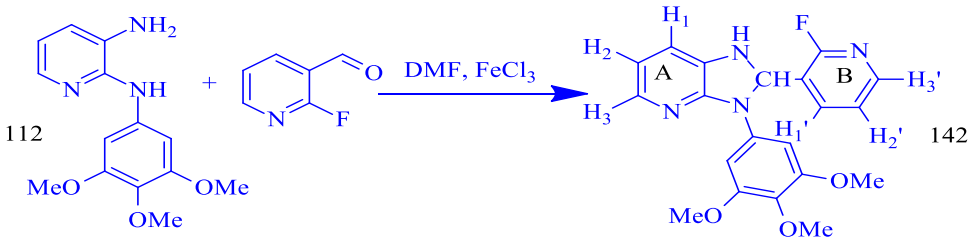

Using N2-(3,4,5-trimethoxyphenyl)pyridine-2,3-diamine (112) (1 mmol., 0.275 g), 2-flouro-3-pyridinecarboxaldehyde (1.2 mmol., 0.120 cm^3), and $FeCl_3$ (28 mg, 0.172 mmol.), The above imidazo[4,5,b]pyridine (142) was obtained as a yellow solid (0.128 g, 0.33 mmol., 34%). Mp =166-168 ºC, after purification by column chromatography (SiO_2: hexane: ethyl acetate 9:1, R_f =0.05). HRMS (ESI) calculated for $C_{20}H_{20}FN_4O_3$ (M+H) = 383.1519, found for (M+H) = 383.1518, ΔMs=0.1ppm.

^{1}H NMR (CD_2Cl_2): δ (ppm) =3.63 [3H, s, (OCH_3)], 3.70 [3H, s, (OCH_3)], 3.76 [3H, s, (OCH_3)], 4.79 [1H, d, J= 6.04 Hz, NH], 6.11 [1H, s, Ar-H, trimethoxy ring], 6.17 [1H, s, CH], 6.50 [1H, dd, J=7.58 Hz, 4.881 Hz, Py-H2], 6.76 [1H, m, Py-H2'], 6.84 [1H, d, J=7.57Hz, Py-H1], 7.13 [1H, m, Py-H1'], 7.69 [1H, dd, J=4.88Hz,1.32Hz, Py-H3], 7.92 [1H, d, J=4.72Hz, Py-H3'], 8.08 [1H, s, labile proton].

^{13}C NMR (CD_2Cl_2): δ (ppm) =52.15 [CH-NH, d, J=1.28Hz], 55.74 [(OCH_3], 61.02 [(OCH_3)], 61.23 [(OCH_3)], 97.39 [C-H, *ortho* to methoxy], 110.16 [C-quaternary, Ar-C-], 115.71 [C-H, Py-C-H2], 121.30 [C-H, d, J=4.07 Hz, Py-C-H2'], 124.08 [C-C, d, J=27.8 Hz, Py-C-CH, ring B], 127.30 [C-H, Py-C-H1], 130.27[C-N, Ar-C-N], 135.20 [C-O, Ar-C-OCH_3], 137.58 [C-N, Py-C-N, ring A], 139.55 [C-H, d, J=4.07Hz, Py-C-H1'], 140.70 [C-H, Py-C-H3], 146.13 [C-H, d, J=15.42Hz, Py-C-H3'], 147.01 [C=N, Py-C=N, ring A], 150.93 [C-O, Ar-C-OCH_3], 153.59 [C-O, Ar-C-OCH_3], 161.38 [C-F,, d=239.14 Hz, Py-C-F].

FT-IR: ν_{max} (cm^{-1}): 3384 (NH str.), 2986 (C-H, str., aromatic), 2941 (C-H, str., aliphatic), 1598 (NH ben.), 1528, 1495 (C=C, str., aromatic), 1096 (C-O-CH_3, asy. str.), 997 (C-F).

2-(3,5-Difluoro-4-methoxyphenyl)-3-(3,4,5-trimethoxyphenyl)-3H-imidazo[4,5-b]pyridine (143):

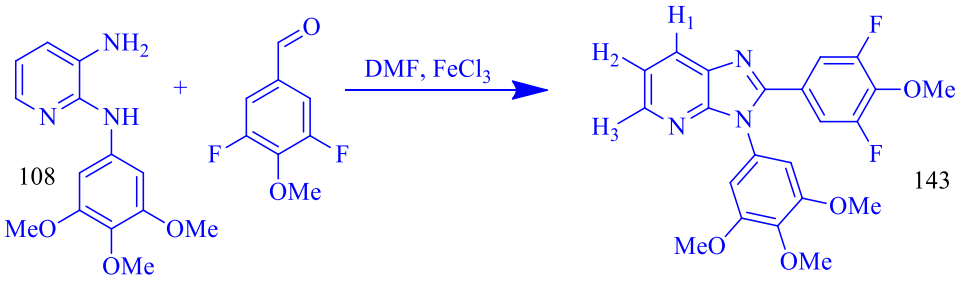

Using N2-(3,4,5-trimethoxyphenyl)pyridine-2,3-diamine (112) (1 mmol., 0.275 g), 3,5-difluoro-4-methoxybenzaldehyde (1.2 mmol., 0.206 g), and $FeCl_3$ (28 mg, 0.172 mmol.), the above Imidazo[4,5,b]pyridine (143) was obtained as a yellow solid (0.163 g, 0.38 mmol., 38%). Mp =244-246ºC, after purification by column chromatography (SiO_2: hexane: ethyl acetate 7:3, R_f = 0.15). HRMS (ESI): calculated for $C_{22}H_{20}F_2N_3O_4$ = 428.1428, found for (M+H) = 428.1425, ΔMs=0.3ppm.

^{1}H NMR: δ (ppm) =3.77 [6 H, s, 2 x (OCH_3)], 3.97 [3 H, s, (OCH_3)], 4.05 [3H, d, J = 2.66 Hz, (OCH_3), difluoro ring], 6.52 [2H, s, *ortho* to methoxy (trimethoxy ring)], 7.18 [2H, dd, J = 6.52 Hz, 9.82 Hz, Ar-H *ortho* to F], 7.24 [1H, dd, J = 8.03 Hz, 4.82 Hz, Py-H2], 8.04 [1H, dd, J = 8.03 Hz, 1.49 Hz, Py-H1], 8.33 [1H, dd, J = 4.87 Hz, 1.49 Hz, Py-H3].

^{13}C NMR: δ (ppm) =56.37 [2 x (OCH_3)], 61.74 [(OCH_3)], 61.78 [(OCH_3), t, J = 7.32 Hz, *ortho* to F], 105.36 [C-H, *ortho* to methoxy (trimethoxy ring)], 113.06 [C-H, dd, J = 8.03 Hz, 7.75 Hz, *ortho* to F], 119.47 [C-H, Py-C-H2], 123.72 [C-C, t, J=19.42 Hz, *meta* to F], 127.61 [C-H, Py-C-H1], 130.43 [C-N, Ar-C-N, trimethoxy ring], 134.82 [C-N, Py-C-N], 137.95 [C-O, t, J = 27.18 Hz, ortho to F], 138.81 [C-O, Ar-C-OCH_3], 149.73 [C=N, Py-C-N], 150.52 [N-C=N, t, J = 5.88Hz], 154.93 [C-F, dd, J=248.97 Hz, 6.57 Hz], 154.14 [C-O, 2 x Ar-C-OCH_3].

FT-IR: ν_{max} (cm^{-1}): 2942 (C-H, str., aromatic), 2834 (C-H, str., aliphatic), 1594 (C=C, str., aromatic), 1130 (C-O-CH_3, asy. str.), 994 (C-F).

2-(3-Fluoro-4-Hydroxy-5-methoxyphenyl)-3-(3,4,5-trimethoxyphenyl)-3H-imidazo[4,5-b]pyridine (144):

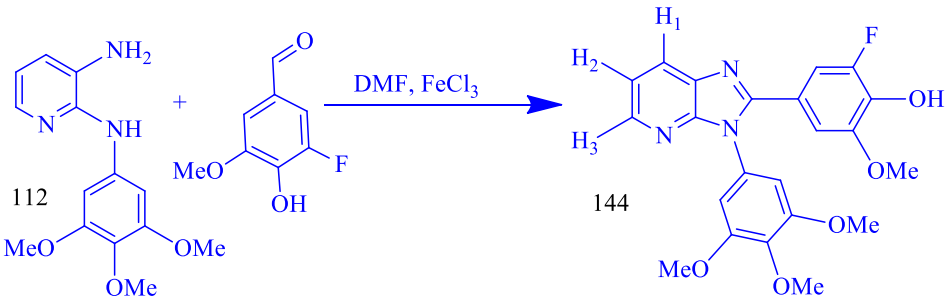

Using N2-(3,4,5-trimethoxyphenyl)pyridine-2,3-diamine (112) (0.5 mmol., 0.137 g), 3-fluoro-4-hydroxy-5-methoxybenzaldehyde (0.6 mmol., 0.102 g), and $FeCl_3$ (14 mg, 0.086 mmol.), the above imidazo[4,5,b]pyridine (144) was obtained as a pale white solid (0.163 g, 0.38 mmol., 38%). Mp > 250ºC, after purification by flash chromatography (SiO_2: hexane: ethyl acetate 1:1, R_f = 0.11). HRMS (ESI): calculated for $C_{22}H_{21}FN_3O_5$ (M+H) = 426.1460, found for (M+H) = 426.1466, ΔMs=0.6ppm.

^{1}H NMR (d6-dmso): δ (ppm) =3.62 [3 H, s, (OCH_3)], 3.69 [9 H, 2 x s, 3 x (OCH_3)], 6.87 [2 H, s, *ortho* to methoxy (trimethoxy ring)], 7.03 [1H, t, J = 1.9 Hz, Ar-H *para* to F] 7.09 [1H, dd, J = 11.56 Hz, 1.9 Hz, Ar-H *ortho* to F], 7.34 [1H, dd, J = 8.18 Hz, 4.86 Hz, Py-H2], 8.15 [1H, dd, J = 8.18 Hz, 1.33 Hz, Py-H1], 8.31 [1H, dd, J = 4.86 Hz, 1.33 Hz, Py-H2], 9.88 [1H, s, (OH)].

^{13}CNMR (d6-dmso): δ (ppm) = 55.77 [(OCH_3)], 56.31 [2 x (OCH_3)], 60.15 [(OCH_3)], 106.52 [C-H, *ortho* to methoxy (trimethoxy ring)], 108.47 [C-H, d, J = 1.49 Hz, Ar-C-H *para* to F], 109.25 [C-H, d, J = 21.49 Hz, Ar-C-H *ortho* to F], 119.02 [C-H, Py-C-H2], 119.30 [C-C, d, J = 9.86 Hz, Ar-C-C], 126.60 [C-H, Py-C-H1], 131.27 [C-N, Ar-C-N], 134.26 [C-N, Py-C-N], 136.28 [C-O, d, J = 14.18 Hz, Ar-C-OH], 137.38 [C-O, Ar-C-OCH_3, trimethoxy ring], 143.92 [[C-H, Py-C-H3], 148.84 [C-O, d, J = 6.70 Hz, Ar-C-OCH_3 *meta* to F], 150.76 [C-F, d, J=237.96 Hz], 149.81 [C-N, Py-C=N], 151.51[N-C=N, d, J=3.03 Hz], 153.39 [C-O, 2 x Ar-C-OCH_3, trimethoxy ring].

FT-IR: ν_{max} (cm^{-1}): 3497 (OH, str.), 2938(C-H, str., aromatic), 2840 (C-H, str., aliphatic), 1595 (C=C, str., aromatic), 1184 (C-O-CH_3, asy. str.), 1001 (C-F).

2-(3-Hydroxy-4,5-dimethoxyphenyl)-3-(3,4,5-trimethoxyphenyl)-3H-imidazo[4,5-b]pyridine (145):

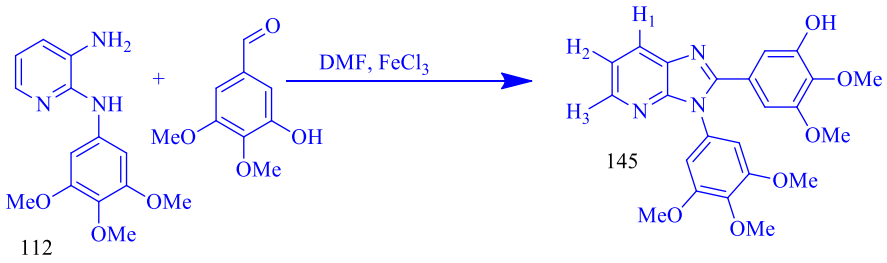

Using N2-(3,4,5-trimethoxyphenyl)pyridine-2,3-diamine (112) (0.5 mmol., 0.137 g), 3-hydroxy-4,5-dimethoxybenzaldehyde (0.6 mmol., 0.109 g), and $FeCl_3$ (14 mg, 0.086 mmol.), the above imidazo[4,5,b]pyridine (145) was obtained as a pale yellow solid (0.128 g, 0.29 mmol., 57%). Mp = 244-246 ºC, after purification by flash chromatography (SiO_2: hexane: ethyl acetate 1:1, R_f = 0.12). HRMS (ESI): calculated for $C_{23}H_{24}N_3O_6$ (M+H) = 438.1665, found for (M+H) = 438.1674, ΔMs=-0.9ppm.

^{1}H NMR (d6-dmso): δ (ppm) =3.58 [3H, s, (OCH_3)], 3.70 [9 H, 2 x s, 3 x (OCH_3)], 3.74 [3H, s, (OCH_3)], 6.78 [1H, d, J=1.78 Hz, Ar-H4], 6.90 [2 H, s, Ar-H trimethoxy ring], 6.94 [1H, d, J =1.80 Hz, Ar-H5], 7.43 [1H, dd, J = 8.03 Hz, 4.79 Hz, Py-H2], 8.12 [1H, dd, J = 8.03 Hz, 1.13 Hz, Py-H1], 8.38 [1H, dd, J = 4.79 Hz, 4.86 Hz, Py-H3], 9.78 [1H, s, (OH)].

^{13}CNMR (d6-dmso): δ (ppm) = 55.46 [(OCH_3)], 56.29 [2 x (OCH_3)], 59.97 [(OCH_3)], 60.15 [(OCH_3)], 104.81 [C-H, Ar-C-H *ortho* to OH], 106.45 [C-H, Ar-H *ortho* to methoxy (trimethoxy ring)], 110.82 [C-H, Ar-C-H *para* to OH], 119.87 [C-H, Py-C-H2], 122.51 [C-C, Ar-C-C], 125.83 [C-H, Py-C-H1], 130.49 [C-N, Ar-C-N], 131.55 [C-O, Ar-C-OCH_3], 138.01 [C-N, Py-C-N], 138.54 [C-O, Ar-C-OCH_3], 144.83 [C-H, Py-C-H3], 148.75 [C-O, Ar-C-OCH_3], 150.52 [C-N, Py-C=N], 151.85 [C-O, Ar-C-OH], 152.59 [C-N, N-C=N], 153.34 [C-O, 2 x Ar-C-OCH_3].

FT-IR: ν_{max} (cm^{-1}): 3354 (OH, str.), 2943 (C-H, str., aromatic), 2840 (C-H, str., aliphatic), 1594 (C=C, str., aromatic), 1232 (C-O-CH3, asy. str.).

2-(3,4-Dihydroxy-5-methoxyphenyl)-3-(3,4,5-trimethoxyphenyl)-3H-imidazo[4,5-b]pyridine (146):

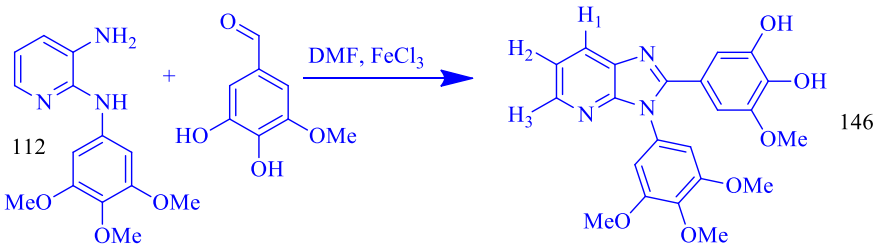

Using N2-(3,4,5-trimethoxyphenyl)pyridine-2,3-diamine (112) (0.5 mmol., 0.137 g), 3,4-dihydroxy-5-methoxybenzaldehyde (0.6 mmol., 0.100 g), and $FeCl_3$ (14 mg, 0.086 mmol.), the above imidazo[4,5,b]pyridine (146) was obtained as a pale purple solid (0.125 g, 0.29 mmol., 59%). Mp = 228-230 ºC) after purification by flash chromatography (SiO_2: hexane: ethyl acetate 1:1, R_f = 0.11). HRMS (ESI) calculated for $C_{22}H_{22}N_3O_6$ (M+H) = 424.1508, found for (M+H) = 424.1512, ΔMs=-0.4ppm.

^{1}H NMR (d4-methanol): δ (ppm) =3.68 [3H, (OCH_3)], 3.71 [6H, 2 x (OCH_3)], 3.74 [3H, (OCH_3)], 6.64 [1H, d, J=1.98 Hz, Ar-H *para* to OH], 6.67 [2H, s, *ortho* to methoxy (trimethoxy ring)], 6.78 [1H, d, J= 1.98 Hz, Ar-H *ortho* to OH], 7.28 [1H, dd, J= 8.05 Hz, 4.85 Hz, Py-H2], 8.01 [1H, dd, J= 8.05 Hz, 1.22 Hz, Py-H1], 8.18 [1H, dd, J=4.85 Hz, 1.22 Hz, Py-H3].

^{13}CNMR (d4-methanol): δ (ppm) =56.52 [(OCH_3)], 56.93 [2 x (OCH_3)], 61.26 [(OCH_3)], 106.26 [C-H, Ar-C-H *para* to OH], 107.34 [C-H, *ortho* to methoxy (trimethoxy ring)], 111.70 [C-H, Ar-C-H *ortho* to OH], 120.27 [C-C, Ar-C-C], 120.54 [C-H, Py-C-H2], 127.95 [C-H, Py-C-H1], 132.53 [C-N, Ar-C-N], 136.00 [C-N, Py-C-N], 138.21 [C-O, Ar-C-OCH_3], 139.85 [C-O, Ar-C-OCH_3], 144.87 [C-H, Py-C-H3], 146.78 [C=N, Py-C=N], 149.27 [C=N, N-C=N], 150.41[C-O, Ar-C-OH], 155.39 [C-O, 2 x Ar-C-OCH_3], 155.81 [C-O, Ar-C-OH].

FT-IR: ν_{max} (cm^{-1}): 3499 (OH Str.), 2937 (C-H str., aromatic), 2848 (C-H str., aliphatic), 1594 (C=C Str., aromatic), 1125 (C-O-CH_3 asy. str.).

2-(4-Hydroxy-3,5-dimethoxyphenyl)-3-(3,4,5-trimethoxyphenyl)-3H-imidazo[4,5-b]pyridine (147):

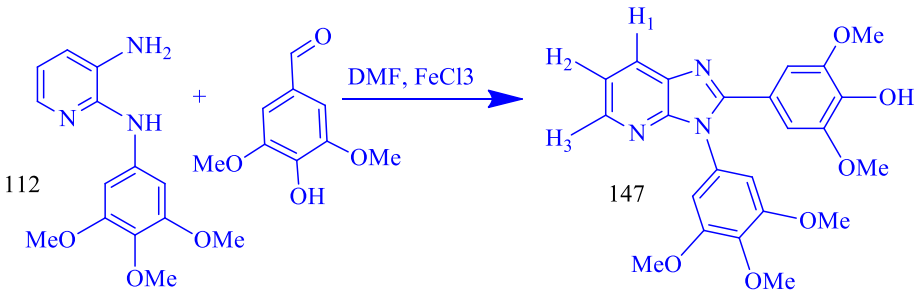

Using N2-(3,4,5-trimethoxyphenyl)pyridine-2,3-diamine (112) (0.5 mmol., 0.137 g), 4-hydroxy-3,5-dimethoxybenzaldehyde (0.6 mmol., 0.109 g), and $FeCl_3$ (14 mg, 0.086 mmol.), the above Imidazo[4,5,b]pyridine (147) was obtained as a yellow solid (0.132 g, 0.30 mmol., 61%). Mp =189-190 ºC, after purification by flash chromatography (SiO_2: hexane: ethyl acetate 1:1, R_f = 0.12). HRMS (ESI): calculated for $C_{23}H_{24}N_3O_6$ (M+H) = 438.1665, found for (M+H) = 438.1670, ΔMs=-0.5ppm.

^{1}H NMR (d6-dmso): δ (ppm) =3.66 [6 H, s, 2 x (OCH_3)], 3.77 [9 H, 2 x s, 3 x (OCH_3)], 6.92 [2H, s, *ortho* to methoxy (trimethoxy ring)], 7.02 [2H, s, *meta* to OH], 7.37 [1H, dd, J = 8.04 Hz, 4.86 Hz, Py-H2], 8.18 [1H, dd, J = 8.05 Hz, 1.31 Hz, Py-H1], 8.32[1H, dd, J= 4.86 Hz, 1.31 Hz, Py-H3], 9.06 [1H, s, OH].

^{13}CNMR (d6-dmso): δ(ppm) = 55.58 [2 x (OCH_3)], 56.34 [2 x (OCH_3)], 60.09 [(OCH_3)], 106.41 [C-H, *ortho* to methoxy (trimethoxy ring)], 106.66 [C-H, Ar-C-H *meta* to OH], 118.85 [C-H, Py-C-H2], 119.00 [C-C, Ar-C-C], 126.28 [C-H, Py-C-H1], 131.76 [C-N, Ar-C-N], 134.34 [C-N, Py-C-N], 137.56 [C-O, Ar-C-OCH_3 trimethoxy ring], 137.82 [C-O, Ar-C-OH], 143.56 [C-H, Py-C-H3], 147.44 [C-O, 2 x Ar-C-OCH_3 *ortho* to OH], 149.97 [C=N, Py-C=N], 152.61 [C=N, N-C=N], 153.45 [C-O, 2 x Ar-C-OCH_3 trimethoxy ring].

FT-IR: ν_{max} (cm^{-1}): 3317 (OH str.), 2934 (C-H, str.,aromatic), 2839 (C-H, str., aliphatic), 1594 (C=C str., aromatic), 1124 (C-O-CH_3 asy. str.).

2-(4-Hydroxy-3,5-difluorophenyl)-3-(3,4,5-trimethoxyphenyl)-3H-imidazo[4,5-b]pyridine (148):

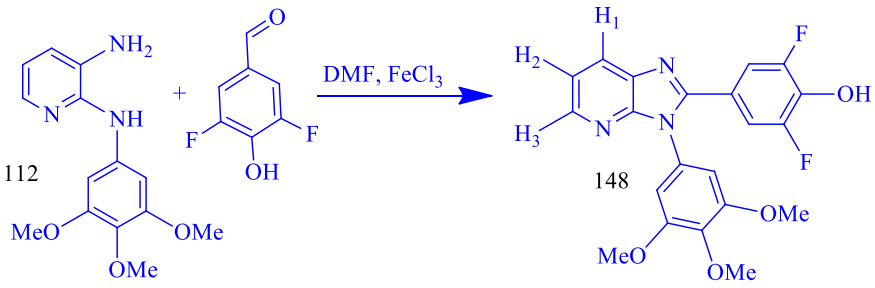

Using N2-(3,4,5-trimethoxyphenyl)pyridine-2,3-diamine (112) (0.5 mmol., 0.137g), 4-hydroxy-3,5-diflourobenzaldehyde (0.6 mmol.,0.094 g), and $FeCl_3$ (14 mg, 0.086 mmol.), the above imidazo[4,5,b]pyridine (148) was obtained as a white solid (0.120 g, 0.29 mmol., 58%). Mp >250 ºC, after purification by column chromatography (SiO_2: hexane: ethyl acetate 1:1, R_f= 0.17). HRMS (ESI): calculated for $C_{21}H_{18}F_2N_3O_4$ (M+H) = 414.1265, found for (M+H) = 414.1270, ΔMs=-0.5ppm.

^{1}H NMR (d6-dmso): δ (ppm) =3.72 [6 H, s, 2 x (OCH_3)], 3.76 [3 H, (OCH_3)], 6.87 [2 H, s, *ortho* to *methoxy*], 7.19 [2H, m, Ar-H, *ortho* to F], 7.35 [1H, dd, J = 8.01 Hz, 4.82 Hz, Py-H2], 8.16 [1H, dd, J = 8.04 Hz, 1.37 Hz, Py-H1], 8.32 [1H, dd, J = 4.80 Hz, 1.37 Hz, Py-H3], 10.95 [1H, s, OH].

^{13}CNMR (d6-dmso): δ (ppm) = 56.26 [2 x (OCH_3)], 60.22 [(OCH_3)], 106.33 [C-H, *ortho* to methoxy], 112.34 [C-H, dd, J = 16.22 Hz, 8.09 Hz, *ortho* to F], 1119.13 [C-H, Py-C-H2], 119.32 [C-C, t, J = 9.36 Hz, Ar-C-C, *meta* to F], 126.82 [C-H, Py-C-H1], 130.62 [C-N, Ar-C-N], 134.2 [C-N, Py-C-N], 135.61 [C-O, t, J= 16.29 Hz, Ar-C-OH *ortho* to F], 137.86 [C-O, Ar-C-OCH_3], 144.23 [C-H, Py-C-H3], 149.62 [C=N, Py-C=N], 150.54 [C-F, dd, J=242.89 Hz, 7.76 Hz], 150.58 [N-C=N, t, J=2.92 Hz,], 153.28 [C-O, 2 x Ar-C-OCH_3].

FT-IR: ν_{max} (cm^{-1}): 3323 (OH str.), 2937 (C-H, str., aromatic), 2827 (C-H, str., aliphatic), 1593 (C=C str., aromatic), 1127 (C-O-CH_3 asy. str.), 1024 (C-F).

2-(3,5-Dihydroxyphenyl)-3-(3,4,5-trimethoxyphenyl)-3H-imidazo[4,5-b]pyridine (149):

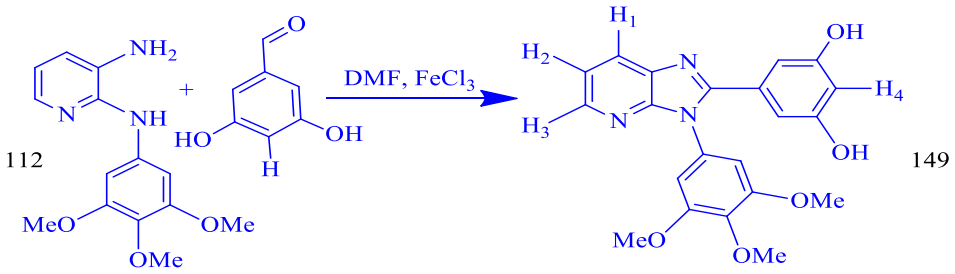

Using N2-(3,4,5-trimethoxyphenyl)pyridine-2,3-diamine (112) (0.5 mmol., 0.137 g), 3,5-dihydroxybenzaldehyde (0.6 mmol., 0.082 g),and $FeCl_3$ (14 mg, 0.086 mmol.), the above imidazo[4,5,b]pyridine (149) was obtained as a white solid (0.120 g, 0.30 mmol., 54%). Mp <250 ºC, after purification by column chromatography (SiO_2: hexane: ethyl acetate 1:1, R_f = 0.17). HRMS (ESI): calculated for $C_{21}H_{20}N_3O_5$ (M+H) = 394.1402, found for (M+H) = 394.1410, ΔMs=-0.5ppm.

^{1}H NMR from (d6-dmso): δ (ppm) =3.70 [6H, s, 2 x (OCH_3)], 3.75 [3H, (OCH_3)], 5.95 [1H, t, J= 2.21 Hz, Ar-H4], 6.29 [2H, d, J= 2.21 Hz, Ar-H *ortho* to OH], 6.78 [2H, s, *ortho* to methoxy], 7.34 [1H, dd, J= 7.99 Hz, 4.75 Hz, Py-H2], 8.15 [1H, dd, J= 8.01 Hz, 1.56 Hz, Py-H1], 8.31 [1H, dd, J= 4.74 Hz, 1.56 Hz, Py-H3], 10.95 [1H, s, OH].

^{13}CNMR from (d6-dmso): δ (ppm) = 56.09 [2 x (OCH_3)], 60.08 [(OCH_3)], 104.11 [C-H, Ar-C-H4], 106.05 [C-H, Ar-C-H *ortho* to OH], 107.31 [C-H, *ortho* to methoxy], 118.90 [C-H, Py-C-H2], 119.75 [C-C, Ar-C-C], 126.73 [C-H, Py-C-H1], 131.09 [C-N, Ar-C-N], 134.20 [C-N, Py-C-N], 137.47 [C-O, Ar-C-OCH_3], 143.89 [C-H, Py-C-H3], 149.47 [C=N, Py-C=N], 152.89 [C=N, N-C=N], 153.02 [C-O, 2 x Ar-C-OH]. 157.97 [C-O, 2 xAr-C-OCH_3].

FT-IR: ν_{max} (cm^{-1}): 3485 (OH str.), 2993 (C-H, str., aromatic), 2827 (C-H, str., aliphatic), 1593, 1542 (C=C str., aromatic), 1127 (C-O-CH_3 asy. str.).

2-(4-Hydroxy-3,5-dimethylphenyl)-3-(3,4,5-trimethoxyphenyl)-3H-imidazo[4,5-b]pyridine (150)

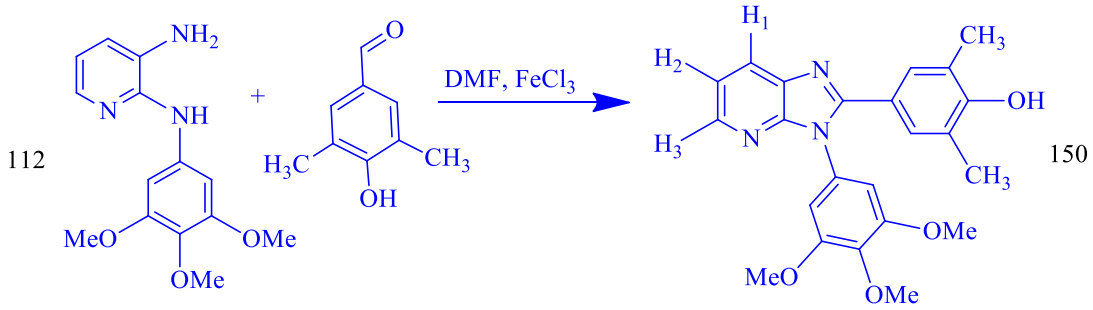

Using N2-(3,4,5-trimethoxyphenyl)pyridine-2,3-diamine (112) (1mmol., 0.275 g), 4-hydroxy-3,5-dimethylbenzaldehyde (1.2mmol.,0.180g),and $FeCl_3$ (28 mg, 0.172 mmol.), the above imidazo[4,5,b]pyridine (150) was obtained as a white solid (0.235 g, 0.58 mmol., 58%). Mp =208-209 ºC, after purification by column chromatography (SiO_2: hexane: ethyl acetate 6:4, R_f = 0.18). HRMS (ESI): calculated for $C_{23}H_{24}N_3O_4$ (M+H) = 406.1766, found for (M+H) = 406.1755, ΔMs=0.11ppm.

^{1}H NMR : δ (ppm) = 1.93 [6 H, s, 2 x (CH_3)], 3.78 [6 H, s, 2 x (OCH_3)], 3.90 [3 H, (OCH_3)], 5.73 [1H, s, OH], 6.61 [2 H, s, *ortho* to CH_3], 7.27 [3H, m, (2 H, Ar-H, *ortho* to methoxy), (1H, Py-H2)], 8.09 [1H, dd, J = 7.99 Hz, 1.35 Hz, Py-H1], 8.36 [1H, dd, J = 4.65 Hz, 1.39 Hz, Py-H3].

^{13}CNMR : δ (ppm) =16.11 [2 x (CH_3)], 56.35 [2 x (OCH_3)], 60.97 [(OCH_3)], 105.66 [C-H, Ar-C-H *orhto* to CH_3], 119.03 [C-H, Py-H2], 120.87 [C-C, Ar-C-C], 123.54 [C-C, 2 x Ar-C-CH_3], 126.82 [C-H, Py-H1], 131.28[C-H, Ar-C-H *ortho* to methoxy], 134.99 [C-N, Ar-C-N], 138.33 [C-N, Py-C-N], 144.12 [C-O, Ar-C-OCH_3], 149.62 [C-H, Py-H3], 153.69 [C=N, Py-C=N], 153.69 [C=N, N-C=N], 153.82 [C-O, 2 x Ar-C-OCH_3], 154.52 [C-O, Ar-C-OH].

FT-IR: ν_{max} (cm^{-1}): 3422 (OH str.), 2988 (C-H, str., aromatic), 2830 (C-H, str., aliphatic), 1597 (C=C str., aromatic), 1129 (C-O-CH_3 asy.str.).

2-(3-Hydrox-4-methoxyphenyl)-3-(3,4,5-trimethoxyphenyl)-2,3-dihydro-1H-imidazo[4,5-b]pyridine (151):

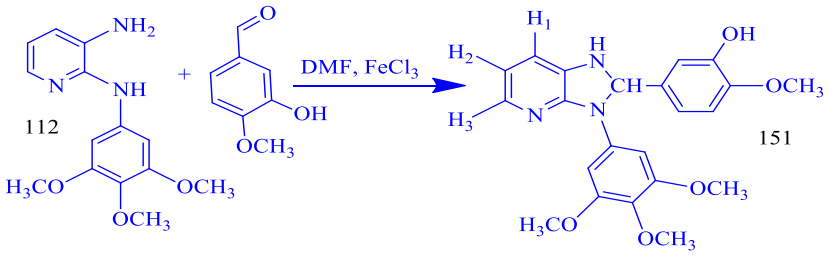

Using N2-(3,4,5-trimethoxyphenyl)pyridine-2,3-diamine (112) (1mmol., 0.275 g), 3-hydroxy-4-methoxybenzaldehyde (1.2 mmol., 0.182 g), and $FeCl_3$ (28 mg, 0.172 mmol.), the above imidazo[4,5,b]pyridine (151) was obtained as a white solid (0.192 g, 0.46 mmol., 47%). Mp =179-181ºC, after purification by column chromatography (SiO_2: hexane: ethyl acetate 6:4, R_f = 0.11). HRMS (ESI): calculated for $C_{23}H_{24}N_3O_4$= 410.1715, found for (M+H) = 410.1707, ΔMs=0.8ppm.

^{1}H NMR from (d6-dmso, at 80 ºC): δ (ppm) =3.63 [12 H, 4 x s, 4 x (OCH_3)], 5.68 [1H, d, J = 5.86 Hz, CH-NH], 5.96 [1H, d, J= 5.89 Hz, NH-CH], 6.41 [1H, dd, J = 7.56 Hz, 4.76 Hz, Py-H2], 6.48 [1H, dd, J= 8.36 Hz, 1.12 Hz Ar-H *para* to OH], 6.55 [1H, d, J = 2.04 Hz, Ar-H, *ortho* to OH], 6.66 [2H, m, (1H, Ar-H, *ortho* to methoxy trimethoxy ring), (1H, d, J= 8.32 Hz Ar-H *meta* to OH)], 6.80 [1H, dd, J = 7.56 Hz, 1.51 Hz, Py-H1], 7.42 [1H, dd, J= 4.76 Hz, 1.51 Hz, Py-H3], 8.08 [2H, 2 x s, (OH), (labile proton, NH)].

^{13}C NMR from (d6-dmso, at 80 ºC): δ (ppm) = 54.70 [CH, CH-NH], 55.33 [(OCH_3)], 55.44 [(OCH_3)], 60.47 [(OCH_3)], 60.87 [(OCH_3)], 98.42 [C-H, *ortho* to methoxy (trimethoxy ring)], 111.51 [C-H, Ar-C-H *meta* to OH], 113.97 [C- quaternary, Ar-C], 114.62 [C-H, Ar-C-H *para* to OH], 114.89 [C-H, Ar-C-H *ortho* to OH], 118.01 [C-H, Py-C-H2], 125.31 [C-H, Py-C-H1], 131.88 [C-C, Ar-C-C], 133.98 [C-N, Ar-C-N], 136.05 [C-N, Py-C-N], 137.95 [C-H, Py-C-H3], 138.07 [C-O, Ar-C-OCH_3], 145.75 [C-O, Ar-C-OCH_3], 145.92 [C-O, Ar-C-OCH_3], 146.41 [C-O, Ar-C-OCH_3], 150.16 [C-O, Ar-C-OH], 152.06 [C=N, Ar-C=N].

FT-IR: ν_{max} (cm^{-1}): 3445 (OH str.) 3301 (NH str.), 2956 (C-H, str., aromatic), 2838 (C-H, str., aliphatic), 1601 (NH, ben.), 1512 (C=C str., aromatic), 1125 (C-O-CH_3 asy. str.).

2-(2,3,4-Trifluorophenyl)-3-(3,4,5-trimethoxyphenyl)-2,3-dihydro-1H-imidazo[4,5-b]pyridine (152):

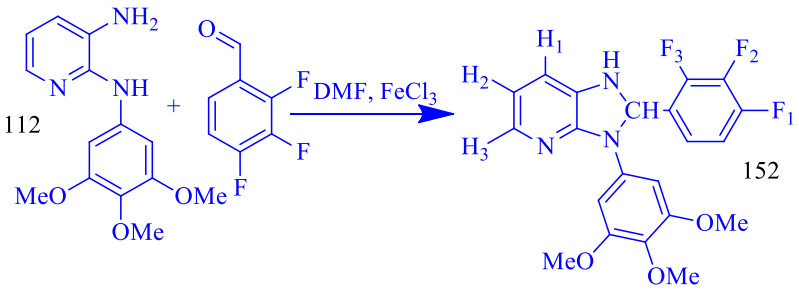

Using N2-(3,4,5-trimethoxyphenyl)pyridine-2,3-diamine (112) (1 mmol., 0.275 g), 2,3,4-trifluorobenzaldehyde (1.2 mmol., 0.182 g), and $FeCl_3$(28 mg, 0.172 mmol.), the above imidazo[4,5,b]pyridine (152) was obtained as light-brown solid (0.192 g, 0.46 mmol., 47%, Mp =119-120 ºC) after purification by column chromatography (SiO_2: hexane: ethyl acetate 10:1, TLC 6:4, R_f = 0.4). HRMS (ESI): calculated for $C_{23}H_{19}F_3N_3O_3$ (M+H) = 418.1378, found for (M+H) = 418.1372, ΔMs=0.6ppm.

^{1}H NMR from (Acetone-D6): δ (ppm) =3.69 [3H, s, (OCH_3)], 3.74 [3H, s, (OCH_3)], 3.83 [3H, s, (OCH_3)], 5.63 [1H, d, J = 6.29 Hz, NH-CH,], 6.26 [1H, d, J= 6.23 Hz, C-H,], 6.49 [1H, dd, J = 7.51 Hz, 4.81 Hz, Py-H2], 6.64, [1H, m, ortho to F], 6.73 [1H, s, *ortho* to methoxy (trimethoxy ring)], 6.84 [1H, m, *meta* to F], 6.94 [1H, dd, J= 7.51 Hz, 1.46 Hz, Py-H1], 7.60 [1H, dd, J=4.83 Hz, 1.46 Hz, Py-H3], 8.15 [1H, s, labile proton (NH)].

^{13}C NMR from (Aceton-D6): δ (ppm) =52.41 [C-H, t, J= 2.17 Hz, NH-CH], 56.05 [(OCH_3)], 60.97 [(OCH_3)], 61.35 [(OCH_3)], 98.88 [C-H, ortho to methoxy], 112.16 [C-H, dd, J= 17.25 Hz, 3.87 Hz, Ar-C-H *ortho* to F], 112.27 [C-quaternary, Ar-C-C], 116.13 [C-H, Py-C-H2], 123.72 [C-H, m, Ar-C-H *meta* to F], 127.28 [C-H, Py-C-H1], 129.24 [C-C, m, Ar-C-C *ortho* to F], 131.60 [C-N, Ar-C-N], 135.94 [C-O, Ar-C-OCH_3], 139.14 [C-N, Py-C-N], 140.47 [C-F, dt, J= 250.77 Hz, 15.85 Hz, Ar-C-F1], 140.92 [C-H, Py-C-H3], 148.29 [C-O, Ar-C-OCH_3], 148.88 [C-F, ddd, J=248.90 Hz, 10.85 Hz, 3.61 Hz, Ar-C-F3], 151.32 [C-O, Ar-C-OCH_3], 151.54 [C-F, ddd, J= 247.49 Hz, 10.12 Hz, 2.71 Hz, Ar-C-F2], 154.49 [C=N, Py-C=N].

FT-IR: ν_{max} (cm^{-1}): 3334, 3270 [NH, str.], 2938 (C-H, str., aromatic), 2838 (C-H, str., aliphatic), 1600 (NH, ben.), 1541, 1498 (C=C str., aromatic), 1101 (C-O-CH_3 asy. str.), 1032 (C-F ben.).

2-(3-fluoropyridin-4-yl)-3-(3,4,5-trimethoxyphenyl)-2,3-dihydro-1H-imidazo[4,5-b]pyridine (153):

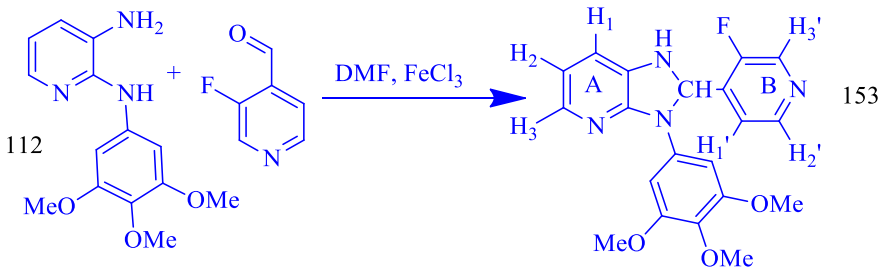

Using N2-(3,4,5-trimethoxyphenyl)pyridine-2,3-diamine (112) (1mmol., 0.275 g), 3-fluoro-4-pyridinecarbaldehyde (1.2 mmol., 0.150 g), and $FeCl_3$ (28 mg, 0.172 mmol.), the above imidazo[4,5,b]pyridine (153) was obtained as pale-yellow solid (0.192 g, 0.5 mmol., 47%). Mp =140-141ºC, after purification by flash chromatography (SiO_2: hexane: ethyl acetate 10:1, TLC 7:3 R_f =0.14). HRMS (ESI): calculated for $C_{20}H_{20}FN_4O_3$ (M+H) = 383.1519, found for (M+H) = 383.1521, ΔMs=0.7ppm.

^{1}H NMR from (CD_2Cl_2): δ (ppm) = 3.70 [3 H, s, (OCH_3)], 3.76 [3 H, s, (OCH_3)], 3.82 [3 H, s, (OCH_3)], 4.61 [1H, d, J = 6.16 Hz, NH], 6.23-6.27 [2 H, (1H, s, *ortho* to methoxy (trimethoxy ring)), (1H, d, J = 6.16 Hz, CH)], 6.49 [1H, dd, J = 7.55 Hz, 4.86 Hz, Py-H2, ring A], 6.68 [1H, dd, J = 6.27 Hz, 5.25 Hz, Py-H2', *para* to F ring B], 6.78 [1H, dd, J= 7.54 Hz, 1.40 Hz, Py-H1, ring A], 7.20 [1H, labile proton], 7.63 [1H, dd, J = 4.86 Hz, 1.41 Hz, Py-H3, ring A], 8.06 [1H, d, J = 4.89 Hz, Py-H1' *meta* to F ring B], 8.35 [1H, d, J= 4.89 Hz, Py-H3', *ortho* to F ring B].

^{13}C NMR from (CD_2Cl_2): δ (ppm) =51.76 [CH-NH, d, J=2.03 Hz], 55.87 [(OCH_3], 61.04 [(OCH_3)], 61.24 [(OCH_3)], 97.92 [C-H, *ortho* to methoxy], 109.94 [C-quaternary, Ar-C-C], 115.46 [C-H, Py-C-H2 ring A], 123.16 [C-H, Py-C-H1 ring A], 127.31 [C-H, Py-C-H2' *para* to F ring B], 130.63[C-N, Ar-C-N], 135.72 [C-O, Ar-C-OCH_3], 136.99[C-N, Py-C-N, ring A], 137.45 [C-C, d, J = 10.77 Hz, Py-C-C, ring B], 137.78[C-H, d, J = 24.41 Hz, Py-C-H3' *ortho* to F ring B], 138.82 [C-H, Py-C-H3 ring A], 146.06 [C-H, d, J=4.90 Hz, Py-C-H1' *meta* to F ring B], 146.44 [C=N, Py-C=N, ring A], 150.92 [C-O, Ar-C-OCH_3], 153.84 [C-O, Ar-C-OCH_3], 157.795 [C-F, d=255.11 Hz, Py-C-F].

FT-IR: ν_{max} (cm^{-1}): 3384 (NH str.), 2986 (C-H, str., aromatic), 2941 (C-H, str., aliphatic), 1598 (NH ben.), 1528, 1495 (C=C, str., aromatic), 1096 (C-O-CH_3, asy. str), 997 (C-F).

2-(3,5-Difluorophenyl)-3-(3,4,5-trimethoxyphenyl)-3H-imidazo[4,5-b]pyridine (154): and

2-(3,5-Difluorophenyl)-3-(3,4,5-trimethoxyphenyl)-2,3-dihydro-1H-imidazo[4,5-b]pyridine (155):

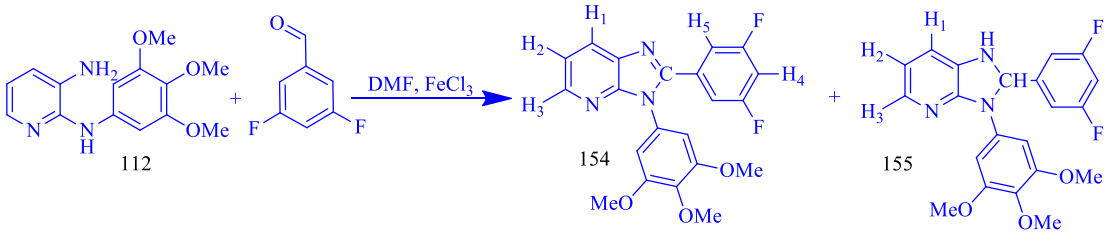

Using N2-(3,4,5-trimethoxyphenyl)pyridine-2,3-diamine (112) (1mmol., 0.275 g), 3,5-difluorobenzaldehyde (1.2 mmol., 0.114 cm^3), and $FeCl_3$ (28 mg, 0.172 mmol.), the above two imidazo[4,5,b]pyridines were obtained as: (**154**) as a white crystalline solid (0.065 g, 0.16 mmol., 16%, Mp =195-196 ºC), and (**155**) as a pink solid (0.175 g, 0.43 mmol., 44%). Mp=169-170 ºC, after purification by flash chromatography (SiO_2: hexane: ethyl acetate 10:1, TLC 7:3 R_f = 0.18). HRMS (ESI) for (**154**): calculated for $C_{21}H_{18}F_2N_3O_3$ (M+H) = 398.1316, found (M+H) = 398.1317, ΔMs=-0.1ppm. HRMS (ESI) for (**155**) calculated for $C_{21}H_{20}F_2N_3O_3$ (M+H) = 400.1472, found for (M+H) = 400.1473, ΔMs=-0.1.

^{1}H NMR for (154): δ (ppm) =3.82 [6H, s, 2 x (OCH_3)], 3.95 [3H, s, (OCH_3)], 6.61[2H, s, *ortho* to methoxy], 6.87 [1H, dt, J=18.65 Hz, 2.22 Hz, Ar-H4, difluoro ring], 7.22 [2H, m, Ar-H5, difluoro ring], 7.35 [1H, dd, J= 8.05 Hz, 4.77 Hz, Py-H2], 8.18 [1H, dd, J=8.05 Hz, 1.42 Hz, Py-H1], 8.46 [1H, dd, J= 4.77 Hz, 1.42 Hz, Py-H3].

^{13}C NMR (154): δ (ppm) =56.36 [2 x (OCH_3)], 61.02 [(OCH_3)], 105.28 [C-H, *ortho* to methoxy], 105.40 [C-H, t, J= 25.33 Hz, Ar-C-H4], 112.05 [C-H, dd, J=19.67 Hz, 8.08Hz, Ar-C-H5], 119.61[C-H, Py-C-H2], 127.95 [C-H, Py-C-H1], 130.29 [C-N, Ar-C-N], 132.48 [C-C, t, J=10.25 Hz, *meta* to F], 134.29 [C-N, Py-C-N], 138.82 [C-O, Ar-C-OCH_3], 145.58 [C-H, Py-C-H3], 149.62 [C=N, Py-C=N] 150.56[N-C=N, d, J=3.49 Hz], 154.12 [C-O, 2 x Ar-C-OCH_3], 162.71 [C-F, dd, J = 248.52 Hz, 12.67 Hz, Ar-C-F].

FT-IR ν_{max} (cm^{-1}): 2958 (C-H, str., aromatic), 2828 (C-H, str., aliphatic), 1598 (C=C str., aromatic), 1123 (C-O-CH_3 asy.str.), 1028 (C-F ben.).

^{1}H NMR for (155): δ (ppm) =3.77 [3H, s, (OCH_3)] 3.80 [6H, s, 2 x (OCH_3)], 4.56 [1H, d, J=6.15 Hz, CH-NH], 5.94 [1H, t, J= 6.13 Hz, NH], 6.19 [1H, s, *ortho* to methoxy], 6.57 [2H, m, Ar-H5], 6.80 [1H, m, Ar-H4], 7.27 [2H, (1H, dd, J = 8.07 Hz, 4.80 Hz, Py-H2),

(1H, s, labile H)], 7.64 [1H, dd, J = 8.02 Hz, 1.25 Hz, Py-H1], 8.16 [1H, dd, J = 4.81 Hz, 1.25 Hz, Py-H3].

^{13}C NMR (155): δ (ppm) =55.857[(OCH_3)], 56.36 [(OCH_3)], 61.02 [(OCH_3], 61.32 [CH-NH], 98.30 [C-H, *ortho* to methoxy], 102.2 [C-H, t, J = 25.51 Hz, Ar-C-H4], 109.94 [C-H, dd, 18.65Hz, 6.65 Hz, Ar-C-H5], 113.04 [C-quaternary, Ar-C, trimethoxy ring], 115.80 [C-H, Py-C-H2], 119.61[C-C, m, *meta* to F], 126.87 [C-H, Py-C-H1], 130.29 [C-N, Ar-C-N], 136.98 [C-N, Py-C-N], 137.08, 139.25 [C-H, Py-C-H3], 139,18, [C-H, Py-C-H3], 146.18 [C=N, Py-C=N], 147.15 [C-O, Ar-C-OCH_3], 151.04 [C-O, Ar-C-OCH_3], 154.12 [C-O, Ar-C-OCH_3]. 161.86 [2C-F, dd, J = 248.03 Hz, 12.40 Hz, Ar-C-F].

FT-IR: ν_{max} (cm^{-1}): 3374 (NH str.), 2958 (C-H, str., aromatic.), 2844 (C-H, str., aliphatic), 15925 (C=C, str., aromatic), 1213 (C-O-CH_3, asy. str), 1008 (C-F).

4.3 Discussion:

2,3-Diarylimidazo[4,5,b]pyridines have been synthesised from substituted aldehydes due to the broad range of commercially available substrates along with previously prepared N2-(3,4,5-trimethoxyphenyl)pyridine-2,3-diamine as a starting material in presence of catalytic amount of $FeCl_3$.

The cyclisation process during the reaction of ortho-diamine substrates likely undergoes in two pathway (scheme-20), however, both leading to the formation of 2,3-dihydro-1*H*-imidazo[4,5,b]pyridine, which in turn undergo aromatization to form the final product (Padmaja *et al.*, 2018).

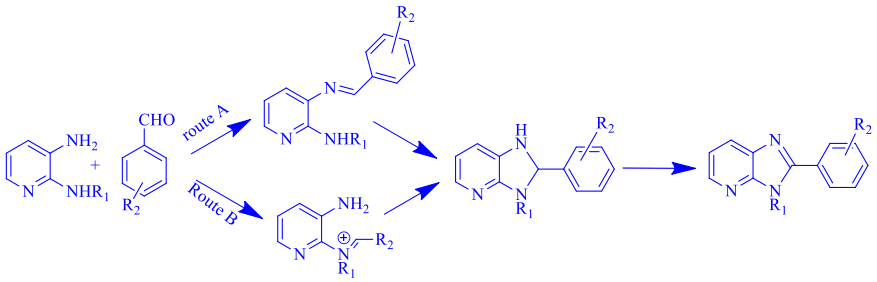

Scheme 20: Cyclization pathway of 2,3-diarylimidazo[4,5,b]pyridines (Padmaja *et al.*, 2018)

According to the above cyclization a full mechanism can be drawn as shown in scheme 21.

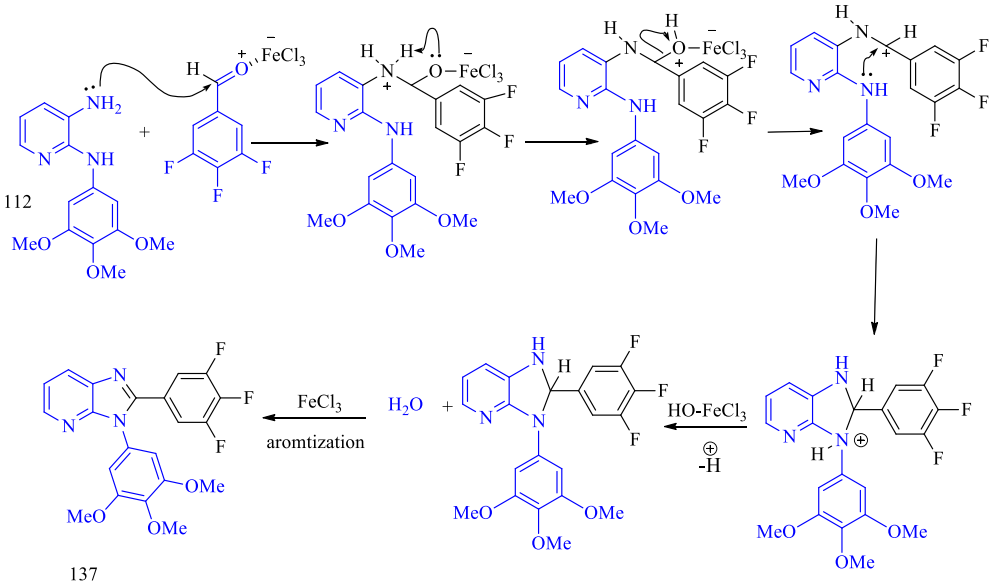

Scheme 21: Suggested mechanism for imidazo[4,5,b]pyridines cyclization (Padmaja *et al.*, 2018; Singh *et al.*, 2000).

From 24 novel compounds synthesised, 7 imidazopyridines were obtained in the reduced form. Compounds (**137**, **141**, **142**, **151**, **152**, **153**, and **154**) didn't show the expected NMR spectra. For example, the ^{1}H NMR spectra of compound (**137**) shows only one proton for the trimethoxy ring at 6.12 ppm (figure 21), as well as one labile proton at 7.29 ppm, which disappeared from the spectrum when shaken with D_2O and trifluoro acetic (figure 25). On the other hand, ^{13}C NMR spectra revealed additional number of carbon atoms and Jmod-^{13}CNMR showed there is one extra quaternary carbon at 112.83 ppm figures (22). However, high resolution mass spectroscopy analysis of this compound showed the expected molecular weight.

There are two possible interpretation from the NMR spectra. Either the proton is exchanged by resonance hybrids between the nitrogen of pyridine and ortho C-H of the trimethoxy ring (156) or the proton is migrated to the nitrogen of the pyridine ring to form a pyridinium ion and leaves the carbon on the trimethoxy ring with a negative charge (157). The appereance of the trimethoxy groups as three singlets in the ^{1}HNMR, and the extra-quaternary carbon in the ^{13}CNMR, indicates that the trimethoxy ring is retained by the positive-negative charge of the pyridinium ion. The expected structure of (157) is supported by NMR data and literature (Kumar *et al.*, 2011) more so than (156). The defectiveness of (157) is that the negative charge on the aromatic ring destabilised by the trimethoxy groups.

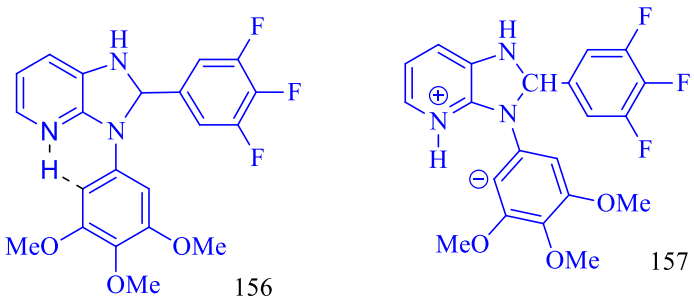

Figure 19: Suggested structures for reduced form of substituted imidazo[4,5,b]pyridines compounds.

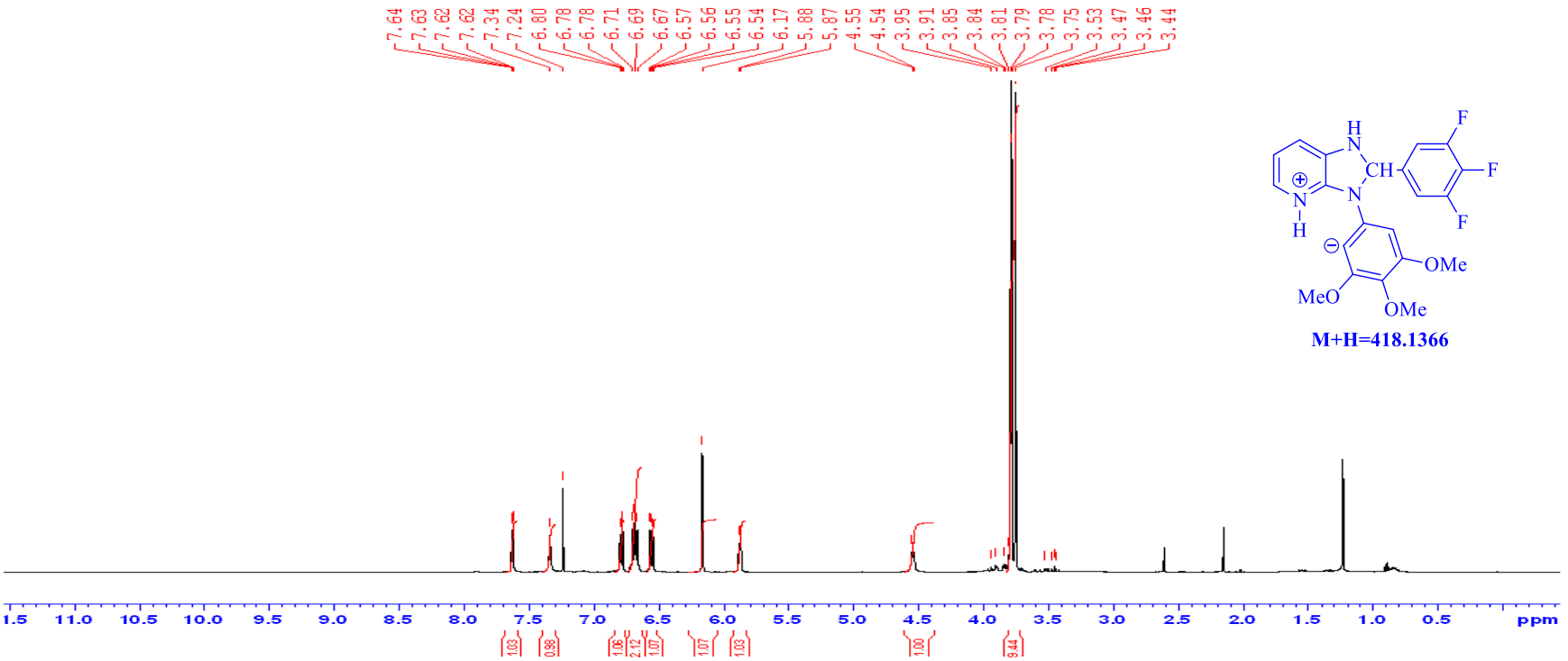

Figure 20: ^{1}H NMR for compound (137), structure (157).

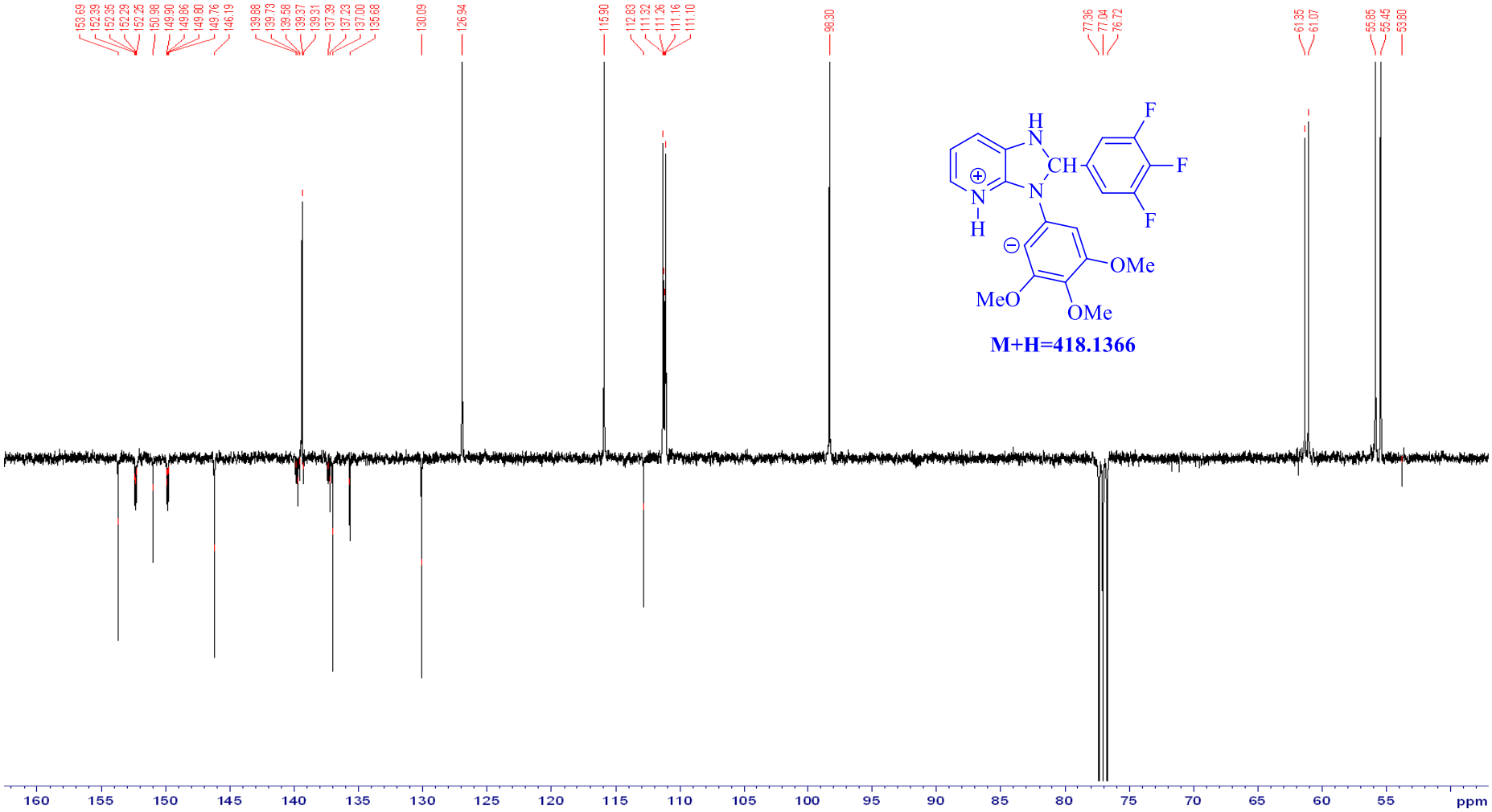

Figure 21: ^{13}C NMR- APT(Jmod) for compound (137), structure (157).

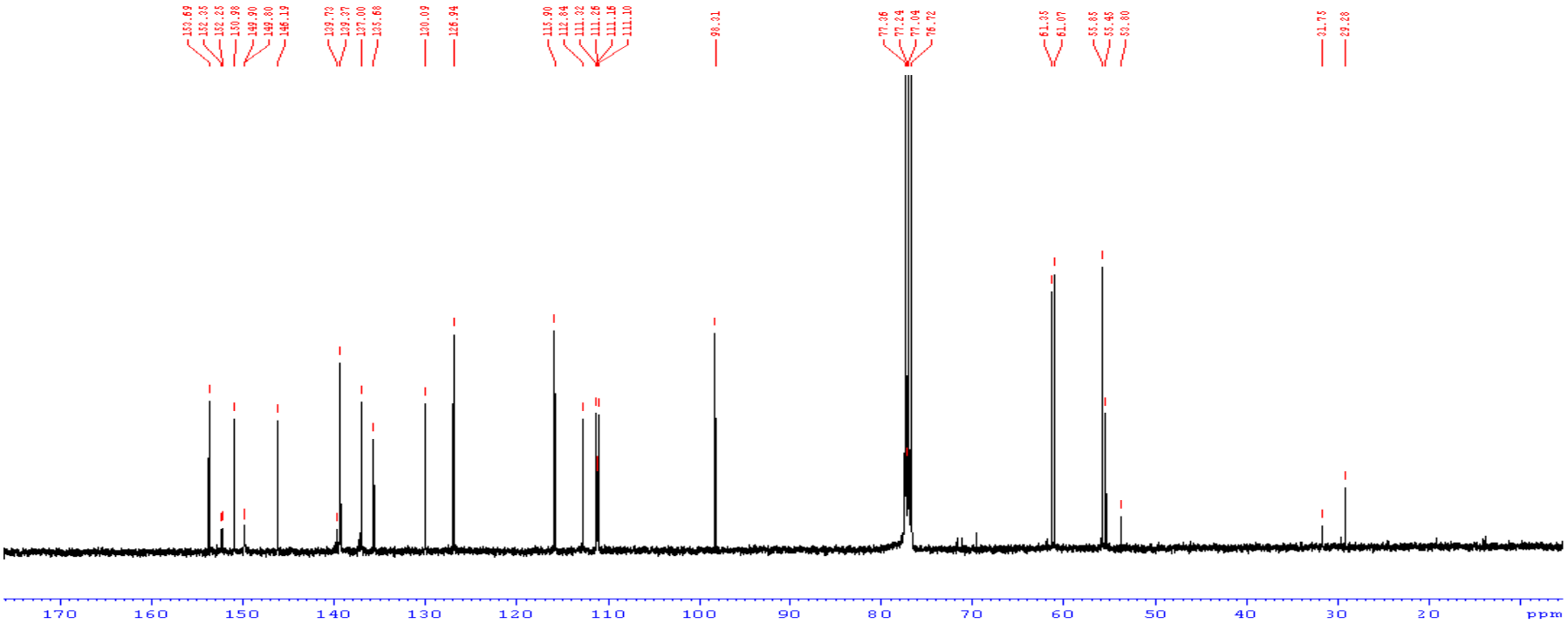

Figure 22: ^{13}C NMR for compound (137), structure (157).

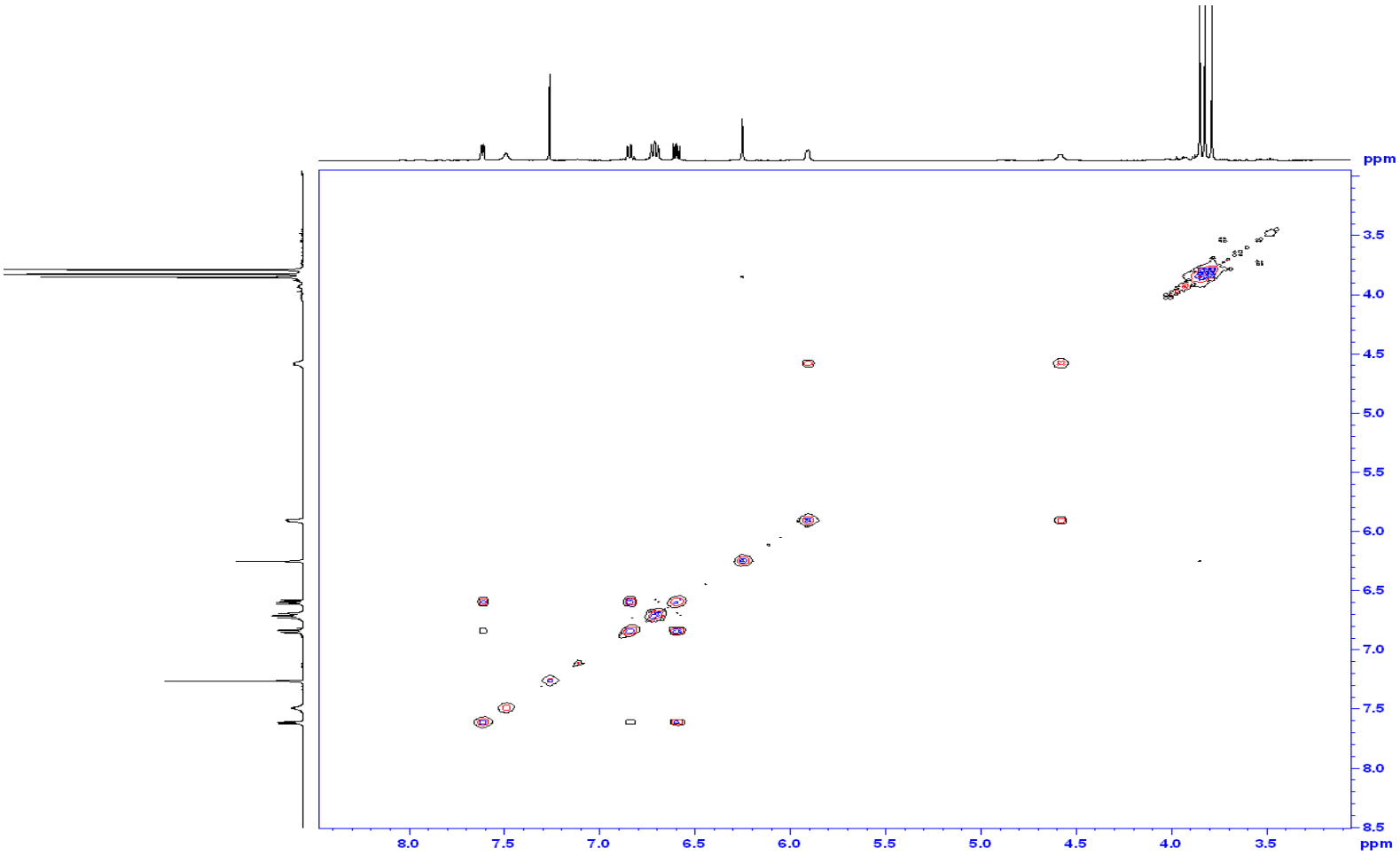

Figure 23: 2D-1H NMR for compound (137), structure (157).

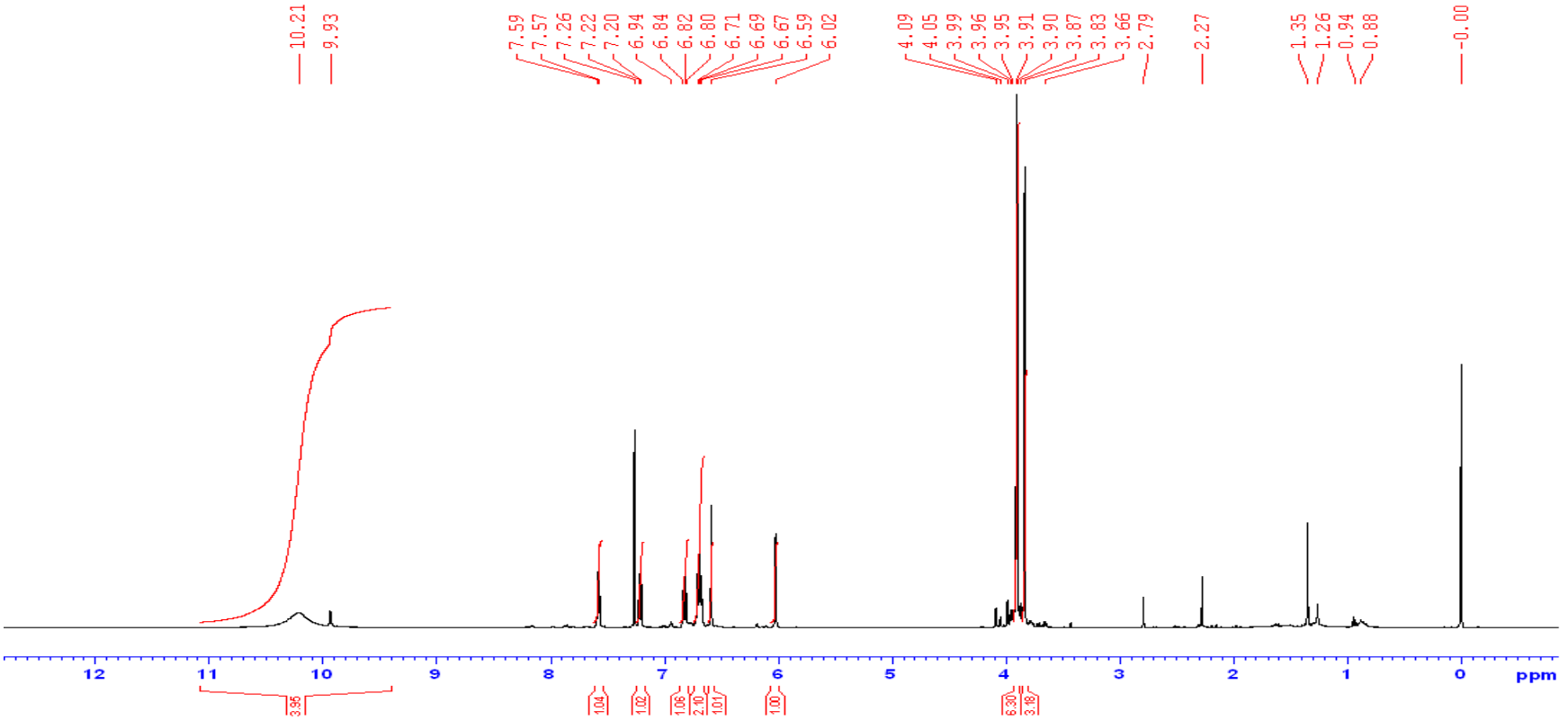

Figure 24: ^{1}H NMR with D_2O + trifluoro acetic acid for compound (137), structure (157).

Chapter 5

Cytotoxic evaluation of synthesised analogues

5 Biological assesment

Healthy cells divide and increase in number as the normal tissue grow. However, some cells which are exposed to different diseases may show a higher proliferation rate than the normal cells. Consequently, proliferating cells could be a valuable clue for the general health of cells and tissues. Evaluating the rate of cells proliferation can be used to diagnose various cancers, and to scale the responses of the toxic effect. Cell viability is defined as a percentage of healthy cells in a whole culture (Kwolek-Mirek & Zadrag-Tecza, 2014), therefore, it is considered as a direct assessment of cell proliferation. However, other measurements such as metabolic activity and DNA measurements provide a valuable information about the cells condition and its cycle stages.

Generally, the process of drug development in medicinal and natural product chemistry uutilises assays through which evaluation of anticancer activity is carried out. One of these processes is the cell proliferation assay. This type of assay has been used extensively for evaluation of anticancer agents derived from natural extracts or through synthetic means. As cancer is known for its uncontrolled cells production that arise from disorders in regulatory genes, various methods have been used to score proliferated cells based on different cellular activities, which in turn could be categorized into diverse groups such as cell membrane permeability, metabolic activity, cell adherence, enzyme releasing, dye uptake, coenzyme production, DNA synthesis and nucleotide uptake activity, and ATP production, (Adan *et al.*, 2016). However, the most common methods are DNA measurements, metabolic activity measurements, and proliferating protein measurements.

Common assays to determine cell viability and cytotoxicity are MTT, protein, LDH leakage, and neutral red assay (Fotakis & Timbrell, 2006). Owing to its practicality, precision, and quick indication of toxicity, MTT [3-(4,5-dimethylthiazol-2-yl)-2,5-diphenyltetrazolium bromide] is regarded as the most economic, dependable, and favourable anticancer screening method (McCauley *et al.*, 2013). It employs a colourimetric technique to measure the number of active cells after exposure to a toxic agents.

Cytotoxic evaluation of synthesised analogues

5.1 MTT Assay

This assay determines mitochondrial bioconversion of a yellow water soluble MTT into insoluble coloured formazan by the activity of the succinate dehydrogenase enzyme, which breaks down the tetrazolium ring. The mechanism of this conversion is not clear yet, however, opinions from the literature reported a reduction process by NADH or any other reducing agents that donate electrons to the MTT (scheme-21) (Liu *et al.*, 1997; Stockert *et al.*, 2012). A solubilizing agent is used to convert insoluble formazan into a soluble tincture and the concentration is directly proportional to the number of viable cells. Many solvents have been used as a solubilising solution. Commonly used solvents include dimethyl sulfoxide (DMSO), isopropanol, acidic ethanol solution, mineral oil, and solution of sodium dodecyl sulphate in dilute hydrochloric acid (Twentyman & Luscombe, 1987).

Furthermore, the number of viable cells is linearly related to the optical density of formazan as it is produced only by the living species. Consequently, the optical density can be measured by a spectrophotometer (ELISA) on a plate reader at wavelength 540-720 nm (Denizot & Lang, 1986; van Meerloo *et al.*, 2011). Using DMSO as a solubilising agent is more desirable than acidic isopropyl alcohol, as the latter brings about lowering optical density values (Carmichael *et al.*, 1987).

However, many parameters affects on the results from the assay such as the metabolic activity of the viable cells, incubation period, and the concentration of MTT (Riss *et al.*, 2016).

Because of the insolubility of formazan produced by the MTT reagent different compounds that form a water-soluble formazan such as MTS, XTT, and WTS were developed (Riss *et al.*, 2016). Consequently, the addition of the solubilising agent step of the protocol would be inevitably worthless.

However, many drawbacks have been reported for the MTT assay. For instance, the linearity of the MTT assay is not related to the cell abundance at high densities, the ability of the reduction varies according to cell-lines, and the coefficients of variability whether it was intra- assay or inter-assay largely depend on specific conditions (Keepers *et al.*, 1991). In addition, differentiating between cytotoxic and cytostatic agents by the MTT

assay is also accompanied with difficulty, and the results would be unreliable at low cell densities (Berridge *et al.*, 2005).

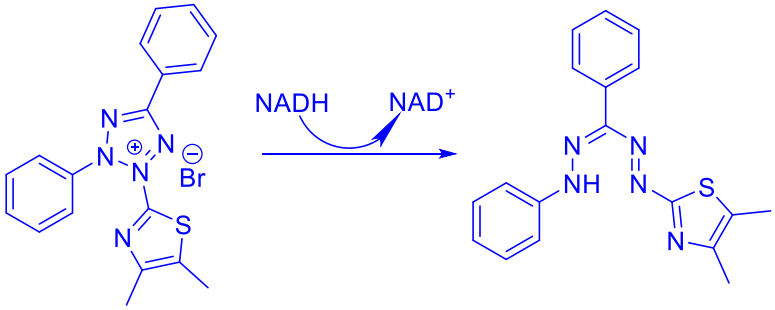

MTT FORMAZAN

Scheme 22: the bioconversion of MTT to Formazan.

5.2 Cell line

Permanently proliferative cells that arise from normal multicellular organisms, which have been mutated intentionally or naturally to keep growing in vitro for extended timespans, have been widely used in biochemistry, cell biology, and biotechnology research as a substitute for primary cells. In addition to their use in cancer research, they have been used to study vaccines, antibodies, and artificial skin. For instance, hormones, clotting factors, enzymes, and growth factors by genetic engineering (Macdonald, 1990). Owing to its practicality, cost-efficiency, and not requiring strict ethical implications with animal and humans, cell lines are considered as valuable tool in drug metabolism and cytotoxicity research (Kaur & Dufour, 2012). All the cell lines have been provided by the biobank of Salford University.

5.2.1 HepG2

Primary liver cancer, hepatocellular carcinoma (HCC) and cholangiocarcinoma (CC), have been reported as the second cause of cancer related fatality and the sixth prevailing malignant disease in the world respectively (Forner *et al.*, 2012; Mittal & El-Serag, 2013), with more than half a million new diagnoses every year. HCC is responsible for more than 80% of liver tumour mortality.

Numerous human hepatoma cell lines have been established for hepatotoxicity and drug metabolism. These include, HLE, Hepa-RG, PLC/PRF/5, HuH6, HuH7, Hep-3B, and Hep-G2. Hep-G2 is extensively used among other cell lines in pharmaco-toxicological

studies, because of their proliferative character, and their hepatic function, such as secretion and synthesis of cholesterol, bile acid, glycogen and major plasma proteins as well as lipoprotein metabolism and triglyceride metabolism (Knowles *et al.*, 1980). Hep-G2 cells are viable as a mono-layer aggregation and show epithelial morphology under specific cultural environments.

The major limitation of HepG2 is the small expression of DMETs, drug-metabolizing enzymes and transporters (Guo *et al.*, 2011). Also there is the difficulty of accurate evaluation of the viable cells due to their tendency to form aggregates, which prevents the precise use of the haemocytometer (Sgouras & Duncan, 1990).

5.2.2 U2OS

U2OS was originally established in 1964 from a shinbone biopsy of 15 year old Caucasian female suffering from osteosarcoma (or osteogenic sarcoma), which is quite common in children and teenagers, although, it can be grow at any stage of life (Walia *et al.*, 2018). 26 different cell lines have been reported, however, U2OS, SAOS-2, MG-63, and KHOS family are the most frequently practised cell line in biomedical research (Bernhard Palsson & Masters, 2002). Among other cell lines U2OS is characterised by few changes in chromosome number and an insignificant proportion of multipolar divisions (Niforou *et al.*, 2008).

5.2.3 SAOS-2

Saos-2 was cultivated by (Fogh *et al.*, 1977; Rousseau *et al.*, 2010) from osteosarcoma of an 11-year old Caucasian girl. Although, U2OS and SAOS-2 cell lines were isolated from osteosarcoma tissues, they vary substantially from each other. For instance, while tumour suppressor genes such as p53 and pRb are mutated in the SAOS-2 cell line, they are active in U2OS. On the other hand, SAOS-2 possess exceptional osteoinductive properties compared to other osteosarcoma's cell lines, and so SAOS-2 is considered an ideal osteoplastic cells supplier (Rodan *et al.*, 1987). Owing to its good properties such as extremely fast-growing cells, global accessibility, and well-researched cell line, SAOS-2 is widely used for scientific research (Hausser & Brenner, 2005).

5.2.4 A204

Rhabdomyosarcoma (RMS) is one of the soft tissue sarcoma that is responsible for 7% of cancer in children, around the age of 10, with almost 5 new cases per million every year among children (Ognjanovic *et al.*, 2009). It was derived from pelvic carcinoma of a seven-year old girl (McAllister *et al.*, 1969). There are three different subtypes of RMS: embryonal, alveolar, and pleomorphic RMS, however, the latter is more related to the arms and legs of adults than children. 18 different cell lines of embryonal RMS, and 12 alveolar have been reported. Alveolar RMS is more aggressive than embryonal RMS , while the former shows almost 50% of 5 year survival rates, the embryonal RMS presents around 75% (Hinson *et al.*, 2013).

5.2.5 A549

This cell line has been used as human lung cancer model since it was isolated and cultivated from pulmonary adenocarcinoma of a 58- year old Caucasian male in 1973 (Giard *et al.*, 1973). It has also been employed as a model for in vitro research of type II alveolar pulmonary epithelium (Foster *et al.*, 1998). Owing to its ability to produce chemokines as a response to viral infection, A549 was used in viral research(Lin *et al.*, 1998).

5.2.6 Beas-2B

Normal human immortalised lung cell line has been established and cultured by (Reddel *et al.*, 1988), via infection or transfection of healthy bronchial epithelial cells with viral carcinogenic DNA genes such as Ad12-SV40 hybrid virus and SV40. Beas-2B has been widely employed in lung cancer research, especially with molecular mechanisms of epithelial-mesenchymal transition (Veljkovic *et al.*, 2011). Beas-2B has also been used to explore the protective activity of bronchial epithelial cells toward endogenous and exogenous oxidizing agents (Kinnula *et al.*, 1994). Owing to its epithelial merits, Beas-2B has been extensively used in vitro to evaluate reactivity and toxicity of chemical agents (Ha *et al.*, 2007; Vergaro *et al.*, 2016).

5.3 Experimental: cytotoxicity assay.

5.3.1 General procedure for thawing adherent cell line (Yokoyama *et al.*, 2012):

Cryogenic vial containing desired cell line (1cm^3 in DMSO), was recovered from a -80 ˚C freezer and placed into a pre-heated water bath at 37˚C for 1-2 minutes. The suspension was transferred into a (15 cm^3) falcon tube and the cryovial was rinsed off with (1 cm^3) media to fully transfer of the cell line, which in turn, was added to the (15 cm^3) tube. Further (8 cm^3) of the fresh media was added to the tube, with gentle shaking. Cells were centrifuged for 5 minutes at 1344 G and the supernatant was discarded. The cell line was resuspended into two T75 culture vessels, and cells were investigated, after 24 hours, under a microscope and the media was replaced with fresh culture media to remove residual DMSO.

5.3.2 General procedure for sub-culturing mammalian cell line and maintenance (adherent) (Philippeos *et al.*, 2012):

The old medium was removed from T75 flask and the cells were flushed with sterile phosphate buffer saline (1x PBS, 2 x 7cm^3). The flask was incubated for 2 minutes to detach the cells, after the addition of trypsin (trypsin-EDTA in PBS) (2 cm^3), and fresh media (8 cm^3) was added. The solution was distributed between 2-3 T75 flask that contained fresh complete media (10 cm^3). The T75 flask was transferred to the humidifier incubator at 37˚C, 5% CO_2 to allow cells to be attached and proliferate. This process was repeated regularly according to cells confluency.

General procedure for counting mammalian cell line (Louis & Siegel, 2011)

Cells were counted using a disposable haemocytometer slides (C-Chips) and trypan blue. Cells were suspended in fresh complete media (10 cm^3) as described in the sub-culturing procedure, and a mixture (1:1) has been made from (10 µL) cells and (10 µL) Trypan blue solution 0.4%. The mixture was left for 5 minutes at room temperature, 10 µL was applied to the chamber, and counting was carried out under the microscope.

5.3.3 General procedure for the growth assay

The MTT assay was carried out as described in (Sung *et al.*, 2003). Hep-G2, U-2OS, Saos-2, Beas-2B, A549, and A204 cell lines, were grown in fresh media solution of

DMEM and RPMI (Dulbecco's modified Eagle's medium) that was supplemented with 1% penicillin-streptomycin solution. Cells were cultured in a 96 well plate at 5000 cells / 100 µL concentration and incubated for 24 hours to stay attached in a 5% CO_2 atmosphere in a humidified incubator. The cells were treated with drugs, which were administered as a solution in DMSO and fresh media and sterilized by MillixGP Filter 0.22µm. After the addition of different concentrations of analogues, cells were cultured for 5 days and 50µg/well of MTT solution was added for 3hrs. DMSO (200 µL) was used to disolve the formed formazan and the optical density was recorded at 570 nm by microplate reader.

5.3.4 General procedure for flowcytometry (Darzynkiewicz *et al.*, 2017):

Cell cycle analysis was conducted on the A549 cell line. Cells were detached, counted, and seeded at 2 million cells per well in 12-well plates as formerly mentioned. Cells were incubated for 24 hours at 37 ºC to be attached to the plate, treated with the synthesised drugs at concentrations of 25, 50, 100 µM, and incubated for 24 hours to be exposed to the drugs. The adherent cells were harvested from the 12-well plates as previously mentioned in the sub-culturing cell line procedure, through removal of old media, washing with PBS, trypsinisation and transfer of cells into an Eppendorf tube. After removing the supernatant, pellets were collected by centrifugation at 1344 G for 5 minutes, flushed with phosphate buffer saline (2 cm3) and centrifuged back to obtain pellets after removing phosphate buffer saline. The pellets were suspended in ice cold ethanol (70%, 1 cm3) and kept in a freezer at -20 ºC for 30 minutes. Following fixation, the suspension was centrifuged at 12096 G to obtain pellets, and the supernatant was removed carefully.

A solution of ribonuclease A was added (100 µL, 100 µg/cm3), and the tube was incubated at room temperature for 15 minutes. The cells were analysed based on cellular DNA content by using flowcytometry (BD FACSVerse flow cytometer), following the addition of propidium iodide solution (50 µL/ 1m, 50 µg/ cm^3).

Compound	structure	IC_{50} in µM					
		A204	A549	SAOS-2	HEP-G2	BEAS-2B	U2OS
132	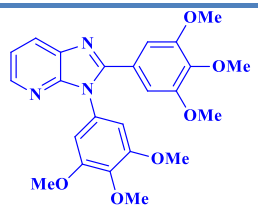	2.226 ± 0.66	3.151±0.569	15.18±0.15	9.496±0.69	64.64±0.70	60.04±0.72
133	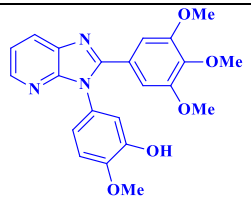	3.825 ± 0.197	37.46±0.143	14.59±0.813	4.058±0.185	51.20±0.108	17.53±0.616
134	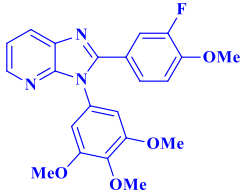	6.58 ± 0.199	38.69±0.322	14.59±0.812	8.567±0.362	94.05±0.67	34.08±0.744
135	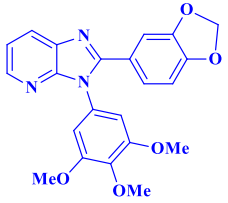	67.06 ± 2.354	15.96±0.248	63.46±0.778	85.47±1.502	87.53±2.801	38.69±0.566

136	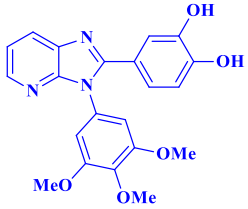	15.62 ± 0.225	10.12±0.286	54.49±0.710	70.48±2.303	79.12±1.5415	29.68±0.314
137	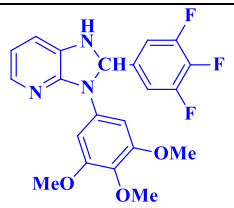	28.94 ± 0.384	15.03±0.309	68.34±1.028	44.19±1.557	73.79±0.757	31.91±0.496
138	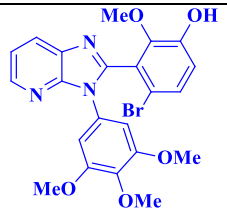	4.947 ± 0.208	26.20±0.997	58.72±8.362	34.01±1.51	45.83±1.50	58.51±1.424
139	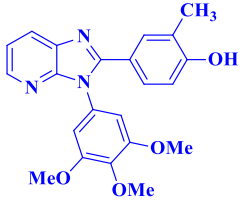	12.84 ± 0.522	3.732±0.082	30.4±0.524	2.894±0.107	27.59±0.926	22.99±0.771
140	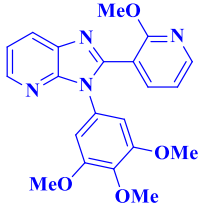	2.53±0.864	4.743±1.11	38.23±1.17	12.98±2.94	58.15±1.638	16.15±7.14

141	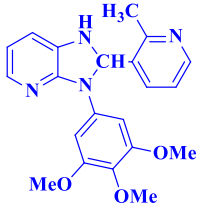	16.49±3.53	inactive	59.28±3.17	29.65±6.39	58.64±2.412	12.64±5.17
142	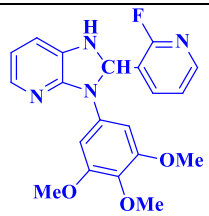	14.02±0.224	inactive	56.84±1.34	37.04±1.05	31.54±1.366	inactive
143	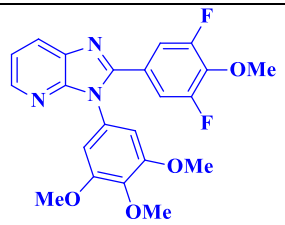	13.90±1.79	7.745±1.21	41.18±1.828	9.216±0.225	55.60±3.56	23.04±0.991
144	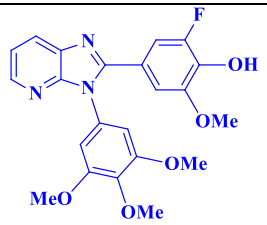	14.14±0.28	41.94±1.56	57.79±1.28	27.62±3.585	39.29±4.23	58.02±0.866

145	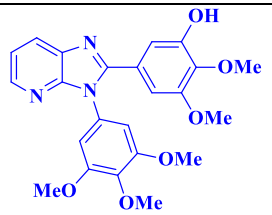	11.01±0.252	8.432±0.159	18.14±0.455	20.06±0.475	18.09±0.309	12.17±0.164
146	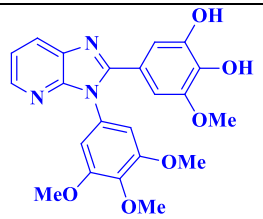	16.60±1.78	18.37±2.495	56.63±0.60	19.50±3.21	58.77±3.347	30.07±1.33
147	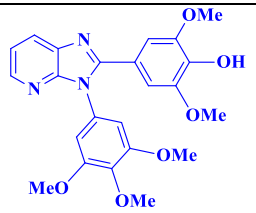	42.85±1.22	65.63±8.82	51.54±1.80	24.20±6.75	68.40±1.58	40.84±7.27
148	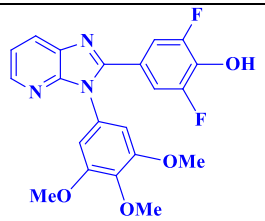	3.022±0.88	1.37±0.138	23.90±1.73	8.712±1.78	29.83±6.20	12.33±2.51

149	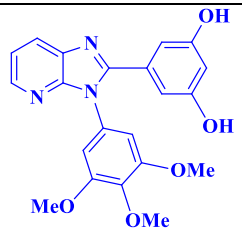	14.94±0.31	61.17±5.32	33.01±13.09	27.83±1.11	77.14±1.84	29.50±0.832
150	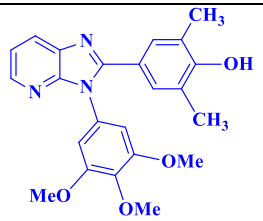	9.22±0.205	86.12±1.447	62.77±1.23	50.35±3.63	64.83±1.23	13.21±0.382
151	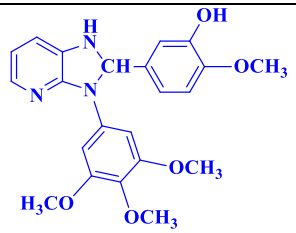	28.68±0.64	56.64±1.07	64.62±3.46	10.43±0.207	123.6±6.558	23.61±0.624
152	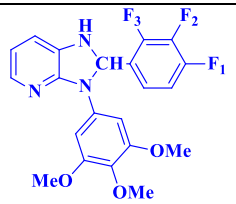	43.92±0.40	80.74±0.82	inactive	40.84±1.185	inactive	158.6±6.46

153	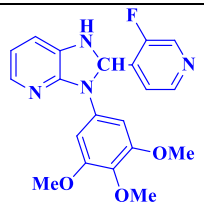	22.03±0.41	217.93±7.85	138.8±1.66	48.37±4.81	53.88±2.57	38.54±1.21
154	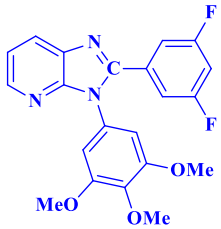	27.27 ± 0.37	60.03±1.02	47.08±0.71	62.85±1.66	54.40±2.20	76.07±780
155	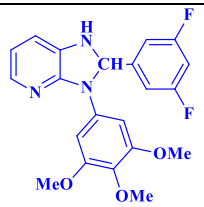	89.56 ± 0.25	159.78±0.53	95.68 ± 0.45	120.54±0.24	inactive	98.68 ± 0.14
CA-4	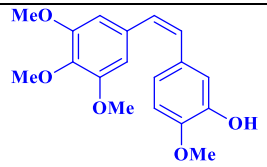	0.0212±0.01	0.0132±0.02	0.0291±0.03	0.022±0.011	2.163±0.07	0.012±0.04

Table 6: half-maximal inhibitory concentration of synthesised imidazo[4,5,b]pyridine analogues in A204, A549, Saos-2, Hep-G2, BEAS-2B, and U2OS.

Cytotoxic evaluation of synthesised analogues

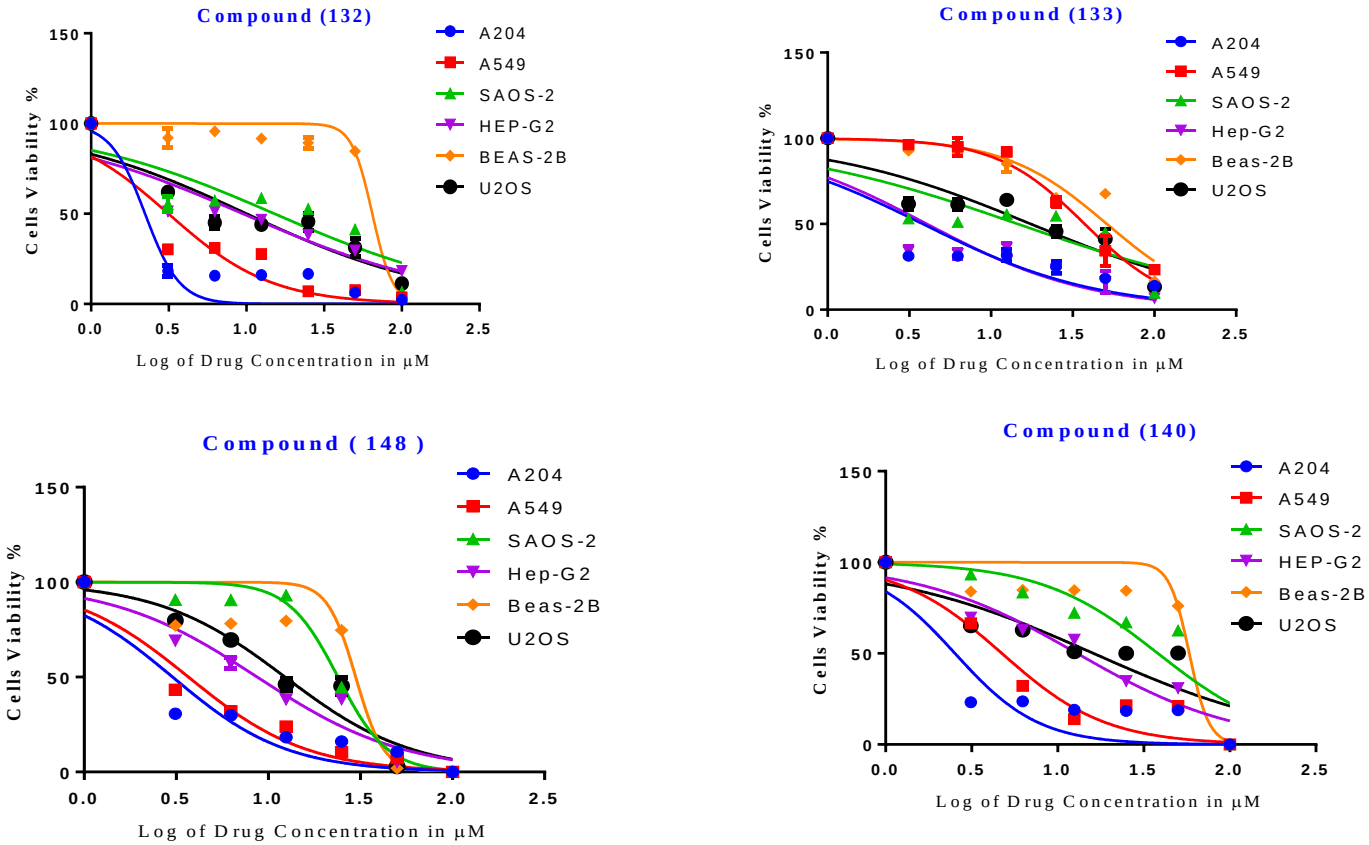

Figure 25: effect of compounds (132,133,140,148) on cells viability.

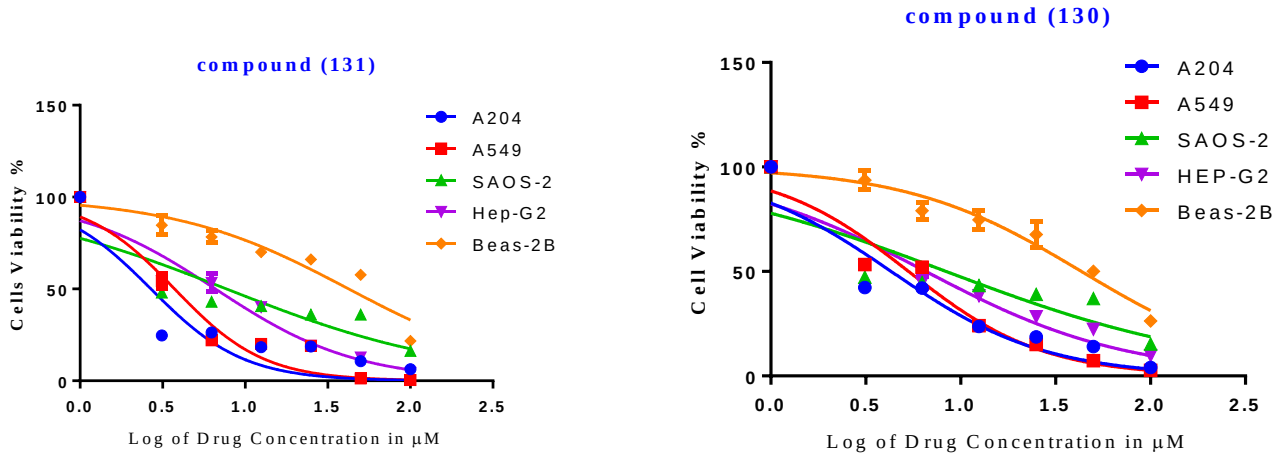

Figure 26: effect of compounds (130, 131) on cells viability.

Cytotoxic evaluation of synthesised analogues

Compound	structure	IC_{50} in µM				
		A204	A549	SAOS-2	HEP-G2	BEAS-2B
123	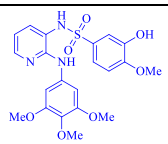	24.79 ±0.48	67.24 ± 0.31	35.78±0.722	19.57±0.206	57.52±0.342
125	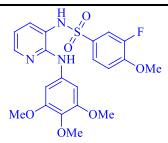	48.02±1.28	82.54 ± 3.36	70.32±0.728	60.76±1.46	69.85±0.458
126	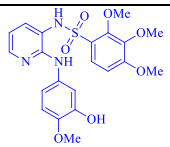	40.29±0.35	107.7±0.41	81.17±1.49	inactive	78.58±0.243
127	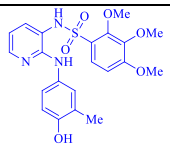	15.77±0.41	124.4±2.73	56.07±0.44	40.45±0.647	122.2±1.32
128	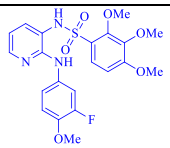	36.28±0.42	73.61±0.52	59.31±0.57	60.94±0.67	73.13±0.324
129	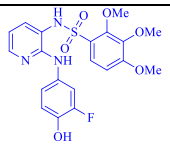	26.04±0.25	63.08±1.14	41.61±0.43	48.22±0.895	48.48±0.628
130	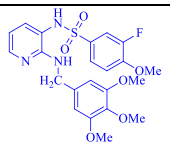	2.309±0.11	1.347±0.06	8.391±0.41	6.55±0.188	43.31±0.695
131	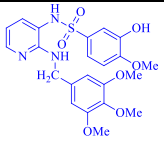	2.687±0.08	1.15±0.035	7.70±0.365	6.60±0.143	42.37±1.096

Table 7: half-maximal inhibitory concentration of synthesised substituted pyridinyl-phenyl sulphonamide analogues in A204, A549, Saos-2, Hep-G2, and Beas-2B cells.

5.4 Cell cycle analysis

Cell cycle is a process of producing two new daughter cells by which DNA, cytoplasm, and organelles are duplicated and divide in a sequential steps. This process lasts 24 hours in typical eukaryotic cells such as human cells. The cell cycle can be divided into two characteristic periods: interphase and mitosis (figure-29). The latter lasts only one hour in which two chromosomes are separated leading to cell division. Whereas, cells spends almost all their time in the former phase growing steadily and preparing for the division (Cooper, 2016). The interphase consists of three phases depending on the period of DNA synthesis: G_1, S, G_2.

G_1, gap phase, occurs from the end of the M phase untill the DNA synthesis S phase, during which time the cell is growing for 11 hours. S, synthesis phase, starts with the synthesis of DNA and results in doubling the total numbers of DNAs and lasts for 8 hours. The following phase is G_2, growth phase, in which within 4 hours cells continue growing and synthesising proteins to be prepared for the ensuing mitosis M phase.

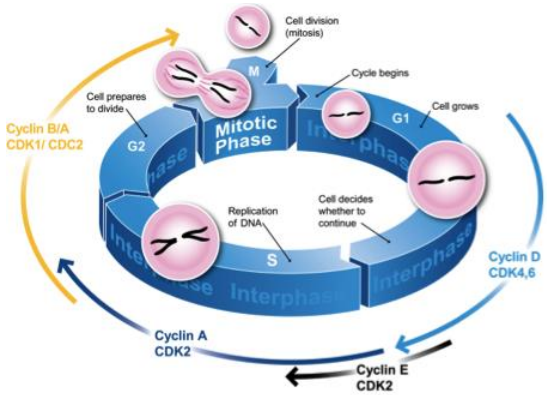

Figure 27: the cell cycle diagram (Cobb & Das, 2013).

Because of the variation of the DNA in different phases, cells can be distinguished according to DNA content. For example, cells in the S phase have almost double the number of chromosomes than cells in the G_1 phase, similarly DNA content in G_2 phase will be greater than in G_1. Consequently, the quantity of cellular DNA can be measured analytically by staining the cells with DNA binding dyes and recording the intensity of fluorescence by flowcytometry. However, not all DNA binding stains can be applied, solely fluorescent DNA dyes can be used with the flowcytometry. Microscopic and autoradiographic methods can be used to analyse cell cycle, however flowcytometry is one of the most powerful technologies and has been used in many applications such as cell sorting and molecular

biology, immunology, infectious disease and cancer biology, and virology (McKinnon, 2018). One of the first applications of flowcytometry was quantification of cellular DNA content by incubating fluorescent dye with a suspension of fixed cells. The intensity of fluorescent signal will increased proportionally to the quantity of DNA which result in differentiation between cell cycle phases (Cobb & Das, 2013). Many dyes have been widely used in flowcytometry such as propidium iodide (PI), Hoeochst 33342, Dye Cycle Violet, 4,6-diamino-2-phenylindole (DAPI), and 7-amino actinomycin-D (7-AAD)(McKinnon, 2018).

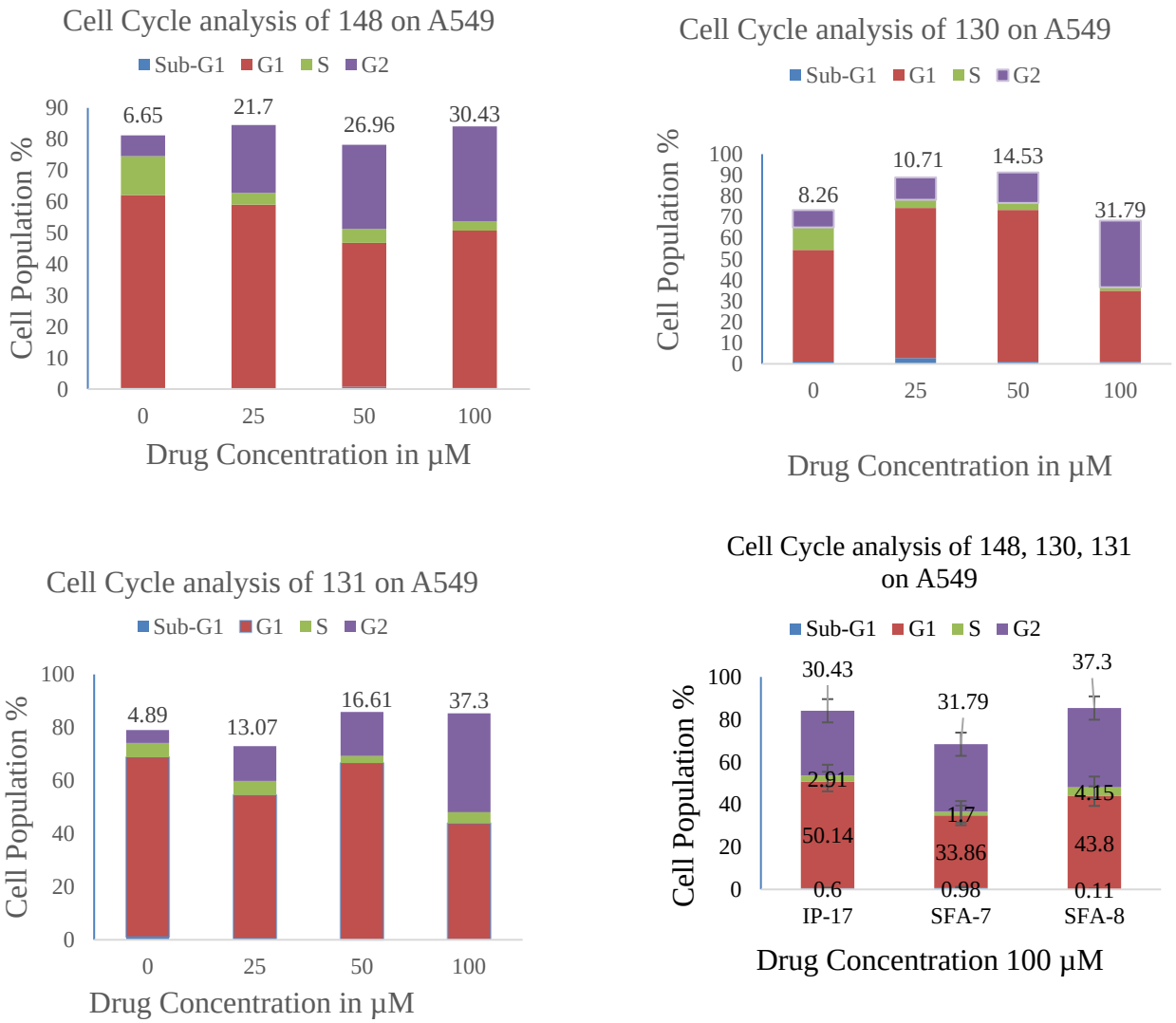

Figure 28: the effect of compounds (130, 131, and 148) on cell cycle progress tested by flowcytometry on A549 cell line.

Cytotoxic evaluation of synthesised analogues

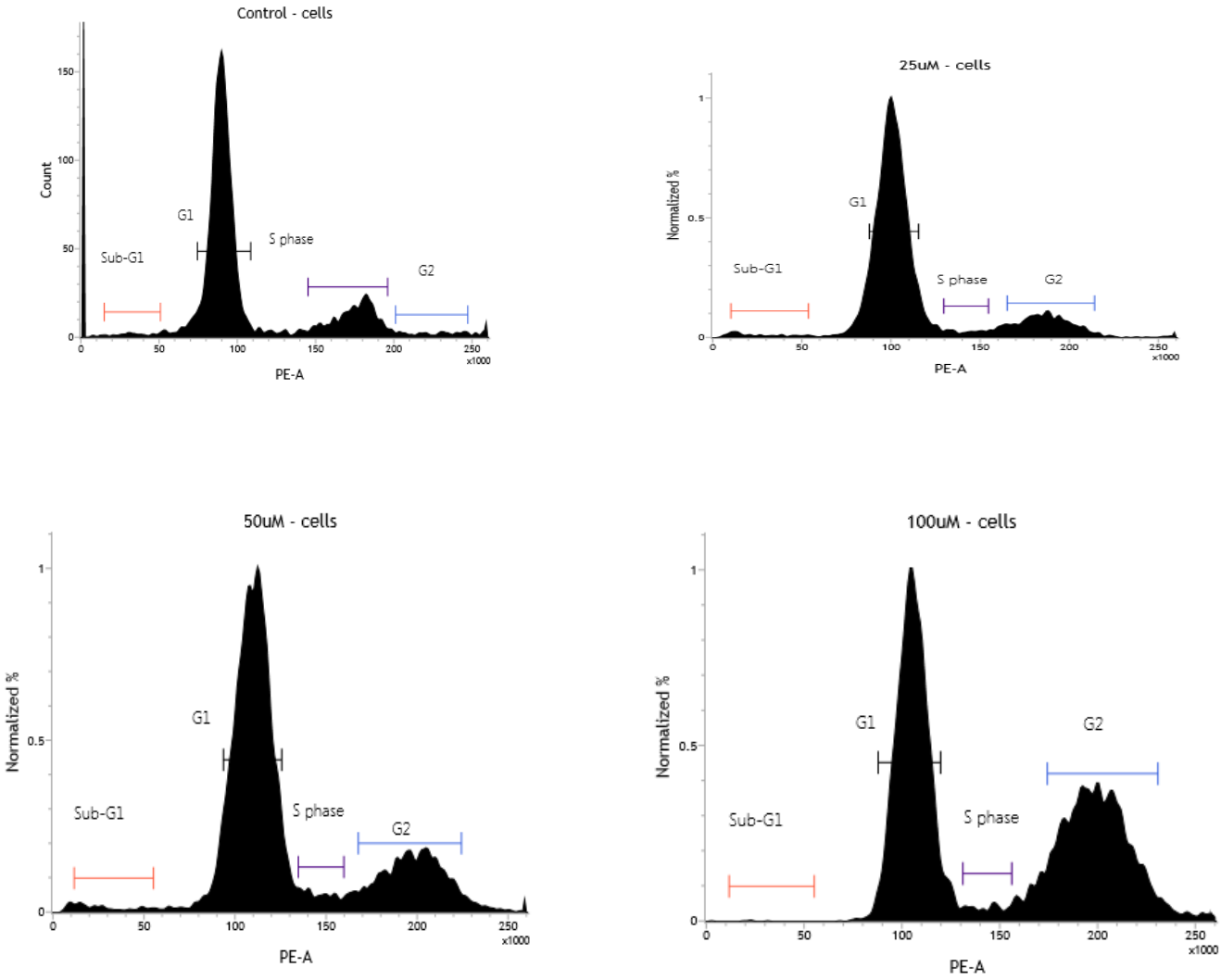

Figure 29: propidium iodide diagram vs cell count to identify cell cycle phases for compound 148.

Cytotoxic evaluation of synthesised analogues

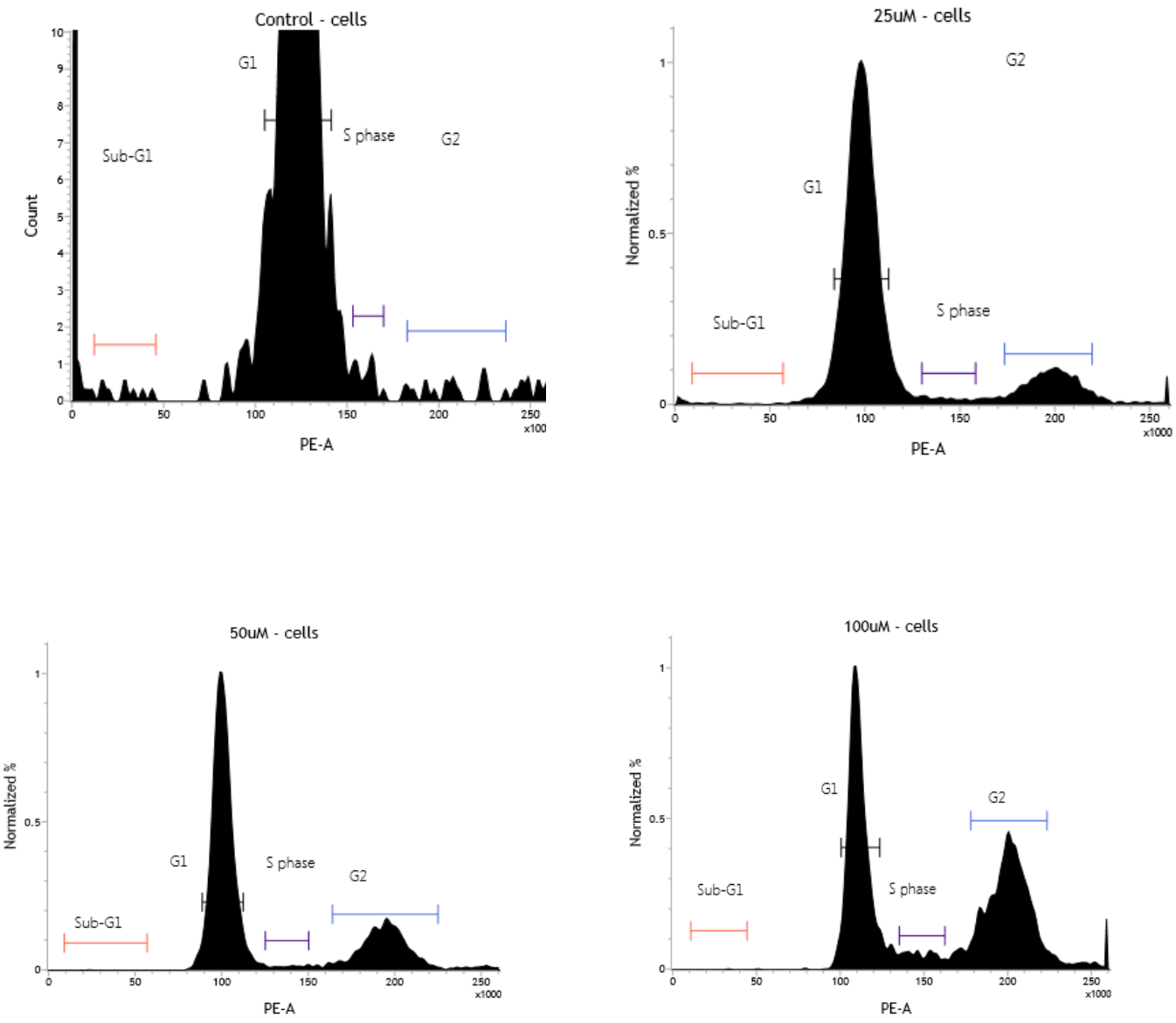

Figure 30: propidium iodide diagram vs cell count to identify cell cycle phases for compound 130.

Cytotoxic evaluation of synthesised analogues

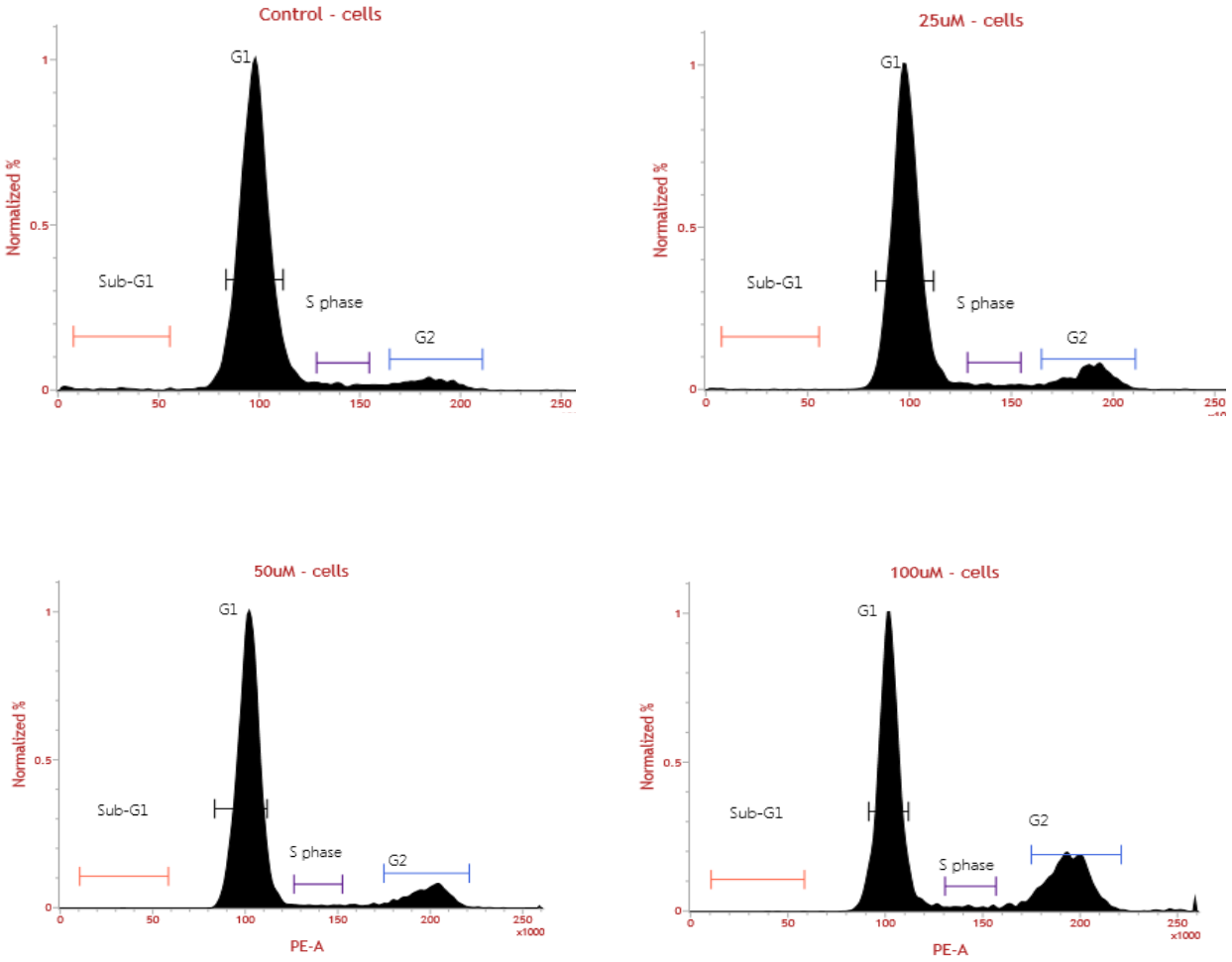

Figure 31: propidium iodide diagram vs cell count to identify cell cycle phases for compound 131.

Cytotoxic evaluation of synthesised analogues

5.5 Discussion:

The biological activity of the synthesised compounds was evaluated via MTT assay to calculate the half maximal inhibitory concentration (IC_{50}), which is the concentration required to inhibit the population of the cells by 50%. It is calculated as a mean for no less than two separated experiments (Fassy *et al.*, 2017). Combretastatin A-4 was used as a positive control in order to assess the reliability of the experiment. The IC_{50} for 32 novel compounds were screened on A204, A549, SAOS-2, Hep-G2, Beas-2B, and U2OS cell lines and are listed in tables 6 and 7. Out of the 32 novel compounds, (148, 130, 131) were found to efficiently supress the proliferation of almost all the cell lines (figure 26, 27) . Comparing the IC_{50} values of compounds 148, 154, and 143 (figure-33), on A549 cell line (table 6), compound (148, IC_{50} = 1.37 µM) has a higher potency than compound (143, IC_{50} = 7.74) and (154, IC_{50} = 60.03). This might be due to the ability of the OH group to interact with tubulin more than OCH_3 group.

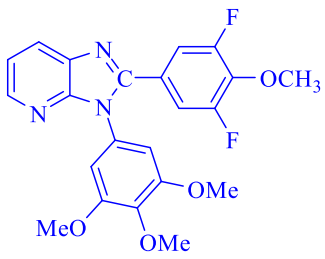

143

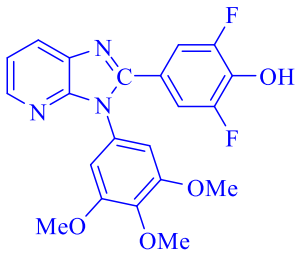

148

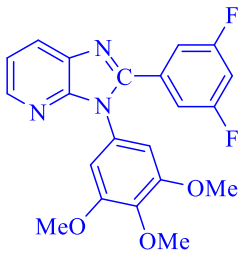

154

Figure 32: The chemical structures of compounds 143, 148, 154.

Most tested compounds appeared to be most potent in the A204 cell line, this may be due to their slow growth rate. A literature search showed that A204 cells had lower IC_{50} values than others tested (Anderson *et al.*, 2015; Chauvin *et al.*, 2017). Compounds 132, 133, 134, 140, and 150 have shown a good cytotoxic activity against A204 cell line.

Cytotoxic evaluation of synthesised analogues

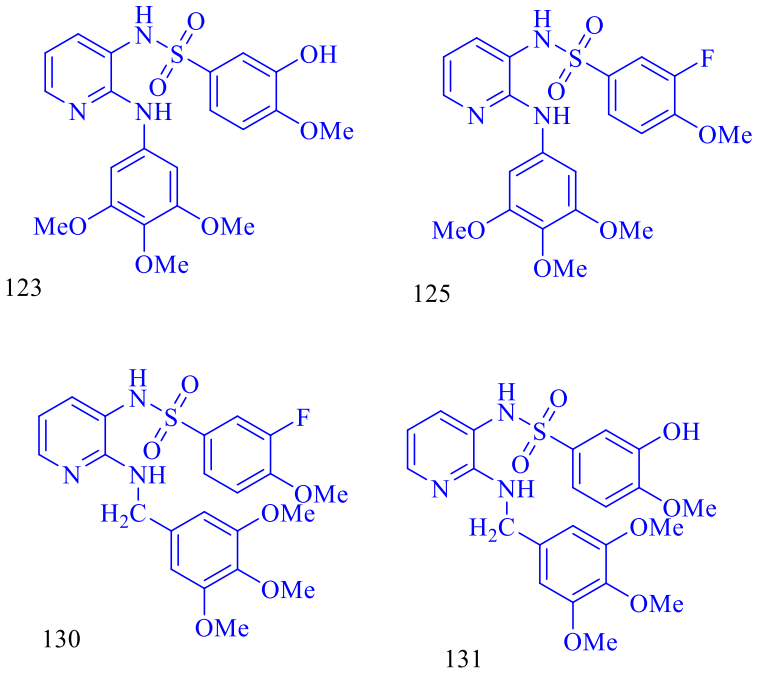

Figure 33: the chemical structures of compounds 123, 125, 130, and 131.

Hep-G2 are epithelial-like cells that grow as monolayers. Endothelial cells line the interior of blood vessels and so are a good model to test combretastatin derivatives. Compounds 130 and 131 (figure 33) have substitution patterns similar to that of CA4F and CA4. Low IC_{50} values were observed (6.55 and 6.60 µM respectively). The potency of combretastatins relies on the interactions of the compound with the colchicine binding site of tubulin (Gaspari *et al.*, 2017). 4-OMe group, as in CA4, could form hydrophobic interactions with a pocket in the binding site located below the combretastatins. Compounds 123 and 125 have a similar substitution pattern, with the removal of CH_2, the activity decreased drastically to 19.57 and 60.76 µM respectively. This suggests pyridinyl-phenyl sulphonamide analogues with the CH_2 more closely resemble the stilbene structure and fit into the binding pocket better.

Cis-locked compounds with imidazo[4,5,b]pyridine in place of the double bond in general had better IC_{50} values across all cell lines. In Hep-G2 compounds 132 and 131 had improved IC_{50} values (4.06 and 8.57 µM) compared to the corresponding pyridinyl-phenyl sulphonamide analogues 123 and 125. The imidazo[4,5,b]pyridine locks the combretastatin derivatives in the cis conformation. These molecules would be capable of fitting into the binding site of tubulin better.

Cytotoxic evaluation of synthesised analogues

The effect of the most active compounds (148, 130, 131) on the cell cycle were explored for the A549 cell line. They show a significant increase in cell population in the G_2/M phase (37.3 % in comparison with 4.89% in control for 131). In G_2/M phase, mitotic spindles are preparing to duplicate chromosomes of DNA to be separated into two daughter cells, therefore antimitotic agents cause the cells to be retained in G_2 phase (DiPaola, 2002). Flowcytometry results, figures (29-32), shows that compounds 148, 130, and 131 lead to considerable G_2/M arrest and therefore these compounds can be considered as antimitotic agents.

6 Conclusion and Future perspectives

Throughout this study many heterocyclic compounds have been synthesised as analogues of combretastatin A-4 and E7010. CA-4 analogues include substituted 5,6-diaryl-1,2,4-triazine-3(2H)-ones and substituted 2,3-diaryl imidazo[4,5,b]pyridines, whereas E7010 analogues were pyridinyl-benzene sulphonamides derivatives. Although many attempts, in acidic and basic medium, have been carried out to synthesise triazines, the required final product could not be synthesised when electron donating groups were present. 24 novel imidazo[4,5,b]pyridines and 8 pyridine-benzene sulphonamides have been successfully synthesised through multistep synthetic routes, as well as 36 novel intermediate compounds. 7 imidazo[4,5,b]pyridines have shown unexpected NMR spectra where the phenyl ring bearing trimethoxy moiety has only one out of two protons as well as one labile proton and a quaternary carbon. The biggest challenge in multistep synthesis is finding high yield protocols that required trying out several methodologies for one single reaction. However, most of the synthesised compounds have been obtained in a good to excellent yields. Owing to the crucial role of the trimethoxy moiety as microtubules inhibitors (Ma *et al.*, 2013), all the analogues have been synthesised bearing trimethoxy moiety in its structure.

The candidates have been evaluated for their cytotoxic activity in several cell lines using the MTT assay. Moreover, cell cycle analysis was conducted to explore their ability to block cells in the G_2/M phase for the most potent analogues.

The half maximal inhibitory concentration IC_{50} of the synthesised compounds were evaluated in vitro on (A204, A549, SAOS-2, Hep-G2, Beas-2B, and U2OS cells) by MTT assay.

Several analogues have shown low IC_{50} with values of about 1 µM and caused cell cycle arrest in G2/M phase with 37% of cells population in comparison with the population of cells at zero concentration of drug.

Cytotoxic evaluation of synthesised analogues

6.1 Future work

Owing to many obstacles encountered in synthesis of 1,2,4-triazine-3(2H)-one derivatives, future work would be focusing on optimization of the cyclocondensation protocol and to consider utilizing different catalysts to allow a successful reaction. Moreover, future work might involve the synthesis of substituted cyclohexadiene derivatives as combretastatin A-4 analogues through (4+2) Diels -Alder cycloaddition which remains unexplored by using diarlyalkyne and butadiene (scheme 23).

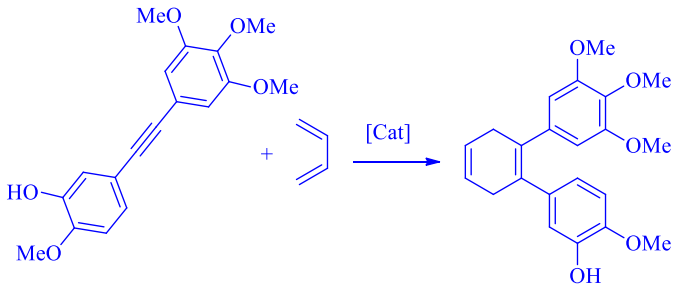

Scheme 23: synthesis of cyclohexadiene derivatives as combretastatin A-4 analogues.

Tubulin assembly assays would be very useful in the future. However, compounds that are biologically inactive or showing high IC_{50} values can be evaluated as protein kinase inhibitors, AKT inhibitors, aurora kinases inhibitors, and anti-inflammatory agents.

Acevedo, O., & Jorgensen, W. L. (2004). Solvent Effects and Mechanism for a Nucleophilic Aromatic Substitution from QM/MM Simulations. *Organic Letters, 6*(17), 2881-2884. doi:10.1021/ol049121k

ACS. (2020, 27th March 2020). Oncogenes and tumor suppressor genes. Retrieved from https://www.cancer.org/cancer/cancer-causes/genetics/genes-and-cancer/oncogenes-tumor-suppressor-genes.html

Adan, A., Kiraz, Y., & Baran, Y. (2016). Cell Proliferation and Cytotoxicity Assays. *Curr Pharm Biotechnol, 17*(14), 1213-1221.

Agabekov, V., Seiche, W., & Breit, B. (2013). Rhodium-catalyzed hydroformylation of alkynes employing a self-assembling ligand system. *Chemical Science, 4*(6), 2418-2422. doi:10.1039/C3SC50725D

Ahmed, B., Van Eijk, L. I., Bouma-Ter Steege, J. C., Van Der Schaft, D. W., Van Esch, A. M., Joosten-Achjanie, S. R., . . . Griffioen, A. W. (2003). Vascular targeting effect of combretastatin A-4 phosphate dominates the inherent angiogenesis inhibitory activity. *Int J Cancer, 105*(1), 20-25. doi:10.1002/ijc.11010

Al-Husein, B., Abdalla, M., Trepte, M., DeRemer, D. L., & Somanath, P. R. (2012). Anti-angiogenic therapy for cancer: An update. *Pharmacotherapy, 32*(12), 1095-1111. doi:10.1002/phar.1147

Almansa, C., de Arriba, A. F., Cavalcanti, F. L., Gómez, L. A., Miralles, A., Merlos, M., . . . Forn, J. (2001). Synthesis and SAR of a New Series of COX-2-Selective Inhibitors: Pyrazolo[1,5-a]pyrimidines. *Journal of Medicinal Chemistry, 44*(3), 350-361. doi:10.1021/jm0009383

Amsterdam, A., Pitzer, F., & Baumeister, W. (1993). Changes in intracellular localization of proteasomes in immortalized ovarian granulosa cells during mitosis associated with a role in cell cycle control. *Proceedings of the National Academy of Sciences, 90*(1), 99-103.

Anand, P., Kunnumakara, A. B., Sundaram, C., Harikumar, K. B., Tharakan, S. T., Lai, O. S., . . . Aggarwal, B. B. (2008). Cancer is a Preventable Disease that Requires Major

Lifestyle Changes. *Pharmaceutical Research, 25*(9), 2097-2116. doi:10.1007/s11095-008-9661-9

Anderson, J. L., Park, A., Akiyama, R., Tap, W. D., Denny, C. T., & Federman, N. (2015). Evaluation of in vitro activity of the class I PI3K inhibitor buparlisib (BKM120) in pediatric bone and soft tissue sarcomas. *PLOS ONE, 10*(9).

Arcamone, F. (1985). Properties of Antitumor Anthracyclines and New Developments in Their Application: Cain Memorial Award Lecture. *Cancer research, 45*(12 Part 1), 5995.

Arquero, A., Cañadas, M., Martinez-Ripoll, M., Antonia Mendiola, M., & Rodriguez, A. (1998). Selective access to new semicarbazones and thiosemicarbazones derived from benzil. Study of their conversion reactions. *Tetrahedron, 54*(37), 11271-11284. doi:https://doi.org/10.1016/S0040-4020(98)00667-X

Avendano, C., & Menendez, J. C. (2015). Medicinal Chemistry of Anticancer Drugs (pp. 25): Elsevier Science.

Avendano, C., & Menéndez, J. C. (2015). Medicinal Chemistry of Anticancer Drugs. In J. C. Menendez (Ed.), *Medicinal Chemistry of Anticancer Drugs* (2nd ed., pp. 198). Burlington: Elsevier Science.

Balcome, S., Park, S., Quirk Dorr, D. R., Hafner, L., Phillips, L., & Tretyakova, N. (2004). Adenine-containing DNA-DNA cross-links of antitumor nitrogen mustards. *Chem Res Toxicol, 17*(7), 950-962. doi:10.1021/tx0499463

Bavetsias, V., Sun, C., Bouloc, N., Reynisson, J., Workman, P., Linardopoulos, S., & McDonald, E. (2007). Hit generation and exploration: imidazo[4,5-b]pyridine derivatives as inhibitors of Aurora kinases. *Bioorg Med Chem Lett, 17*(23), 6567-6571. doi:10.1016/j.bmcl.2007.09.076

Bernhard Palsson, & Masters, J. (2002). *Cancer Cell Lines Part 2* (1 ed. Vol. 2): Springer Netherland.

References

Berridge, M. V., Herst, P. M., & Tan, A. S. (2005). Tetrazolium dyes as tools in cell biology: New insights into their cellular reduction *Biotechnology Annual Review* (Vol. 11, pp. 127-152): Elsevier.

Bhattacharya, B., & Mukherjee, S. (2015). Cancer Therapy Using Antibiotics. *Journal of Cancer Therapy, 6*(10), 849.

Binisti, C., Assogba, L., Touboul, E., Mounier, C., Huet, J., Ombetta, J.-E., . . . Godfroid, J.-J. (2001). Structure–activity relationships in platelet-activating factor (PAF). 11-From PAF-antagonism to phospholipase A2 inhibition: syntheses and structure–activity relationships in 1-arylsulfamido-2-alkylpiperazines. *European Journal of Medicinal Chemistry, 36*(10), 809-828. doi:https://doi.org/10.1016/S0223-5234(01)01274-0

Blackburn, E. K., King, G. M., & Swan, H. T. (1956). Myleran in Treatment of Chronic Myeloid Leukaemia. *British Medical Journal, 1*(4971), 835-837.

Borrel, C., Thoret, S., Cachet, X., Guénard, D., Tillequin, F., Koch, M., & Michel, S. (2005). New antitubulin derivatives in the combretastatin A4 series: synthesis and biological evaluation. *Bioorganic & Medicinal Chemistry, 13*(11), 3853-3864. doi:https://doi.org/10.1016/j.bmc.2005.02.039

Boulikas, T. (2007). Molecular mechanisms of cisplatin and its liposomally encapsulated form, Lipoplatin™. Lipoplatin™ as a chemotherapy and antiangiogenesis drug. *Cancer ther, 5*, 351-376.

Braig, M., Lee, S., Loddenkemper, C., Rudolph, C., Peters, A. H., Schlegelberger, B., . . . Schmitt, C. A. (2005). Oncogene-induced senescence as an initial barrier in lymphoma development. *Nature, 436*(7051), 660-665. Retrieved from doi:10.1038/nature03841

Bray, F., Ferlay, J., Soerjomataram, I., Siegel, R. L., Torre, L. A., & Jemal, A. (2018). Global cancer statistics 2018: GLOBOCAN estimates of incidence and mortality worldwide for 36 cancers in 185 countries. *CA: A Cancer Journal for Clinicians, 68*(6), 394-424. doi:10.3322/caac.21492

References

Burroughs, L., Ritchie, J., Ngwenya, M., Khan, D., Lewis, W., & Woodward, S. (2015). Anionic sigmatropic-electrocyclic-Chugaev cascades: accessing 12-aryl-5-(methylthiocarbonylthio)tetracenes and a related anthra[2,3-b]thiophene. *Beilstein Journal of Organic Chemistry*, *11*, 273-279. doi:10.3762/bjoc.11.31

Caley, A., & Jones, R. (2012). The principles of cancer treatment by chemotherapy. *Surgery (Oxford)*, *30*(4), 186-190. doi:https://doi.org/10.1016/j.mpsur.2012.01.004

Cao, S.-L., Zhao, J., Zhang, N., Wang, Y., Jiang, Y.-Y., & Feng, Y.-P. (2011). Synthesis and Crystal Structures of 4-(3-Nitropyridin-2-ylamino)phenol and 4-(3-Aminopyridin-2-ylamino)phenol. *Journal of Chemical Crystallography*, *41*(10), 1456-1460. doi:10.1007/s10870-011-0121-8

Caporale, A., Tartaggia, S., Castellin, A., & De Lucchi, O. (2014). Practical synthesis of aryl-2-methyl-3-butyn-2-ols from aryl bromides via conventional and decarboxylative copper-free Sonogashira coupling reactions. *Beilstein journal of organic chemistry*, *10*(1), 384-393. doi:10.3762/bjoc.10.36

Carmichael, J., DeGraff, W. G., Gazdar, A. F., Minna, J. D., & Mitchell, J. B. (1987). Evaluation of a tetrazolium-based semiautomated colorimetric assay: assessment of chemosensitivity testing. *Cancer research*, *47*(4), 936-942.

Chauvin, C., Leruste, A., Tauziede-Espariat, A., Andrianteranagna, M., Surdez, D., Lescure, A., . . . Bourdeaut, F. (2017). High-Throughput Drug Screening Identifies Pazopanib and Clofilium Tosylate as Promising Treatments for Malignant Rhabdoid Tumors. *Cell Reports*, *21*(7), 1737-1745. doi:https://doi.org/10.1016/j.celrep.2017.10.076

Chen, J., Liu, T., Dong, X., & Hu, Y. (2009). Recent development and SAR analysis of colchicine binding site inhibitors. *Mini Rev Med Chem*, *9*(10), 1174-1190.

Cheng, J., Sun, Y., Wang, F., Guo, M., Xu, J.-H., Pan, Y., & Zhang, Z. (2004). A Copper- and Amine-Free Sonogashira Reaction Employing Aminophosphines as Ligands. *The Journal of organic chemistry*, *69*(16), 5428-5432. doi:10.1021/jo049379o

References

Chinchilla, R., & Najera, C. (2007). The Sonogashira reaction: a booming methodology in synthetic organic chemistry. *Chem Rev, 107*(3), 874-922. doi:10.1021/cr050992x

Chinchilla, R., & Najera, C. (2011). Recent advances in Sonogashira reactions. *Chemical Society Reviews, 40*(10), 5084-5121. doi:10.1039/C1CS15071E

Clayden, J., Nick, G., & Stuart, W. (2012). *Organic chemistry* (Second edition. ed.). Oxford: Oxford : Oxford University Press.

Cobb, L., & Das, S. (2013). The Cell Cycle Analysis. *MATER METHODS, 3*(172). Retrieved from https://www.labome.com/method/Cell-Based-Assays-the-Cell-Cycle-Cell-Proliferation-and-Cell-Death.html doi:dx.doi.org/10.13070/mm.en.3.172

Colvin, M. (2003, 10th February2003). Alkylating Agents. *Holland-Frei Cancer Medicine.* 6th. Retrieved from https://www.ncbi.nlm.nih.gov/books/NBK12772/

Coniglio, A., Bassetti, M., García-Garrido, S. E., & Gimeno, J. (2012). Dimerization of Terminal Arylalkynes in Aqueous Medium by Ruthenium and Acid Promoted (RAP) Catalysis: Acetate- Assisted (sp)C□(sp2)C Bond Formation. *Advanced Synthesis & Catalysis, 354*(1), 148-158. doi:10.1002/adsc.201100600

Cooper, G. M. a. (2016). The cell : a molecular approach. In R. E. a. Hausman (Ed.), (Seventh edition / Geoffrey M. Cooper, Robert E. Hausman. ed.): Sunderland, Massachusetts U.S.A. : Sinauer Associates, Inc.

Cooper., G. M. (2000). *The Cell A Molecular Approach* (2nd edition ed.): Sinauer Associates.

Cortes-Funes, H., & Coronado, C. (2007). Role of anthracyclines in the era of targeted therapy. *Cardiovasc Toxicol, 7*(2), 56-60. doi:10.1007/s12012-007-0015-3

Cox, M. M., Doudna, J. A., & O'Donnel, M. (2015). *Molecular biology : principles and practice* (2nd ed.). New York: W.H. Freeman & Company.

CRUK. (2020a, 21th March 2020
). Cancer incidence by age. Retrieved from http://www.cancerresearchuk.org/health-professional/cancer-statistics/incidence/age#ref-0

CRUK. (2020b, 30th March 2020
30 November 2017). Types of cancer. Retrieved from http://www.cancerresearchuk.org/about-cancer/what-is-cancer/how-cancer-starts/types-of-cancer

Csékei, M., Novák, Z., & Kotschy, A. (2008). Development of a one-pot sequential Sonogashira coupling for the synthesis of benzofurans. *Tetrahedron, 64*(37), 8992-8996. doi:https://doi.org/10.1016/j.tet.2008.05.100

Danaei, G., Vander Hoorn, S., Lopez, A. D., Murray, C. J., & Ezzati, M. (2005). Causes of cancer in the world: comparative risk assessment of nine behavioural and environmental risk factors. *Lancet, 366*(9499), 1784-1793. doi:10.1016/s0140-6736(05)67725-2

Dark, G. G., Hill, S. A., Prise, V. E., Tozer, G. M., Pettit, G. R., & Chaplin, D. J. (1997). Combretastatin A-4, an agent that displays potent and selective toxicity toward tumor vasculature. *Cancer research, 57*(10), 1829-1834.

Darzynkiewicz, Z., Huang, X., & Zhao, H. (2017). Analysis of Cellular DNA Content by Flow Cytometry. *Curr Protoc Cytom, 82*, 7.5.1-7.5.20. doi:10.1002/cpcy.28

Davis, P. P., Grossert, J. S., Langler, R. F., & Mantle, W. S. (1977). Rearrangements in the electron impact induced fragmentations of sulfonyl chlorides. *Organic Mass Spectrometry, 12*(11), 659-662. doi:10.1002/oms.1210121102

De Luca, L., & Giacomelli, G. (2008). An easy microwave-assisted synthesis of sulfonamides directly from sulfonic acids. *The Journal of organic chemistry, 73*(10), 3967-3969.

Demchuk, D. V., Samet, A. V., Chernysheva, N. B., Ushkarov, V. I., Stashina, G. A., Konyushkin, L. D., . . . Zavelevich, M. P. (2014). Synthesis and antiproliferative activity of conformationally restricted 1, 2, 3-triazole analogues of combretastatins in the sea urchin embryo model and against human cancer cell lines. *Bioorganic & Medicinal Chemistry, 22*(2), 738-755.

References

Denizot, F., & Lang, R. (1986). Rapid colorimetric assay for cell growth and survival: Modifications to the tetrazolium dye procedure giving improved sensitivity and reliability. *Journal of Immunological Methods, 89*(2), 271-277. doi:https://doi.org/10.1016/0022-1759(86)90368-6

Di Marco, A., Gaetani, M., Orezzi, P., Scarpinato, B., Silvestrini, R., Soldati, M., . . . Valentini, L. (1964). Daunomycin', a new antibiotic of the rhodomycin group. *Nature, 201*, 706-707.

DiPaola, R. S. (2002). To Arrest or Not To G₂-M Cell-Cycle Arrest. *Clinical Cancer Research, 8*(11), 3311.

Donzelli, E., Carfì, M., Miloso, M., Strada, A., Galbiati, S., Bayssas, M., . . . Tredici, G. (2004). Neurotoxicity of platinum compounds: Comparison of the effects of cisplatin and oxaliplatin on the human neuroblastoma cell line sh-sy5y. *Journal of Neuro-Oncology, 67*(1), 65-73. doi:10.1023/B:NEON.0000021787.70029.ce

Doucet, H., & Hierso, J. C. (2007). Palladium‐Based Catalytic Systems for the Synthesis of Conjugated Enynes by Sonogashira Reactions and Related Alkynylations. *Angewandte Chemie International Edition, 46*(6), 834-871. doi:doi:10.1002/anie.200602761

Dowsett, M., Smithers, D., Moore, J., Trunet, P. F., Coombes, R. C., Powles, T. J., . . . Smith, I. E. (1994). Endocrine changes with the aromatase inhibitor fadrozole hydrochloride in breast cancer. *European Journal of Cancer, 30*(10), 1453-1458. doi:https://doi.org/10.1016/0959-8049(94)00281-9

Dyminska, L. (2015). Imidazopyridines as a source of biological activity and their pharmacological potentials-Infrared and Raman spectroscopic evidence of their content in pharmaceuticals and plant materials. *Bioorg Med Chem, 23*(18), 6087-6099. doi:10.1016/j.bmc.2015.07.045

Eckhouse, S., Lewison, G., & Sullivan, R. (2008). Trends in the global funding and activity of cancer research. *Mol Oncol, 2*(1), 20-32. doi:10.1016/j.molonc.2008.03.007

References

Elangovan, A., Wang, Y. H., & Ho, T. I. (2003). Sonogashira coupling reaction with diminished homocoupling. *Org Lett, 5*(11), 1841-1844. doi:10.1021/ol034320+

Emmett, E. J., Hayter, B. R., & Willis, M. C. (2014). Palladium‐Catalyzed Synthesis of Ammonium Sulfinates from Aryl Halides and a Sulfur Dioxide Surrogate: A Gas‐and Reductant‐Free Process. *Angewandte Chemie International Edition, 53*(38), 10204-10208.

Fassy, F., Dureuil, C., Lamberton, A., Mathieu, M., Michot, N., Ronan, B., & Pasquier, B. (2017). Chapter Twenty-Six - In Vitro Characterization of VPS34 Lipid Kinase Inhibition by Small Molecules. In L. Galluzzi, J. M. Bravo-San Pedro, & G. Kroemer (Eds.), *Methods in Enzymology* (Vol. 587, pp. 447-464): Academic Press.

Feng, S.-S., & Chien, S. (2003). Chemotherapeutic engineering: application and further development of chemical engineering principles for chemotherapy of cancer and other diseases. *Chemical Engineering Science, 58*(18), 4087-4114.

Flynn, B. L., Flynn, G. P., Hamel, E., & Jung, M. K. (2001). The synthesis and tubulin binding activity of thiophene-based analogues of combretastatin A-4. *Bioorganic & Medicinal Chemistry Letters, 11*(17), 2341-2343. doi:https://doi.org/10.1016/S0960-894X(01)00436-X

Fogh, J., Fogh, J. M., & Orfeo, T. (1977). One hundred and twenty-seven cultured human tumor cell lines producing tumors in nude mice. *J Natl Cancer Inst, 59*(1), 221-226. doi:10.1093/jnci/59.1.221

Forner, A., Llovet, J. M., & Bruix, J. (2012). Hepatocellular carcinoma. *The Lancet, 379*(9822), 1245-1255. doi:https://doi.org/10.1016/S0140-6736(11)61347-0

Foster, K. A., Oster, C. G., Mayer, M. M., Avery, M. L., & Audus, K. L. (1998). Characterization of the A549 Cell Line as a Type II Pulmonary Epithelial Cell Model for Drug Metabolism. *Experimental Cell Research, 243*(2), 359-366. doi:https://doi.org/10.1006/excr.1998.4172

References

Fotakis, G., & Timbrell, J. A. (2006). In vitro cytotoxicity assays: comparison of LDH, neutral red, MTT and protein assay in hepatoma cell lines following exposure to cadmium chloride. *Toxicology Letters, 160*(2), 171-177. doi:10.1016/j.toxlet.2005.07.001

Fürstner, A., & Nikolakis, K. (1996). Ethynylation of Aryl Halides by a Modified Suzuki Reaction: Application to the Syntheses of Combretastatin A‐4, A‐5 and Lunularic Acid. *Liebigs Annalen, 1996*(12), 2107-2113.

Gao, A., Yang, F., Li, J., & Wu, Y. (2012). Pd/Cu-catalyzed oxidation of alkynes into 1,2-diketones using DMSO as the oxidant. *Tetrahedron, 68*(25), 4950-4954. doi:https://doi.org/10.1016/j.tet.2012.04.069

Gaspari, R., Prota, A. E., Bargsten, K., Cavalli, A., & Steinmetz, M. O. (2017). Structural Basis of cis- and trans-Combretastatin Binding to Tubulin. *Chem, 2*(1), 102-113. doi:10.1016/j.chempr.2016.12.005

Gates, K. S. (2009). An overview of chemical processes that damage cellular DNA: spontaneous hydrolysis, alkylation, and reactions with radicals. *Chem Res Toxicol, 22*(11), 1747-1760. doi:10.1021/tx900242k

Gaukroger, K., Hadfield, J. A., Lawrence, N. J., Nolan, S., & McGown, A. T. (2003). Structural requirements for the interaction of combretastatins with tubulin: how important is the trimethoxy unit? *Organic & Biomolecular Chemistry, 1*(17), 3033-3037.

Giannakakou, P., Sackett, D., & Fojo, T. (2000). Tubulin/microtubules: still a promising target for new chemotherapeutic agents. *J Natl Cancer Inst, 92*(3), 182-183. doi:https://doi.org/10.1016/0163-7258(93)90044-E

Giard, D. J., Aaronson, S. A., Todaro, G. J., Arnstein, P., Kersey, J. H., Dosik, H., & Parks, W. P. (1973). In vitro cultivation of human tumors: establishment of cell lines derived from a series of solid tumors. *J Natl Cancer Inst, 51*(5), 1417-1423. doi:10.1093/jnci/51.5.1417

Gille, L., & Nohl, H. (1997). Analyses of the molecular mechanism of adriamycin-induced cardiotoxicity. *Free Radical Biology and Medicine, 23*(5), 775-782.

Giraud, A., Provot, O., Peyrat, J.-F., Alami, M., & Brion, J.-D. (2006). Microwave-assisted efficient synthesis of 1,2-diaryldiketones: a novel oxidation reaction of diarylalkynes with DMSO promoted by FeBr3. *Tetrahedron, 62*(33), 7667-7673. doi:https://doi.org/10.1016/j.tet.2006.05.072

Gniazdowski, M., Denny, W. A., Nelson, S. M., & Czyz, M. (2005). Effects of anticancer drugs on transcription factor–DNA interactions. *Expert Opinion on Therapeutic Targets, 9*(3), 471-489. doi:10.1517/14728222.9.3.471

Goldstein, S. W., Bill, A., Dhuguru, J., & Ghoneim, O. (2017). Nucleophilic Aromatic Substitution—Addition and Identification of an Amine. *Journal of Chemical Education, 94*(9), 1388-1390. doi:10.1021/acs.jchemed.6b00680

Greene, L. M., Nathwani, S. M., Bright, S. A., Fayne, D., Croke, A., Gagliardi, M., . . . Zisterer, D. M. (2010). The Vascular Targeting Agent Combretastatin-A4 and a Novel cis-Restricted β-Lactam Analogue, CA-432, Induce Apoptosis in Human Chronic Myeloid Leukemia Cells and Ex Vivo Patient Samples Including Those Displaying Multidrug Resistance. *Journal of Pharmacology and Experimental Therapeutics, 335*(2), 302-313. doi:10.1124/jpet.110.170415

Grossman, R. B. (1999). *The art of writing reasonable organic reaction mechanisms*. New York: New York : Springer.

Guo, L., Dial, S., Shi, L., Branham, W., Liu, J., Fang, J. L., . . . Ning, B. (2011). Similarities and differences in the expression of drug-metabolizing enzymes between human hepatic cell lines and primary human hepatocytes. *Drug Metab Dispos, 39*(3), 528-538. doi:10.1124/dmd.110.035873

Ha, M. H., Ham, S. Y., Lee, D. H., & Choi, J. (2007). In vitro toxicity assay using human bronchial epithelial cell, Beas-2B, for the screening of toxicological risk of dioxin-like compounds sampled from small sized Korean waste incineration plants. *Chemosphere, 70*(1), 20-28. doi:10.1016/j.chemosphere.2007.07.055

Habrant, D., Rauhala, V., & Koskinen, A. M. P. (2010). Conversion of carbonyl compounds to alkynes: general overview and recent developments. *Chemical Society Reviews, 39*(6), 2007-2017. doi:10.1039/B915418C

Hadfield, J. A., Gaukroger, K., Hirst, N., Weston, A. P., Lawrence, N. J., & McGown, A. T. (2005). Synthesis and evaluation of double bond substituted combretastatins. *European Journal of Medicinal Chemistry, 40*(6), 529-541. doi:https://doi.org/10.1016/j.ejmech.2004.12.008

Hadfield, J. A., & McGown, A. T. (1998). Preparation and Evaluation of Diarylalkynes as Antitumour Agents. *Synthetic Communications, 28*(8), 1421-1431. doi:10.1080/00397919808006841

Hasegawa, M., Nishigaki, N., Washio, Y., Kano, K., Harris, P. A., Sato, H., . . . Cheung, M. (2007). Discovery of novel benzimidazoles as potent inhibitors of TIE-2 and VEGFR-2 tyrosine kinase receptors. *J Med Chem, 50*(18), 4453-4470. doi:10.1021/jm0611051

Hausser, H.-J., & Brenner, R. E. (2005). Phenotypic instability of Saos-2 cells in long-term culture. *Biochemical and Biophysical Research Communications, 333*(1), 216-222. doi:https://doi.org/10.1016/j.bbrc.2005.05.097

Heilman, W. P., Heilman, R. D., Scozzie, J. A., Wayner, R. J., Gullo, J. M., & Ariyan, Z. S. (1979). Synthesis and antihypertensive activity of novel 3-hydrazino-5-phenyl-1,2,4-triazines. *J Med Chem, 22*(6), 671-677. doi:10.1021/jm00192a012

Hinson, A., Jones, R., Crose, L., Belyea, B., Barr, F., & Linardic, C. (2013). Human Rhabdomyosarcoma Cell Lines for Rhabdomyosarcoma Research: Utility and Pitfalls. *Frontiers in Oncology, 3*(183). doi:10.3389/fonc.2013.00183

Huntress, E. H., & Carten, F. H. (1940). Identification of Organic Compounds. I. Chlorosulfonic Acid as a Reagent for the Identification of Aryl Halides. *Journal of the American Chemical Society, 62*(3), 511-514. doi:10.1021/ja01860a014

Isanbor, C., & Emokpae, T. A. (2008). Nucleophilic heteroaromatic substitution: Kinetics of the reactions of nitropyridines with aliphatic amines in dipolar aprotic

solvents. *International Journal of Chemical Kinetics, 40*(3), 125-135. doi:10.1002/kin.20297

Ji, Y. Z., Li, H. J., Zhang, J. Y., & Wu, Y. C. (2019). Switchable regioselection of C-H thiolation of indoles using different TMS counterions. *Chem Commun (Camb), 55*(79), 11864-11867. doi:10.1039/c9cc05652a

Johnstone, T. C., Park, G. Y., & Lippard, S. J. (2014). Understanding and Improving Platinum Anticancer Drugs – Phenanthriplatin. *Anticancer research, 34*(1), 471-476.

Johnstone, T. C., Suntharalingam, K., & Lippard, S. J. (2015). Third row transition metals for the treatment of cancer. *Philosophical Transactions of the Royal Society of London A: Mathematical, Physical and Engineering Sciences, 373*(2037), 20140185.

Jung, M. E., & Deng, G. (2014). Synthesis of α-Diketones from Alkylaryl- and Diarylalkynes Using Mercuric Salts. *Organic Letters, 16*(8), 2142-2145. doi:10.1021/ol500592m

Jutand, A., Négri, S., & Principaud, A. (2005). Formation of ArPdXL(amine) Complexes by Substitution of One Phosphane Ligand by an Amine in trans-ArPdX(PPh3)2 Complexes. *European Journal of Inorganic Chemistry, 2005*(4), 631-635. doi:10.1002/ejic.200400413

Kabalka, G. W., Wang, L., Namboodiri, V., & Pagni, R. M. (2000). Rapid microwave-enhanced, solventless Sonogashira coupling reaction on alumina. *Tetrahedron Letters, 41*(27), 5151-5154. doi:https://doi.org/10.1016/S0040-4039(00)00774-7

Kaur, G., & Dufour, J. M. (2012). Cell lines: Valuable tools or useless artifacts. *Spermatogenesis, 2*(1), 1-5. doi:10.4161/spmg.19885

Kavallaris, M., Verrills, N. M., & Hill, B. T. (2001). Anticancer therapy with novel tubulin-interacting drugs. *Drug Resistance Updates, 4*(6), 392-401. doi:10.1054/drup.2002.0230

Keepers, Y. P., Pizao, P. E., Peters, G. J., van Ark-Otte, J., Winograd, B., & Pinedo, H. M. (1991). Comparison of the sulforhodamine B protein and tetrazolium (MTT) assays

for in vitro chemosensitivity testing. *European Journal of Cancer and Clinical Oncology, 27*(7), 897-900. doi:https://doi.org/10.1016/0277-5379(91)90142-Z

Kim Choong Hahn, Beak Young Mi, Park Ho Cheol, Lee Chang Jun, Shin Jin Yong, Lee Jae Hoon, . . . Sung, C. N. (2015). KR101556826 (B1). K. Patent.

Kim, J.-G., & Jang, D. O. (2007). Mild and efficient indium metal catalyzed synthesis of sulfonamides and sulfonic esters. *Synlett, 2007*(16), 2501-2504.

Kinnula, V. L., Yankaskas, J. R., Chang, L., Virtanen, I., Linnala, A., Kang, B. H., & Crapo, J. D. (1994). Primary and immortalized (BEAS 2B) human bronchial epithelial cells have significant antioxidative capacity in vitro. *Am J Respir Cell Mol Biol, 11*(5), 568-576. doi:10.1165/ajrcmb.11.5.7946385

Kiyomiya, K., Matsuo, S., & Kurebe, M. (2001). Mechanism of specific nuclear transport of adriamycin: the mode of nuclear translocation of adriamycin-proteasome complex. *Cancer research, 61*(6), 2467-2471.

Knowles, B., Howe, C., & Aden, D. (1980). Human hepatocellular carcinoma cell lines secrete the major plasma proteins and hepatitis B surface antigen. *Science, 209*(4455), 497-499. doi:10.1126/science.6248960

Kovač, T., Oklobdžija, M., Comisso, G., Decorte, E., Fajdiga, T., Moimas, F., . . . Šunjić, V. (1983). New synthesis of 11 ‐ acyl ‐ 5, 11 ‐ dihydro ‐ 6H ‐ pyrido [2, 3 ‐ b][1, 4] ‐ benzodiazepin ‐ 6 ‐ ones and related studies. *Journal of heterocyclic chemistry, 20*(5), 1339-1349.

Koyanagi, N., Nagasu, T., Fujita, F., Watanabe, T., Tsukahara, K., Funahashi, Y., . . . Kitoh, K. (1994). In vivo tumor growth inhibition produced by a novel sulfonamide, E7010, against rodent and human tumors. *Cancer research, 54*(7), 1702-1706.

Kratzl, K., & Nelböck-Hochstetter, M. (1952). Die Synthese sulfonsäure-analoger Vanillinsäure- und Isovanillinsäurederivate. *Monatshefte für Chemie und verwandte Teile anderer Wissenschaften, 83*(4), 1038-1044. doi:10.1007/BF00899640

Kumar, A., Gupta, G., & Srivastava, S. (2011). Synthesis of New Class of Alkyl Azarene Pyridinium Zwitterions via Iodine Mediated sp3 C–H Bond Activation. *Organic Letters, 13*(24), 6366-6369. doi:10.1021/ol202654j

Kuper, H., Adami, H. O., & Boffetta, P. (2002). Tobacco use, cancer causation and public health impact. *J Intern Med, 251*(6), 455-466.

Kushi, L. H., Doyle, C., McCullough, M., Rock, C. L., Demark-Wahnefried, W., Bandera, E. V., . . . Gansler, T. (2012). American Cancer Society Guidelines on nutrition and physical activity for cancer prevention: reducing the risk of cancer with healthy food choices and physical activity. *CA Cancer J Clin, 62*(1), 30-67. doi:10.3322/caac.20140

Kwolek-Mirek, M., & Zadrag-Tecza, R. (2014). Comparison of methods used for assessing the viability and vitality of yeast cells. *FEMS Yeast Research, 14*(7), 1068-1079. doi:10.1111/1567-1364.12202

Lai, M.-J., Ojha, R., Lin, M.-H., Liu, Y.-M., Lee, H.-Y., Lin, T. E., . . . Nepali, K. (2019). 1-Arylsulfonyl indoline-benzamides as a new antitubulin agents, with inhibition of histone deacetylase. *European Journal of Medicinal Chemistry, 162*, 612-630.

Lan, P., Chen, W. N., & Chen, W. M. (2011). Molecular modeling studies on imidazo[4,5-b]pyridine derivatives as Aurora A kinase inhibitors using 3D-QSAR and docking approaches. *Eur J Med Chem, 46*(1), 77-94. doi:10.1016/j.ejmech.2010.10.017

Langer, S. Z., & Arbilla, S. (1988). Imidazopyridines as a tool for the characterization of benzodiazepine receptors: a proposal for a pharmacological classification as omega receptor subtypes. *Pharmacol Biochem Behav, 29*(4), 763-766. doi:10.1016/0091-3057(88)90202-x

Lara-Ochoa, F., & Espinosa-Pérez, G. (2007). A new synthesis of combretastatins A-4 and AVE-8062A. *Tetrahedron Letters, 48*(39), 7007-7010. doi:https://doi.org/10.1016/j.tetlet.2007.07.151

Lavanya, R. (2017). Sulphonamides: a pharmaceutical review. *International Journal of Pharmaceutical Science Invention, 6*(2).

Lawrence, N. J., Ghani, F. A., Hepworth, L. A., Hadfield, J. A., McGown, A. T., & Pritchard, R. G. (1999). The synthesis of (E) and (Z)-combretastatins A-4 and a phenanthrene from Combretum caffrum. *Synthesis, 1999*(09), 1656-1660. doi:10.1055/s-1999-3570

Leadbeater, N. E., & Tominack, B. J. (2003). Rapid, easy copper-free Sonogashira couplings using aryl iodides and activated aryl bromides. *Tetrahedron Letters, 44*(48), 8653-8656. doi:http://dx.doi.org/10.1016/j.tetlet.2003.09.159

Li, W., Yin, Y., Shuai, W., Xu, F., Yao, H., Liu, J., . . . Xu, S. (2019). Discovery of novel quinazolines as potential anti-tubulin agents occupying three zones of colchicine domain. *Bioorganic Chemistry, 83*, 380-390. doi:https://doi.org/10.1016/j.bioorg.2018.10.027

Li, Y., Dong, K., Wang, Z., & Ding, K. (2013). Rhodium(I)-Catalyzed Enantioselective Hydrogenation of Substituted Acrylic Acids with Sterically Similar β,β-Diaryls. *Angewandte Chemie, 125*(26), 6880-6884. doi:10.1002/ange.201302349

Liang, Y., Xie, Y.-X., & Li, J.-H. (2006). Modified Palladium-Catalyzed Sonogashira Cross-Coupling Reactions under Copper-, Amine-, and Solvent-Free Conditions. *The Journal of organic chemistry, 71*(1), 379-381. doi:10.1021/jo051882t

Lin, Y., Zhang, M., & Barnes, P. F. (1998). Chemokine Production by a Human Alveolar Epithelial Cell Line in Response to Mycobacterium tuberculosis. *Infection and Immunity, 66*(3), 1121-1126.

Lipshutz, B. H., Chung, D. W., & Rich, B. (2008). Sonogashira Couplings of Aryl Bromides: Room Temperature, Water Only, No Copper. *Organic Letters, 10*(17), 3793-3796. doi:10.1021/ol801471f

Littke, A. F., & Fu, G. C. (2002). Palladium-catalyzed coupling reactions of aryl chlorides. *Angew Chem Int Ed Engl, 41*(22), 4176-4211. doi:10.1002/1521-3773(20021115)41:22<4176::aid-anie4176>3.0.co;2-u

Liu, Y., Peterson, D. A., Kimura, H., & Schubert, D. (1997). Mechanism of Cellular 3 - (4,5 - Dimethylthiazol - 2 - yl) - 2,5 - Diphenyltetrazolium Bromide (MTT)

Reduction. *Journal of Neurochemistry, 69*(2), 581-593. doi:doi:10.1046/j.1471-4159.1997.69020581.x

Longmuir, K. J., Haynes, S. M., Baratta, J. L., Kasabwalla, N., & Robertson, R. T. (2009). Liposomal delivery of doxorubicin to hepatocytes in vivo by targeting heparan sulfate. *International Journal of Pharmaceutics, 382*(1–2), 222-233. doi:https://doi.org/10.1016/j.ijpharm.2009.07.030

Louis, K. S., & Siegel, A. C. (2011). Cell viability analysis using trypan blue: manual and automated methods *Mammalian cell viability* (pp. 7-12): Springer.

Lu, Y., Chen, J., Xiao, M., Li, W., & Miller, D. D. (2012). An overview of tubulin inhibitors that interact with the colchicine binding site. *Pharm Res, 29*(11), 2943-2971. doi:10.1007/s11095-012-0828-z

Lu, Y., Chen, J., Xiao, M., Li, W., & Miller, D. D. (2012). An Overview of Tubulin Inhibitors That Interact with the Colchicine Binding Site. *Pharmaceutical research, 29*(11), 2943-2971. doi:10.1007/s11095-012-0828-z

Lv, W.-X., Zeng, Y.-F., Zhang, S.-S., Li, Q., & Wang, H. (2015). Mild Mn(OAc)3-Mediated Aerobic Oxidative Decarboxylative Coupling of Arylboronic Acids and Arylpropiolic Acids: Direct Access to Diaryl 1,2-Diketones. *Organic Letters, 17*(12), 2972-2975. doi:10.1021/acs.orglett.5b01265

Ma, M., Sun, L., Lou, H., & Ji, M. (2013). Synthesis and biological evaluation of Combretastatin A-4 derivatives containing a 3'-O-substituted carbonic ether moiety as potential antitumor agents. *Chemistry Central journal, 7*(1), 179-179. doi:10.1186/1752-153X-7-179

Macdonald, C. (1990). Development of New Cell Lines for Animal Cell Biotechnology. *Critical Reviews in Biotechnology, 10*(2), 155-178. doi:10.3109/07388559009068265

Macdonald, J., Oldfield, V., Bavetsias, V., & Blagg, J. (2013). Regioselective C2-arylation of imidazo[4,5-b]pyridines. *Organic & Biomolecular Chemistry, 11*(14), 2335-2347. doi:10.1039/C3OB27477B

References

Mahesh, R., Nayak, V. L., Babu, K. S., Riyaz, S., Shaik, T. B., Kumar, G. B., . . . Kamal, A. (2017). Design, Synthesis, and in vitro and in vivo Evaluations of (Z)-3,4,5-Trimethoxystyrylbenzenesulfonamides/sulfonates as Highly Potent Tubulin Polymerization Inhibitors. *ChemMedChem, 12*(9), 678-700. doi:10.1002/cmdc.201600643

Marco, A., & Arcamone, F. (1975). DNA complexing antibiotics: daunomycin, adriamycin and their derivatives. *Arzneimittel-Forschung, 25*(3), 368-374.

Marie Kirwen, E., Batra, T., Karthikeyan, C., Deora, G. S., Rathore, V., Mulakayala, C., . . . Tiwari, A. K. (2017). 2,3-Diaryl-3H-imidazo[4,5-b]pyridine derivatives as potential anticancer and anti-inflammatory agents. *Acta Pharmaceutica Sinica B, 7*(1), 73-79. doi:https://doi.org/10.1016/j.apsb.2016.05.003

Markus, G., Michael, A. J., & Bernhard, K. K. (2005). Update of the Preclinical Situation of Anticancer Platinum Complexes: Novel Design Strategies and Innovative Analytical Approaches. *Current medicinal chemistry, 12*(18), 2075-2094. doi:http://dx.doi.org/10.2174/0929867054637626

McAllister, R. M., Melnyk, J., Finkelstein, J. Z., Adams, E. C., Jr., & Gardner, M. B. (1969). Cultivation in vitro of cells derived from a human rhabdomyosarcoma. *Cancer, 24*(3), 520-526. doi:10.1002/1097-0142(196909)24:3<520::aid-cncr2820240313>3.0.co;2-m

McCauley, J., Zivanovic, A., & Skropeta, D. (2013). Bioassays for Anticancer Activities. In U. Roessner & D. A. Dias (Eds.), *Metabolomics Tools for Natural Product Discovery: Methods and Protocols* (pp. 191-205). Totowa, NJ: Humana Press.

McKinnon, K. M. (2018). Flow Cytometry: An Overview. *Curr Protoc Immunol, 120*, 5.1.1-5.1.11. doi:10.1002/cpim.40

Merck. (2020, 5th March 2020). DNA Damage and Repair. *technical documents.* Retrieved from http://www.sigmaaldrich.com/technical-documents/articles/biofiles/dna-damage-and-repair.html#ref

Mery, D., Heuze, K., & Astruc, D. (2003). A very efficient, copper-free palladium catalyst for the Sonogashira reaction with aryl halides. *Chemical Communications*(15), 1934-1935. doi:10.1039/B305391C

Mikashima, H., & Goto, K. (1982). Inhibitory effect of 2-(4-(2-imidazo (1, 2-a) pyridyl) phenyl) propionic acid (miroprofen) on platelet aggregation and prostaglandin I2 generation (author's transl). *Yakugaku zasshi: Journal of the Pharmaceutical Society of Japan, 102*(1), 99-103.

Missailidis, S. (2008). *Anticancer Therapeutics* (4th ed.): John Wiley & Sons, Ltd.

Mittal, S., & El-Serag, H. B. (2013). Epidemiology of HCC: Consider the Population. *Journal of clinical gastroenterology, 47*(0), S2-S6. doi:10.1097/MCG.0b013e3182872f29

Mori, S., Takubo, M., Yanase, T., Maegawa, T., Monguchi, Y., & Sajiki, H. (2010). Palladium on Carbon‐Catalyzed Synthesis of Benzil Derivatives from 1,2‐Diarylalkynes with DMSO and Molecular Oxygen as Dual Oxidants. *Advanced Synthesis & Catalysis, 352*(10), 1630-1634. doi:doi:10.1002/adsc.201000173

Mousset, C., Giraud, A., Provot, O., Hamze, A., Bignon, J., Liu, J.-M., . . . Alami, M. (2008). Synthesis and antitumor activity of benzils related to combretastatin A-4. *Bioorganic & Medicinal Chemistry Letters, 18*(11), 3266-3271. doi:https://doi.org/10.1016/j.bmcl.2008.04.053

Mullick, P., Khan, S. A., Begum, T., Verma, S., Kaushik, D., & Alam, O. (2009). Synthesis of 1,2,4-triazine derivatives as potential anti-anxiety and anti-inflammatory agents. *Acta Pol Pharm, 66*(4), 379-385.

Muniz, K. (2009). High-oxidation-state palladium catalysis: new reactivity for organic synthesis. *Angew Chem Int Ed Engl, 48*(50), 9412-9423. doi:10.1002/anie.200903671

Murty, M. S. R., Penthala, R., Polepalli, S., & Jain, N. (2016). Synthesis and biological evaluation of novel resveratrol-oxadiazole hybrid heterocycles as potential antiproliferative agents. *Medicinal Chemistry Research, 25*(4), 627-643. doi:10.1007/s00044-016-1514-1

Nagy, A., Novák, Z., & Kotschy, A. (2005). Sequential and domino Sonogashira coupling: Efficient tools for the synthesis of diarylalkynes. *Journal of Organometallic Chemistry, 690*(20), 4453-4461. doi:https://doi.org/10.1016/j.jorganchem.2004.12.036

Nam, N.-H. (2003). Combretastatin A-4 analogues as antimitotic antitumor agents. *Current medicinal chemistry, 10*(17), 1697-1722. doi:10.2174/0929867033457151

Nandini, C. P., Matthew Merrill Hayward, Thomas Allen, C., & Patrick Robert, V. (2014). USA Patent No. US 2014 235 612 A1.

Nargund, V. H., Raghavan, Derek, Sandler, Howard M. (2008). *Urological Oncology*: Springer London.

Narva, S., Chitti, S., Amaroju, S., Bhattacharjee, D., Rao, B. B., Jain, N., . . . Sekhar, K. (2017). Design and synthesis of 4-morpholino-6-(1,2,3,6-tetrahydropyridin-4-yl)-N-(3,4,5-trimethoxyphenyl)-1,3,5- triazin-2-amine analogues as tubulin polymerization inhibitors. *Bioorg Med Chem Lett, 27*(16), 3794-3801. doi:10.1016/j.bmcl.2017.06.060

Nathwani, S. M., Hughes, L., Greene, L. M., Carr, M., O'Boyle, N. M., McDonnell, S., . . . Zisterer, D. M. (2013). Novel cis-restricted beta-lactam combretastatin A-4 analogues display anti-vascular and anti-metastatic properties in vitro. *Oncol Rep, 29*(2), 585-594. doi:10.3892/or.2012.2181

Newhouse, B. J., Wenglowsky, S., Grina, J., Laird, E. R., Voegtli, W. C., Ren, L., . . . Feng, B. (2013). Imidazo[4,5-b]pyridine inhibitors of B-Raf kinase. *Bioorganic & Medicinal Chemistry Letters, 23*(21), 5896-5899. doi:https://doi.org/10.1016/j.bmcl.2013.08.086

Niforou, K. N., Anagnostopoulos, A. K., Vougas, K., Kittas, C., Gorgoulis, V. G., & Tsangaris, G. T. (2008). The proteome profile of the human osteosarcoma U2OS cell line. *Cancer Genomics-Proteomics, 5*(1), 63-77.

NIH. (2007, 27th March). Understanding Cancer. Retrieved from https://www.ncbi.nlm.nih.gov/books/NBK20362/

Nogales, E. (2000). Structural insights into microtubule function. *Annu Rev Biochem, 69*, 277-302. doi:10.1146/annurev.biochem.69.1.277

Noll, D. M., Mason, T. M., & Miller, P. S. (2006). Formation and repair of interstrand cross-links in DNA. *Chem Rev, 106*(2), 277-301. doi:10.1021/cr040478b

Nowikow, C., Fuerst, R., Kauderer, M., Dank, C., Schmid, W., Hajduch, M., . . . Rinner, U. (2019). Synthesis and biological evaluation of cis-restrained carbocyclic combretastatin A-4 analogs: Influence of the ring size and saturation on cytotoxic properties. *Bioorganic & Medicinal Chemistry*, *27*(19), 115032. doi:https://doi.org/10.1016/j.bmc.2019.07.048

Nunez, J., Fellous, A., Francon, J., & Lennon, A. M. (1979). Competitive inhibition of colchicine binding to tubulin by microtubule-associated proteins. *Proceedings of the National Academy of Sciences of the United States of America, 76*(1), 86-90.

Nussbaumer, S., Bonnabry, P., Veuthey, J.-L., & Fleury-Souverain, S. (2011). Analysis of anticancer drugs: A review. *Talanta, 85*(5), 2265-2289. doi:https://doi.org/10.1016/j.talanta.2011.08.034

Ognjanovic, S., Linabery, A. M., Charbonneau, B., & Ross, J. A. (2009). Trends in childhood rhabdomyosarcoma incidence and survival in the United States, 1975-2005. *Cancer, 115*(18), 4218-4226. doi:10.1002/cncr.24465

Ohsumi, K., Hatanaka, T., Fujita, K., Nakagawa, R., Fukuda, Y., Nihei, Y., . . . Tsuji, T. (1998a). Syntheses and antitumor activity of cis-restricted combretastatins: 5-membered heterocyclic analogues. *Bioorganic & Medicinal Chemistry Letters*, *8*(22), 3153-3158.

Ohsumi, K., Nakagawa, R., Fukuda, Y., Hatanaka, T., Morinaga, Y., Nihei, Y., . . . Tsuji, T. (1998b). Novel combretastatin analogues effective against murine solid tumors: design and structure− activity relationships. *Journal of Medicinal Chemistry, 41*(16), 3022-3032.

Okutani, M., & Mori, Y. (2009). Conversion of Bromoalkenes into Alkynes by Wet Tetra-n-butylammonium Fluoride. *The Journal of organic chemistry*, *74*(1), 442-444. doi:10.1021/jo802101a

Onozuka, T., Tanaka, M., Fujiwara, T., Tamura, M., & Satake, S. (2010). Process For Production of Aromatic Sulfonyl Chloride Compounds (Vol. WO2011058915): Sumitomo Seika Chemicals.

Ottaviani, G., & Jaffe, N. (2010). The Epidemiology of Osteosarcoma. In N. Jaffe, O. S. Bruland, & S. Bielack (Eds.), *Pediatric and Adolescent Osteosarcoma* (pp. 3-13). Boston, MA: Springer US.

Padmaja, R. D., Devi, C. V., Mukku, N., Chanda, K., & Maiti, B. (2018). Rapid Construction of an Imidazo[4,5-b]pyridine Skeleton from 2-Chloro-3-nitropyridine via Tandem Reaction in H2O-IPA Medium. *ACS Omega, 3*(4), 4583-4590. doi:10.1021/acsomega.8b00426

Parisio, C., & Clementi, F. (1976). Surface alterations induced by stress in gastric mucosa: protective effect of zolimidine. A transmission and scanning electron microscope investigation. *Laboratory investigation; a journal of technical methods and pathology, 35*(5), 484-495.

Perego, P., Corna, E., De Cesare, M., Gatti, L., Polizzi, D., Pratesi, G., . . . Zunino, F. (2001). Role of apoptosis and apoptosis-related genes in cellular response and antitumor efficacy of anthracyclines. *Curr Med Chem, 8*(1), 31-37.

Pettit, G. R., Lippert, J. W., Boyd, M. R., Verdier-Pinard, P., & Hamel, E. (2000). Antineoplastic agents 442. Synthesis and biological activities of dioxostatin. *Anti-cancer drug design, 15*(5), 361-371.

Pettit, G. R., Temple, C., Jr., Narayanan, V. L., Varma, R., Simpson, M. J., Boyd, M. R., . . . Bansal, N. (1995). Antineoplastic agents 322. synthesis of combretastatin A-4 prodrugs. *Anticancer Drug Des, 10*(4), 299-309.

Philippeos, C., Hughes, R. D., Dhawan, A., & Mitry, R. R. (2012). Introduction to Cell Culture. In R. R. Mitry & R. D. Hughes (Eds.), *Human Cell Culture Protocols* (pp. 1-13). Totowa, NJ: Humana Press.

Pifferi, G., & Monguzzi, R. (1973). New compounds: Synthesis of 3,4,5-trimethoxybenzenesulfonamides. *Journal of Pharmaceutical Sciences, 62*(8), 1392-1394. doi:https://doi.org/10.1002/jps.2600620847

Pretsch, E. (2000). *Structure determination of organic compounds : tables of spectral data* (3rd completely rev. and enl. English ed. ed.). Berlin
London: Berlin
London : Springer.

Provot, O., Giraud, A., Peyrat, J.-F., Alami, M., & Brion, J.-D. (2005). Synthetic approach to enyne and enediyne analogues of anticancer agents. *Tetrahedron Letters, 46*(49), 8547-8550. doi:https://doi.org/10.1016/j.tetlet.2005.10.001

Ranu, B. C., Das, A., & Hajra, A. (2003). Dichloroindium Hydride (Cl2InH): A Convenient Reagent for Stereoselective Reduction of vic ‐ Dibromides to (E) ‐ Alkenes. *ChemInform, 34*(41). doi:doi:10.1002/chin.200341060

Ravelli, R. B., Gigant, B., Curmi, P. A., Jourdain, I., Lachkar, S., Sobel, A., & Knossow, M. (2004). Insight into tubulin regulation from a complex with colchicine and a stathmin-like domain. *Nature, 428*(6979), 198-202. doi:10.1038/nature02393

Reddel, R. R., Ke, Y., Gerwin, B. I., McMenamin, M. G., Lechner, J. F., Su, R. T., . . . Harris, C. C. (1988). Transformation of human bronchial epithelial cells by infection with SV40 or adenovirus-12 SV40 hybrid virus, or transfection via strontium phosphate coprecipitation with a plasmid containing SV40 early region genes. *Cancer research, 48*(7), 1904-1909.

Ren, W., Xia, Y., Ji, S.-J., Zhang, Y., Wan, X., & Zhao, J. (2009). Wacker-Type Oxidation of Alkynes into 1,2-Diketones Using Molecular Oxygen. *Organic Letters, 11*(8), 1841-1844. doi:10.1021/ol900344g

Riss, T. L., Moravec, R. A., Niles, A. L., Duellman, S., Benink, H. A., Worzella, T. J., & Minor, L. (2016). Cell viability assays *Assay Guidance Manual [Internet]*: Eli Lilly & Company and the National Center for Advancing Translational Sciences.

Robertson, S. (2014Dec 22, 2014). What are Proto-Oncogenes? Retrieved from http://www.news-medical.net/life-sciences/What-are-Proto-Oncogenes.aspx

Robison, M., & Finch, N. (1970). united states Patent No. US3719683A. w. applications.

Rodan, S. B., Imai, Y., Thiede, M. A., Wesolowski, G., Thompson, D., Bar-Shavit, Z., . . . Rodan, G. A. (1987). Characterization of a human osteosarcoma cell line (Saos-2) with osteoblastic properties. *Cancer research*, *47*(18), 4961-4966.

Romagnoli, R., Baraldi, P. G., Salvador, M. K., Preti, D., Aghazadeh Tabrizi, M., Brancale, A., . . . Viola, G. (2012). Synthesis and Evaluation of 1,5-Disubstituted Tetrazoles as Rigid Analogues of Combretastatin A-4 with Potent Antiproliferative and Antitumor Activity. *Journal of Medicinal Chemistry*, *55*(1), 475-488. doi:10.1021/jm2013979

Rosenberg, A. J., Zhao, J., & Clark, D. A. (2012). Synthesis of Imidazo [4, 5-b] pyridines and Imidazo [4, 5-b] pyrazines by Palladium Catalyzed Amidation of 2-Chloro-3-amino-heterocycles. *Organic Letters*, *14*(7), 1764-1767.

Rousseau, J., Lamoureux, F., Picarda, G., Gouin, F., Trichet, V., & Rédini, F. (2010). Chapter 28 - Animal Models of Malignant Primary Bone Tumors and Novel Therapeutic Approaches. In D. Heymann (Ed.), *Bone Cancer* (pp. 333-346). San Diego: Academic Press.

Sajith, A. M., & Muralidharan, A. (2012). Microwave enhanced Suzuki coupling: a diversity-oriented approach to the synthesis of highly functionalised 3-substituted-2-aryl/heteroaryl imidazo[4,5-b]pyridines. *Tetrahedron Letters*, *53*(9), 1036-1041. doi:https://doi.org/10.1016/j.tetlet.2011.12.051

Sanghai, N., Jain, V., Preet, R., Kandekar, S., Das, S., Trivedi, N., . . . Bharatam, P. V. (2014). Combretastatin A-4 inspired novel 2-aryl-3-arylamino-imidazo-pyridines/pyrazines as tubulin polymerization inhibitors, antimitotic and anticancer agents. *MedChemComm*, *5*(6), 766-782. doi:10.1039/C3MD00357D

Segaoula, Z., Leclercq, J., Verones, V., Flouquet, N., Lecoeur, M., Ach, L., . . . Berthelot, P. (2016). Synthesis and biological evaluation of N-[2-(4-Hydroxyphenylamino)-pyridin-3-yl]-4-methoxy-benzenesulfonamide (ABT-751) tricyclic analogues as antimitotic and Antivascular agents with potent in vivo antitumor activity. *Journal of Medicinal Chemistry, 59*(18), 8422-8440.

Sgouras, D., & Duncan, R. (1990). Methods for the evaluation of biocompatibility of soluble synthetic polymers which have potential for biomedical use: 1 — Use of the tetrazolium-based colorimetric assay (MTT) as a preliminary screen for evaluation ofin vitro cytotoxicity. *Journal of Materials Science: Materials in Medicine, 1*(2), 61-68. doi:10.1007/bf00839070

Shapiro, G. I., & Harper, J. W. (1999). Anticancer drug targets: cell cycle and checkpoint control. *Journal of Clinical Investigation, 104*(12), 1645-1653.

Sherr, C. J. (2004). Principles of tumor suppression. *Cell, 116*(2), 235-246. doi:http://dx.doi.org/10.1016/S0092-8674(03)01075-4
showArticle Info

Siemsen, P., Livingston, R. C., & Diederich, F. (2000). Acetylenic Coupling: A Powerful Tool in Molecular Construction. *Angew Chem Int Ed Engl, 39*(15), 2632-2657.

Silverstein, R. M., Webster, F. X., Kiemle, D. J., & Bryce, D. L. (2014). *Spectrometric identification of organic compounds* (8th ed.): John wiley & sons.

Simoni, D., Grisolia, G., Giannini, G., Roberti, M., Rondanin, R., Piccagli, L., . . . Invidiata, F. P. (2005). Heterocyclic and phenyl double-bond-locked combretastatin analogues possessing potent apoptosis-inducing activity in HL60 and in MDR cell lines. *Journal of Medicinal Chemistry, 48*(3), 723-736.

Singh, M. P., Sasmal, S., Lu, W., & Chatterjee, M. N. (2000). Synthetic Utility of Catalytic Fe(III)/Fe(II) Redox Cycling Towards Fused Heterocycles: A Facile Access to Substituted Benzimidazole, Bisbenzimidazole and Imidazopyridine Derivatives. *Synthesis, 2000*(10), 1380-1390. doi:10.1055/s-2000-7111

Singh, U. P., Bhat, H. R., & Gahtori, P. (2012). Antifungal activity, SAR and physicochemical correlation of some thiazole-1,3,5-triazine derivatives. *Journal de Mycologie Médicale, 22*(2), 134-141. doi:https://doi.org/10.1016/j.mycmed.2011.12.073

Singla, P., Luxami, V., & Paul, K. (2015). Triazine as a promising scaffold for its versatile biological behavior. *European Journal of Medicinal Chemistry, 102*, 39-57. doi:https://doi.org/10.1016/j.ejmech.2015.07.037

SJR. (2016, 27th March). World Report. Retrieved from http://www.scimagojr.com/worldreport.php?area=1300

Skibba, J. L., Beal, D. D., Ramirez, G., & Bryan, G. T. (1970). N-demethylation the antineoplastic agent4(5)-(3,3-dimethyl-1-triazeno)imidazole-5(4)-carboxamide by rats and man. *Cancer research, 30*(1), 147-150.

Smeyanov, A., & Schmidt, A. (2013). K3PO4-KOH Mixture as Efficient Reagent for the Deprotection of 4-Aryl-2-methyl-3-butyn-2-ols to Terminal Acetylenes. *Synthetic Communications, 43*(20), 2809-2816. doi:10.1080/00397911.2012.744841

Smith, A. L., D'Angelo, N. D., Bo, Y. Y., Booker, S. K., Cee, V. J., Herberich, B., . . . Norman, M. H. (2012). Structure-Based Design of a Novel Series of Potent, Selective Inhibitors of the Class I Phosphatidylinositol 3-Kinases. *Journal of Medicinal Chemistry, 55*(11), 5188-5219. doi:10.1021/jm300184s

Smith, M. B. (2013). *March's advanced organic chemistry: reactions, mechanisms, and structure*: John Wiley & Sons.

Stanton, R. A., Gernert, K. M., Nettles, J. H., & Aneja, R. (2011). Drugs that target dynamic microtubules: a new molecular perspective. *Med Res Rev, 31*(3), 443-481. doi:10.1002/med.20242

Steliarova-Foucher, E., Colombet, M., Ries, L. A. G., Moreno, F., Dolya, A., Bray, F., . . . Steliarova-Foucher, E. (2017). International incidence of childhood cancer, 2001–10: a population-based registry study. *The Lancet Oncology*. doi:https://doi.org/10.1016/S1470-2045(17)30186-9

Stępiński, D. (2012). Immunofluorescent localization of ubiquitin and proteasomes in nucleolar vacuoles of soybean root meristematic cells. *European Journal of Histochemistry : EJH, 56*(2), e13. doi:10.4081/ejh.2012.e13

Stockert, J. C., Blazquez-Castro, A., Canete, M., Horobin, R. W., & Villanueva, A. (2012). MTT assay for cell viability: Intracellular localization of the formazan product is in lipid droplets. *Acta Histochem, 114*(8), 785-796. doi:10.1016/j.acthis.2012.01.006

Sundstrøm, S., Bremnes, R. M., Kaasa, S., Aasebø, U., Hatlevoll, R., Dahle, R., . . . Vilsvik, J. (2002). Cisplatin and etoposide regimen is superior to cyclophosphamide, epirubicin, and vincristine regimen in small-cell lung cancer: results from a randomized phase III trial with 5 years' follow-up. *Journal of Clinical Oncology, 20*(24), 4665-4672.

Sung, Y. K., Hwang, S. Y., Farooq, M., Kim, J. C., & Kim, M. K. (2003). Growth promotion of HepG2 hepatoma cells by antisense-mediated knockdown of glypican-3 is independent of insulin-like growth factor 2 signaling. *Exp Mol Med, 35*(4), 257-262. doi:10.1038/emm.2003.34

Takacs, J. M., & Jiang, X. t. (2003). The Wacker Reaction and Related Alkene Oxidation Reactions. *ChemInform, 34*(33). doi:doi:10.1002/chin.200333264

Tarade, D., Ma, D., Pignanelli, C., Mansour, F., Simard, D., van den Berg, S., . . . Pandey, S. (2017). Structurally simplified biphenyl combretastatin A4 derivatives retain in vitro anti-cancer activity dependent on mitotic arrest. *PLOS ONE, 12*(3), e0171806. doi:10.1371/journal.pone.0171806

Thathagar, M. B., Beckers, J., & Rothenberg, G. (2004). Palladium-free and ligand-free Sonogashira cross-coupling. *Green Chemistry, 6*(4), 215-218. doi:10.1039/B401586J

Thurston, D. E. (2006). *Chemistry and pharmacology of anticancer drugs*: CRC press.

Tingoli, M., Mazzella, M., Panunzi, B., & Tuzi, A. (2011). Elemental Iodine or Diphenyl Diselenide in the [Bis(trifluoroacetoxy)iodo]benzene‐Mediated Conversion

of Alkynes into 1,2 - Diketones. *European Journal of Organic Chemistry, 2011*(2), 399-404. doi:doi:10.1002/ejoc.201001232

Tron, G. C., Pirali, T., Sorba, G., Pagliai, F., Busacca, S., & Genazzani, A. A. (2006). Medicinal chemistry of combretastatin A4: present and future directions. *J Med Chem, 49*(11), 3033-3044. doi:10.1021/jm0512903

Twentyman, P. R., & Luscombe, M. (1987). A study of some variables in a tetrazolium dye (MTT) based assay for cell growth and chemosensitivity. *Br J Cancer, 56*(3), 279-285.

Uryga, A., Gray, K., & Bennett, M. (2016). DNA damage and repair in vascular disease. *Annual review of physiology, 78*, 45-66. doi:10.1146/annurev-physiol-021115-105127

van Meerloo, J., Kaspers, G. J., & Cloos, J. (2011). Cell sensitivity assays: the MTT assay. *Methods Mol Biol, 731*, 237-245. doi:10.1007/978-1-61779-080-5_20

Vasbinder, M. M., Alimzhanov, M., Augustin, M., Bebernitz, G., Bell, K., Chuaqui, C., . . . Zinda, M. (2016). Identification of azabenzimidazoles as potent JAK1 selective inhibitors. *Bioorg Med Chem Lett, 26*(1), 60-67. doi:10.1016/j.bmcl.2015.11.031

Vasilevsky, S. F., Davydova, M. P., & Tolstikov, G. A. (2008). Heterocyclic analogs of combretastatin A-4. *Chemistry of Heterocyclic Compounds, 44*(10), 1257-1261. doi:10.1007/s10593-009-0171-4

Veisi, H., Ghorbani-Vaghei, R., Hemmati, S., & Mahmoodi, J. (2011). Convenient one-pot synthesis of sulfonamides and sulfonyl azides from thiols using N-chlorosuccinimide. *Synlett, 2011*(16), 2315-2320.

Veljkovic, E., Jiricny, J., Menigatti, M., Rehrauer, H., & Han, W. (2011). Chronic exposure to cigarette smoke condensate in vitro induces epithelial to mesenchymal transition-like changes in human bronchial epithelial cells, BEAS-2B. *Toxicol In Vitro, 25*(2), 446-453. doi:10.1016/j.tiv.2010.11.011

Vergaro, V., Aldieri, E., Fenoglio, I., Marucco, A., Carlucci, C., & Ciccarella, G. (2016). Surface reactivity and in vitro toxicity on human bronchial epithelial cells

(BEAS-2B) of nanomaterials intermediates of the production of titania-based composites. *Toxicol In Vitro, 34*, 171-178. doi:10.1016/j.tiv.2016.04.003

Vogelstein, B., & Kinzler, K. W. (2004). Cancer genes and the pathways they control. *Nat Med, 10*(8), 789-799. doi:10.1038/nm1087

Walia, M. K., Castillo-Tandazo, W., Mutsaers, A. J., Martin, T. J., & Walkley, C. R. (2018). Murine models of osteosarcoma: A piece of the translational puzzle. *Journal of Cellular Biochemistry, 119*(6), 4241-4250. doi:10.1002/jcb.26601

Wang, A., & Jiang, H. (2008). Palladium-Catalyzed Cleavage Reaction of Carbon−Carbon Triple Bond with Molecular Oxygen Promoted by Lewis Acid. *Journal of the American Chemical Society, 130*(15), 5030-5031. doi:10.1021/ja8002217

Weinberg, R. A. (2014). *The biology of cancer* (2nd ed.): Garland Science.

WHO. (2020, 21th March). Data and statistics. Retrieved from http://gco.iarc.fr/today/data/factsheets/populations/994-who-europe-region-euro-fact-sheets.pdf

Wilson, R. J., Rosenberg, A. J., Kaminsky, L., & Clark, D. A. (2014). Copper-and palladium-catalyzed amidation reactions for the synthesis of substituted imidazo [4, 5-c] pyridines. *The Journal of organic chemistry, 79*(5), 2203-2212.

Woolven, H., González-Rodríguez, C., Marco, I., Thompson, A. L., & Willis, M. C. (2011). DABCO-Bis(sulfur dioxide), DABSO, as a Convenient Source of Sulfur Dioxide for Organic Synthesis: Utility in Sulfonamide and Sulfamide Preparation. *Organic Letters, 13*(18), 4876-4878. doi:10.1021/ol201957n

Wu, Y., Xia, C., Fiordeliso, J., Layek, S., Alleyne, B., Dyatkin, A. B., . . . Brooks, J. (2014). Pyridyl carbene phosphorescent emitters: Google Patents.

Xu, N., Gu, D.-W., Dong, Y.-S., Yi, F.-P., Cai, L., Wu, X.-Y., & Guo, X.-X. (2015). Copper-catalyzed synthesis of 1,2-diketones via oxidation of alkynes. *Tetrahedron Letters, 56*(12), 1517-1519. doi:https://doi.org/10.1016/j.tetlet.2015.01.195

Xue, J. W., Zeng, M., Hou, X., Chen, Z., & Yin, G. (2018). Catalytic Oxidation of Alkynes into 1,2 - Diketone Derivatives by Using a PdII/Lewis - Acid Catalyst. *Asian Journal of Organic Chemistry*, *7*(1), 212-219. doi:doi:10.1002/ajoc.201700556

Yang, D., Fokas, D., Li, J., Yu, L., & Baldino, C. M. (2005). A Versatile Method for the Synthesis of Benzimidazoles from o-Nitroanilines and Aldehydes in One Step via a Reductive Cyclization. *Synthesis, 2005*(01), 47-56. doi:10.1055/s-2004-834926

Yokoyama, W. M., Thompson, M. L., & Ehrhardt, R. O. (2012). Cryopreservation and thawing of cells. *Current protocols in immunology*, *99*(1), A. 3G. 1-A. 3G. 5. doi:https://doi.org/10.1002/0471142735.ima03gs99

Yoshimatsu, K., Yamaguchi, A., Yoshino, H., Koyanagi, N., & Kitoh, K. (1997). Mechanism of action of E7010, an orally active sulfonamide antitumor agent: inhibition of mitosis by binding to the colchicine site of tubulin. *Cancer research*, *57*(15), 3208-3213.

Yuan, L.-Z., Hamze, A., Alami, M., & Provot, O. (2017). Synthesis of Substituted Benzils from Diarylalkyne Oxidation. *Synthesis*, *49*(03), 504-525. doi:10.1055/s-0036-1588608

Yusubov, M. S.-o., & Filimonov, V. D. (1991). Iodine in Dimethyl Sulfoxide as a New General Reagent for the Preparative Oxidation of 1,2-Diarylethenes and 1,2-Diarylethynes to Aromatic 1,2-Diketones. *Synthesis*, *1991*(02), 131-132. doi:10.1055/s-1991-26397

Zhang, S., Liu, X., Bawa-Khalfe, T., Lu, L. S., Lyu, Y. L., Liu, L. F., & Yeh, E. T. (2012). Identification of the molecular basis of doxorubicin-induced cardiotoxicity. *Nat Med*, *18*(11), 1639-1642. doi:10.1038/nm.2919

Zheng, N., Anderson, K. W., Huang, X., Nguyen, H. N., & Buchwald, S. L. (2007). A palladium-catalyzed regiospecific synthesis of N-aryl benzimidazoles. *Angew Chem Int Ed Engl*, *46*(39), 7509-7512. doi:10.1002/anie.200702542

Zou, B., Yuan, Q., & Ma, D. (2007). Synthesis of 1,2-disubstituted benzimidazoles by a Cu-catalyzed cascade aryl amination/condensation process. *Angew Chem Int Ed Engl, 46*(15), 2598-2601. doi:10.1002/anie.200700071

Zwelling, L. A., Anderson, T., & Kohn, K. W. (1979). DNA-protein and DNA interstrand cross-linking by cis- and trans-platinum(II) diamminedichloride in L1210 mouse leukemia cells and relation to cytotoxicity. *Cancer research, 39*(2 Pt 1), 365-369.